

**BIOSYNTHESIS AND CELLULAR ACTIONS OF
BIOACTIVE NATURAL PRODUCTS**

A Dissertation

by

SHOGO MORI

Submitted to the Office of Graduate and Professional Studies of
Texas A&M University
in partial fulfillment of the requirements for the degree of

DOCTOR OF PHILOSOPHY

Chair of Committee,	Coran M. H. Watanabe
Committee Members,	Tadhg P. Begley
	David P. Barondeau
	Gregory D. Reinhart
Head of Department,	Francois P. Gabbai

December 2015

Major Subject: Chemistry

Copyright 2015 Shogo Mori

ABSTRACT

The utilization of natural products as therapeutic agents has been an invaluable resource throughout medicinal history. Through the combined application of combinatorial biosynthesis, the modification of a natural product by engineered enzymes, and the isolation of new bioactive natural products, the discovery of new therapeutic agents may be achieved. This work shows the novel enzymatic interaction in the biosynthesis of a known therapeutic agent and the isolation of a new bioactive natural product.

Azinomycin A and B are antitumor natural products, isolated from *Streptomyces sahachiroi*. It was proposed that the biosynthesis of azinomycins is achieved through polyketide synthase (PKS) and non-ribosomal peptide synthetase (NRPS) machinery. In order to characterize the role of the PKS (AziB), enzymatic assays were analyzed by HPLC, LC-MS, and spectrophotometric methods. Although AziB was predicted to catalyze the production of 5-methyl-1-napthoic acid, a building block of azinomycins, a thioesterase (AziG) was found to be essential. Kinetic and crystallographic studies suggested the importance of the interaction of AziB and AziG to facilitate optimal enzymatic activity. The derivative of the AziB-AziG product is hypothesized to be assembled into the azinomycin backbone by NRPSs. In order to confirm the significance of a NRPS (AziA2) in the azinomycin biosynthetic pathway, gene knockout studies were performed. Fermentation of Δ *aziA2* *S. sahachiroi* led to an cryptic overproduction of dimethyl furan-2,4-dicarboxylate. This showed an example of bacterial adaptation where bacteria start overproducing a new secondary metabolite to deal with the absence of a bioactive natural product.

A novel bioactive 40-membered macrolactone, Nuiapolide, was identified from a cyanobacterium collected from the Hawaiian ocean. This molecule has a rare *tert*-butyl side chain and nine hydroxyl groups distributed through the large hydrocarbon ring structure. Nuiapolide could inhibit metastatic activity of Jurkat at the concentration of as low as 1.3 μ M without killing the cells.

In this dissertation, the new functionality of a class of enzyme, the effect of biosynthetic disruption, and a novel anti-metastatic natural product from a marine source will be discussed. This information leads to a new understanding of natural products and their biosynthesis, which will eventually help researchers developing novel therapeutic agents.

ACKNOWLEDGEMENTS

First and foremost, I would like to greatly thank my academic advisor Dr. Coran M. H. Watanabe. Her keen and critical advice allowed me to achieve this scientific accomplishment in my doctoral years. Without her guidance, I could never complete my Ph. D works. She also keeps the lab safe, clean, and organized, which makes the lab an ideal place for research.

My committee members, Dr. David P. Barondeau, Dr. Tadhg P. Begley, and Dr. Gregory D. Reinhart provided me with critical advice in or out of committee meetings. I also would like to thank our collaborators, Dr. F. David Horgen in the Hawaii Pacific University for his help with the marine natural product project and Dr. Steven E. Ealick in the Cornell University for his help with the enzymology project. The flow cytometry operator Dr. Roger Smith III at the Department of Veterinary Pathobiology kindly instructed me on how to use the instrument to analyze the cell cycle of Jurkat cells. Dr. Howard Williams was able to take clean NMR spectra with a small amount of sample. This was a great help on determining the structure of the novel natural product. When I needed unique biomolecules, Dr. Dmytro Fedoseyenko could synthesize either known or novel compounds incredibly fast. I could not achieve any of my dissertation work without the help of these great scientists.

I am grateful to my previous and current labmates, especially my senior Dr. Hillary Agbo. All my primary work was accomplished by his kind assistance, helping me learn the fundamental techniques and start becoming a biochemist. I would also like to acknowledge postdoctoral members Dr. Huitu Zhang, Dr. Dinesh Simkhada, and Dr. Keshav Nepal who all had extensive knowledge about *Streptomyces* species. They were role models as well as experienced researchers. I was given a lot of help from my current graduate student labmates, Vishruth Gowda, Irum Perveen, Brian Young, Brendan Foley, and Lauren A. Washburn. I wish them success in their graduate years.

Thanks to all my friends who shared time with me in a city soccer league and weekend parties, I could survive this long path to gain the degree by easing my stress

and pressure. Finally, I will not have to worry my family anymore because they have always been doing so. I have just kept their words since coming here, “do as you like, but never give up.”

TABLE OF CONTENTS

	Page
ABSTRACT	ii
ACKNOWLEDGEMENTS	iv
TABLE OF CONTENTS	vi
LIST OF FIGURES	x
LIST OF SCHEMES	xv
LIST OF TABLES	xvi
CHAPTER I INTRODUCTION: NATURAL PRODUCTS AND THEIR BIOSYNTHESIS	1
Introduction	1
Historical Perspective	2
Primitive Use of Natural Products	2
Development of Natural Product Pharmacology	3
Current Status	4
Natural Products in Cancer Therapy	8
Biosynthesis of Natural Products	12
Importance of Enzymology	12
Polyketide Synthase (PKS)	13
Nonribosomal Peptide Synthetase (NRPS)	16
Thioesterase (TE)	17
Combinatorial Biosynthesis	19
Azinomycins	20
Antitumor Natural Products	21
Mode of Action: Interstrand Cross Link Formation	23
Mode of Action: Role of Moieties	27
Biosynthesis: Hybrid Functionality	32
Biosynthesis: Genetics	36
Statement of Purpose	39

CHAPTER II	AZINOMYCIN BIOSYNTHESIS: FORMATION OF THE	
	NAPHTHOATE MOIETY BY PKS-TE INTERACTION	40
	Introduction	40
	Preliminary Research	41
	Results and Discussion.....	45
	Production of 5-Methyl-1-Naphthoic Acid by AziB and AziG	45
	Comparison to Synthetic Standard of 5-Methyl-1-Naphthoic Acid.....	47
	AziB-AziG <i>In Vitro</i> Binding Assay	48
	Bioinformatic Study and Crystal Structure of AziG	49
	Site Directed Mutagenesis and Effect to the Production.....	53
	Kinetics of AziG and Its Mutants.....	55
	Significance	56
	Materials and Methods	58
	General Experimental Procedure.....	58
	Reagents and Materials	58
	Cloning of <i>AziA6</i> into an Expression Vector for <i>E. coli</i>	59
	Site Directed Mutagenesis of <i>AziG</i>	59
	Overexpression of AziB, Svp, <i>AziA6</i> , AziG, and AziG Mutants.....	60
	Posttranslational Modification of AziB with Svp and Coenzyme A	61
	Purification of AziB-Svp, <i>AziA6</i> , AziG, and AziG Mutants.....	62
	<i>In Vitro</i> Synthesis of 5-Methyl-1-Naphthoic Acid by AziB and TE	
	Domains	62
	LC-MS Analysis of AziB and <i>AziA6</i> or AziG Products	63
	Synthesis of 5-Methyl-1-Naphthoic Acid (Dr. Dmytro Fedoseyenko).....	63
	LC-MS Analysis of AziB-AziG Product with the Synthetic Standard	65
	Preparation of Cell Free Extract of <i>S. sahachiroi</i>	65
	AziB-AziG <i>In Vitro</i> Binding Assay	65
	Gel Filtration Chromatography of AziG Native Form.....	66
	Crystallization of AziG (Dr. Megan D. Sikowitz)	66
	X-Ray Data Collection and Processing (Dr. Megan D. Sikowitz).....	67
	Structure Determination, Model Building, and Refinement	
	(Dr. Megan D. Sikowitz).....	67
	Kinetics of AziG Hydrolysis	68
	Molar Absorptivity of TNB.....	69
	Synthesis of 5-Methyl-1-Naphthoate-SNAC Ester	
	(Dr. Dmytro Fedoseyenko)	70
CHAPTER III	AZINOMYCINS: EVALUATION OF BIOLOGICAL	
	ACTIVITY OF CRYPTIC PRODUCT FROM Δ <i>AZIA2</i> <i>STREPTOMYCES</i>	
	<i>SAHACHIROI</i>	73

Introduction	73
Preliminary Research	74
Results and Discussion.....	76
Cytotoxicity and Chemotaxis Assays against Jurkat Cells	76
Anti-Bacterial and Anti-Fungal Assays	77
Neurite Outgrowth Assay	78
Significance	79
Materials and Methods	81
Chemicals and General Procedures.....	81
Cytotoxicity Assay against Jurkat Cells, Human Cell Line of T Lymphocyte	81
Chemotaxis Assay against Jurkat Cells, Human Cell Line of T Lymphocyte	82
Anti-Bacterial and Anti-Fungal Assays	82
Neurite Outgrowth Assay.....	83

CHAPTER IV DISCOVERY AND EVALUATION OF MACRO-LACTONE

ANTI-METASTATIC MARINE NATURAL PRODUCT, NUIAPOLIDE	84
Introduction	84
Results and Discussion.....	87
Evaluation of Hawaiian Marine Natural Product Extracts for Anti-Chemotactic Behavior.....	87
Cytotoxicity Assay for Active Crude Extracts	88
Evaluation of Fractionated Extracts for Anti-Chemotactic Behavior	89
Cell Cycle Analysis of Nuiapolide (56)	92
Structural Analysis of Nuiapolide (56)	93
Significance	99
Methods and Materials	100
General Experimental Procedures	100
Reagents and Chemicals.....	101
Sample Preparation for Assay Analysis (Hawaii Pacific University).....	101
Details on Cyanobacteria Biomass (Hawaii Pacific University)	102
DNA Extraction and Sequencing (Hawaii Pacific University).....	102
Scaled-Up Extraction of the Active Cyanobacterial Species (Hawaii Pacific University).....	103
Bioassay-Linked Fractionation of Methanol and Dichloromethane Extracts of the Cyanobacterium 071905-NII-01 (Hawaii Pacific University).....	104
Isolation of Nuiapolide (56) (Hawaii Pacific University).....	105
Structural Analysis of Nuiapolide (56)	105

Chemotaxis and Cytotoxicity Assay against Jurkat Cells, Human Cell Line of T Lymphocyte.....	106
Cell Cycle Analysis by Flow Cytometry.....	106
Spectral Data of Nuiapolide (56)	106
CHAPTER V CONCLUSION.....	124
REFERENCES	127
APPENDIX FIGURES AND TABLES.....	146

LIST OF FIGURES

	Page
Figure 1 Structures of penicillin derivatives.....	2
Figure 2 Drug trend from 1981 to 2010 ¹	7
Figure 3 Small molecule drugs for cancer therapy from 1930 to 2012 ²	9
Figure 4 Anticancer drugs	10
Figure 5 Anthracycline analogs	12
Figure 6 Polyketide (PK), nonribosomal peptide (NRP), or hybrid natural products	14
Figure 7 Three types of combinatorial biosynthesis ³	21
Figure 8 Azinomycins and relative compounds	23
Figure 9 Sequence selectivity and covalent interaction ⁴⁻⁷	25
Figure 10 <i>In vivo</i> action of azinomycin B ⁸	26
Figure 11 Azinomycin synthetic analogs for evaluation of the role of naphthoate epoxide moiety	28
Figure 12 Azinomycin analogs for evaluation of aziridine and epoxyaziridine derivatives	30
Figure 13 Dimeric naphthoate epoxyamides linked by flexible or non-flexible arms	31
Figure 14 Aziridine containing natural products	33
Figure 15 Isotopic labeling studies for the origin of the naphthoate moiety ⁷	34
Figure 16 Biosynthetic origins of azinomycins	36
Figure 17 Biosynthetic gene cluster of azinomycins	38
Figure 18 <i>In situ</i> biosynthesis of azinomycin analog in target cells.....	41

Figure 19	Enhanced naphthoate moiety production with over expressed AziB (Dr. Huitu Zhang).....	42
Figure 20	Phosphopantetheinylation of AziB with ³ H-CoA (Dr. Huitu Zhang)	43
Figure 21	<i>In vitro</i> product of AziB (Dr. Huitu Zhang and Dr. Dinesh Simkhada) .	44
Figure 22	Induced naphthoic acid synthesis by AziB and AziG (Dr. Dinesh Simkhada).....	45
Figure 23	LC-MS traces that demonstrate lack of formation of 5-methyl-1-naphthoic acid by AziA6, AziA7, and AziA8 (Dr. Dinesh Simkhada for AziA7 and AziA8)	46
Figure 24	LC-MS analysis of AziB-AziG product with the buffer treated standard	48
Figure 25	AziB-AziG <i>in vitro</i> binding assay	49
Figure 26	Sequence alignment of AziG homologs and AziG crystal structures	53
Figure 27	LC-MS analysis of AziB-AziG mutant products	54
Figure 28	Kinetic parameters of AziG and its mutants	56
Figure 29	Azinomycin NRPS modules and their substrates.....	74
Figure 30	HPLC analysis of WT and Δ <i>aziA2</i> mutant.....	75
Figure 31	Cytotoxicity and chemotaxis assay against Jurkat cells.....	77
Figure 32	Antibacterial and antifungal assays.....	78
Figure 33	Neurite outgrowth assay.....	79
Figure 34	Evaluation of Jurkat cultures in the Boyden chamber assay	88
Figure 35	Cytotoxicity profile analysis of extracts.....	89
Figure 36	Fragmentation of CL013-F10 (Dr. David Horgen) and chemotaxis assays.....	90
Figure 37	Evaluation of nuiapolide (56) activity at 1 μ g/mL.....	91

Figure 38	Cell cycle analysis of nuiapolide (56) treated Jurkat cells	93
Figure 39	Partial structure of nuiapolide (56) with key HMBC correlations	94
Figure 40	Structure of nuiapolide (56) and caylobolides A (57) and B (58).....	99
Figure 41	¹ H NMR of nuiapolide (56) in methanol- <i>d</i> ₄	109
Figure 42	¹³ C NMR of nuiapolide (56) in methanol- <i>d</i> ₄	110
Figure 43	DEPT-90 of nuiapolide (56) in methanol- <i>d</i> ₄	111
Figure 44	DEPT-145 of nuiapolide (56) in methanol- <i>d</i> ₄	112
Figure 45	COSY of nuiapolide (56) in methanol- <i>d</i> ₄	113
Figure 46	TOCSY of nuiapolide (56) in methanol- <i>d</i> ₄	114
Figure 47	HSQC of nuiapolide (56) in methanol- <i>d</i> ₄	115
Figure 48	HSQC-TOCSY of nuiapolide (56) in methanol- <i>d</i> ₄	116
Figure 49	HMBC of nuiapolide (56) in methanol- <i>d</i> ₄	117
Figure 50	¹ H NMR of nuiapolide (56) in DMSO- <i>d</i> ₄	118
Figure 51	¹³ C NMR of nuiapolide (56) in DMSO- <i>d</i> ₄	119
Figure 52	COSY of nuiapolide (56) in DMSO- <i>d</i> ₄	120
Figure 53	TOCSY of nuiapolide (56) in DMSO- <i>d</i> ₄	121
Figure 54	HSQC of nuiapolide (56) in DMSO- <i>d</i> ₄	122
Figure 55	HMBC of nuiapolide (56) in DMSO- <i>d</i> ₄	123
Appendix Figure 56	BLAST search of AziB.....	146
Appendix Figure 57	Multiple alignment of AziB and its homologous enzymes (0-400 aa).....	146
Appendix Figure 58	Preparation of pure AziA6.....	147
Appendix Figure 59	BLAST search of AziG.....	147

Appendix Figure 60	Multiple alignment of AziG and its characterized homologous enzymes which share the conserved active site .	148
Appendix Figure 61	AziG tetramer and monomer	149
Appendix Figure 62	Expression plasmid of AziG (and its mutants) and SDS-PAGE analysis of overexpression and purification	150
Appendix Figure 63	Numbering of 5-methyl-1-napthoic acid (49) and HMBC correlations.....	151
Appendix Figure 64	LC-MS analysis with the standard.....	151
Appendix Figure 65	¹ H NMR (500 MHz, CD ₃ OD) for 5-methyl-1-napthoic acid (49).....	152
Appendix Figure 66	¹ H NMR (500 MHz, CD ₃ OD) for 5-methyl-1-napthoic acid (49), 7.0-9.0 ppm	153
Appendix Figure 67	¹³ C NMR (500 MHz, CD ₃ OD) for 5-methyl-1-napthoic acid (49).....	154
Appendix Figure 68	¹³ C NMR (500 MHz, CD ₃ OD) for 5-methyl-1-napthoic acid (49), >120 ppm.	155
Appendix Figure 69	COSY (500 MHz, CD ₃ OD) for 5-methyl-1-napthoic acid (49).....	156
Appendix Figure 70	COSY (500 MHz, CD ₃ OD) for 5-methyl-1-napthoic acid (49), 7.0-9.0 ppm	157
Appendix Figure 71	HSQC (500 MHz, CD ₃ OD) for 5-methyl-1-napthoic acid (49).....	158
Appendix Figure 72	HSQC (500 MHz, CD ₃ OD) for 5-methyl-1-napthoic acid (49), aromatic region.....	159
Appendix Figure 73	HMBC (500 MHz, CD ₃ OD) for 5-methyl-1-napthoic acid (49).....	160
Appendix Figure 74	HMBC (500 MHz, CD ₃ OD) for 5-methyl-1-napthoic acid (49), methyl group region.	161

Appendix Figure 75	HMBC (500 MHz, CD ₃ OD) for 5-methyl-1-napthoic acid (49), aromatic region.....	162
Appendix Figure 76	Individual kinetic parameters including R ² values and error bars of standard deviations	163
Appendix Figure 77	Determination of molar absorptivity of Ellman's reagent in the reaction buffer	164
Appendix Figure 78	Gel filtration of native AziG.....	165
Appendix Figure 79	Gel filtration analysis of AziG: calibration curves and tabulated data	166
Appendix Figure 80	Cytotoxicity and chemotaxis assay against Jurkat cells	168
Appendix Figure 81	Chemotaxis assay of CL013-F10 at lower doses.....	169
Appendix Figure 82	PDA map of active fractions in FR022.....	169
Appendix Figure 83	LCMS analysis of FR022	170
Appendix Figure 84	PDA map of active fractions in FR023.....	171
Appendix Figure 85	LCMS analysis of NP988	172
Appendix Figure 86	Purified nuiapolide (56) and NP982	173
Appendix Figure 87	Chemotaxis assay for purified active fractions.....	174
Appendix Figure 88	Cell cycle analysis of nuiapolide (56) treated Jurkat cells.....	175
Appendix Figure 89	Number of carbons in ¹³ C NMR grouped regions	176

LIST OF SCHEMES

	Page
Scheme 1 General scheme of PKS.....	15
Scheme 2 General scheme of NRPS	17
Scheme 3 General scheme of product release by TE domain.....	19
Scheme 4 Predicted mechanisms of AziG catalyzed hydrolysis	51
Appendix Scheme 5 AziG kinetic experiment utilizing Ellman's reagent	164

LIST OF TABLES

	Page
Table 1 Primers used in Chapter II.....	70
Table 2 Strains and plasmids used in Chapter II.....	71
Table 3 NMR spectral data for nuiapolide (56)	96
Appendix Table 4 Characterized homologous enzymes of AziG	148
Appendix Table 5 NMR spectral data for 5-methyl-1-naphthoic acid (49) (500 MHz, CD ₃ OD).	150
Appendix Table 6 AziG data collection and refinement statistics.....	167

CHAPTER I

INTRODUCTION: NATURAL PRODUCTS AND THEIR BIOSYNTHESIS

INTRODUCTION

Natural products are secondary metabolites which living organisms synthesize to survive the stress of various environmental conditions including changes in the weather and the existence of competitors or invaders. Many of these molecules are used as weapons to attack competitors. Plants produce antibiotics or antifungals to defend against invading pathogens, and microorganisms produce toxic materials to kill other microbes living in the same habitat.^{9, 10} These natural products can often be used as therapeutic agents for higher-order organisms when they are properly applied because many of these anti-infectious molecules are effective against a broad spectrum of microorganisms.¹¹ The first antibiotic used as a therapeutic agent, penicillin (Figure 1), was isolated from the mold *Penicillium glaucum*. It was initially observed as having antibiotic activity against *Staphylococcus* spp.,¹² but its derivatives have been shown to be effective against many other bacterial infections including Gram-positive bacteria, such as *Streptococci*, *Clostridium*, and *Listeria genera*.¹³ Since then natural product exploration has been one of the primary interests in drug discovery because the large degree of structural diversity can deliver highly potent lead compounds.

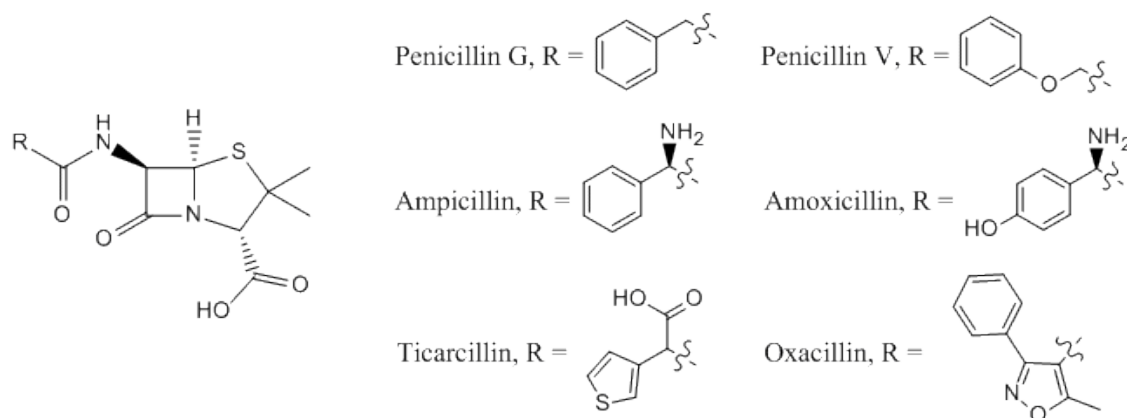


Figure 1. Structures of penicillin derivatives

HISTORICAL PERSPECTIVE

Primitive Use of Natural Products

Plants have been used by humans as herbal drugs for a long time. Archaeological evidence suggests that medicinal plants were used by Neanderthals during the Paleolithic period, approximately 60,000 years ago.¹⁴ A large amount of pollen from eight flowering plants, seven of which are currently used as herbal remedies, was found at Shanidar cave located in northern Iraq. More recent work has shown that dental plaques isolated from 50,000 year old Neanderthals at El Sidrón site in northern Spain contained trace amounts of the known herbal plant *Achillea millefolium*.¹⁵ The plant was unlikely suitable for regular consumption because of its extremely bitter taste which is sensed by a taste receptor shared with Neanderthals and modern humans.¹⁶

The oldest written history describing the medicinal uses of herbs dates back to 3,000 B.C. when Sumerians in Mesopotamia documented the practice of preparing clay tablets with hundreds of medicinal plants including myrrh and opium.¹⁷ Ancient Egyptians wrote Ebers Papyrus in approximately 1500 B.C. containing information of more than 850 herbal medicines made from garlic, juniper, cannabis, castor bean, aloe, and mandrake.¹⁸ This list included many plants of foreign origin, suggesting that they had been trading for these medicinal plants with other nations. Through development of

Ayurveda (science of long life) in India, spices which could be either food components or medicines were developed more than 5,000 years ago. For example, turmeric was derived from the rhizome of the plant *Curcuma longa* which contains a variety of bioactive natural products.¹⁹ The history of China has been written since 722 B.C. during the Zhou dynasty when Chinese medicine had already been established as an independent field of study with a variety of practitioners, such as physicians, surgeons, dietitians, and veterinarians. Archeological evidence from the Shang dynasty (16-11th century B.C.) has demonstrated their utilization of herbal medicines at that time.²⁰

Plants for medical purposes are consumed not only by humans but also by animals, and it is often observed in both mammals and birds. These behaviors are discussed in zoopharmacognosy.²¹ A well known example of animal self-medication is that chimpanzees consume the plant *Aspilia* spp. for the treatment or prevention of intestinal nematode parasites.^{22, 23} The plant contains a bioactive natural product, thiarubrine A, which is toxic to several parasitic nematode species.^{21, 24} Chimpanzees have a unique practice of using the plant. They eat only young leaves with 2-10 cm long and up to 4 cm broad by rolling it around in their mouth and swallow a whole without chewing so that a sufficient amount of bioactive molecules is protected by leaf structure and kept from digestion by stomach acid.²¹ Another well known example is anting, observed in more than 200 species of song birds, when birds wipe ants or other insects vigorously through their plumage.²⁵ It is theorized that the behavior is to protect themselves with chemical fluids secreted by insects, such as formic acid, which act as anti-infectious agents.²⁶

Development of Natural Product Pharmacology

The Significance of natural products had been naturally and empirically shown, but the common viewpoint changed dramatically with the advancement of chemistry in the early nineteenth century. During this time, practitioners and physicians began to identify chemical compounds in medical plants which led to vigilant research on the therapeutic potential of plant components.²⁷ Apothecaries and then pharmaceutical

companies developed relatively crude therapeutic formulations from plant extracts, which had become purer and purer through the development of chemical analysis techniques until the mid-twentieth century when single molecule drugs derived from natural products started emerging.²⁸

The use of natural products entered into a new era with the discovery of penicillin, the first pure antibiotic drug, by Alexander Fleming in 1928. He showed that *Penicilium rubens* cultured in appropriate condition secreted an antibiotic substance which inhibited growth of other bacteria.^{12, 29} Penicillin was not introduced to the public market until the mid-1940s due to the lack of mass production techniques, although the therapeutic potential had already been displayed by Howard Florey and his colleagues. They showed that the antibiotic had a high toxicity against certain bacteria with a low toxicity to humans.^{30, 31} In a few years after their studies were published, thousands of cases were treated with penicillin and reported in hundreds of papers in the scientific community after production difficulties were overcome during World War II.³² Success of penicillin led researcher to investigate microbes as sources of potential therapeutic agents. Technological advancement has broadened explorable sites on earth over time allowing researchers to obtain novel sources of natural products.

Current Status

Natural product research began declining in the late 1980s due to the increasing development of synthetic drugs thanks to the technological development of organic synthesis.³³ Synthetic drugs had a high impact on the pharmacological society because these molecules can be produced at a much larger scale with a much smaller facility. As comparing a small round bottomed flask producing grams of product in synthetic methods to a large fermenter producing milligrams of product in biological methods, the synthetic method provides robust drugs at a cheap price, which is crucial for poor people, especially in developing countries. Structures of synthetic drugs are typically simpler than ones of natural products, which make the synthetic compounds easy to be

mass produced and to be handled, but the simpler structures tend to lack the specificity and selectivity to drug targets leading to greater adverse effects to patients.

The continuous exploration of natural products has supplied a great diversity of bioactive compounds which cannot be replaced by synthetic drugs. Natural products have demonstrated their importance in drug discovery, especially after the substantial innovation of high throughput screening (HTS) in the early 1990s. HTS uses automated robots and powerful computers to screen and analyze a large number of molecules at a time. The number of assays per day had reached 200,000 by the middle 2000s; although lack of facilities, which required expensive equipment that was only accessible by big pharmaceutical companies, still limited access to the procedure.³³ One of the recent advancements in the HTS method was grown out of conventional plate assays. The well plates were replaced by pico-litter scale aqueous drops spread on oil surface as the reaction vessel. Thousands of these could be screened in a second, allowing $\sim 1 \times 10^8$ enzymatic reactions with a total of $< 150 \mu\text{L}$ reagent to be performed in 10 h.³⁴ These technological advances made research much quicker, providing an enormous library of bioactive compounds to be studied. These compounds provided leads which researchers could use for designing novel therapeutic agents.

Natural product exploration has been a leading theme in drug discovery for more than 50 years and never lost attention, although interest rose and fell occasionally due to changing trends. For 30 years, from 1981 to 2010, 33.8% of approved small molecule drugs were natural products, natural product botanical (botanical defined mixture), or natural product derived, and 16.5% of them were synthetic compounds with the same pharmacophore as natural products (Figure 2).¹ The high ratio of natural product related drugs, and their steady contribution to drugs available, shows the significance of natural product research. This research will likely receive more attention in the future because new sources of natural products have been recognized recently. Natural product botanical extracts (NB) are a mixture of multiple weak bioactive materials or of previously known drugs that have been shown to significantly elevate the therapeutic effect of a treatment when compared to an equal amount of the active single drug. The

plant extracts have been recognized again as novel drug formulations, although the individual molecules had been extensively focused since the discovery and success of penicillin.^{35, 36}

Sources of natural products which people can access and investigate has significantly extended thanks to technological, engineering, and scientific development. Marine natural products produced by invertebrates or microorganisms were made possible to investigate by the advancement of scuba technologies in the late twentieth century. This has lead to a growing number of marine natural products in preclinical studies and following clinical trials, and a few that have passed clinical trials in recent years. The quantity of clinically applicable marine natural products is thought to increase in the near future. In Europe no antitumor drug of marine origin had been approved since cytarabine come onto the market in 1969 until trabectedin (Yondelis®), isolated from the seasquirt *Ecteinascidia turbinata*, was approved for treatment of advanced or metastatic soft tissue sarcoma in 2007.³⁷ Other sources of natural product drugs include venom or secretion of higher-order organisms, such as insects, reptiles, and amphibians, which often formulate a cocktail of bioactive peptides and/or small molecules to catch pray or to protect themselves from enemies or infection.³⁸

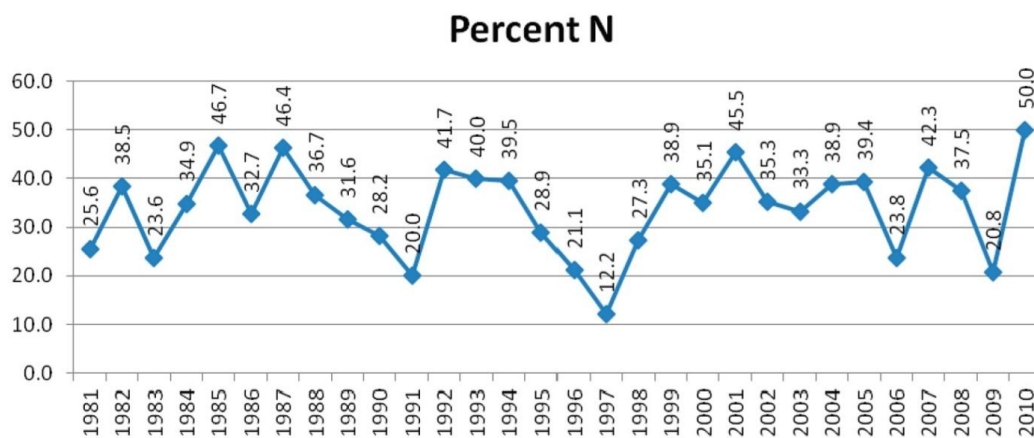
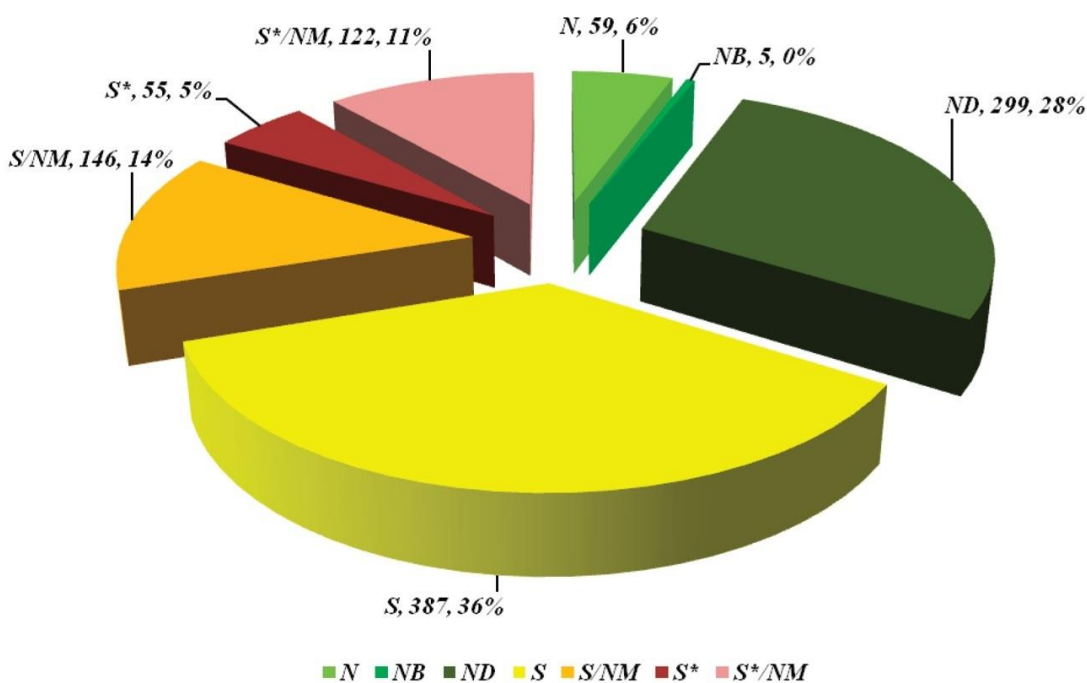


Figure 2. Drug trend from 1981 to 2010¹

N: natural product, NB: natural product botanical, ND: natural product derived, S: synthetic, S/NM: synthetic of a competitive inhibitor of an enzyme or receptor (natural product mimic), S*: synthetic with a natural product pharmacophore, S*/NM: synthetic with a natural product pharmacophore of a competitive inhibitor. Total number is 1073. The top graph displays the ratio of the source of approved small molecule drugs in the period, and the bottom one shows the percentage of natural product in approved small molecule drugs in each year.

NATURAL PRODUCTS IN CANCER THERAPY

Cancer is one of the primary causes of death in developed countries, which tend to have higher average life expectancy, because the number of cases increases as the population ages. In The United States of America cancer was the second highest cause of death, preceded by heart (cardiovascular) diseases in 2010.³⁹ In The European Union (EU), Australia, Canada, and Japan, cancer was the leading cause of death in 2010 (EU and Australia), in 2011 (Canada), and in 2012 (Japan).⁴⁰⁻⁴³ Cancer is traditionally treated by surgery, radiotherapy, chemotherapy, or their combination. In surgery and radiotherapy, cancer cells are physically removed from the affected sites or destroyed with high energy radiation. Drugs are used in chemotherapy for killing the cancerous cells or limiting cell behaviors, such as growth and spreading. Because sensitivity to these treatment strategies is varied in each cancer type and in each patient, other options are not likely to disappear even if one of them becomes predominantly effective and common. Most patients diagnosed with cancers have received chemotherapy in some form. Cancer is caused by failure of apoptosis after bodily cells undergo certain mutations, which occur due to either internal or external factors. Internal factors include inherited traits passed down by parents, and genetic mutations caused by aging. The primary example of an external source is exposure to carcinogens. There are countless numbers of cancer types because all body cells have the possibility to become cancerous. Some cancers are much more common than others, such as lung cancer, prostate cancer for men, and breast cancer for women. Therefore, an active drug to a particular cancer may not necessarily be active against other cancers, which make cancer therapies highly complicated.

The enormous structural diversity of natural products, which can often selectively affect certain types of cancer cells, provides a solution to this problem. Bioactive natural products against cancer cells have been found from various sources, such as plants, terrestrial microorganisms, and marine microbes or invertebrates. Several successful antitumor natural products or natural product derivatives include paclitaxel,

vinorelbine, and vindesine from plants, bleomycins, anthracyclines, and epothilones from terrestrial microbes, and didemnin B, trabectedin, and halichondrin B from marine organisms (Figure 4).⁴⁴⁻⁴⁶ From 1930 to 2012, natural products, natural product botanical, or natural product derived small molecules accounted for 46.6% of all approved small molecules for cancer therapy, and synthetic compounds sharing a pharmacophore with natural products accounted for 20.4 % of all (Figure 3).² This clearly shows the importance of natural products and their structural properties.

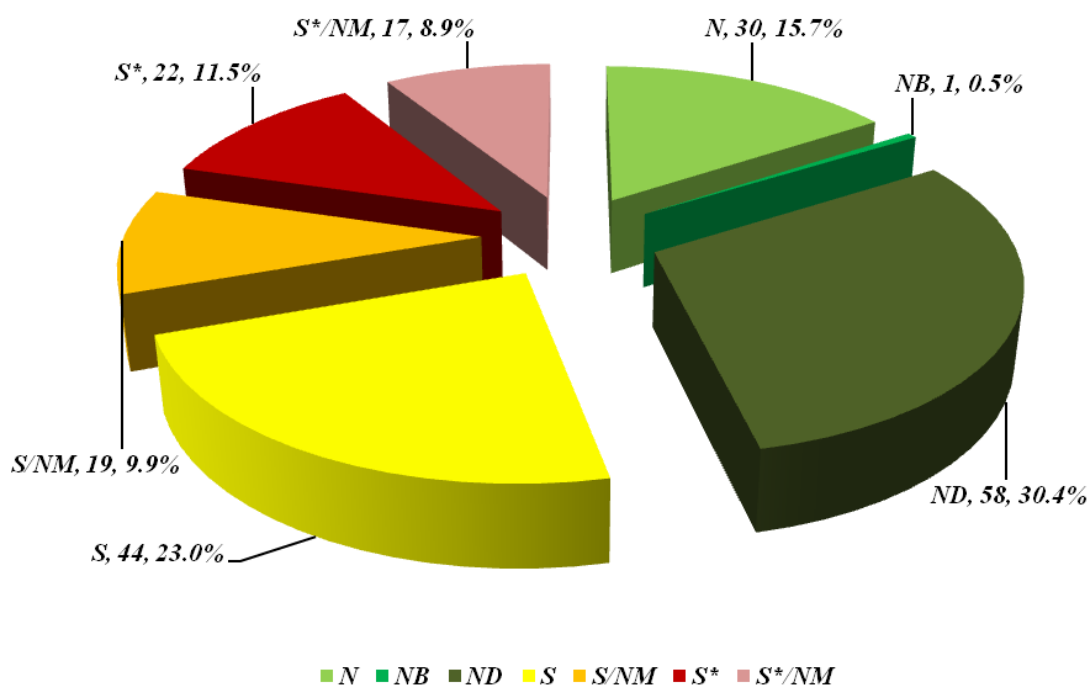
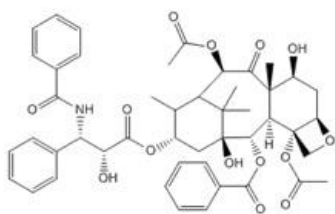
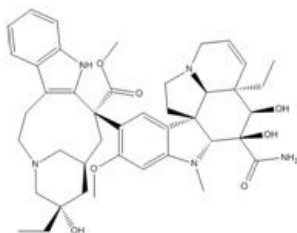


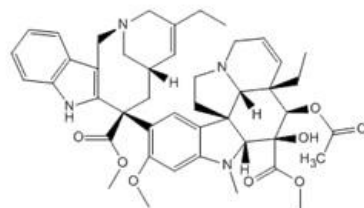
Figure 3. Small molecule drugs for cancer therapy from 1930 to 2012²
Abbreviations are identified in Figure 2. Total number is 191.



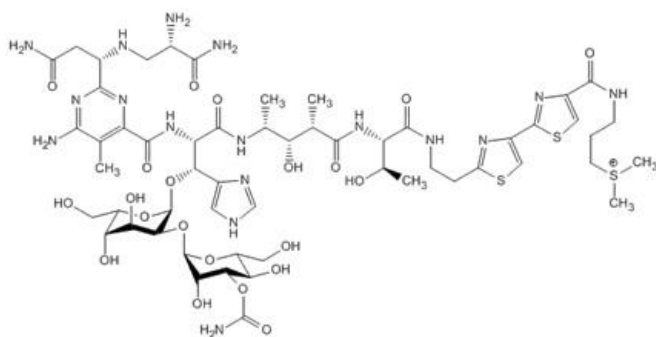
Paclitaxel



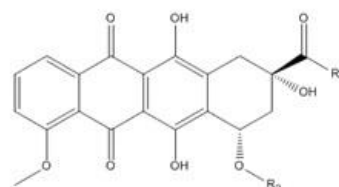
Vindesine



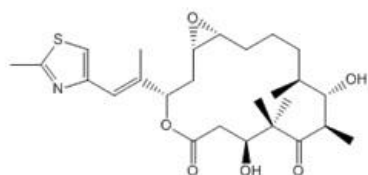
Vinorelbine



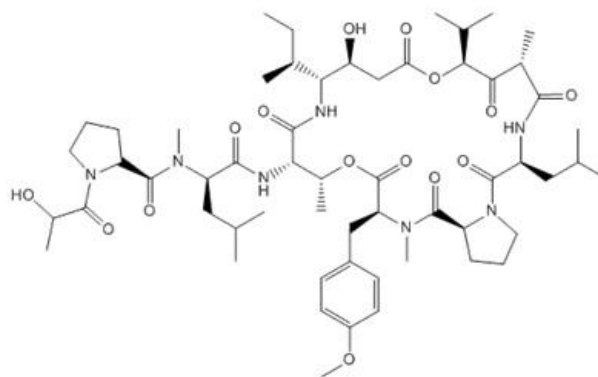
Bleomycine



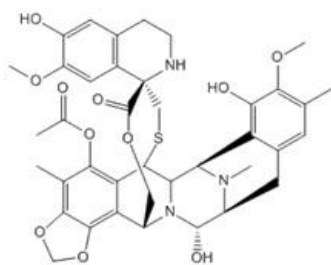
Anthracyclines
(core structure)



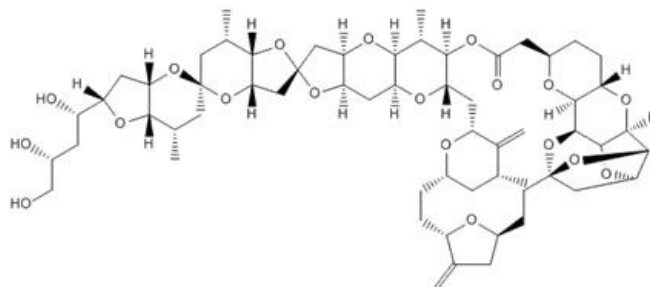
Epothilone A



Didemnin B



Trabectedin



Halichondrin B

Figure 4. Anticancer drugs

One of the most notable antitumor drugs of natural source is paclitaxel (taxol®), which is used for the treatment of breast, ovarian, lung, bladder, prostate, melanoma, esophageal, Kaposi's sarcoma, and some other solid tumors. Paclitaxel was discovered in 1962 by the National Cancer Institute (NCI) granted large scale screening program for antitumor agents from 1960s to early 1980s when 15,000 plant samples worldwide were evaluated against the mouse leukemia cell line.⁴⁷ It was originally isolated from bark of the Pacific yew *Taxus brevifolia* and later found that it was produced by the fungus *Taxomyces andreanae* infecting the plant surface.⁴⁸ Although it spent more than 10 years to be confirmed as an antitumor agent, 20 years to begin phase I clinical trials, and 30 years to be approved by FDA, the plant alkaloid is now one of the most successful antitumor drugs on the market. It was the first one to reach sales greater than \$1 billion, and peaked at \$1.6 billion in late 2000 when the generic form was available on the market.⁴⁹ Natural sources of bioactive compounds are not always sufficient for investigations, clinical trials, and practical uses. For example, *T. brevifolia* had already been scarce at the time of paclitaxel discovery, and it could not meet increasing demand of the compound. This issue was later solved by the establishment of the practical semi-synthetic route from its analogous compound isolated from *T. baccata*.^{50, 51}

This kind of problem can also be tackled by total synthesis which allows for the generation of an enormous library of small molecule analogs. These can be screened to identify the pharmacophore of the parental compound, allowing for the development of safer or more powerful drugs. Pixantrone (pixuvri®) and mitoxantrone (novantrone®) are examples of synthetic drugs possessing a shared pharmacophore with natural products, the anthracyclines produced by *Streptomyces* spp. Anthracyclines are a class of drugs among the most effective anticancer treatments, but they have an irreversible cardiotoxic adverse reaction. This was settled by synthetic studies uncovering compounds with low toxicity that retained their antitumor activity. (Figure 5).⁵²

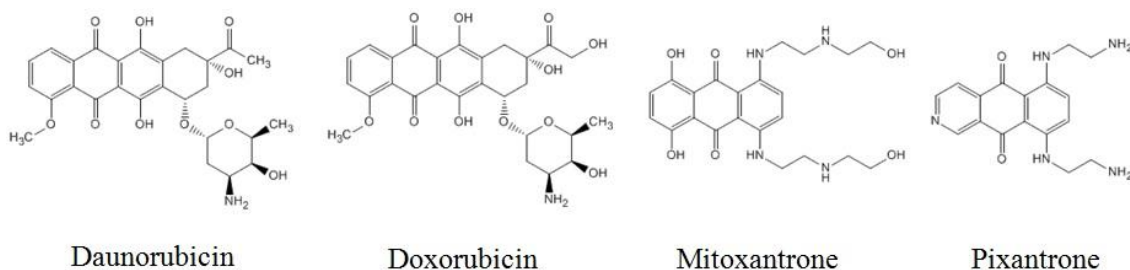


Figure 5. Anthracycline analogs

Daunorubicin and doxorubicin are natural origin prototypes of anthracycline drugs. Mitoxantrone is a synthetic drug derived from anthracyclines. Pixantrone is an experimental drug which is less toxic than mitoxantrone.

BIOSYNTHESIS OF NATURAL PRODUCTS

Importance of Enzymology

Natural products are synthesized by the combination of diverse enzymes. Enzyme structures have been optimized through the process of evolution since the appearance of the first organism, or even before that, for specific functions which are essential or desired for survival and reproduction. This has created a magnificent variety of enzymes. The structure of an enzyme is coded by a gene whose sequence is easily altered, but these mutations do not necessarily lead to bad outcomes. The mutated enzyme sometimes produces a new metabolite which increases the organism's survivability in its environment, and may become the new standard for the organism in the later generations.

In other words, modifications to the biosynthetic pathway of a particular natural product may lead to novel bioactive compounds which are difficult to obtain through total or semi synthetic methods.^{53, 54} The expanded diversity of small molecules by combinatorial biosynthesis, generating non-natural natural products by engineered proteins, may relieve some of the difficulties on time and cost in drug discovery. Releasing a new drug currently takes approximately 13.5 years and costs about \$1.8 billion.⁵⁵ The large modular proteins polyketide synthases (PKSs) and non-ribosomal

peptide synthetases (NRPSs) are well suited for the purpose of modifications on natural product structures by swapping or deleting the catalytic domains.⁵⁶

Polyketide Synthase (PKS)

PKS is one of the largest class of enzyme families synthesizing an enormous variety of natural products including long chained, cyclic, and aromatic compounds (Figure 6).⁵⁷⁻⁶³ The highly diversified structures are constructed by the complex combination of enzyme modules which consist of multiple functional domains. The fundamental domains which essentially all PKS proteins possess include acyl-transferase (AT), keto-synthase (KS), and acyl carrier protein (ACP) domains.⁶⁴ These domains catalyze polyketide chain elongation with coenzyme A (CoA) derived monomer units of one starter unit (typically acetyl-CoA) and multiple malonyl-CoA or methaylmalonyl-CoA for building blocks. An AT domain transfers a (methyl)malonyl group onto an ACP domain, which posttranslationally obtains a flexible pantetheinyl arm from CoA on its active site serine residue. This process is catalyzed by a phosphopantetheinyl transferase (PPTase).⁶⁵ The (methyl)malonyl group is subsequently condensed with either the starter unit or the elongating chain. The elongating chain is transferred from a previous ACP domain to the active site cysteine residue of a KS domain, which gives an additional unit onto the polyketide intermediate. Side chains of elongating polyketides can be modified by multiple sub domains. For instance, the ketone would be reduced to alcohol by keto reductase (KR) domain, which can be further reduced to alkene by dehydratase (DH) domain, which could be reduced more to alkane by enoyl reductase (ER) domain. The final product is generated by cycles of these amalgamated enzymatic functions and released from the final ACP domain by hydrolysis or intramolecular cyclization catalyzed by thioesterase (TE) domain (Scheme 1 and Scheme 3).

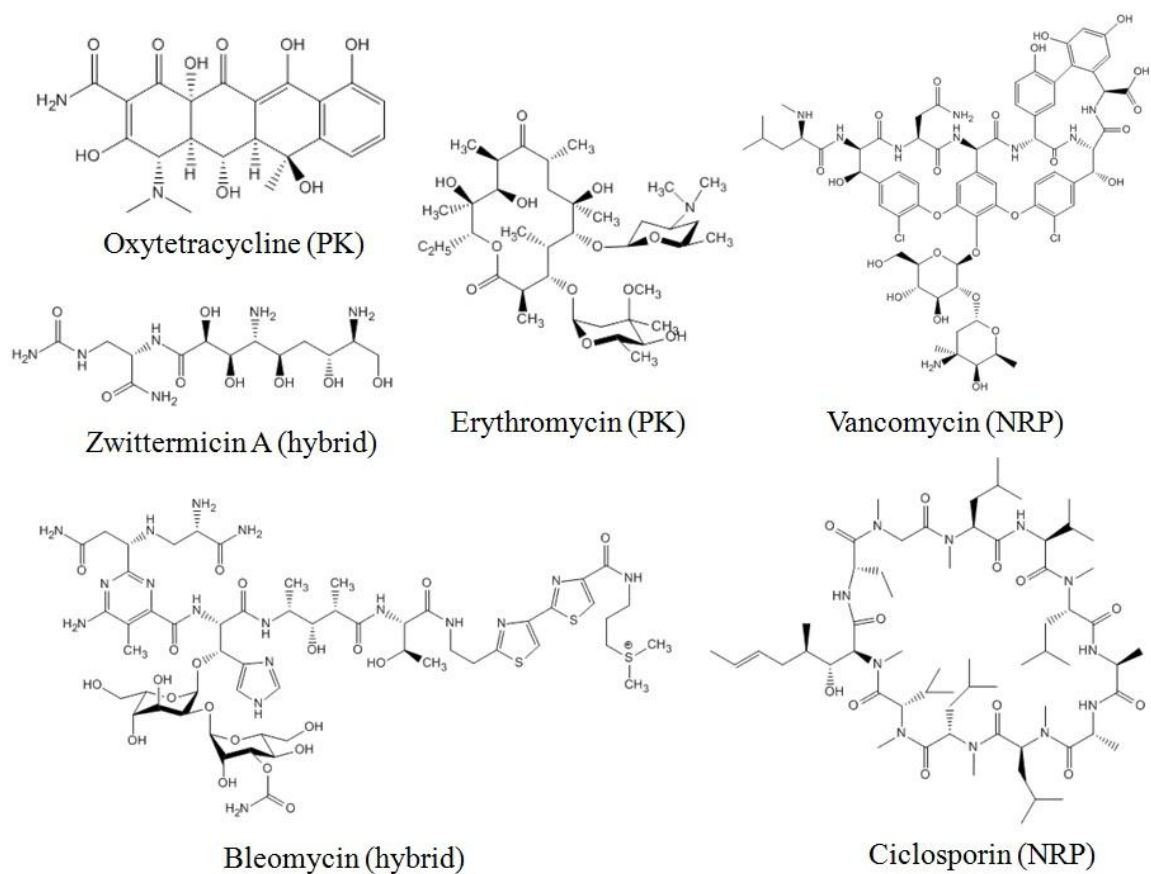
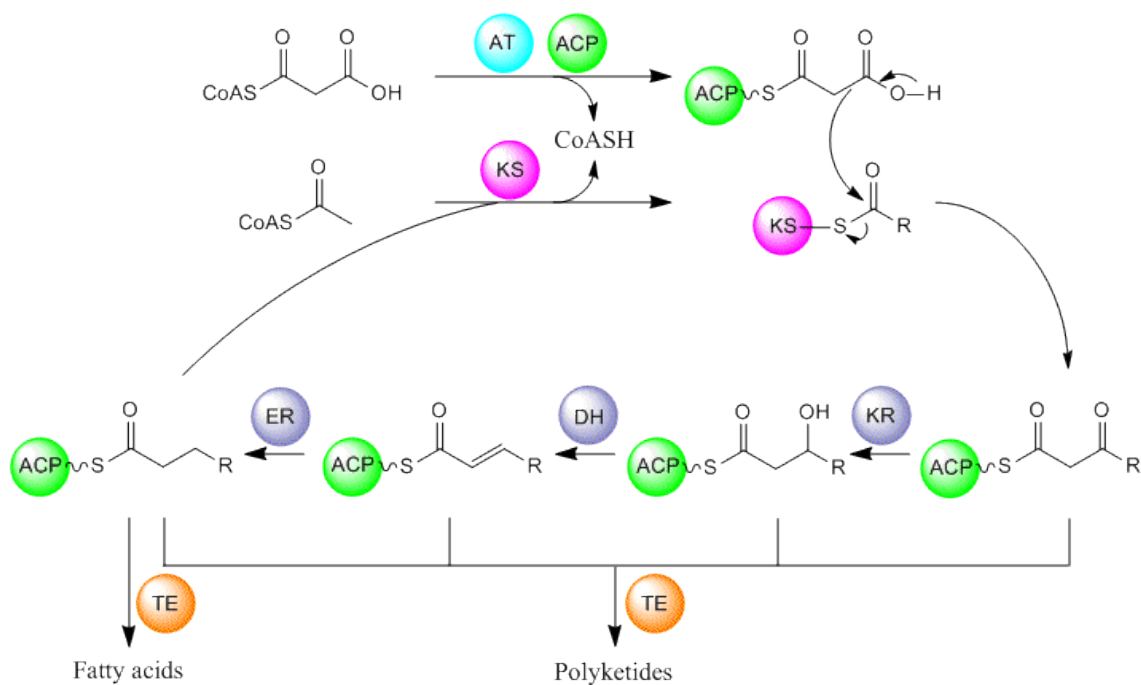


Figure 6. Polyketide (PK), nonribosomal peptide (NRP), or hybrid Natural Products



Scheme 1. General scheme of PKS

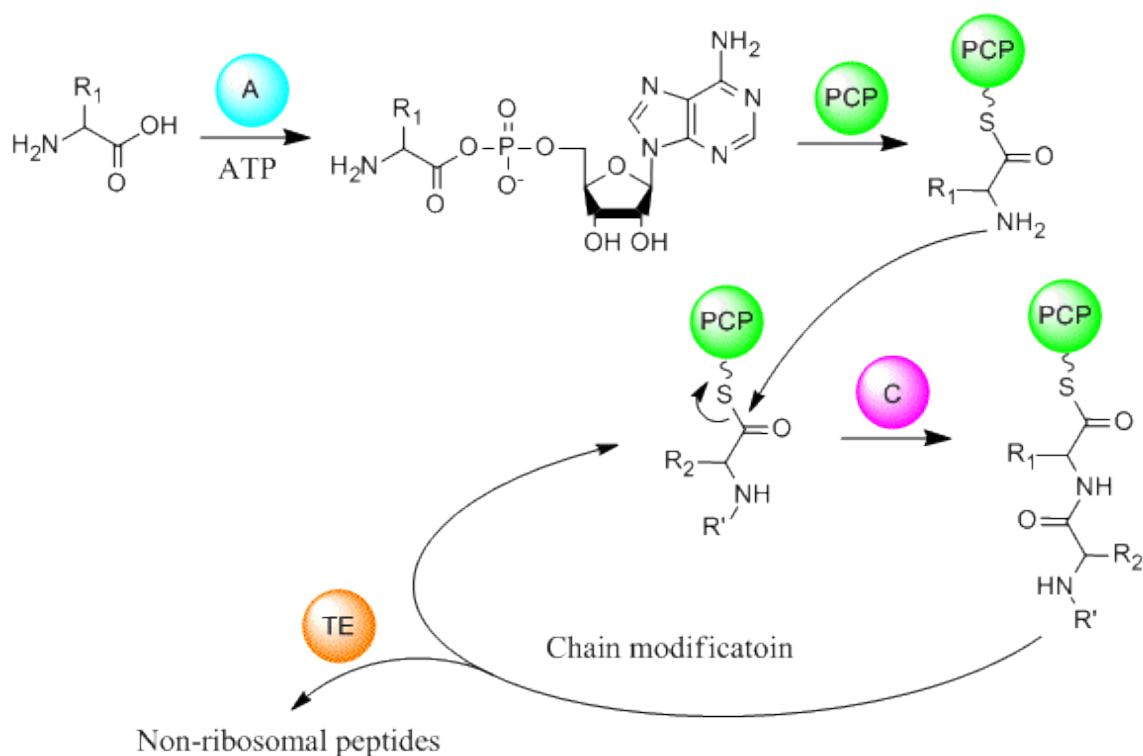
AT: acyltransferase, KS: keto-synthase, ACP: acyl carrier protein, KR: ketoreductase, DH: dehydrogenase, ER: enoylreductase, TE: thioesterase.

PKS is classified into three types.⁶⁴ Type I PKS is large modular protein in which each domain is interacted *in cis*. Type I PKS is further divided into two sub groups, iterative PKS (IPKS) and modular PKS. In IPKS, the cycle of catalytic actions is repeated until the polyketide chain reaches a specific length, which enables one module alone to synthesize the final product from scratch. Therefore, products of IPKSs regularly possess repeated units with the same structural properties. Fatty acid derivatives are synthesized by fully reductive IPKSs. In contrast to IPKS, modular PKS synthesizes the product with multiple modules, each of which consists of domains responsible for constructing individual building block of the final product. Products of modular PKSs have diversified structural features in each unit resulting highly complex natural products. In type II PKS, also known as aromatic polyketide producers, individual catalytic domains are not physically connected but interacted with *in trans*.⁶⁶ Its minimal set of

enzyme contains ACP, KS $_{\alpha}$, and KS $_{\beta}$ (or CLF: chain length factor) which has high sequence similarity to KS $_{\alpha}$ but lacks the key cysteine residue.⁶⁷ Type II PKSs synthesize aromatic natural products by elongating polyketide chain iteratively in the active site between KS $_{\alpha}$ and KS $_{\beta}$, which is thought to be a factor determining the chain length, followed by cyclization and aromatization. Type III PKS is identified as a PKS lacking its ACP domain. It directly uses malonyl-CoA as a substrate instead of transferring it onto the posttranslationally modified long flexible phosphopantetheinyl arm on ACP domain.⁶⁸

Nonribosomal Peptide Synthetase (NRPS)

NRPS is another class of enzyme family that produces an immense variety of natural products (Figure 6).^{62, 63, 69, 70} NRPSs are modular proteins consisting of multiple catalytic domains in a similar style as PKSs, but NRPSs produce peptide natural product instead of polyketides. The catalytic domains in NRPS include adenylation (A), condensation (C), and peptidyl carrier protein (PCP) domains, each of which corresponds to AT, KS, and ACP domains, respectively.⁶⁴ The A domain activates a peptide building block with adenosine triphosphate (ATP) to transfer it onto a posttranslationally modified PCP domain. An amide bond formation between two substrates is catalyzed by a C domain, and the product is eventually released by a TE domain (Scheme 2). NRPS generally has a wider variety of subdomains for structural modification on the side chain which allows for nonribosomal peptides to increase the complexity, such as cyclization (Cy), epimerization (E), methyltransferases (MT), reductase (Re), oxidase (Ox) and halogenation (Hal) domains.⁶⁴ Contrary to the numbers of subdomains NRPSs have only one type, the large non-iterative modular protein likewise modular type I PKS.



Scheme 2. General scheme of NRPS

A: adenylation, C: condensation, PCP: peptidyl carrier protein, TE: thioesterase.

Thioesterase (TE)

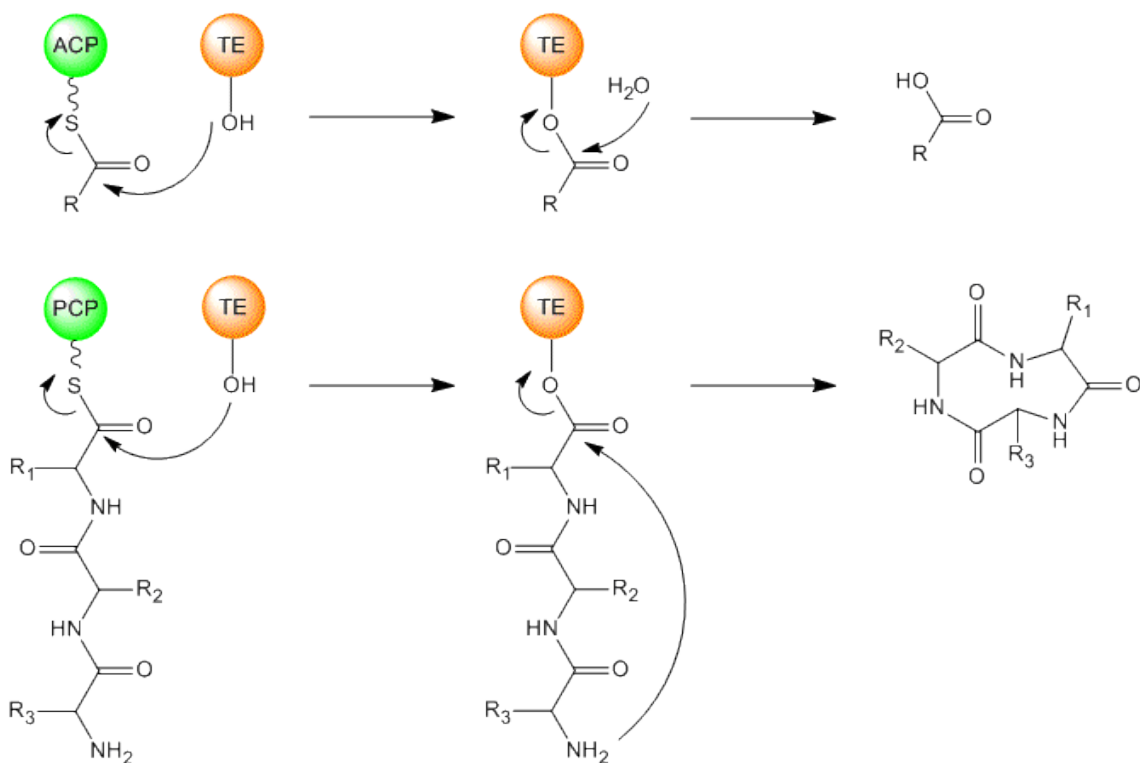
PKSs, NRPSs, and fatty acid synthases (FASs) typically have a thioesterase (TE) domain at the final stage of the sequential reaction to release the product through thioester hydrolysis or macrocyclization (Scheme 3).⁷¹ It has been recently recognized that TE domains do not only catalyze the release of the product but, can also catalyze other chemistries such as chain elongation, epimerization, Dieckmann or Claisen condensation, and deacetylation. The wide diversity of the thioesterase enzyme family may lead to novel modification strategies of natural products.

Elongation by a TE domain is seen in biosynthesis of enterobactin, which is known as the strongest siderophore binding ferrous ions (Fe^{2+}) with the affinity $K = 10^{52} \text{ M}^{-1}$. The natural product found in Gram-negative bacteria is constructed by NRPS enzymes, but it contains trilactone core structure with three identical subunits. It has

been shown that the core structure is assembled by the TE domain which covalently binds and holds an intermediate on its active site serine residue until another identical unit is ready on the neighboring PCP domain.⁷² These two intermediates are condensed together on the TE domain, and the new intermediate waits until the next identical unit is located on the PCP domain for the second condensation, and finally the trimer molecule is released by intramolecular cyclization to form the trilactone.

The TE domain NocTE catalyzes epimerization at the final stage of NRPS machineries acquiring nocardicin G which is an intermediate of the β -lactam antibiotic nocardicin A produced by the Gram-positive bacterium, *Nocardia uniformis* subspecies *Tsuyamenensis*.⁷³ It was previously proposed that NocTE catalyzed β -lactam formation out of the peptide product of five NRPS modules, but NocTE did not recognize any of the predicted or activated substrates. It was found that β -lactam formation was achieved prior to loading onto NocTE, which subsequently epimerized α -center of the substrate to produce nocardicin G.⁷⁴

TE domains do not only catalyze one additional reaction but may also catalyze two additional reactions. For example, the TE domain in a nonreducing PKS Pks1 catalyzes Claisen/Dieckmann cyclization and deacetylation to synthesize 1,3,6,8-tetrahydroxynaphthalene (THN), which is a precursor in melanin biosynthesis in the fungi *Colletotrichum lagenarium*. Pks1 consists of the following domains: acyl-carrier protein transacylase (SAT), KS, malonyl-CoA:acyl-carrier protein transacylase (MAT), product template (PT), ACP, another ACP, and a TE domain. The TE domain was previously known as the Claisen/Dieckmann cyclase class, which was thought to catalyze six-membered aromatic ring formation through Claisen/Dieckmann cyclization, although formation of the δ -lactone was observed without the TE domain by a reduced hydroxyl group and thioester.^{75, 76} The mystery behind construction of THN was that the starter unit acetyl group was not incorporated in the product although the SAT domain was shown to selectively transfer acetyl group from acetyl-CoA onto the protein.^{77, 78} It was finally revealed that the TE domain catalyzed deacetylation in addition to cyclization in a single enzymatic step.⁷⁹



Scheme 3. General scheme of product release by TE domain

Combinatorial Biosynthesis

Three strategies are currently used in combinatorial biosynthesis: precursor-directed biosynthesis, enzyme-level modification, and pathway-level recombination (Figure 7).³ One of the most important properties of many enzymes is substrate specificity, but it is not absolute because some enzymes recognize their substrates by a part of the structures. When the substrate and its close relatives are not both found in the environment, it is not crucial for an enzyme to distinguish between these structures. This may result in an enzyme that can accept a relatively broad spectrum of structures and may catalyze the following reactions. Precursor-directed biosynthesis describes the technique of utilizing this property to produce derivatives of the enzyme's original

product by adding synthetic analogs of the substrate which are chosen by crystal structure and computational analysis.⁸⁰

Enzyme-level modification can be divided into three sub-divisions: domain swapping, site-specific mutagenesis, and directed evolution. In each of these divisions, mutation or replacement is carried out to alter the specific function of enzyme.³ In the domain swapping method, a domain of a modular enzyme is replaced with the same type of domain from another enzyme to manufacture non-predictable natural products. This procedure is often invasive and the yield of the novel product is significantly lowered because of the inaccessibility of the intermediate to the following enzymes. The resulting mega-protein also tends to become insoluble because of the structure change. This problem is resolved by the application of site-specific mutagenesis onto a particular sequence of proteins. The mutations are normally performed onto reductive domains which do not catalyze backbone construction, but catalyze side chain alteration which does not appreciably affect the overall structure of the enzyme or the product. The directed evolution method is more powerful than site-specific mutagenesis, which does not produce a wide variety of derivatives because of the limited scope of mutation. In this technique a library of vectors which express randomly mutated proteins is introduced into a host organism in which synthesis of the original protein is disrupted. The organism then naturally selects acceptable mutations to produce novel natural product derivatives. Its multiple outcomes also surpass the domain swapping method which produces only one derivative from one successful replacement.

The most prosperous strategy so far has been pathway-level recombination since mederrhodin A was achieved in 1985 which produces a novel compound by heterologous expression of biosynthetic genes from separate species.³ This procedure is not only applied to the novel derivative formation but also utilized for addition of the specific substitution on natural product, such as halogenation which has an important role in bioactivity of secondary metabolite. It is essential to understand the biosynthetic pathway of the original natural product, including the function of enzymes, domains, and amino acid residues required for its production.

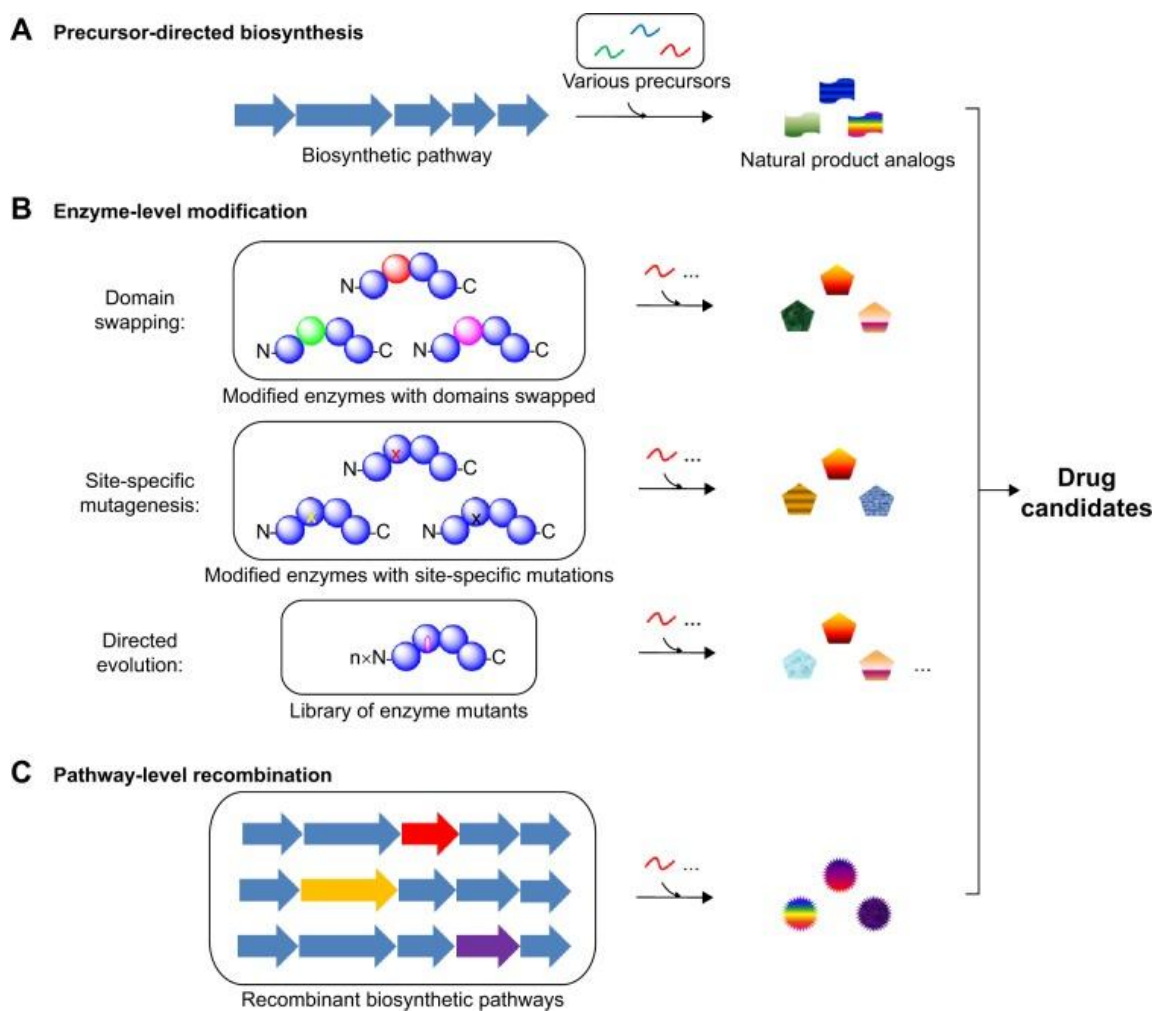


Figure 7. Three types of combinatorial biosynthesis³

AZINOMYCINS

Antitumor Natural Products

Azinomycin A and B (**1** and **2**, Figure 8) are antitumor natural products produced by *Streptomyces* spp., a Gram positive bacteria predominately found in soil. Azinomycin A was originally isolated from *Streptomyces sahachiroi* as carzinophilin A in 1954. Its antitumor activity was identified against Yoshida sarcoma cells, and it was also shown to have antibacterial activity against several Gram negative bacteria.⁸¹ The natural product

was reisolated from *S. griseofuscus* in 1986 with its close structural relatives azinomycin B and their derivatives (**3-5**) which lack the 1-azabicyclo[3.1.0] ring system (Figure 8). Azinomycins were subsequently shown to have *in vitro* cytotoxicity against the mouse lymphoma cell line (L5178Y), with a half maximal inhibitory concentration (IC_{50}) of 0.07 $\mu\text{g/mL}$ and 0.11 $\mu\text{g/mL}$ for azinomycin A and B, respectively. They also showed bioactivity against both Gram positive and negative bacteria but not against yeast and fungi.⁸² The *in vivo* antitumor effects in mice were published in the next year. They showed positive results against Ehrlich carcinoma, where azinomycin A and B had 161 % and 15 % increase in lifespan (ILS) at a dose of 32 $\mu\text{g/kg/day}$ and 8 $\mu\text{g/kg/day}$ with a 45 day survival of 5/8 and 3/8 respectively. They were also effective against P388 leukemia, where azinomycin B exhibited ILS of 193 % at the dose of 32 $\mu\text{g/kg/day}$ with 45 days survival of 4/7. This dosage was much lower than the well known antitumor drug mitomycin C which showed 204 % ILS at the 1 mg/kg/day dose with 4/7 survival after 45 days.⁸³ The structures of the azinomycins were determined at the same time, showing that they had characteristic epoxide and aziridine ring structures on separate side chains with a naphthoate and peptide backbone. The difference between azinomycin A and B was found at the peptide end of these structures, where azinomycin B possessed an additional enol substituent and a slightly elevated molecular weight of 623 g/mol compared to 593 g/mol for azinomycin A. Their structures corresponded to molecular formula of $\text{C}_{30}\text{H}_{33}\text{N}_3\text{O}_{10}$ and $\text{C}_{31}\text{H}_{33}\text{N}_3\text{O}_{11}$, respectively.⁸⁴

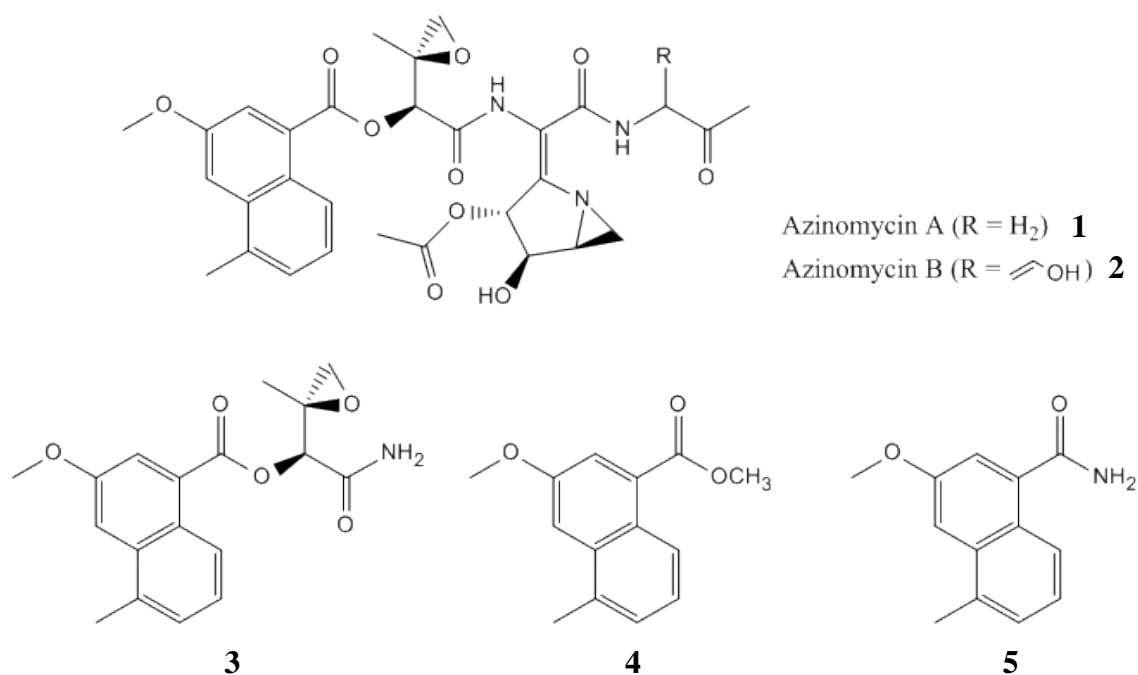


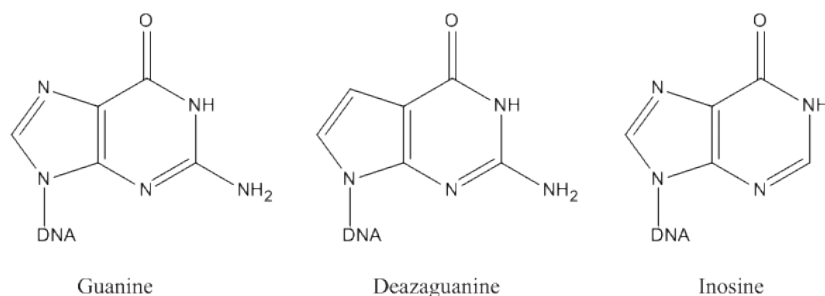
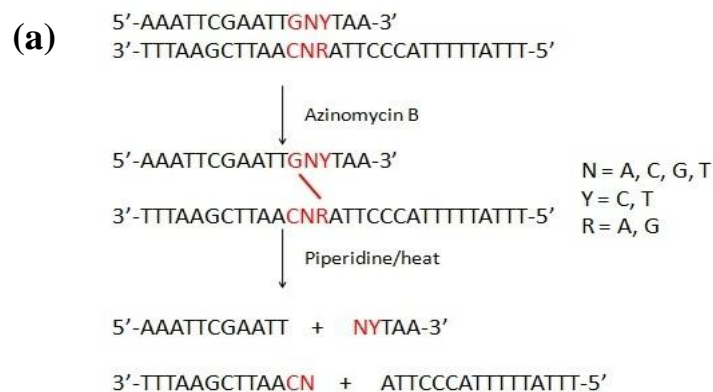
Figure 8. Azinomycins and relative compounds

Mode of Action: Interstrand Cross Link Formation

The azinomycins and their related analogs have been shown to induce apoptosis of living cells through the formation of sequence specific DNA cross-links in the major groove of double stranded DNA. The cross-link is formed by covalent interactions between DNA bases and two ring structures of azinomycins, while the naphthoate moiety non-covalently interacts with non-polar regions of DNA to enhance the cross-link formation. It was shown first in 1966 that azinomycin B inhibited DNA synthesis in the azinomycin sensitive strain *Escherichia coli* B₀, but neither RNA nor protein synthesis were inhibited.⁸⁵ DNA isolated from *E. coli* and *Bacillus subtilis* was not irreversibly denatured when treated with azinomycin B, suggesting formation of interstrand cross-links (ISCs).⁸⁶ This was further confirmed by an ethidium fluorescent based investigation which uncovered extensive alkylation and covalent links between complementary strands of a variety of short DNA sequences, especially with high G + C contents, without modification of the azinomycin structure.⁸⁷ Occurrence of ISC and

alkylation was dependent on low pH, indicating that the basic functional groups on azinomycin B were the electrophilic reactive centers. This would also provide some specificity for cancer cells, which tend to have a lower pH than healthy cells.

Azinomycin B's (**2**) sequence specificity was observed by treating ^{32}P labeled 17-mer synthetic oligonucleotides with the compound and producing cross-links with the complementary DNA strands. This was followed by piperidine cleavage of alkylation sites and analysis of the scission fragments by polyacrylamide gel electrophoresis. This established that the covalent linkage occurred between G and R (A or G) which were two base pairs away on each complementary DNA strand (Figure 9-a).⁴ The cross-linking site of guanine was confirmed as G-N7 by replacement of guanine with deazaguanine, which causes complete loss of the activity compared to slight reduction of the activity by substituting to inosine. Evidence of the sequence selectivity of azinomycin B was added by employing varied triplet (purine-pyridine-pyridine) sequences in 15-mer DNA duplex. This determined an optimal recognition sequence of 5'-d(GCC)-3' (Figure 9-b).⁵ The covalent correlation was shown by isolation of monoalkylated and cross linked products from the reaction between 4-*O*-methyl-azinomycin derivative (**6**) and self-complementary deoxyoligonucleotide d(TAGCTA)₂ (Figure 9-c).⁶ Monoalkylation was found only at the aziridine ring moiety which instantaneously led to the cross-link, indicating two step mechanism was initiated by alkylation at the aziridine C10 followed by at the epoxide C21.



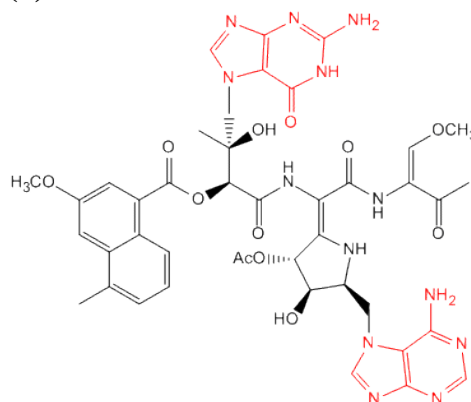
(b)

Table 1. Sequence Selectivity of Azinomycin B^a

	triplet sequence	cross-link (%)	mono (%)	starting DNA (%)
1	5'-GCC-3' 3'-CGG-5'	77	5	18
2	5'-GTC-3' 3'-CAG-5'	18	12	70
3	5'-GCT-3' 3'-CGA-5'	24	37	39
4	5'-GTT-3' 3'-CAA-5'	3	19	73
5	5'-ATC-3' 3'-TAG-5'	0	0	98
6	5'-ACC-3' 3'-TGG-5'	2	7	91

^a Reaction conditions: 10 mM Tris-HCl (pH 7.5), 5 mM NaCl, 10 μ L reaction volume, 20 h, 8 $^{\circ}$ C, 10 μ M duplex DNA, and 400 μ M azinomycin B. Numbers opposite sequences refer to yields when that strand of the duplex DNA was 5' end-labeled with ³²P.

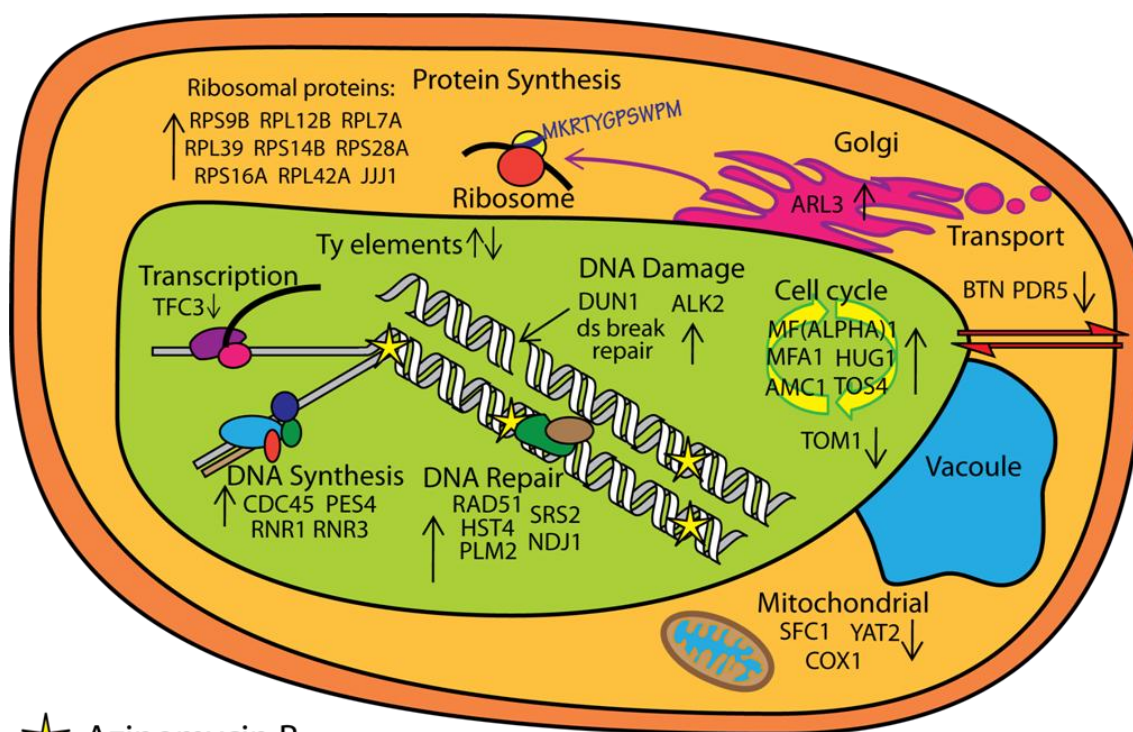
(c)



6

Figure 9. Sequence selectivity and covalent interaction⁴⁻⁷

The cellular effects of azinomycin B *in vivo* were evaluated by cellular localization pattern in the yeast *Saccharomyces cerevisiae*, where fluorescence of the naphthoate moiety was visualized as a marker localizing in the cell's nucleus (Figure 10). This resembled the behavior of the DNA intercalator, propidium iodide.⁸ Targeting of DNA was observed in genomic DNA of treated yeast as significant breakage, and transcriptional effects due to DNA damage and repair were displayed by oligonucleotide microarrays. Expression of genes involved in DNA synthesis and cell cycle were affected, suggesting that the S phase was altered. This was confirmed by a fluorescence based cell cycle assay.



★ Azinomycin B

Figure 10. *In vivo* action of azinomycin B⁸

The results of Affymetrix GeneChip profile were summarized in the cartoon.

Mode of Action: Role of Moieties

The biological activity of azinomycin analogs has been studied through a synthetic approach which led to an understanding of the key moieties present in the natural product (Figure 11). An analog consisting of naphthoate, epoxide, and aziridine moieties **7** possessed remarkable preference of cross-linking sequence in 15-mer DNA duplexes.⁸⁸ The epoxide stereochemistry was responsible for the sequence specificity, which was revealed by synthesizing partial structures of azinomycins with four epoxide stereoisomers **8-11** showing that only the natural **8** and enantiomeric epoxyamide **9** formed DNA cross-links and had cytotoxicity. Compound **9** was subsequently found to alkylate 3'G in the triplet sequence of nucleotide 5'-CGG-3' instead of 5'G in 5'-GGC-3' which is preferred by azinomycins.⁸⁹⁻⁹¹ In the naphthoate epoxyamide structures **8** and **9**, it was critical to preserve both naphthoate and epoxyamide moieties because each separate moiety **12-14** failed to react with DNA and was not biologically active.^{5, 92} This suggested that the naphthoate moiety also serves an important purpose in interaction with DNA. It added evidence to the previously shown data where an azinomycin derivative **15** showed reduced cytotoxic activity without the naphthalene ring **16**.⁵⁴ Weak but significant interaction of the naphthoate moiety with DNA was observed based on fluorescence and viscosity measurements by employing the epoxide-broken partial structures **17** and **18** in order to avoid the covalent association with DNA.⁹³ Removing C5'-methyl **19**, C3'-methoxy **20**, or both of them **21** from the naphthoate ring uncovered the significance of methyl group at C5' position although substituting methoxy functional group to ethoxy group also diminished cytotoxicity by an average of 25-fold.^{89, 94}

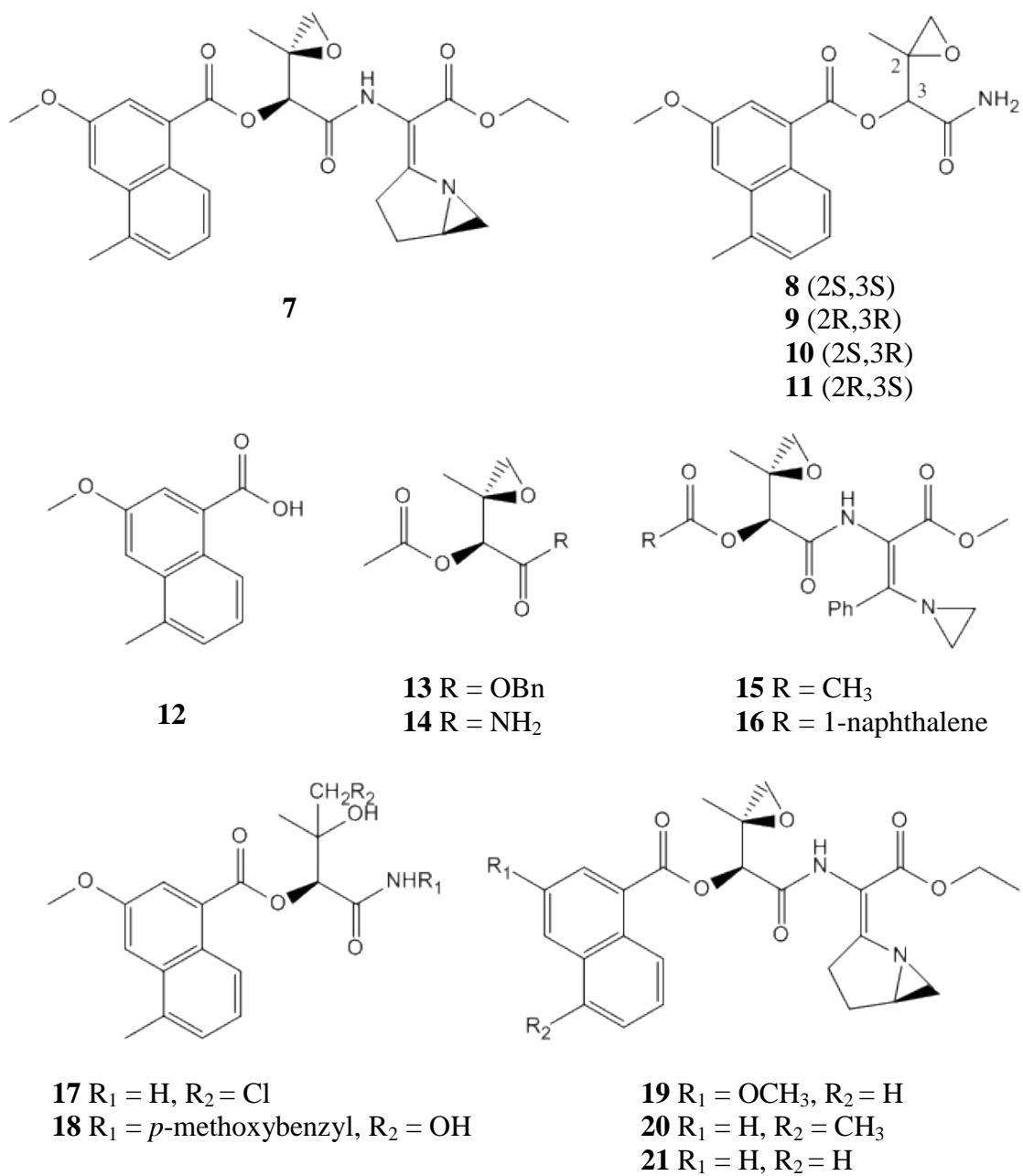


Figure 11. Azinomycin synthetic analogs for evaluation of the role of naphthoate epoxide moiety

Less attention has been paid to the primary alkylating agent, the azabicyclo[3.1.0]hexane ring, because instability of the structure makes its study challenging. Several simple azabicyclo analogs **22-31** were synthesized and tested for biological activity, but they did not show activity as potent as naphthoate epoxyamide analogs. This indicates that the substantially powerful activity of azinomycins results from the tandem function of naphthoate, epoxide, and aziridine moieties (Figure 12).⁹⁵⁻⁹⁸ The epoxyaziridine analogs are still largely appealing because of the bisalkylating role of two combinatorial cyclic structures which cannot be achieved by the single ring structure of epoxyamide analogs. Some potent derivatives were synthesized, and their bioactivity was determined. The stereoisomeric derivatives **32** and **33** had IC₅₀ of 2.3 ng/mL and 3.6 ng/mL respectively against P388 murine leukemia,⁹⁵ and a single ring opening from the azabicyclo structure **34** showed IC₅₀ of 3.2 ng/mL.⁹⁹ These two derivatives displayed higher bioactivity than the azinomycins. A few other relative compounds **35-36** were bioactive in <1.0 μM concentrations against the same cell line.^{95,}

99, 100

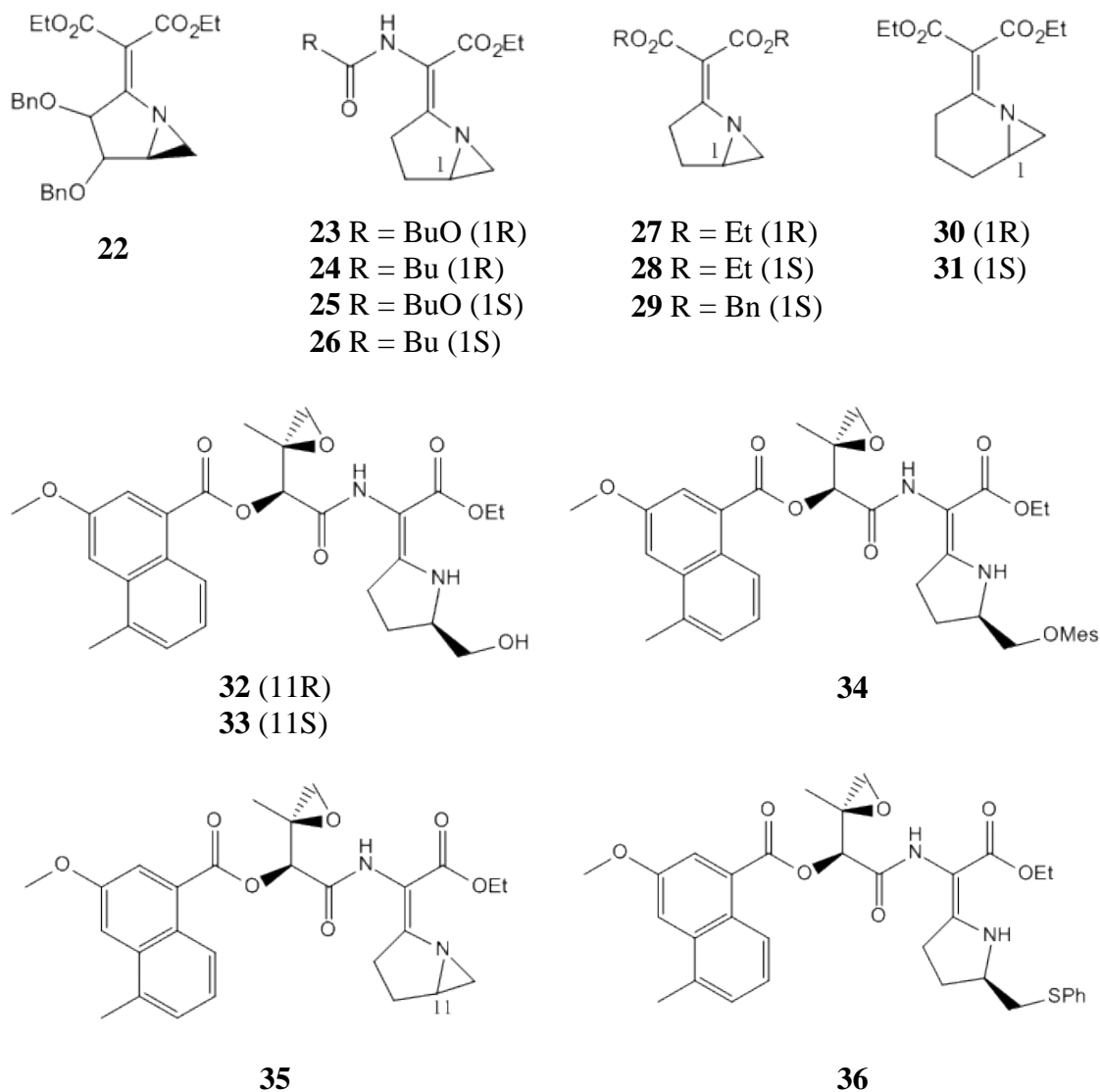


Figure 12. Azinomycin analogs for evaluation of aziridine and epoxyaziridine derivatives

The analog studies inspired some researchers to utilize linkers connecting two of the naphthoate epoxyamide **7** so the dimer, including two alkylating agents and non-polar naphthoate moieties, could form ISC in double stranded DNA like azinomycins (Figure 13). Several flexible **37-42** and non-flexible **43-45** linkers were applied and

assessed for ISC formation and cytotoxic potencies.^{101, 102} A compound containing the flexible linker **42** had the best ISC activity among them showing 70 % of cross-link formation within 15-mer oligonucleotide. Compound with linker **38** showed a modest activity (40%) while others had much lower bioactivity than these two. Assays targeting 60 cancer cell lines found that linker **38** possessed significant cytotoxicity with an LC₅₀ (lethal concentration of 50 % population) of 3.2 μM, which was 11-fold active comparing to the monomer compound **7**. Linkers **42** and **39** also demonstrated cytotoxicity which was more than 2-fold higher than compound **7**. Compounds synthesized with non-flexible linkers, however, did not have reasonable potency of ISC and cytotoxicity. This data suggests that linking an analog with flexible arms of a certain length may have promise in terms of developing high bioactivities with easily synthesizable units.

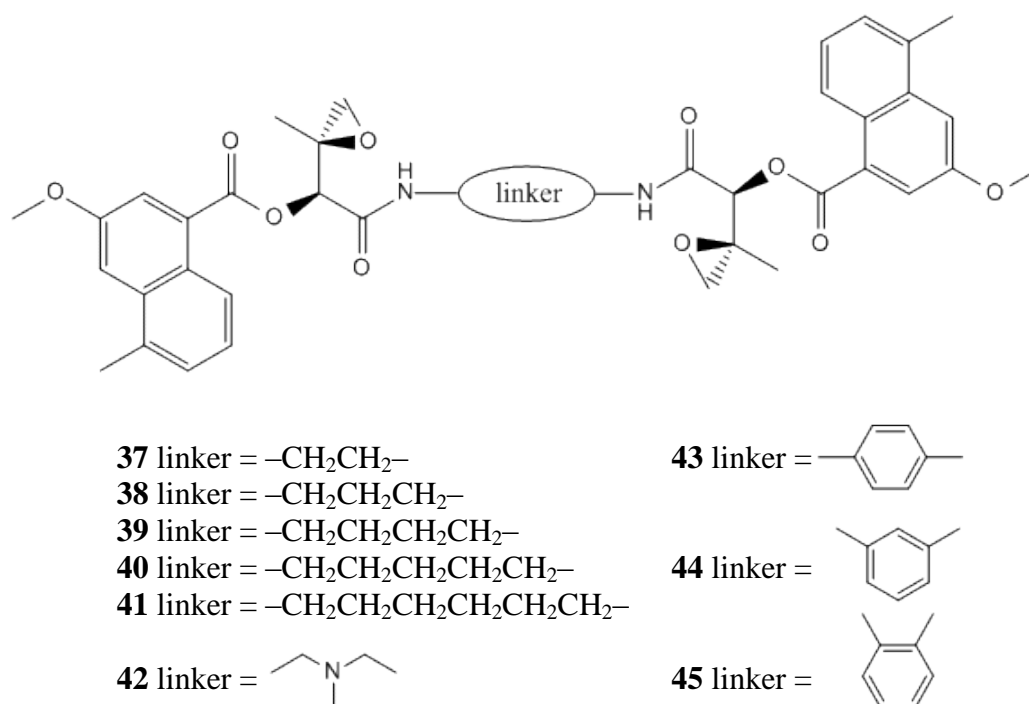


Figure 13. Dimeric naphthoate epoxyamides linked by flexible or non-flexible arms

Biosynthesis: Hybrid Functionality

Azinomycin biosynthesis is a fascinating subject to study because its hybrid biosynthetic origin, utilizing both PKS and NRPS machinery with an alkaloid derivative has been suggested by the structures. The naphthoate and azabicyclo ring moieties would be derived from a polyketide and an alkaloid, respectively. The skeletal backbone of the molecule consisting of ester and amide functional groups could be produced by modular NRPSs which would condense the naphthoate moiety and amino acid like substrates. The alkaloid-derived azabicyclo[3.1.0]hexane ring is especially captivating because of its rarity in natural products. Only a handful of aziridine containing molecules are known within more than 100,000 of natural products isolated to date (Figure 14). The biosynthetic clusters of some aziridine containing natural products have been proposed, but none of the biosynthetic routes have been characterized yet. It has been predicted that the structure arises from β -carbon activations, such as halogenation, adenylation, sulfonylation, or phosphorylation, followed by condensation of nucleophilic attack of nitrogen to the electrophilic carbon.

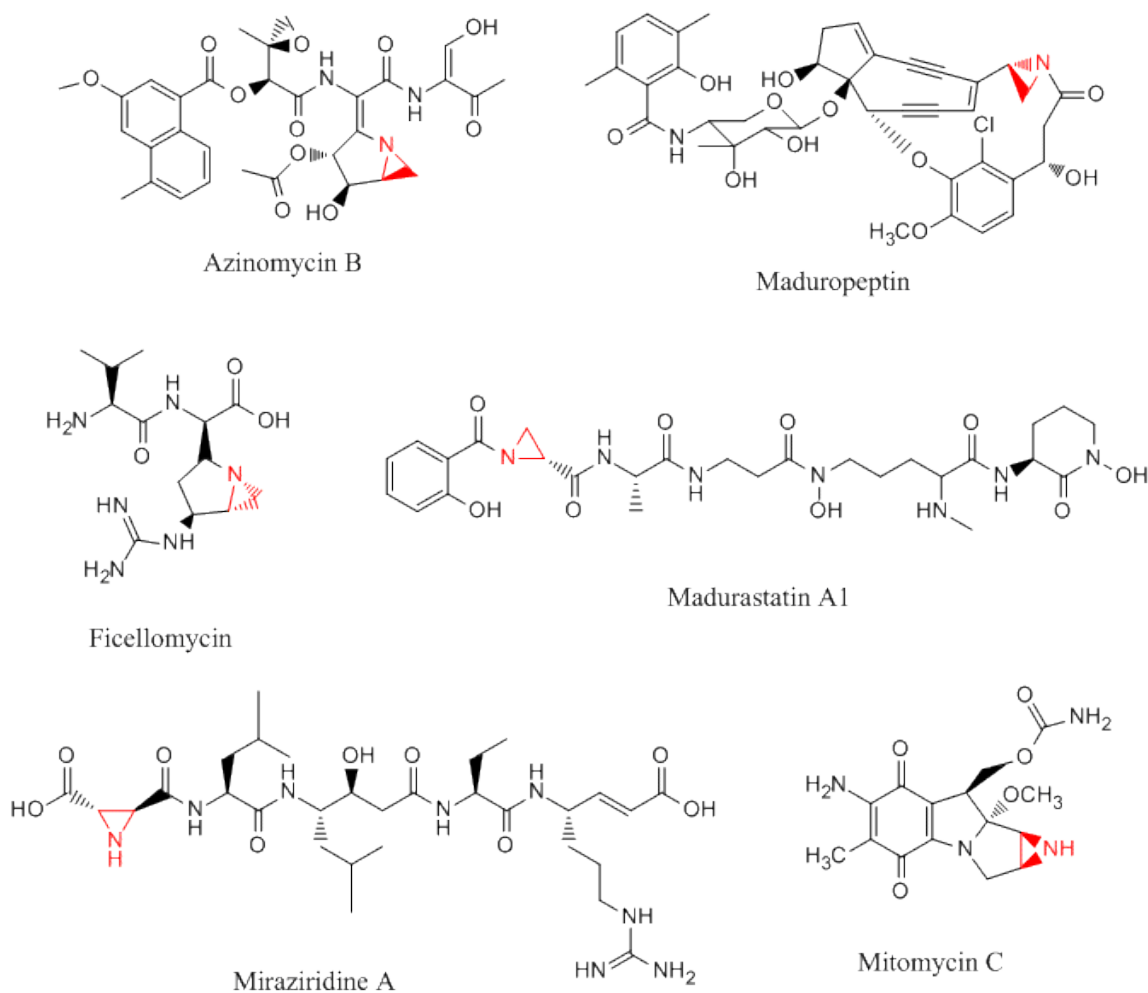


Figure 14. Aziridine containing natural products

The PKS origin of the naphthoate moiety was firstly validated through feeding isotopic labeled acetate to *S. sahachiroi* culture followed by ^{13}C NMR resonance spectroscopy to observe incorporation of the labeled substrate into the azinomycins' structure (Figure 15).¹⁰³ The result showed expected sequential pattern of labeled carbons in the naphthoate moiety. This was consistent with PKS mediated biosynthesis derived from acetyl- and malonyl-CoA units. The acetate carbons also incorporated with C1-C4 of the keto-enol unit and pairs of C6-C7 and C12-C13 in the azabicyclic moiety. L-Threonine, which is derived from oxaloacetate, was proposed as the substrate of C1-

C4 unit, and the azabicyclic moiety was suggested to be produced from α -ketoglutarate derived amino acids, such as glutamate, glutamine, arginine, and proline. The hypothesis of the naphthoate origin was supported by another isotopic labeling study which deuterated 5-methyl hydrogens of naphthoic acid analogs **46-48**, all of whose deuterium were detected in ^2H NMR of resulting azinomycins. This indicated consistent outcome that the naphthoic acid is synthesized before introducing into the rest of the molecule (Figure 15).¹⁰⁴

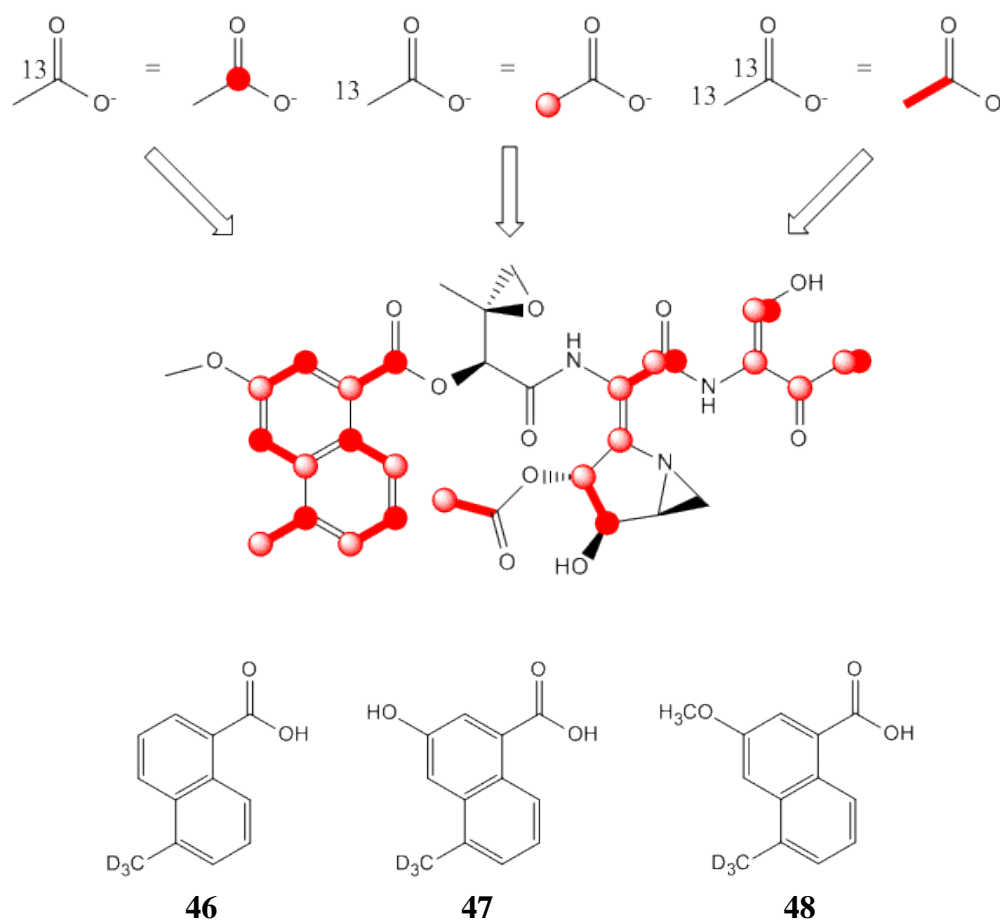


Figure 15. Isotopic labeling studies for the origin of the naphthoate moiety ⁷

Feeding of isotopic labeled amino acids and their derivatives as NRPS substrates showed the skeletal construction of azinomycins (Figure 16). As predicted by the acetate feeding observations, L-threonine was confirmed as the substrate of C1-C4 unit of azinomycin B by supplementation of ^{13}C labeled L-threonine in the culture.¹⁰⁵ It was further demonstrated that other possible intermediates (β -ketoamino acid, β -hydroxyamino aldehyde, and β -ketoamino aldehyde) acquired from L-threonine did not incorporate with the enol moiety. This proposed that the NRPS accepted L-threonine without any structural modifications prior to condensation with other units. Azinomycin A lacks the enol functional group at C1-C3 position, which suggested a different origin from the unit of azinomycin B. This was validated by feeding study of ^{13}C labeled tentative substrates, such as L-threonine, L-glycine, and aminoacetone.¹⁰⁶ The result displayed significant incorporation of aminoacetone while slight incorporation of L-threonine and glycine was also observed. This suggested that aminoacetone was the direct substrate of the NRPS although it was derived from L-threonine and glycine by separate enzymes. These possible homologs were found in *S. sahachiroi* genome by a draft genome sequence. The greater modification of amino acids occurred during the epoxide moiety formation, where the α -methyl group of L-valine was oxidized into hydroxyl methyl followed by alkene formation in tandem with the replacement of the amino acid amine with a carbonyl group. This would enable the substrate to condense with PKS derived naphthoic acid.¹⁰⁷ The most complex unit of azinomycins, azabicyclo, has been under investigation; however, the current available data strongly suggests the glutamate origin that was extensively modified prior to establishment of the skeletal substrate.

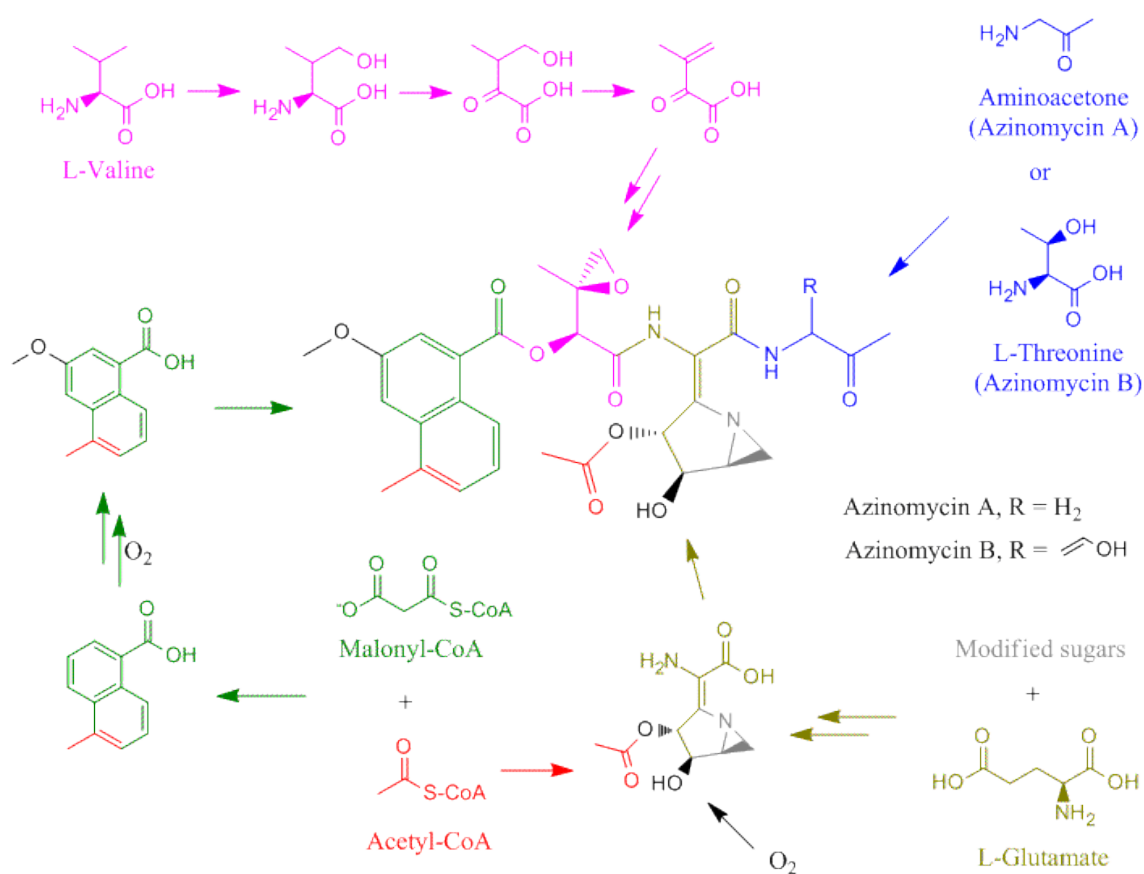


Figure 16. Biosynthetic origins of azinomycins

Biosynthesis: Genetics

Enzymatic studies were extensively enhanced by uncovering the biosynthetic gene cluster of azinomycin B. The informative data was discussed based on homologous searches through publicly available database for each gene to theorize functions of individual enzymes, and involvement of a type I iterative PKS (AziB) in production of the naphthoate moiety was confirmed (Figure 17).¹⁰⁸ The key genes include five NRPS, one PKS, four TE, and many possible alkaloid deriving genes out of more than forty total genes. This added strong evidence to the hypothesis of the molecular construction, where azinomycins are produced by orchestrated functionality of PKS, NRPSs, and alkaloid deriving enzymes. Although most genes have yet to be characterized, there have been a few genes identified as essential for the production of azinomycins. Azinomycins

were not synthesized when either the NRPS gene *aziA2* or an unknown gene *aziU3* were disrupted.^{109, 110}

The resistance protein against azinomycins, AziR, was identified and functionally characterized.¹¹¹ The protein is homologous to aminoglycoside 3'-phosphotransferase (APH-3'), which is a member of the protein kinase superfamily that inactivates aminoglycoside antibiotics. APH-3' catalyzes phosphorylation on a hydroxyl group of the target molecule by γ -phosphate transferred from ATP or CTP. AziR showed a protective effect against DNA damage in *S. lividans* and *E. coli* caused by azinomycin B when the protein was heterologously expressed in these organisms. AziR was not active against other aminoglycoside antibiotics probably because it lacks key residues in the active site seen in other APH-3' members, which is proposed to form a salt bridge when binding and coordinating with ATP. Understanding of the function and mechanism of resistance proteins including AziR could aid the engineered biosynthesis of functionally useful anzinomycin analogs in the future.

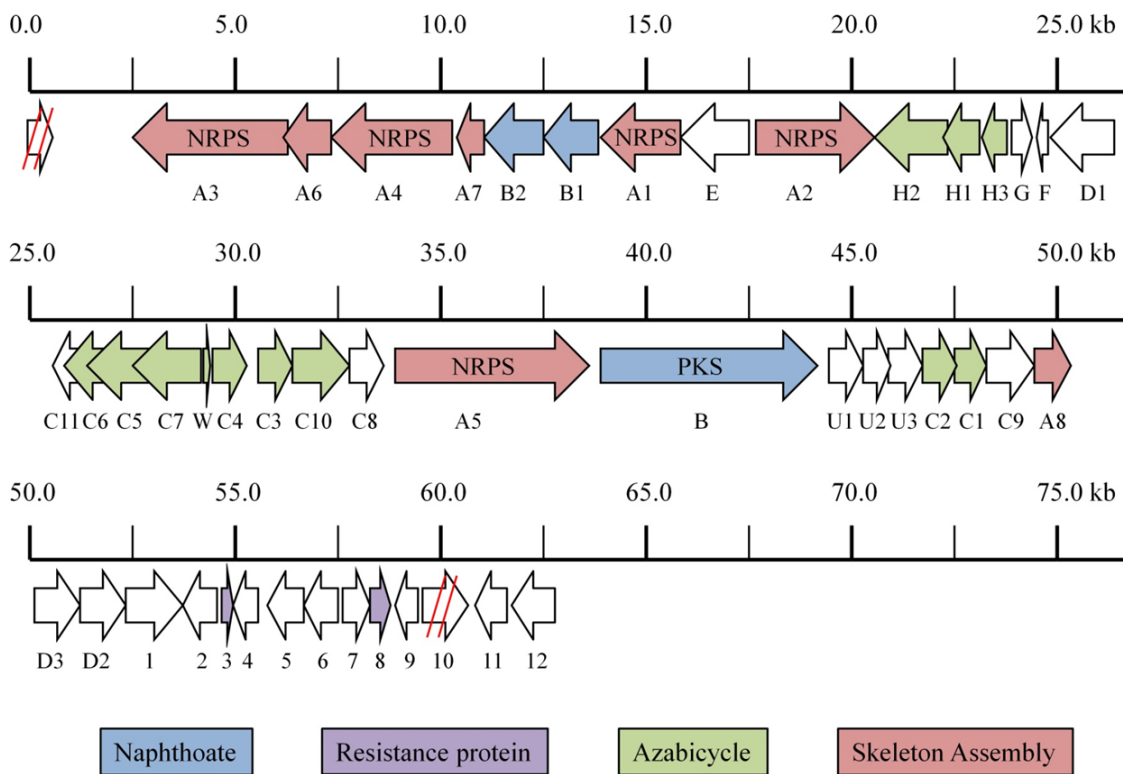


Figure 17. Biosynthetic gene cluster of azinomycins

STATEMENT OF PURPOSE

The introductory materials of this chapter highlight the importance of natural products and their biosynthesis. High structural diversity of natural products provides more options to development of drug therapies. All possible sources on earth have not been completely explored. The marine organisms in particular are one of the largest unexplored sources. Looking for bioactive natural products in marine sources may supply new therapeutic agents or new classes of natural product, which may become a basis of many novel drugs. The diversity can be expanded by engineered biosynthesis of unnatural natural products. Modular proteins, such as PKSs and NRPSs, have great potential for modification, which has already provided many bioactive molecules. For more efficient and highly controlled production of these compounds, understanding protein function is crucial because seemingly simple catalytic domains are still found to possess novel functions. Enzymatic characterization of azinomycin producing proteins and evaluation of new natural product from marine source will be discussed in the following chapters.

CHAPTER II

AZINOMYCIN BIOSYNTHESIS: FORMATION OF THE NAPHTHOATE MOIETY BY PKS-TE INTERACTION

INTRODUCTION

Azinomycins are antitumor agents produced by a soil bacterium, *Streptomyces sahachiroi* as detailed in Chapter I. The structures suggest that these natural products are produced by the combination of polyketide synthases (PKSs) and nonribosomal peptide synthetases (NRPSs).⁸⁴ The naphthoate moiety is produced by a PKS, while the amide bonds and the ester with the naphthoate moiety are constructed by NRPSs. This hypothesis is supported by feeding studies identifying the precursors of each moiety and bioinformatic studies finding the gene cluster of azinomycins (Figure 16 and Figure 17).¹⁰³⁻¹⁰⁸ The gene cluster contains more than forty genes including one PKS, five NRPS, and four thioesterase (TE) genes. TE domains are known to encode proteins that catalyze hydrolysis of thioesters or intermolecular cyclization to release the products from PKS or NRPS proteins. TEs consist of families with broad functionalities, including coenzymatic activity with PKSs or NRPSs. For example, several TEs are known to function by holding an intermediate of a PKS or an NRPS while other intermediates are produced. TEs can then combine these intermediates together to build the final product.^{72, 112}

The naphthoate moiety has an important role in the interaction of azinomycins within the major groove of double stranded DNA. Its hydrophobic property helps azinomycins interact with the non-polar region of DNAs, which enhances the antitumor activity of the compound.⁹⁴ Antitumor activity was also observed in a partial compound which consists of only the naphthoate and epoxide moieties **8**, although the naphthoic acid **12** itself does not induce apoptosis of cancer cells (Figure 11).^{5, 89-92} Thus, it could be applied to cancer therapy as *in situ* biosynthesis of the active compound. A patient is

given the non-toxic fragment of the compound **12** and a vector with a cancer specific promoter which expresses proteins leading the fragment to a bioactive molecule to treat the cancer cells (Figure 18). This chapter will provide insight into the functionality of the PKS called AziB and its coenzyme TE called AziG.

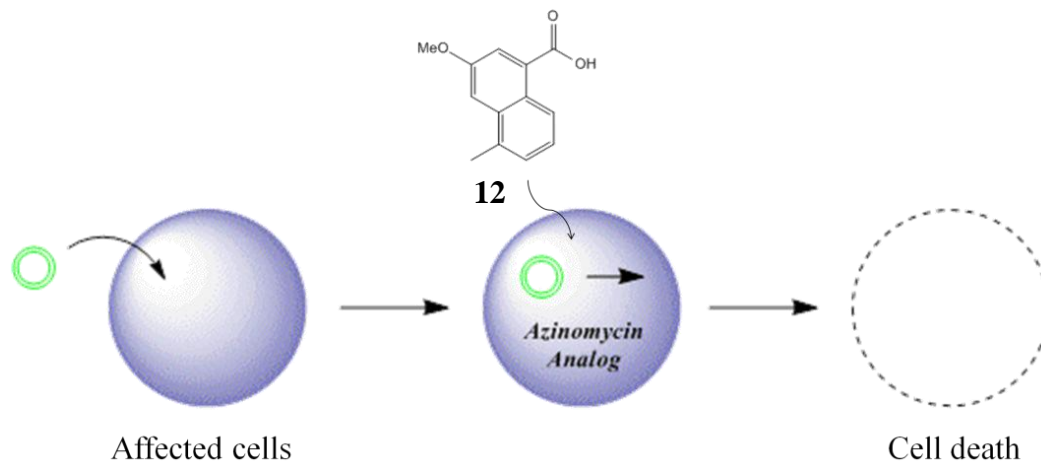


Figure 18. *In situ* biosynthesis of azinomycin analog in target cells

PRELIMINARY RESEARCH

The major part of the naphthoate fragment, 3-methoxy-5-methyl-1-naphthoic acid, has been hypothesized to be produced by a PKS. This was supported by feeding and bioinformatic studies. The feeding study showed that the moiety is produced from acetyl carbons of acetyl-CoA and malonyl-CoA which are typical substrates of PKSs.^{103, 104} The bioinformatic study showed there is only one PKS gene in the gene cluster which contains the following domains: ketosynthase (KS), acyl transferase (AT), dehydratase (DH), ketoreductase (KR), and acyl carrier protein (ACP) (Appendix Figure 56).¹⁰⁸ The protein also has homologous proteins which produce aromatic natural products (Appendix Figure 57).¹¹³⁻¹¹⁵ The involvement of the PKS protein, AziB, was further supported by the enhanced production of the naphthoate moiety in the presence of

additional AziB which was overexpressed in *Escherichia coli* (Figure 19). The cell free extract of *S. sahachiroi* contains all the soluble molecules of the cells including proteins and their precursors. Since malonyl-CoA is used only for the production of azinomycin's naphthoate moiety, [¹⁴C] labeled malonyl-CoA can be used to measure a change in the amount of naphthoate moiety produced.

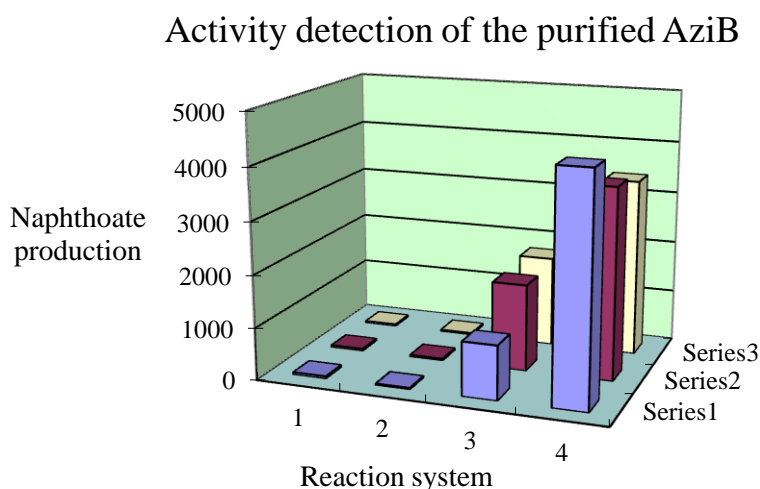


Figure 19. Enhanced naphthoate moiety production with over expressed AziB (Dr. Huitu Zhang)

The production of the naphthoate moiety was measured as the radiation from [¹⁴C] malonyl-CoA which is incorporated in azinomycin B. 1: Boiled cell free extract + [¹⁴C] malonyl-CoA, 2: Boiled cell free extract + AziB + [¹⁴C] malonyl-CoA, 3: Cell free extract + [¹⁴C] malonyl-CoA, 4: Cell free extract + AziB + [¹⁴C] malonyl-CoA. The experiment was triplicated (series 1-3).

AziB used in the following experiments was heterologously expressed in *E. coli*, and it needed to be posttranslationally modified to produce an active holo-enzyme. All ACP domains of PKSs are expressed as a non-active apo-enzyme which is subsequently modified with a flexible phosphopantetheinyl arm from coenzyme A on its serine residue. This is catalyzed by a phosphopantetheinyl transferase (PPTases).⁶⁵ The

posttranslational modification of AziB was catalyzed by a well established PPTase, Svp, found in *Bacillus subtilis* and two PPTases found in *S. sahachiroi* (Figure 20).¹¹⁶ One of the PPTases is associated with fatty acid synthase (FAS) and the other is not. AziB was successfully modified by all of the PPTases, but Svp has been used in the following experiments to activate AziB because it was able to be overexpressed in a large amount.

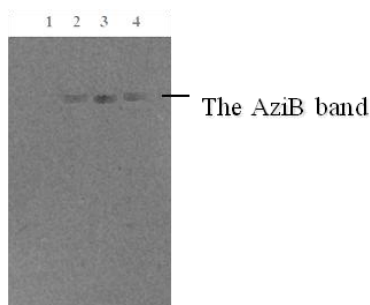


Figure 20. Phosphopantetheinylation of AziB with ³H-CoA (Dr. Huitu Zhang)

The posttranslationally modified AziB with radio labeled CoA was assessed by SDS-PAGE autoradiography. 1: AziB + No PPTase (negative control), 2: AziB + Svp, 3: AziB + FA associated PPTase, 4: AziB+ FA non-associated PPTase.

The product of AziB was assessed by TLC autoradiography using radiolabeled acetyl-CoA and malonyl-CoA. Because the product had been predicted to be 5-methyl-1-naphthoic acid **49**, 1-naphthoic acid was used as a control hypothesizing it should have a similar R_f value to the product due to the related structures. The R_f value of the major product of AziB, however, was significantly different from the one of 1-naphthoic acid, which suggested that the product was in fact not a naphthoic acid (Figure 21-a). The product of AziB was subsequently isolated by a preparative TLC, and its structure was identified by NMRs and MS analysis as 2-methylbenzoic acid **50** (Figure 21-b).

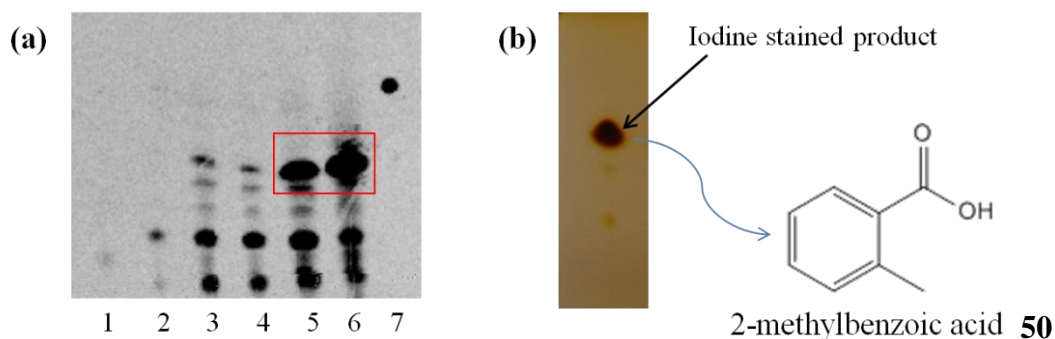


Figure 21. *In vitro* product of AziB (Dr. Huitu Zhang and Dr. Dinesh Simkhada)

(a): TLC autoradiography of AziB product with radio labeled substrates. 1: ^{14}C acetyl-CoA, 2: ^{14}C malonyl-CoA, 3 and 4: Boiled AziB + labeled substrates, 5 and 6: AziB + labeled substrates, 7: 1-naphthoic acid, **(b):** Purification of AziB product by preparative TLC with iodine stain. The major product was identified as 2-methylbenzoic acid.

This suggested the involvement of another enzyme in the production of 5-methyl-1-naphthoic acid since AziB alone produces a different compound, 2-methylbenzoic acid. It was hypothesized that the curator was a TE because there are several TE domains known to function as coenzymes.^{72, 73, 79} It was supported by a LC-MS study which showed that AziB alone produces a compound with the mass of 2-methylbenzoic acid (Figure 22-a), but a compound with the mass of 5-methyl-1-naphthoic acid was produced only when AziG, one of the four TEs in the gene cluster, was added in the reaction (Figure 22-b).

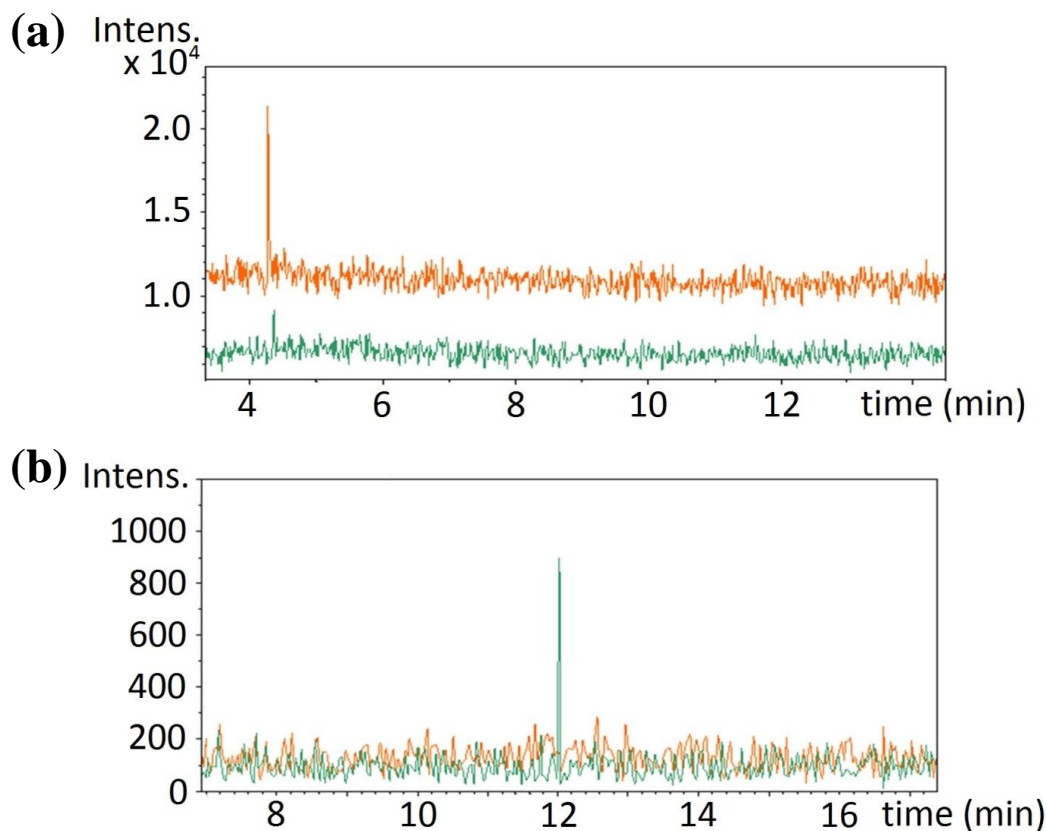


Figure 22. Induced naphthoic acid synthesis by AziB and AziG (Dr. Dinesh Simkhada)

Reaction with AziB alone (orange line) and AziB+AziG (green line). (a): LC profile at the mass 137 m/z, (b): LC profile at the mass 187 m/z.

RESULTS AND DISCUSSION

Production of 5-Methyl-1-Naphthoic Acid by AziB and AziG

The production of the putative 5-methyl-1-naphthoic acid peak by AziB and AziG is described in the introduction section above. It was subsequently shown by Dr. Dinesh Simkhada that two other TEs in the azinomycin gene cluster, AziA7 and AziA8, did not enhance the production of the naphthoic acid (Figure 23-b and Figure 23-c). AziA6 was also found to have no involvement in the naphthoic acid production (Figure

23-a), which proved that the 187 m/z peak in LC-MS chromatogram was obtained by the use of AziG with AziB rather than any of other TEs with AziB. All proteins used in the experiments were overexpressed in *E. coli* using Novagen pET expression vectors. These proteins are small, soluble, and relatively stable, thus the pure proteins were easily obtained by regular preparation procedures, with the exception of AziA6 which needed to be purified by a size exclusion chromatography in addition to the Histidine-tagged (His-tag) Ni²⁺ affinity chromatography (Appendix Figure 58).

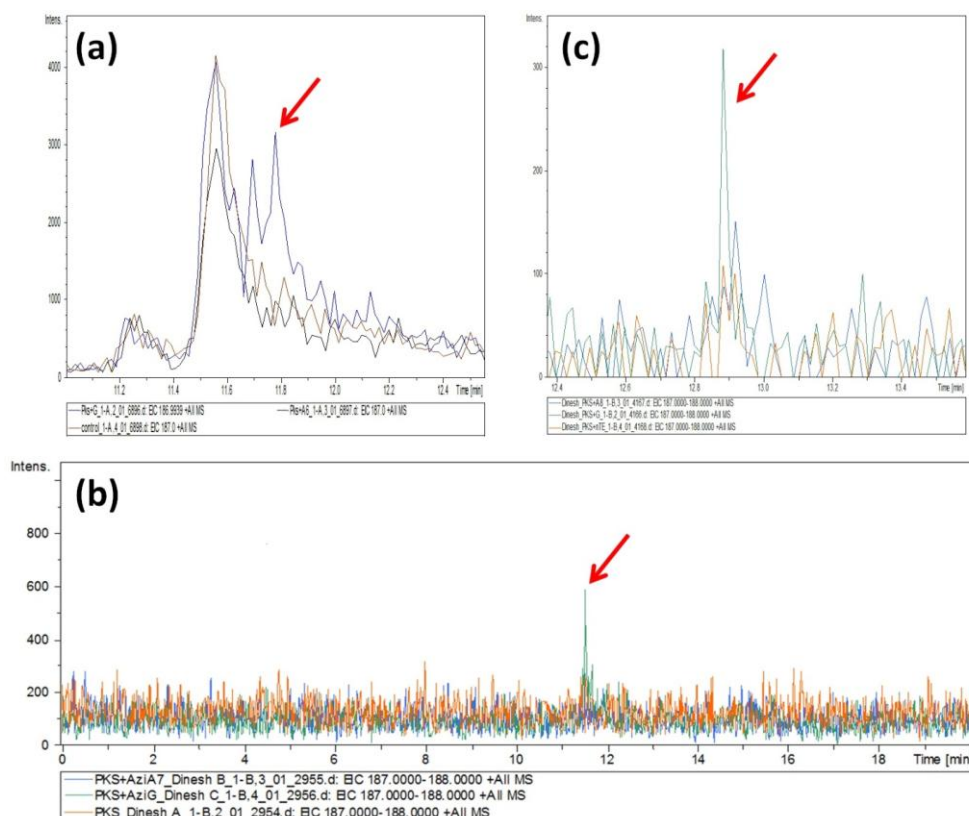


Figure 23. LC-MS traces that demonstrate lack of formation of 5-methyl-1-naphthoic acid by AziA6, AziA7, and AziA8 (Dr. Dinesh Simkhada for AziA7 and AziA8)

(a): AziA6: blue line: AziB+AziG (control), black line: AziB+AziA6, orange line: AziB only (control). (b): AziA7: green line: AziB+AziG (control), blue line: AziB+AziA7, orange line: AziB only (control). (c): AziA8: green line: AziB+AziG (control), blue line: AziB+AziA8, orange line: AziB only (control). The red arrow shows the production of 5-methyl-1-naphthoic acid.

Comparison to Synthetic Standard of 5-Methyl-1-Naphthoic Acid

The synthetic standard of 5-methyl-1-naphthoic acid was synthesized by Dr. Dmytro Fedoseyenko, and the structure was further confirmed by ^1H NMR, ^{13}C NMR, COSY, HSQC, and HMBC which showed the desired peaks and correlations (Appendix Figure 63-Appendix Figure 75 and Appendix Table 5).

The synthetic standard was analyzed by LC-MS with and without the product of the AziB-AziG reaction before being absolutely purified to assess whether there was a peak matching the AziB-AziG product. When it was injected alone, there were some peaks in the LC profile around the mass of 187 m/z, but none of them matched the peak of AziB-AziG product. The apparent mass on the MS profile was slightly different from the AziB-AziG product (187.13 m/z for AziB-AziG product and 187.08 m/z for the standard). When the standard was co-injected with the AziB-AziG product, however, all of the peaks in the LC profile for the standard disappeared while one new peak, which is identical to the AziB-AziG product, appeared. In addition, the mass of the peak was the same as the one seen in the AziB-AziG MS profile (Appendix Figure 64). It is hypothesized that AziB and AziG produce 5-methyl-1-naphthoic acid, but during either the reaction or its workup there was a slight modification to the product, which made a change in the LC-MS profile.

The synthetic compound was further purified and treated with the AziB-AziG reaction buffer and either acid or base, and it was extracted by the same way as in the AziB-AziG reaction before being analyzed in LC-MS (Figure 24). The buffer treatment shifts the retention time moderately, and the base extinguishes the second peak which was shorter than the first peak and is possibly identical to the synthetic standard without treatment. The mass of the sample treated by buffer and base was identical to AziB-AziG product. This observation suggests that the basic and acidic forms of 5-methyl-1-naphthoic acid show separate peaks in the chromatogram and slightly different mass in the mass spectrometry.

Collectively, it was concluded that AziG is responsible for the production of 5-methyl-1-naphthoic acid in tandem with AziB, which alone produces 2-methylbenzoic acid.

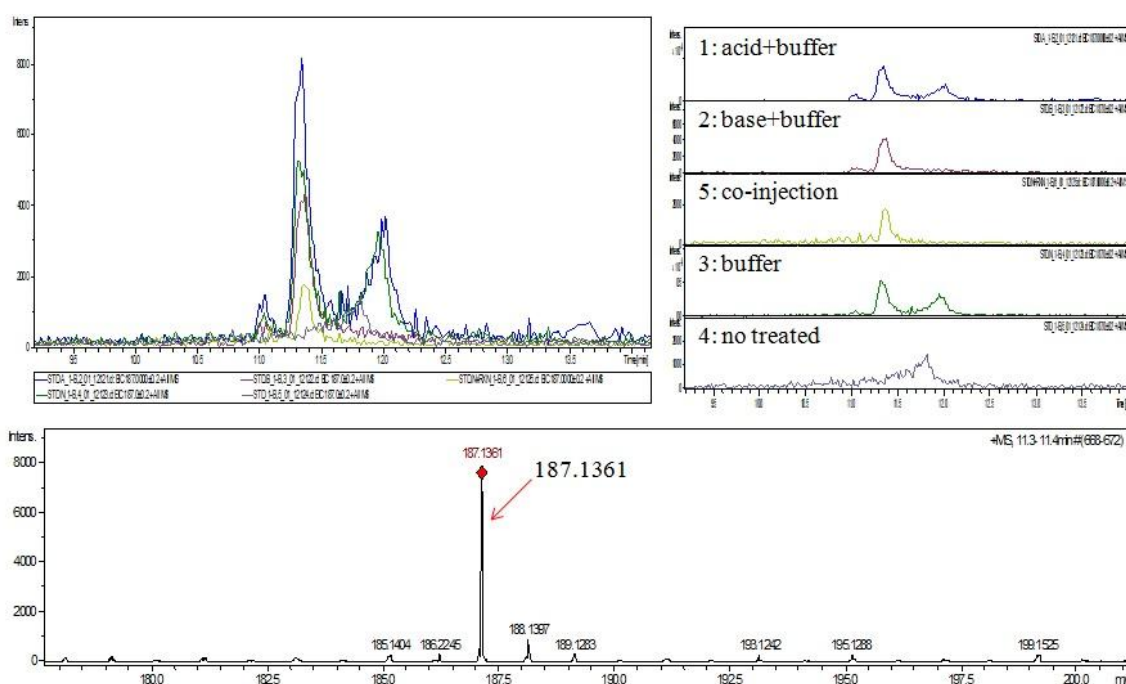


Figure 24. LC-MS analysis of AziB-AziG product with the buffer treated standard
 1: Acid + buffer treated, 2: base + buffer treated, 3: buffer treated, 4: no treatment, 5: co-injection with the AziB-AziG product and base + buffer treated sample. The mass of the co-injection sample matches to the mass of the AziB-AziG product.

AziB-AziG *In Vitro* Binding Assay

AziB and AziG have been shown to work in tandem to produce 5-methyl-1-naphthoic acid. It was evaluated if these two proteins stably bind each other *in vitro*. For the assay His-tag Ni²⁺ affinity column chromatography was used to hold the purified AziG while it was washed with *S. sahachiroi* cell free extract containing all the components of the cell residue including AziB. It was shown that there was no AziB

found in either the coomassie brilliant blue or the silver stained SDS-PAGE, which suggested that the affinity of AziB and AziG is not reasonably high *in vitro* (Figure 25).

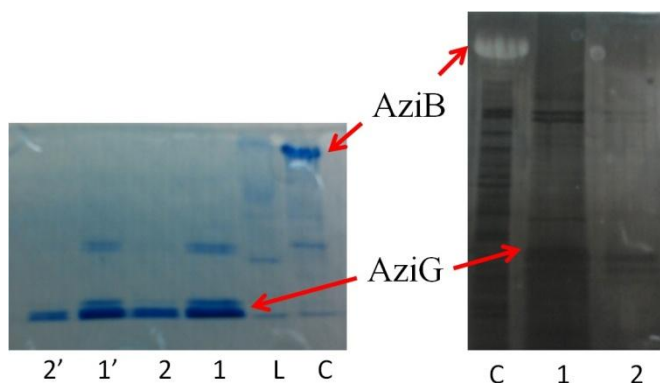


Figure 25. AziB-AziG *in vitro* binding assay

Binding affinity of AziB and AziG was assessed in His-tag Ni²⁺ affinity column followed by SDS-PAGE detection with staining by coomassie brilliant blue or silver. C: Control (red arrow indicates AziB), 1: concentrated samples, 2: non-concentrated samples.

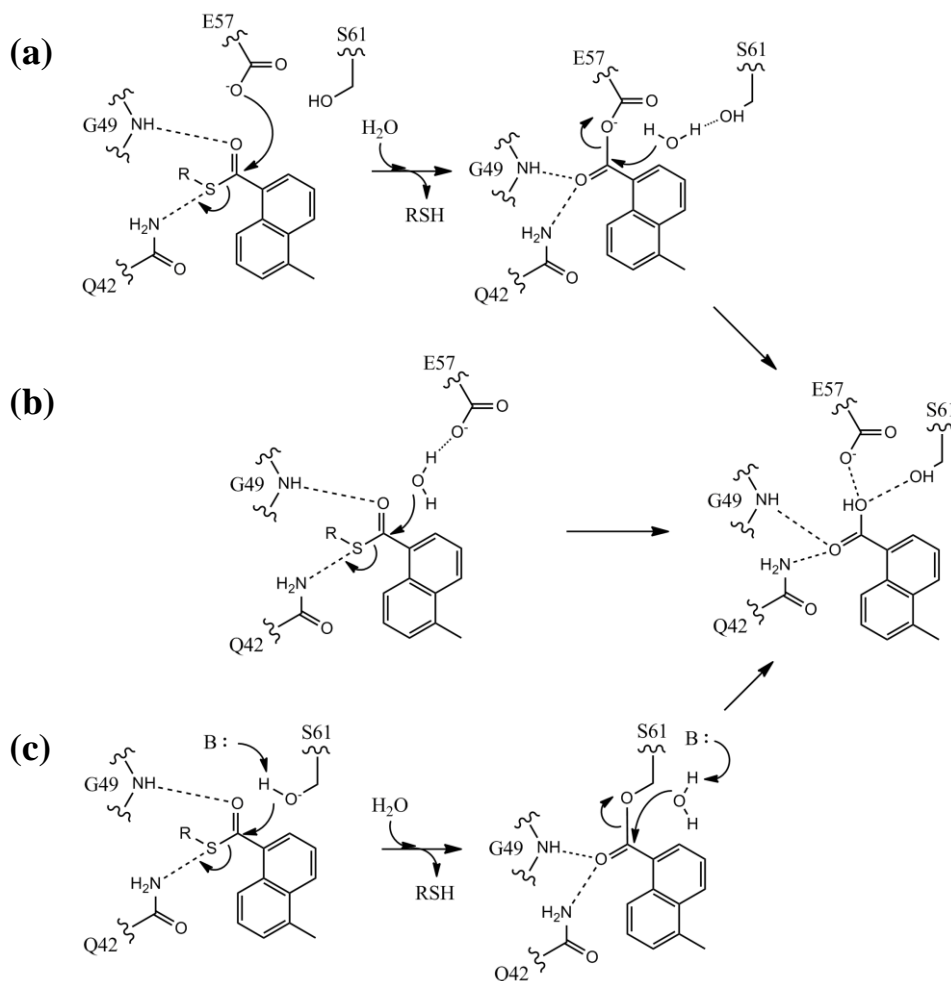
Bioinformatic Study and Crystal Structure of AziG

AziG has been hypothesized by a bioinformatic study including a BLAST search as a member of the family of Hotdog fold thioesterase (Appendix Figure 59 and Appendix Table 4). The Hotdog fold TE is characterized by the anti-parallel β -sheet as the bun wrapping around the long α -helical sausage.¹¹⁷ It forms a functional dimer, and two independent active sites are located between these two. One of the homologous enzymes of AziG is PaaI found in the phenylacetate degradation pathway in bacteria including *Escherichia coli*.¹¹⁸ It is proposed that PaaI hydrolyzes early dead-end products of the pathway, such as 2- or 3-hydroxyphenylacetyl-CoA, to salvage CoA.¹¹⁹ The gel filtration chromatography and crystallographic analysis showed that PaaI forms a tetramer in which two dimers place their β -sheet buns face to face with each other. Comparing to these previously studied thioesterases with a BLAST search, some highly conserved regions in the active site had been identified, which were G49, E57, S58, S61,

and A62 (Figure 26 and Appendix Figure 60). The E57 residue was predicted to be the most critical because this glutamic acid has been shown to covalently bind the carbonyl carbon in order to hydrolyze the thioester in the homologous enzymes. A serine residue, corresponding to S61 in AziG, then activates a water molecule to release the product as a carboxylic acid (Scheme 4-a).^{120, 121} An alternative mechanism includes hydrolytic cleavage of enzyme-anhydride intermediate, in which nucleophilic residues including aspartic acid, corresponding to E57 in AziG, activate a water molecule to hydrolyze the thioester (Scheme 4-b).¹²² This mechanism is found in E73D mutant of 4-HB-CoA whose native form catalyzes hydrolysis by the covalent mechanism.¹²⁰ These previous studies suggest that the catalytic mechanism of AziG homologous enzymes depends on the length of side chain of carboxylate amino acids in the active site. If the side chain is long enough (E), the nucleophilic carboxylate can reach the electrophilic carboxyl carbon, but if it is not (D), it has to employ a water molecule to reach the reaction site. S61 of AziG is not highly conserved in hotdog TEs because it is not necessary when they catalyze one-step base catalyzed hydrolysis. The serine is only needed when they do two-step reaction where a water molecule is employed for the hydrolysis of enzyme-anhydride intermediate. AziG is more closely related to the homologous enzymes which have the second mechanism. The other serine and histidine residues in the active site of some of the homologous Hotdog fold TEs have been shown to be important for their optimal activity.^{112, 118, 121, 122} Although there is no direct interaction between the substrate and serine or histidine, mutation on these residues significantly affects the kinetics.

The other possible mechanism is serine hydrolase, which is seen almost all characterized TEs for FASs and PKSs (Scheme 4-c).¹²³⁻¹²⁶ These TEs contain characteristic catalytic triad residues within the active site consisting of amino acids Ser-His-Asp.¹²⁶ It has been proposed that histidine which is stabilized by aspartic acid deprotonates serine. The activated serine simultaneously attacks the carbonyl carbon of the substrate. The histidine residue again activates a water molecule or a side chain of

the substrate to catalyze hydrolysis or cyclization respectively. The amino acid sequence analysis, however, could not identify the catalytic triad of Ser-His-Asp in AziG.



Scheme 4. Predicted mechanisms of AziG catalyzed hydrolysis

(a): Base catalyzed mechanism, (b): hydrolytic cleavage of enzyme-anhydride intermediate. (c): Serine hydrolase mechanism

AziG was crystallized by Dr. Megan D. Sikowitz (Cornell University) to observe the detailed peptide structure, particularly in the active site. It was also crystallized with the substrate (Figure 26 and Appendix Figure 61). It was shown that AziG forms a

tetramer as expected considering homologous enzymes. The tetramer formation was also confirmed by gel filtration analysis where native AziG gave calculated mass of 62.2 kDa which was significantly close to the theoretical mass of 4 × expressed AziG, 63.4 kDa (Appendix Figure 78 and Appendix Figure 79). As predicted by the homologous enzymes, it forms functional dimer containing two active sites with approximately 7 Å in diameter and 20 Å deep between each monomer unit. Two dimers form a tetramer by interaction between each β-sheet bun. The crystal structures validated the bioinformatic study for the key residues by displaying the amino acids in the active site and their interaction with the substrate. This also added H44 and H48 as study targets. The probable binding location of the PPT arm was predicted by alignment with *Anthrobacter* thioesterase with 4-hydroxybenzoyl-CoA (PDB 1Q4U).¹²⁰ From these analyses, it was determined that amino acid residues, H44, H48, E57, S58, and S61, were the targets for mutation studies. Since all of them can work as a nucleophile, they were mutated into alanine to inhibit the nucleophilic function.

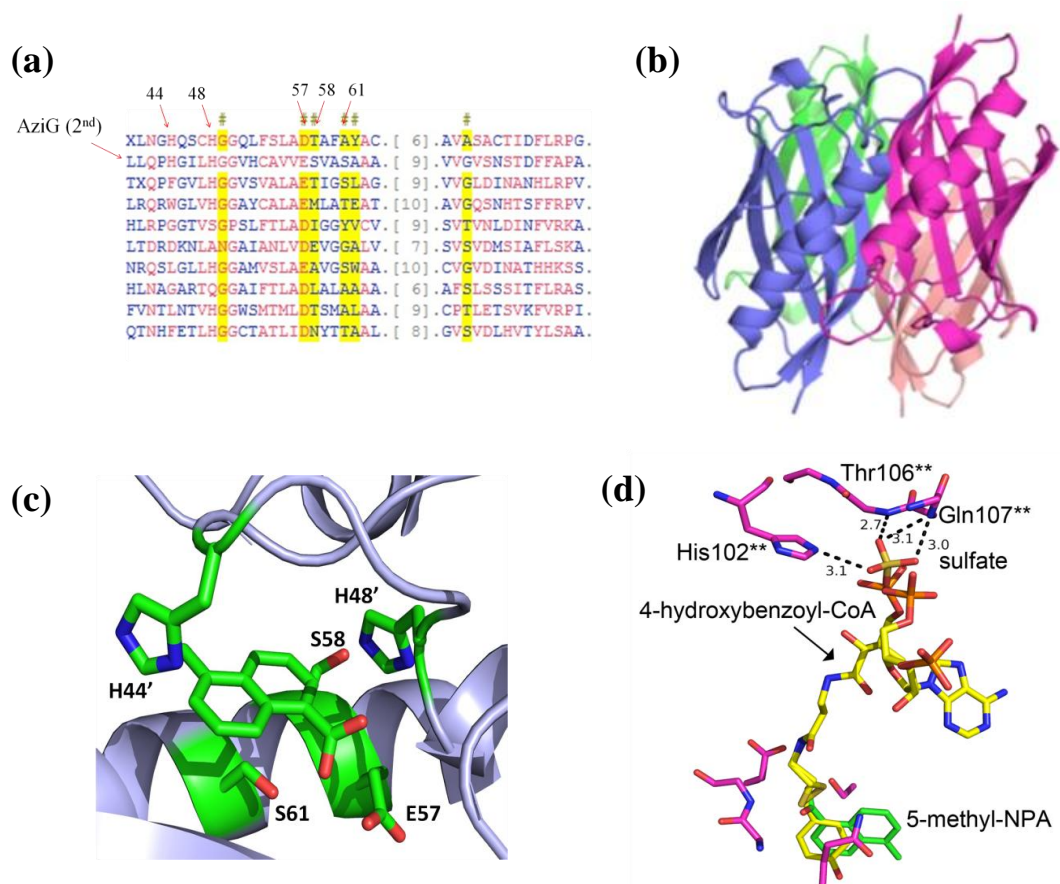


Figure 26. Sequence alignment of AziG homologs and AziG crystal structures

(a) Sequence alignment of AziG and its homologs to show the conserved features for the substrate binding site. Yellow: the most conserved regions, red: conserved regions, and blue: the least conserved regions. (b) Crystal structure of AziG tetramer. (c) Active site of AziG with 5-methyl-1-naphthoic acid. (d) Superposition of AziG and 5-methyl-1-naphthoic acid with *Anthrobacter* thioesterase with 4-hydroxybenzoyl-CoA (PDB 1Q4U).¹²⁰

Site Directed Mutagenesis and Effect to the Production

Site directed mutagenesis of the target residues was performed using QuikChange II Site-Directed Mutagenesis Kit as described in the Materials and Methods section. The mutated expression vectors were produced by PCR with primer pairs containing point mutations, and the template WT plasmid was degraded by DpnI restriction enzyme which digests methylated DNAs. All plasmids replicated in *E. coli*

DH10b are naturally methylated, thus only the PCR product could survive in the environment. Since there was no affection on expression and purification of mutants, the mutant proteins could be prepared and used for assays in the same manner as wild type AziG (Appendix Figure 62).

The effect of AziG mutations on the production of 5-methyl-1-naphthoic acid was evaluated by LC-MS, which showed that the product was still produced (Figure 27). Because some known Hotdog fold TEs activate a water molecule to catalyze hydrolysis rather than using a single amino acid to covalently bind the carbonyl carbon of a thioester,^{122, 127} it is possible that a water molecule can still interact with the remaining amino acids to catalyze the reaction. The kinetics of AziG, however, must be affected by the mutations.

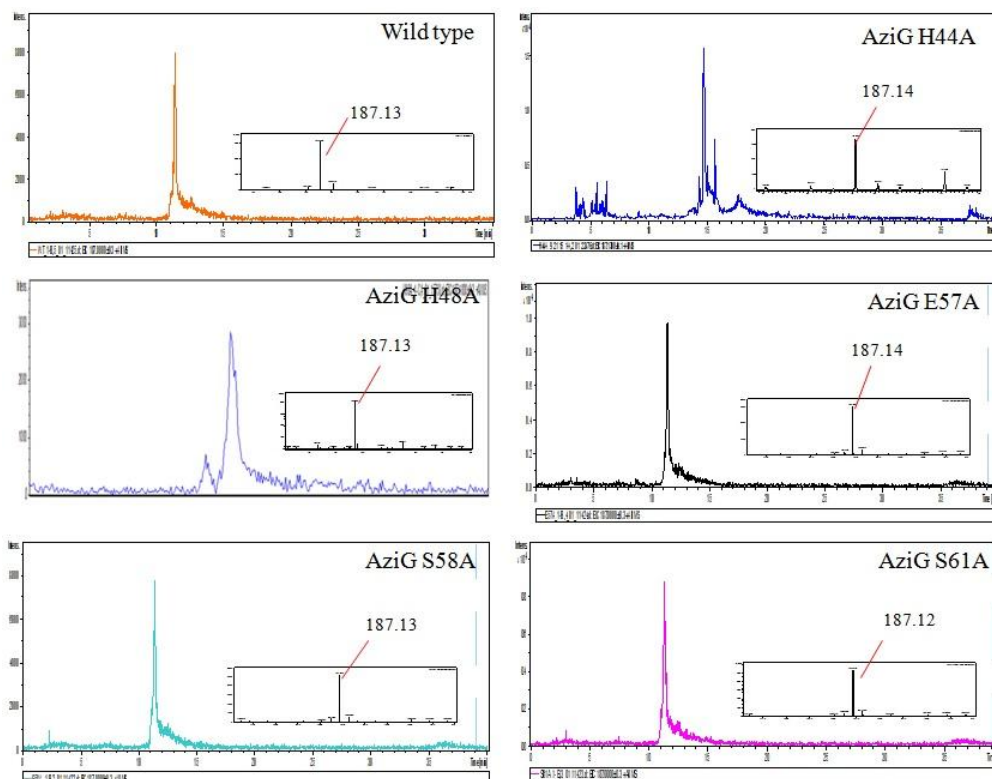


Figure 27. LC-MS analysis of AziB-AziG mutant products

The product of AziB and AziG mutants was analyzed by LC-MS. The wild type AziG was used as the control. There was no affect on the production in the AziG mutants.

Kinetics of AziG and Its Mutants

Kinetic parameters of AziG and its mutants for the hydrolysis of 5-methyl-1-naphthoic acid were measured by using N-acetylcysteamine (NAC)-substrate and Ellman's reagent (5,5'-dithio-bis-(2-nitrobenzoic acid) or DTNB) as described in the Materials and Methods section (Figure 28 and Appendix Figure 76). NAC mimics a pantetheinyl arm of CoA which allows for a TE recognizing NAC-substrate as its target.^{128, 129} The released free thiol is immediately reacted with DTNB to produce mixed disulfide and 2-nitro-5-thiobenzoic acid (TNB) which gives a yellow color and absorbs a light at 412 nm (Appendix Scheme 5).¹³⁰ The absorbance is proportional to the concentration of thiol, which allows measuring the reaction rate of hydrolysis catalyzed by TEs.⁷¹ Because the assay was performed out of the range of the standard buffer for the reagent, molar absorptivity was calculated (Appendix Figure 77). Only k_{cat}/K_m value could be calculated at the low substrate concentrations because the solubility of the substrate was highly limited in the aqueous buffer.

The k_{cat}/K_m value of WT AziG is much lower than homologous hotdog fold TEs.^{112, 120, 121} It still shows significant reduction in the k_{cat}/K_m values of each amino acid mutation, however none of the mutants completely lost their activity and their kinetic values were similar to one another. These data are not consistent with any of predicted mechanisms although it is clear a mutation on polar residues in the active site affects the rate of hydrolysis by AziG. This suggests that interaction with AziB is required for the optimal catalytic activity of AziG as an association between AziB and AziG is essential for production of 5-methyl-1-naphthoic acid. The rate of hydrolysis by AziG with AziB was measured, but it did not produce consistent measurements in the same assay. This was probably because the reaction between AziB's cysteine residues and Ellman's reagent was so robust that it could not be properly eliminated by the control. Although the data was not consistent, significant induction of hydrolysis by adding AziB was never observed. This suggests that covalently attached product on ACP domain of AziB is also necessary for the best activity of AziG. Designing experiments to address these issues and to test the hypothesis is currently in progress.

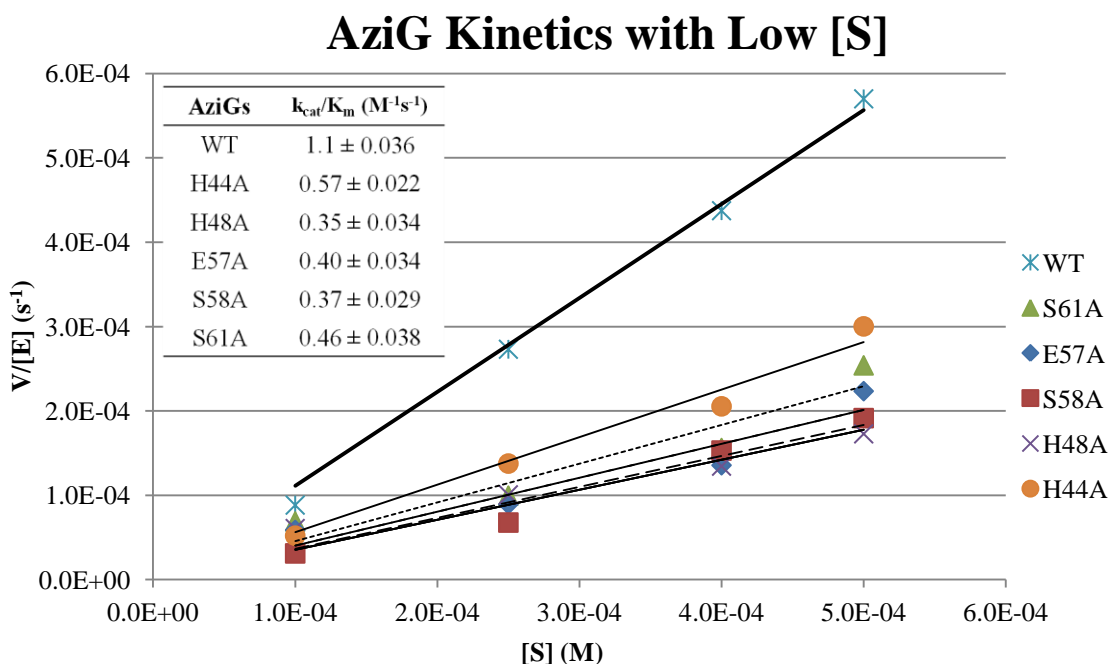


Figure 28. Kinetic parameters of AziG and its mutants

The k_{cat}/K_m value of AziG and its mutants was measured at low substrate concentrations (0.1, 0.25, 0.4, and 0.5 mM).

SIGNIFICANCE

It has been shown that the backbone of the naphthoate moiety, 5-methyl-1-naphthoic acid, is produced by AziB (PKS) and AziG (TE) in tandem while AziB alone produces 2-methylbenzoic acid. The evidence provided by this research strongly supports the hypothesis which has been proposed by previous structural, feeding, and bioinformatic studies that AziB is responsible for the production of the naphthoate moiety. In addition, AziG has been identified as another enzyme involved in the naphthoate production. Although the mechanism is yet to be evaluated, the bioinformatic, crystallographic, and kinetic studies have shown that AziG is a member of the Hotdog fold TE family. The series of experiments discussed here suggest that interaction between AziB and AziG is important for both production and release of the

product. Understanding the novel tandem work of AziB and AziG sheds new light on understanding of PKS-TE interactions.

The naphthoate moiety has the other key residue which is a methoxy group at 3' position, which is thought to be produced by catalytic works of a cytochrome P450 hydroxylase AziB1 and an O-methyltransferase AziB2. Although the 3-methoxy group is not as critical as 5-methyl group in non-covalent interaction with DNAs, replacement of the methoxy group significantly reduce the cytotoxicity of azinomycin analogs.^{89, 94} The formation of the ester bond between the naphthoate moiety and the peptide backbone is also an interesting aspect of azinomycin biosynthesis relating to the naphthoate moiety. There are five NRPS modules in the gene cluster while there are only four substrates including 3-methoxy-5-methyl-1-naphthoic acid.¹⁰⁸ Because 3-methoxy-5-methyl-1-naphthoic acid and α -ketoisovaleric acid are proposed substrates of AziA1 (A-PCP domains) and AziA3 (A-KR-PCP domains) respectively,^{107, 108} AziA2 (C-PCP-C domains) which has additional C and PCP domains has been suggested to be responsible for an ester formation between these two acids. It is unclear, however, why there needs to be additional C and PCP domains for the condensation of these two substrates although the essentiality of AziA2 was shown by the lack of azinomycin production by the *aziA2* disruption mutant (discussed in Chapter III).¹⁰⁹

Understanding the mechanisms, functions and interactions around the naphthoate moiety biosynthesis could lead to a possible application of *in situ* biosynthesis of a bioactive compound in cancer cells where non-toxic substrates and an expression vector with a cancer specific promoter are applied to produce a bioactive molecule. It is essential for the application that detailed knowledge of toxicity of the related compounds and of protein functions is well understood because a minimum number of genes have to be used for the effective expression and reaction. This research is one of the important first steps for understanding the biosynthesis of azinomycins, including the novel interaction of the PKS and the Hotdog fold TE, which will lead to the deeper knowledge not only of azinomycin biosynthesis but also of entire natural product biosynthesis.

MATERIALS AND METHODS

General Experimental Procedure

LC-MS was carried out on a Bruker MicroTOF-QII mass spectrometer (Billerica, MA, USA) coupled to an Agilent 1200 Infinity series liquid chromatography system (Agilent Technologies, Santa Clara, California, USA) with a Prodigy 5 μm ODS-2 150 \AA , LC Column 250 x 4.6 mm (Phenomenex, Torrance, California, USA). NMR spectra were acquired in CDCl_3 or CD_3OD with a Varian Mercury 300 spectrometer or Bruker Advance III 500 MHz spectrometer equipped with a 5 mm H-C-N cryoprobe. UV light absorption was measured by GENESYS 2 UV-Vis Spectrophotometer (Thermo Fisher Scientific, Waltham, Massachusetts, USA). Gel filtration chromatography was performed with Superdex 75 PC HiLoad 16/60 (GE Healthcare, Little Chalfont, UK) at the Protein Chemistry Laboratory at the Texas A&M University.

Reagents and Materials

Streptomyces sahachiroi (NRRL 2485) was obtained from the American Type Culture Collection (ATCC). Cloning steps were performed in *E.coli* DH5 α or *E.coli* TOP10. *E.coli* Rosetta (DE3) or *E.coli* BL21 (DE3) was used for protein expression. PCR was performed using Phusion High-Fidelity DNA Polymerase (New England BioLabs). Plasmids used for gene expression were pET-24a(+) and pET-21-d(+) purchased from Novagen. Plasmid preparation and DNA purification were carried out using commercial kits (Qiagen). Restriction enzymes and other molecular biology reagents were from commercial sources (BioLabs). Unlabeled coenzyme A (CoA), acetyl coenzyme A, malonyl coenzyme A substrates, β -Nicotinamide adenine dinucleotide phosphate reduced form (NADPH), S-(5'-Adenosyl)-L-methionine chloride (SAM), 5,5'-dithiobis(2-nitrobenzoic acid) (DTNB), and chemicals used in organic synthesis were purchased from Sigma-Aldrich. 5-Bromo-1-naphthoic acid was purchased from Ark Pharm, Inc. (Libertyville, IL, USA). The deuterated solvents for

NMR experiments were purchased from Cambridge Isotope Laboratories, and all other solvents were purchased from Fisher Scientific at highest available grade.

Cloning of *AziA6* into an Expression Vector for *E. coli*

A thioesterase gene, *aziA6*, was amplified from genomic DNA of *S. sahachiroi* by PCR with primers AziA6-F and AziA6-R. The PCR reaction was performed in a 25 μ L reaction mixture consisting of: 0.5 μ L Phusion High-Fidelity DNA polymerase, 4 μ L Phusion GC Buffer, 15 ng of *S. sahachiroi* genomic DNA, 0.5 μ L of each 20 mM forward and reverse primer, 0.5 μ L of 20 mM dNTP, 1.25 μ L of DMSO, and water to a total volume of 25 μ L. The PCR condition was optimized as following: initial denaturation for 30 s at 98 $^{\circ}$ C, 25 cycles of 10 s at 98 $^{\circ}$ C, 20 s at 75 $^{\circ}$ C, and 1 min at 72 $^{\circ}$ C, and a final extension for 10 min at 72 $^{\circ}$ C. The DNA fragment of *aziA6* was purified by agarose gel extraction using QIAquick Gel Extraction Kit (Qiagen, Venlo, Netherlands), and it was digested by restriction enzymes HindIII and XhoI. After purified by agarose gel extraction again, the DNA fragment was ligated into HindIII/XhoI multiple cloning site of an expression plasmid vector pET-24b (EMD Millipore, Billerica, Massachusetts, USA) which contains 6xHis-tag at the 3'-end. The resulted plasmid pET24b-*aziA6* was transformed into an *E. coli* strain TOP10 by electroporation, which was cultured on solid LB medium with 50 μ g/mL of kanamycin overnight. Each colony was subsequently cultured in 5 mL of LB medium with the antibiotic overnight for plasmid isolation by QIAprep Spin Miniprep Kit (Qiagen). Cloning of the gene was confirmed by sequencing reaction using BigDye[®] Terminator v3.1 Cycle Sequencing Kit (Applied Biosystems, Foster City, California, USA). The cloned plasmid was transformed again into an *E. coli* expression strain BL21(DE3) for overexpression.

Site Directed Mutagenesis of *AziG*

Cloning of *aziG* was carried out by a former lab mate Michelle Lebo, where *aziG* was inserted into pET-24b multiple cloning site (pET-24b-*aziG*) and was transformed

into BL21(DE3). H44, H48, E57, S58 and S61 of AziG were mutated to alanine using QuikChange II Site-Directed Mutagenesis Kit (Agilent Technologies, Santa Clara, California, USA). Primers containing point mutations were used to amplify mutated plasmids for each. Primer pairs for H44A, H48A, E57A, S58A, and S61A mutations were AziG-H44A-F and AziG-H44A-R, AziG-H48A-F and AziG-H48A-R, AziG-E57A-F and AziG-E57A-R, AziG-S58A-F and AziG-S58A-R, and AziG-S61A-F and AziG-S61A-R, respectively. PCRs were performed as the following program: initial denaturation for 30 s at 95 °C and 12 cycles of 30 s at 95 °C, 1 min at 55 °C, and 6 min at 68 °C. The amplified plasmids were treated with DpnI restriction enzyme for 3 hours to degrade methylated DNA naturally produced by *E. coli*. The mutated plasmids were transformed into DH10b by electroporation, and the mutations were confirmed by sequencing reactions after isolating the plasmids from the strains. The plasmids were subsequently transformed into BL21(DE3) for overexpression.

Overexpression of AziB, Svp, AziA6, AziG, and AziG Mutants

AziB, Svp, AziA6, AziG, and AziG mutants were overexpressed in the same manner. *E. coli* strains which contain their expression plasmids were cultured in 5x5 mL LB media for AziB, 3x5 mL for Svp, 4x5 mL for AziA6, and 2x5 mL for each AziG overnight with proper antibiotics, which are 50 µg/mL kanamycin for AziB, AziA6, and AziGs and 100 µg/mL ampicilin for Svp. Each of the 5 mL overnight cultures was inoculated into 1 L LB medium and grown until OD600 reaches 0.6-0.8. The production of the proteins was induced by 1 mM Isopropyl β-D-1-thiogalactopyranoside (IPTG) and incubation in 16 °C at 250 rpm for 22 hours. The resulted cells were harvested by centrifugation at 7000 rpm for 15 min. After discarding the supernatant, the cells were washed with 250 mL of DI water and centrifuged down again by the same condition. The supernatant was discarded, and the cells were washed again with 30 mL of AziB-Svp reaction buffer (75 mM Tris-HCl, pH 8.0, 10 mM MgCl₂, 5 mM dithiothreitol (DTT), and 20% glycerol). It was centrifuged down again at 9900 rpm for 15 min, and the supernatant was discarded. The remaining steps were performed on ice. The cells

were resuspended into the AziB-Svp reaction buffer of 30 mL for AziA6 and each AziG and total 100 mL for AziB and Svp which were subsequently mixed together. Phenylmethanesulfonylfluoride (PMSF) was added into each solution to the final concentration of 1 mM shortly before the cells were lysed by sonication with Branson Sonifier 450 (Branson Ultrasonics, Danbury, CT) fitted with a 5 mm micro-tip, output setting 6, duty cycle 60%, and 5 cycles for 30 sec each. The lysed cells were removed by centrifugation at 9900 rpm for 45 min twice to remove the cell residues completely. The supernatants which consist of water soluble proteins were stored in 4 °C.

Posttranslational Modification of AziB with Svp and Coenzyme A

Approximately 90 mL of apo-AziB and Svp crude protein extract was obtained following cell lysis and centrifugation. Apo-AziB was converted to the holo-form by adding 5 µmol of coenzyme A, giving a final concentration of ~5.5 µM. The sample was incubated at 28 °C, 250 rpm for 1 h. Any resulting precipitation formed during incubation was removed by centrifugation, 9900 rpm for 45 min. Holo-AziB/Svp were purified by nickel affinity chromatography. A HisTrap FF 5 mL column was equilibrated with PPT buffer and subsequently loaded with the protein mixture at a rate of 0.25 mL/min. The column was washed with 200 mL of PPT column buffer (1 mM DTT, 500 mM NaCl, 40 mM imidazole, 75 mM Tris-HCl, pH 8.0, and 20% glycerol) and eluted with 30 mL of PPT column buffer supplemented with 250 mM imidazole. The buffer was exchanged to the AziB-AziG reaction buffer (50 mM potassium phosphate, pH 7.5, and 20 % glycerol). The purity and quantity of holo-AziB and Svp were assessed by 8 % (v/v) SDS-PAGE and Bradford assay utilizing the Bio-Rad Protein Assay kit (Bio-Rad Laboratories, Hercules, CA, USA); bovine serum albumin (BSA) was implemented as a standard.

Purification of AziB-Svp, AziA6, AziG, and AziG Mutants

The crude solutions, which contained AziA6 or AziGs were applied to pre-equilibrated HisTrap FF 5 mL columns at 0.25 mL/min. The loaded columns were treated as follows:

- For AziA6, the column was washed with 200 mL of column buffer supplemented with 40 mM imidazole, and eluted with 30 mL of column buffer supplemented with 250 mM imidazole
- For AziG and its mutants the column was washed with 200 mL of column buffer supplemented with 60 mM imidazole and eluted with 30 mL of column buffer supplemented with 250 mM imidazole

The buffer was exchanged to AziB-AziG reaction buffer (potassium phosphate: 50 mM, glycerol: 20 %, pH 7.5) by centrifugal ultrafiltration units for 10 kDa (Amicon Ultra - 15) except for AziA6. An additional purification step was required for AziA6. The buffer was exchanged to sephadex column buffer (20 mM sodium phosphate, 150 mM NaCl, pH 7.5). The sephadex G-50 fine (size exclusion) column with 200 mL volume about 1 m height was equilibrated with the sephadex column buffer. The AziA6 solution was concentrated as the total volume reached 1.5 mL which was loaded into the column, and fractions were collected every 3 mL which were later analyzed for quantity and purity by Bradford assay and 12% (v/v) SDS-PAGE. The purified AziA6 fractions were combined together and the buffer was exchanged to AziB-AziG reaction buffer.

***In Vitro* Synthesis of 5-Methyl-1-Naphthoic Acid by AziB and TE Domains**

A 25 mL of the reaction solution consists of 50 μ M of acetyl coenzyme A, 250 μ M of malonyl coenzyme A, 10 μ M of NADPH, about 10 mg of AziB-Svp mixture, and about 10 mg of AziA6 or AziG in the AziB-AziG reaction buffer. The reaction solution was incubated in 30 °C overnight. The product was cleaved from the protein by basification of the solution with NaOH till pH about 12, and it was subsequently acidified by HCl till pH below 5 for the following extraction. The acidified product was extracted with the equal volume of ethyl acetate three times. After dried over anhydrous

sodium sulfate, ethyl acetate was evaporated off in vacuo and gentle flow of dry nitrogen gas. In case of AziG mutant assays, the solution after the reaction was neither basified nor acidified. Alternatively, the reaction solution was filtered out with centrifugal ultrafiltration units for 3 kDa, and the filtrate was extracted with the equal volume of ethyl acetate three times and solidified by the same method.

LC-MS Analysis of AziB and AziA6 or AziG Products

The product was analyzed by LC-MS. It was dissolved in 100 μ L of methanol, and 10-30 μ L of the sample was injected into the reversed-phase HPLC column (Phenomenex, Columbus 5 μ C8 100A, 250 x 3.20 mm 5 μ) which was pre-equilibrated with 80% A (water) and 20% B (75% methanol and 25% isopropanol). The liquid chromatography was ran by the following program: Time 0 min A-80% B-20%; 1 min A-80% B-20%; 15 min A-0% B-100%; 30 min A-0% B-100%; 32 min A-80% B-20% till 40 min at the flow rate 0.75 μ L/min. It was monitored by UV at 254 nm wavelength and by mass at around 136 m/z (2-methylbenzoic acid) and 187 m/z (5-methyl-1-naphthoic acid).

Synthesis of 5-Methyl-1-Naphthoic Acid (Dr. Dmytro Fedoseyenko)

tert-butyl-5-bromo-1-naphthoate **52**¹³¹

Oxalyl chloride (0.4 mL) was added to a suspension of 5-bromo-1-naphthoic acid **51** (1.08 g) in dichloromethane (9.3 mL) containing 3 drops of dimethylformamide and the reaction mixture was stirred at ambient temperature for 6 h. The solution was concentrated to afford a white solid, which was re-dissolved in tetrahydrofuran (THF). The solution was cooled to 2 °C and a solution of potassium *tert*-butoxide (0.72 g) in THF (14.8 mL) was added dropwise, which was stirred at ambient temperature for 3 h. The solution was poured onto ice (20 g) and extracted with ethyl acetate (2 x 10 mL). The combined organic extracts were washed with water (10 mL), dried over sodium sulfate, and concentrated *in vacuo*. The residue was purified by flash column chromatography (cyclohexane:ethyl acetate = 1:1) to give 5-bromo-1-naphthoic acid

tert-butyl ester **52** in 91 % yield (12 g). ^1H NMR (300 MHz, CDCl_3): δ_{H} 8.86 (d, $J = 9.0$ Hz, 1H), 8.48 (d, $J = 8.7$ Hz, 1H), 8.13 (dd, $J = 7.3$, $J = 0.9$ Hz, 1H), 7.86 (dd, $J = 7.5$, $J = 0.9$ Hz, 1H), 7.62 (dd, $J = 8.6$, $J = 7.5$ Hz, 1H), 7.45 (dd, $J = 8.7$, $J = 7.5$ Hz, 1H), 1.71 (s, 9H).

tert-butyl-5-methyl-1-naphthoate **53**¹³²

To a solution of 5-bromo-1-naphthalene-1-carboxylic acid tert-butyl ester **52** (1.00 g, 3.26 mmol) in THF (10 mL), -78 °C, was added n-butyllithium (2.5 M in hexanes, 1.56 mL) over a period of 2 min. After stirring for 40 min, methyl iodide (0.55 g) was added. This reaction mixture was allowed to warm to room temperature over 1.5 h. The reaction was quenched with water (10 mL) and partitioned between water and diethyl ether (3 x 50 mL). The combined organic extracts were dried over MgSO_4 and concentrated *in vacuo*. Purification of the residue by flash-chromatography (hexanes:EtOAc = 98:2) gave compound **53** in 84% yield (660 mg). ^1H -NMR (300 MHz, CDCl_3): δ_{H} 8.70 (d, $J = 8.7$ Hz, 1H), 8.20 (d, $J = 8.7$ Hz, 1H), 8.07 (dd, $J = 7.3$, $J = 1.2$ Hz, 1H), 7.56 (d, $J = 7.2$ Hz, 1H), 7.54-7.48 (m, 1H), 7.42-7.37 (m, 1H), 2.75 (s, 3H), 1.72 (s, 9H).

5-methyl-1-naphthoic acid **49**¹³²

5-Methynaphthalene-1-carboxylic acid tert-butyl ester **53** (1.37 g, 4.45 mmol) was dissolved in dichloromethane (10 mL), and trifluoroacetic acid (3 mL) was added. After stirring for 16 h, the reaction was concentrated *in vacuo* to give compound **49** in quantitative yield. ^1H -NMR (300 MHz, CD_3OD): δ_{H} 8.73 8.74 (d, $J = 8.7$ Hz, 1H), 8.28 (d, $J = 8.4$ Hz, 1H), 8.18 (dd, $J = 7.2$, $J = 1.2$ Hz, 1H), 7.58 (dd, $J = 8.5$, $J = 7.2$ Hz, 1H), 7.52-7.44 (m, 1H), 7.44-7.36 (m, 1H), 2.73 (s, 3H). ^{13}C NMR (125 MHz, CD_3OD): δ_{C} 20.0, 125.0, 125.5, 125.8, 128.0, 128.1, 130.0, 130.4, 132.6, 134.3, 135.9, 171.5. MS (ESI): m/z calculated for $[\text{M}-\text{H}^+]$ $\text{C}_{12}\text{H}_9\text{O}_2$ 185.0603, found 185.0611.

LC-MS Analysis of AziB-AziG Product with the Synthetic Standard

Synthetic 5-methyl-1-naphthoic acid was acquired by Dr. Dmytro Fedoseyenko (Dr. Begley group, Texas A&M University), and the structure was further confirmed by ^1H NMR, ^{13}C NMR, COSY, HSQC, and HMBC. The synthetic compound was treated with acid, base, or nothing followed by the AziB-AziG reaction buffer, and it was extracted and dried by the same method as previously described. Those three samples and untreated compound were analyzed by LC-MS in the same way as described in the last section. The base treated sample had a single peak which was also shown in the AziB-AziG product analysis, and the identity of the two peaks was confirmed by co-injection.

Preparation of Cell Free Extract of *S. sahachiroi*

Cell free extract of *S. sahachiroi* was prepared from 5 L fermentation culture with the previously described procedure.¹⁰⁵ After 72 h fermentation, the cells were harvested by centrifugation at 7000 rpm for 15 min, which were washed with 1.5 L of water twice and with 250 mL of the His-tag binding buffer once. The cell pellet was divided by half and frozen at $-80\text{ }^\circ\text{C}$. The cells were resuspended in 50 mL of the His-tag binding buffer and placed in the bead beater cabinet with 0.1 mm glass beads. The cell membranes were disrupted by ten times of 1 min run with 5 min interval on ice to ensure everything was kept ice cold. The disrupted cell residues were removed by centrifugation at 12,000 rpm for 45 min twice. The supernatant was kept for AziB-AziG *in vitro* binding assay.

AziB-AziG *In Vitro* Binding Assay

AziG-AziB binding assay was carried out on His-tag Ni^{2+} affinity column. AziG was loaded onto the column as described in the previous section (Purification of AziB-Svp, AziA6, AziG, and AziG mutants), and the cell free extract was passed through the column at the same rate as loading AziG. The column was subsequently washed with 200 mL of the His-tag buffer with 60 mM imidazole, and the proteins were eluted with

30 mL of the buffer with 250 mM imidazole. The elution was concentrated to 1 mL by a centrifugal filter unit for 100 kDa. The proteins were assessed by SDS-PAGE following to coomassie blue and silver stains with Silver Stain PlusTM Kit (Bio-Rad, Hercules, California, USA).

Gel Filtration Chromatography of AziG Native Form

Mass of the native state AziG in solution was assessed by gel filtration (size-exclusion) chromatography. Approximately 1 mg of each protein sample was injected into a pre-equilibrated (10 mM phosphate and 150 mM NaCl at pH 7.2) gel filtration column (Superdex 75 PC HiLoad 16/60, GE Healthcare) at room temperature. The elution volume was measured by detecting the sample elution with UV absorbance at λ 280 nm. The calibration curve was generated by chromatography with following protein standards: bovine serum albumin (molecular mass, 67 kDa; elution volume, 55.6 mL), ovalbumin (45 kDa; 61.0 mL), carbonic anhydrase (29 kDa; 69.2 mL), and cytochrome C (13 kDa; 81.6 mL) (Appendix Figure 78-a). Plotting elution volume (mL) vs. molecular mass of standard (kDa) gave a linear trend line with the following equation (Appendix Figure 79):

$$y = -0.475x + 85.1$$

The elution volume of native AziG was 55.6 mL, thus the molecular mass was calculated as 62.2 kDa (Appendix Figure 78-b). Since the theoretical mass of expressed AziG (containing plasmid restriction site and 6 x Histidine) is 15.8 kDa, it is predicted that the native state of AziG in solution is that of a tetramer (\pm 1.61 % error).

Crystallization of AziG (Dr. Megan D. Sikowitz)

The hanging drop vapor diffusion method was used for crystallization. In this method, the frozen protein aliquots were thawed on ice and equal volumes of protein and reservoir solution were mixed and equilibrated at 22 °C against a total volume of 500 μ L well solution. Using the commercially available sparse matrix Wizard screens (Emerald Biosystems), three crystallization conditions were identified. Crystals were observed in

Wizard I condition 13 (1.32 M ammonium sulfate and 0.1 M cacodylate pH 6.5), Wizard II condition 39 (0.1 M CAPS pH 10.5, 0.2 M NaCl, and 20% PEG 8,000), and Wizard III condition 33 (1.6 M magnesium sulfate and 0.1 M MES pH 6.5). Optimized crystals grew in 1.25 M ammonium sulfate and 0.1 M cacodylate pH 6.0, 1.6 M magnesium sulfate and 0.1 M MES pH 5.5, or 0.1 M CAPS pH 10.8, 0.2 M NaCl, and 14% PEG 8000. In all three conditions, crystals with similar morphologies appeared overnight. The crystals were square bipyramidal, 60 μm long, and about 40 μm in width at the center. The crystals were cryoprotected for data collection in a solution composed of their mother liquor supplemented with 15% (v/v) glycerol before flash freezing in liquid nitrogen. For soaking experiments, the crystals were soaked with 10 mM 3-hydroxy-2-NPA for 5 min before cryoprotection and flash freezing.

X-Ray Data Collection and Processing (Dr. Megan D. Sikowitz)

X-ray diffraction experiments were conducted at CHESS (Cornell High Energy Synchrotron Source) beamline F1 using a Q270 detector (Area Detector Systems Corp.) at a distance of 304.7 mm and wavelength of 0.91830 \AA . The oscillation method was used with 1° rotation per frame for 90° with cryocooling and 10 s exposures. Crystals grown in all three conditions were tested for diffraction quality. The data sets reported are for crystals grown in the ammonium sulfate containing condition. Additional diffraction experiments on the ligand soaked crystals were conducted at APS NE-CAT beamline 24-ID-E (Argonne National Laboratory) using a Quantum 315 detector (Area Detector Systems Corp.) at a distance of 325 mm and wavelength of 0.97919 \AA . The oscillation method was also used, with 1° rotation per frame for 70° with cryocooling and 1 s exposure time. HKL2000 was used for indexing, integration, and data scaling.¹³³ Complete data collection and refinement statistics are listed in Appendix Table 6.

Structure Determination, Model Building, and Refinement (Dr. Megan D. Sikowitz)

The AziG crystal belongs to space group $I4_122$ and contains one promoter per asymmetric unit. It has a Matthew's coefficient of 2.73 $\text{\AA}^3/\text{Da}$ with corresponding

solvent content of 54.9%. The structure of AziG was determined using the molecular replacement method, with *Mycobacterium tuberculosis* thioesterase (PDB ID: 3S4K) as the model. The program Chainsaw was used to create a search model from 3S4K. Molecular replacement using this search model was conducted with MolRep. Iterative rounds of model building were conducted with COOT, with refinement using RefMac5 in initial rounds, and PHENIX.refine in final rounds. The quality of the final structure was assessed using MolProbity. The final structure refinement was completed with an R-factor value of 22.2% and R_{free} of 26.6%. This structure was used as the model for refinement of the SsAziG/3-hydroxy-2-NPA structure. PHENIX.elbow was used for ligand generation before placement into $F_o - F_c$ electron density. Model improvement of the liganded structure was performed as described above. Structure refinement for SsAziG/3-hydroxy-2-NPA converged with an R-factor of 20.2% and R_{free} of 25.0%. Complete refinement statistics for both structures are listed in Appendix Table 6.

Kinetics of AziG Hydrolysis

The kinetic parameters of AziG and its mutants were measured as the formation of 2-nitro-5-thiobenzoic acid (TNB) at 412 nm ($\epsilon = 8,857.1 \text{ M}^{-1}\text{cm}^{-1}$) followed by the reaction of 5,5'-dithiobis(2-nitrobenzoic acid) (DTNB or Ellman's reagent) with a free thiol produced by hydrolysis of 5-methyl-1-naphthoate-SNAC by AziGs. 5-methyl-1-naphthoate-SNAC was synthesized by Dr. Dmytro Fedoseyenko, and the absorbance was measured on GENESYSTM 2 UV-Vis Spectrometer (Thermo Fisher Scientific, Waltham, Massachusetts, USA). The reaction was carried out in the AziB-AziG reaction buffer without glycerol, which contains 0.4 mM of DTNB, 20 μM of AziGs, 0.1-0.5 mM of the substrate, and 5% DMSO.

Three types of buffered solutions consisting of DTNB alone, AziG + DTNB, or substrate + DTNB were used to establish a control because DTNB and the substrate are chemically degraded by water molecules and AziG contains cysteine residues, which can react with DTNB. The effect of chemical degradation of DTNB which was counted

twice on the absorbance of two solutions ($A_{\text{AziG-DTNB}}$ and $A_{\text{substrate-DTNB}}$) can be eliminated for utilizing the following equation:

$$A_{\text{control}} = A_{\text{AziG-DTNB}} + A_{\text{substrate-DTNB}} - A_{\text{DTNB}}$$

The control was used to correct these undesired effects with the following equation:

$$A_{\text{corrected}} = A_{\text{AziG+substrate+DTNB}} - A_{\text{control}}$$

The absorbance was observed continuously every 30 s, and the rates of hydrolysis were determined from the initial linear component of the curves. The assays were performed at least 4 times for each data point.

DMSO was used to solubilize the substrate. Since the solubility was highly limited even in 5% DMSO, however, the velocity could be calculated only in low substrate concentrations. Therefore, the limited case of Michaelis–Menten kinetics where $[S] \ll [K_m]$ was applied to obtain k_{cat}/K_m values as the slopes of plotted linear graph of $V/[E]$ vs. $[S]$ by the following equation:

$$\frac{V}{[E]} = \frac{k_{\text{cat}}}{K_m} [S]$$

where V is velocity, $[E]$ is concentration of AziGs, and $[S]$ is concentration of the substrate.

Molar Absorptivity of TNB

Absorbance at 412 nm of TNB with different concentrations of free thiol in the buffer used in kinetic experiments was measured as the product of the reaction with DTNB and N-acetylcysteamine (NAC). The solution contains 50 mM potassium phosphate, 0.4 mM DTNB, 5% DMSO, and varied (10, 20, 30, 40, 50, and 60 μM) concentrations of NAC, and the absorbance at 412 nm was measured on GENESYS™ 2 UV-Vis Spectrometer. The molar absorptivity of TNB was calculated by Beer-Lambert law:

$$A = \epsilon cl$$

where A is the absorbance, ϵ is the molar absorptivity ($\text{M}^{-1} \text{cm}^{-1}$), c is concentration (M), and l is the pathlength (cm). Since the pathlength is 1 cm, the molar absorptivity was calculated as a slope of a linear graph of A vs. c , which was $8,860 \text{ M}^{-1} \text{cm}^{-1}$.

Synthesis of 5-Methyl-1-Naphthoate-SNAC Ester (Dr. Dmytro Fedoseyenko)

S-(2-acetamidoethyl) 5-methylnaphthalene-1-carbothioate **54**

5-methyl-1-naphthoic acid **49** (55 mg, 0.3 mmol), (3-dimethylaminopropyl)-3-ethylcarbodiimide hydrochloride (114 mg, 0.6 mmol), DMAP (37 mg, 0.3 mmol), N-acetylcysteamine (SNAC) (35 mg, 0.3 mmol) and triethylamine (60 mg, 0.6 mmol) were stirred in dichloromethane (10 mL) under argon at room temperature overnight. The organic layer was washed with saturated NaHCO₃ solution, 0.1 N HCl solution and brine (10 mL of each). It was dried over anhydrous sodium sulfate, concentrated *in vacuo* and purified by flash column chromatography (dichloromethane) to provide pure white solid product in 81% yield (70 mg). ¹H NMR (300 MHz, CDCl₃): δ_H 1.99 (s, 3H), 2.71 (s, 3H), 3.27 (t, *J* = 6.3 Hz, 2H), 3.59 (q, *J* = 6.3 Hz, 2H), 6.11 (s, 1H), 7.38 (d, *J* = 7.2 Hz, 1H), 7.44 – 7.55 (m, 2H), 8.01 (d, *J* = 7.2 Hz, 1H), 8.19 (d, *J* = 8.4 Hz, 1H), 8.28 (d, *J* = 8.7 Hz, 1H). ¹³C NMR (75 MHz, CDCl₃): 195.05, 170.4, 135.7, 134.7, 132.9, 129.2, 129.0, 127.7, 127.5, 127.3, 124.3, 123.2, 39.7, 29.5, 23.3, 19.8. MS (ESI): *m/z* calculated for [C₁₆H₁₇NO₂S + Li⁺] 294.1140, found 294.1134

Table 1. Primers used in Chapter II

AziA6-F	5'-GTCAAGCTTATGGACTCGCCCTGGGTGCGCCGC-3'
AziA6-R	5'-GAGCTCGAGCGAAGAGGTCCTTCCGGCCGGAGC-3'
AziG-H44A-F	5'-GCAGTATCCCGGCAGGCTGCAGCAGGTCGG-3'
AziG-H44A-R	5'-CCGACCTGCTGCAGCCTGCCGGGATACTGC-3'
AziG-H48A-F	5'-TGCACCCCGCCGGCCAGTATCCCGTGAGGC-3'
AziG-H48A-R	5'-GCCTCACGGGATACTGGCCGGCGGGGTGCA-3'
AziG-E57A-F	5'-GCGCTGTGGTCGCGTCCGTCGCCAG-3'
AziG-E57A-R	5'-CTGGCGACGGACGCGACCACAGCGC-3'
AziG-S58A-F	5'-CGCTGGCGACGGCCTCGACCACAGC-3'
AziG-S58A-R	5'-GCTGTGGTCGAGGCCGTCGCCAGCG-3'
AziG-S61A-F	5'-GAGTCCGTCGCCGCCGCGGCAGCGGA-3'
AziG-S61A-R	5'-TCCGCTGCCGCGGCGGCGACGGACTC-3'

Table 2. Strains and plasmids used in Chapter II

E. coli TOP10	F- mcrA Δ (mrr-hsdRMS-mcrBC) ϕ 80lacZ Δ M15 Δ lacX74 nupG recA1 araD139 Δ (ara-leu)7697 galE15 galK16 rpsL(Str ^R) endA1 λ^-	Invitrogen
E. coli TOP10/pET-24b-aziA6	F- mcrA Δ (mrr-hsdRMS-mcrBC) ϕ 80lacZ Δ M15 Δ lacX74 nupG recA1 araD139 Δ (ara-leu)7697 galE15 galK16 rpsL(Str ^R) endA1 λ^- with AziA6 expression plasmid	This study
E. coli DH10B	F ⁻ endA1 recA1 galE15 galK16 nupG rpsL Δ lacX74 Φ 80lacZ Δ M15 araD139 Δ (ara,leu)7697 mcrA Δ (mrr-hsdRMS-mcrBC) λ^-	Invitrogen
E. coli DH10B/pET-aziG-H48A	F ⁻ endA1 recA1 galE15 galK16 nupG rpsL Δ lacX74 Φ 80lacZ Δ M15 araD139 Δ (ara,leu)7697 mcrA Δ (mrr-hsdRMS-mcrBC) λ^- with AziG H48A expression plasmid	This study
E. coli DH10B/pET-aziG-E57A	F ⁻ endA1 recA1 galE15 galK16 nupG rpsL Δ lacX74 Φ 80lacZ Δ M15 araD139 Δ (ara,leu)7697 mcrA Δ (mrr-hsdRMS-mcrBC) λ^- with AziG E57A expression plasmid	This study
E. coli DH10B/pET-aziG-S58A	F ⁻ endA1 recA1 galE15 galK16 nupG rpsL Δ lacX74 Φ 80lacZ Δ M15 araD139 Δ (ara,leu)7697 mcrA Δ (mrr-hsdRMS-mcrBC) λ^- with AziG S58A expression plasmid	This study
E. coli DH10B/pET-aziG-S61A	F ⁻ endA1 recA1 galE15 galK16 nupG rpsL Δ lacX74 Φ 80lacZ Δ M15 araD139 Δ (ara,leu)7697 mcrA Δ (mrr-hsdRMS-mcrBC) λ^- with AziG S61A expression plasmid	This study
E. coli BL21(DE3)	B; F-ompT hsdSB(rB- mB-) gal dcm (DE3)	Invitrogen
E. coli BL21(DE3)/pET-24b-aziA6	B; F-ompT hsdSB(rB- mB-) gal dcm (DE3) with AziA6 expression plasmid	This study
E. coli BL21(DE3)/pET-24b-aziG	B; F-ompT hsdSB(rB- mB-) gal dcm (DE3) with AziG expression plasmid	This study
E. coli BL21(DE3)/pET-aziG-H44A	B; F-ompT hsdSB(rB- mB-) gal dcm (DE3) with AziG H44A expression plasmid	This study
E. coli BL21(DE3)/pET-aziG-H48A	B; F-ompT hsdSB(rB- mB-) gal dcm (DE3) with AziG H48A expression plasmid	This study

Table 2 Continued

E. coli BL21(DE3)/ pET-aziG-E57A	B; F-ompT hsdSB(rB ⁻ mB ⁻) gal dcm (DE3) with AziG E57A expression plasmid	This study
E. coli BL21(DE3)/ pET-aziG-S58A	B; F-ompT hsdSB(rB ⁻ mB ⁻) gal dcm (DE3) with AziG S58A expression plasmid	This study
E. coli BL21(DE3)/ pET-aziG-S61A	B; F-ompT hsdSB(rB ⁻ mB ⁻) gal dcm (DE3) with AziG S61A expression plasmid	This study
E. coli BL21(DE3)/ pET-24a-aziB	B; F-ompT hsdSB(rB ⁻ mB ⁻) gal dcm (DE3) with AziB expression plasmid	This study
pET-24a	<i>E. coli</i> expression vector, Km ^r	Novagen
pET-24b	<i>E. coli</i> expression vector, Km ^r	Novagen
pET-24b-aziA6	<i>E. coli</i> expression vector for AziA6, Km ^r	This study
pET-24a-aziG	<i>E. coli</i> expression vector for AziG, Km ^r	This study
pET-aziG-H44A	<i>E. coli</i> expression vector for AziG H44A, Km ^r	This study
pET-aziG-H48A	<i>E. coli</i> expression vector for AziG H48A, Km ^r	This study
pET-aziG-E57A	<i>E. coli</i> expression vector for AziG E57A, Km ^r	This study
pET-aziG-S58A	<i>E. coli</i> expression vector for AziG S58A, Km ^r	This study
pET-aziG-S61A	<i>E. coli</i> expression vector for AziG S61A, Km ^r	This study
pET-24a-aziB	<i>E. coli</i> expression vector for AziB, Km ^r	This study

CHAPTER III

AZINOMYCINS: EVALUATION OF BIOLOGICAL ACTIVITY OF CRYPTIC PRODUCT FROM Δ AZIA2 *STREPTOMYCES SAHACHIROI**

INTRODUCTION

Azinomycins are antitumor natural products produced by *Streptomyces sahachiroi*.⁸¹⁻⁸⁴ As detailed in chapter I, the structural, feeding, and bioinformatic studies have suggested that the compounds are produced by a combination of a polyketide synthase (PKS) and non-ribosomal peptide synthetases (NRPSs).¹⁰³⁻¹⁰⁸ Chapter II discusses the formation of the naphthoate moiety 5-methyl-1-naphthoic acid through the combined efforts of PKS AziB and thioesterase (TE) AziG. This naphthoic acid eventually obtains a methoxy substituent at the 3' position, a fragment installed by AziB1 and AziB2.¹³⁴ The resulting naphthoic acid, 3-methoxy-5-methyl-1-naphthoic acid, forms an ester bond with the epoxide moiety catalyzed by NRPSs. Previous studies have suggested that there are four substrates for the NRPSs while there are five modules in the gene cluster. It has been proposed that 3-methoxy-5-methyl-1-naphthoic acid and 3-methyl-2-oxo-but-3-enoic acid, which eventually forms an epoxide, are substrates of AziA1 and AziA3 respectively.^{107, 108} Thus, there are additional condensation (C) and peptide carrier protein (PCP) domains located on AziA2 between AziA1 and AziA3 (Figure 29). The existence of AziA2 is one of the mysteries in the biosynthesis of azinomycins because condensation between these two substrates seems a simple reaction which occurs between the carbonyl carbon of the naphthoic acid and α -hydroxyl oxygen reduced from α -ketone by keto-reductase (KR) domain on AziA3. It is not clear why the

*Part of the data reported in this chapter is reprinted from "Activation of cryptic metabolite production through gene disruption: Dimethyl furan-2,4-dicarboxylate produced by *Streptomyces sahachiroi*" by Simkhada, D.; Zhang, H.; Mori, S.; and Watanabe C. M. H., 2013. *Beilstein J. Org. Chem.*, 9, 1768-1773, Copyright [2013] by the authors, Licensed by Beilstein-Institut.

naphthoic acid has to be transferred onto another PCP domain prior to the condensation reaction, which is seemingly an inefficient catalytic mechanism.

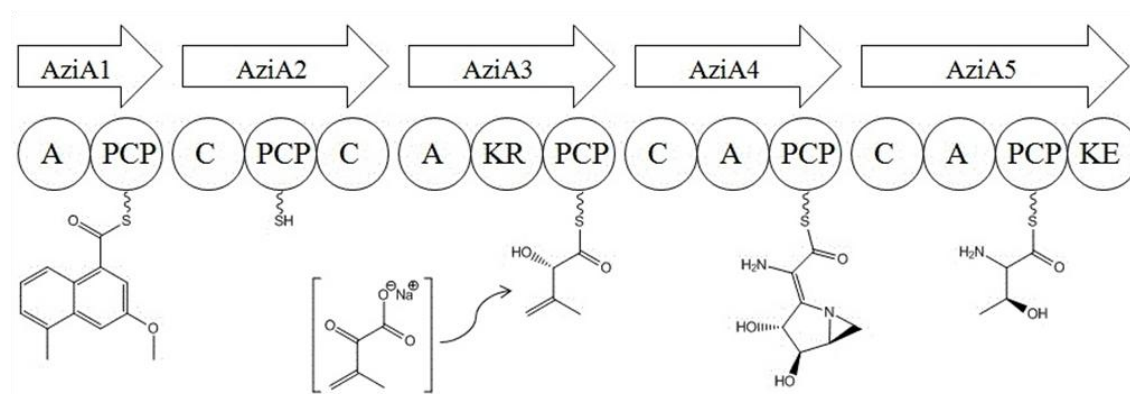


Figure 29. Azinomycin NRPS modules and their substrates

PRELIMINARY RESEARCH

The significance of AziA2 in azinomycin production was assessed by a functional knockout of *aziA2* in *S. sahachiroi*.¹⁰⁹ It was carried out by replacement of the middle portion of *aziA2* with a thiostrepton resistance gene (*tsr*) in the organism's genomic DNA. This was accomplished by double crossover with the shuttle vector pKC-AziA2, which was created from pKC1139 containing the apramycin resistance marker. The mutants were selected by thiostrepton and apramycin for single crossover, and the double crossover mutants were subsequently generated by selection by thiostrepton. The *aziA2* disruption mutant was confirmed by PCR and southern hybridization. Comparing the Reversed-Phase High Performance Liquid Chromatography (RP-HPLC) profile of the organic extract of *S. sahachiroi* wild type and the Δ *aziA2* mutant clearly showed that there was no production of azinomycins in the mutant. This indicated that AziA2 is an essential protein to produce azinomycins. Analysis of the mutant by RP-HPLC showed that the disruption of *aziA2* enhanced production of a non-azinomycin related natural

product which was eventually identified as dimethyl furan-2,4-dicarboxylate **55** (Figure 30).

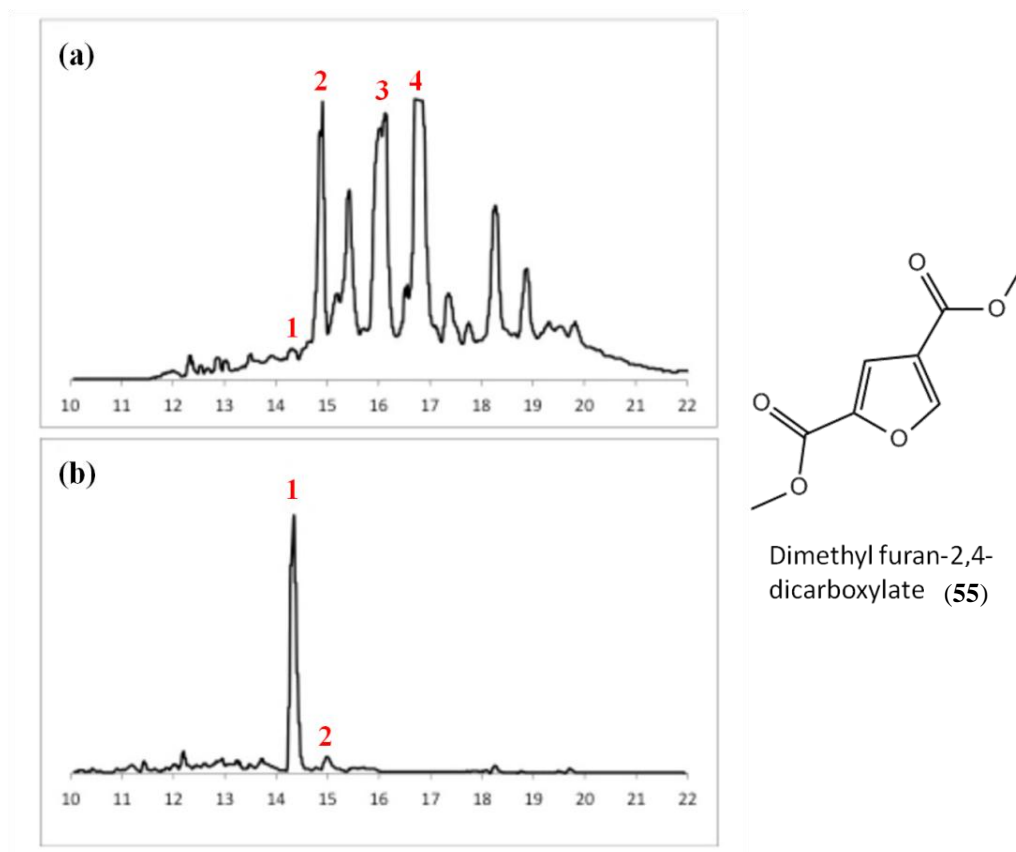


Figure 30. HPLC analysis of WT and $\Delta aziA2$ mutant

RP-HPLC profile of *S. sahachiroi* crude organic extract of WT (a) and of $\Delta aziA2$ (b). 1: dimethyl furan-2,4-dicarboxylate (**55**), 2: 3-methoxy-5-methyl-1-naphthoic acid (**4**), 3: azinomycin A (**1**), 4: azinomycin B (**2**). The chemical structure of dimethyl furan-2,4-dicarboxylate is shown on right.

The overproduction of dimethyl furan-2,4-dicarboxylate in the disruption mutant could be explained by the fact that regulation of genes in microorganisms is highly dependent on the external or internal environment.¹³⁵ Gene clusters in the genome are activated depending on specific factors to which the microorganisms are exposed while

other gene clusters remain silent until they are demanded. In the $\Delta aziA2$ *S. sahachiroi* mutant, genes which produced dimethyl furan-2,4-dicarboxylate were activated. A new question arose from this observation: whether the compound was produced as a replacement of the cytotoxic azinomycins or for other beneficial purposes.

RESULTS AND DISCUSSION

Cytotoxicity and Chemotaxis Assays against Jurkat Cells

Organic extract of *aziA2* disruption mutant and its purified major product, dimethyl furan-2,4-dicarboxylate, were assessed against Jurkat cells, a human T lymphocyte cell line, for cytotoxicity and inhibition of chemotaxis. Cytotoxicity assays were performed by incubation with the samples for 24 h. Chemotaxis assays were performed utilizing Boyden chambers.¹³⁶ FTY720 (fingolimod), a derivative of the natural product myriocin produced by *Iscaria sinclarli*, was used as a control. It is known as an immunomodulating drug that inhibits lymphocyte migration from lymphoid organs.¹³⁷

A Boyden chamber has two wells separated by a membrane which can be penetrated by certain cancer cells but keeps chemical substances from mixing between wells. In the chemotaxis assay, cells are added into the top well with fresh culture medium; a nutrient source (chemotactic agent) and a test substance are added to the bottom well. Following incubation, the bottom well is observed for cells. Cells will be present if the test substance does not inhibit the chemotactic activity, but cells remain in the top well if the test substance is active. The number of live cells in each well was counted by green fluorescent (GR) dye staining of the nuclei followed by fluorescent detection.

Compared to the wild type extract which contains azinomycins as antitumor agents, it was shown that both the crude extract of the *aziA2* disruption mutant and purified dimethyl furan-2,4-dicarboxylate have neither cytotoxicity nor inhibit the chemotactic activity of Jurkat cells (Figure 31 and Appendix Figure 80). This

observation showed no antitumor activities of dimethyl furan-2,4-dicarboxylate and also suggested that *S. sahachiroi* does not produce organic extractable antitumor secondary metabolites other than azinomycins.

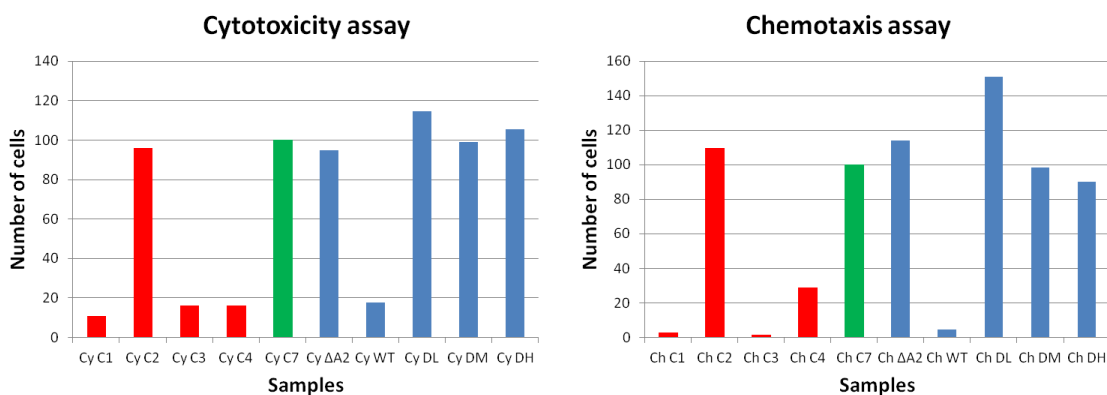


Figure 31. Cytotoxicity and chemotaxis assay against Jurkat cells

The number of cells is the relative numbers to the control (green) which is assumed 100.

Cytotoxicity assay: Cy C1: control without FBS in the culture medium, Cy C2: control without any samples, Cy C3: control with FTY720 (1.0 $\mu\text{g/mL}$), Cy C4: control with FTY720 (0.75 $\mu\text{g/mL}$), Cy C7: control with 1 μL of stock solution (methanol/ethyl acetate/t-butyl methyl ether = 60/30/10), Cy ΔA2 : *aziA2* disruption mutant extract, Cy WT: wild type extract, Cy DL: 1 $\mu\text{g/mL}$ of dimethyl furan-2,4-dicarboxylate, Cy DM: 10 $\mu\text{g/mL}$, Cy DH: 25 $\mu\text{g/mL}$. **Chemotaxis assay:** Ch C1: control without FBS in the bottom well, Ch C2: control without any samples, Ch C3: control with FTY720 (1.0 $\mu\text{g/mL}$), Ch C4: control with FTY720 (0.75 $\mu\text{g/mL}$), Ch C7: control with 1 μL of stock solution, Ch ΔA2 : *aziA2* disruption mutant extract, Ch WT: wild type extract, Ch DL: 1 $\mu\text{g/mL}$ of dimethyl furan-2,4-dicarboxylate, Ch DM: 10 $\mu\text{g/mL}$, Ch DH: 25 $\mu\text{g/mL}$.

Anti-Bacterial and Anti-Fungal Assays

Dimethyl furan-2,4-dicarboxylate was also assayed against two bacteria, the gram-negative *Escherichia coli* and the gram-positive *Bacillus subtilis* for anti-bacterial activity which azinomycins have been shown to have, and against the fungus, *Saccharomyces cerevisiae*, for anti-fungal activity (Figure 32).^{81, 82} It was shown that dimethyl furan-2,4-dicarboxylate did not inhibit growth of these microorganisms, which

suggested that the *aziA2* disruption mutant no longer has its natural defense system against these invaders. This might explain why *S. sahachiroi* has achieved and continued to maintain the production of such complex natural products which require many energy consuming genes and proteins for their biosynthesis. Production of azinomycins seems to be an important survival strategy for the bacterium. It also could be postulated that it was not necessary for *S. sahachiroi* to activate other gene clusters and overproduce alternative weapons for survival because of the sterilized medium environments where there were no other inhabitants. In other words, dimethyl furan-2,4-dicarboxylate could be overproduced for other beneficial purposes.

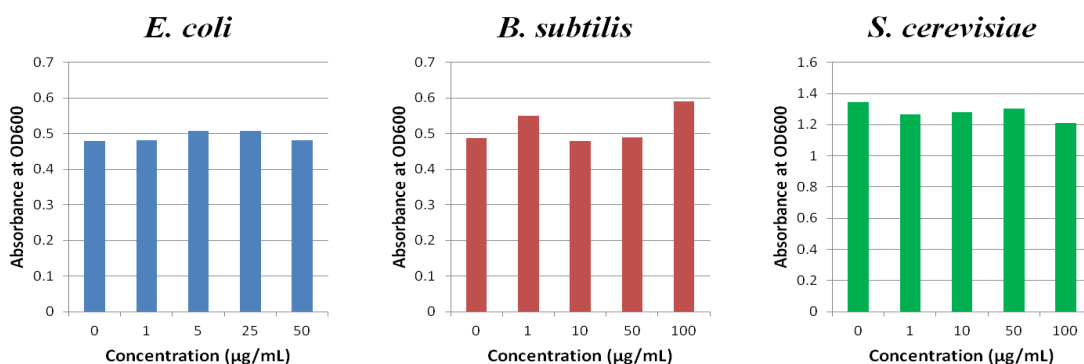


Figure 32. Antibacterial and antifungal assays

Neurite Outgrowth Assay

To evaluate other properties of the natural product purified from the *aziA2* disruption mutant organic extract, dimethyl furan-2,4-dicarboxylate, neurite outgrowth assay was performed on PC-12 cells. The PC-12 cell line which was derived from the rat neuroendocrine tumor, pheochromocytoma, stops dividing and starts differentiating into neuron like cells several days after exposure to an appropriate neural growth factor.^{138, 139} This was observed in the control assay where all-trans-retinoic acid was used as the growth factor.^{140, 141} PC-12 cells incubated with dimethyl furan-2,4-dicarboxylate,

however, continued growing in number (Figure 33). This observation showed that the novel natural product does not possess activity as a neurite outgrowth factor.

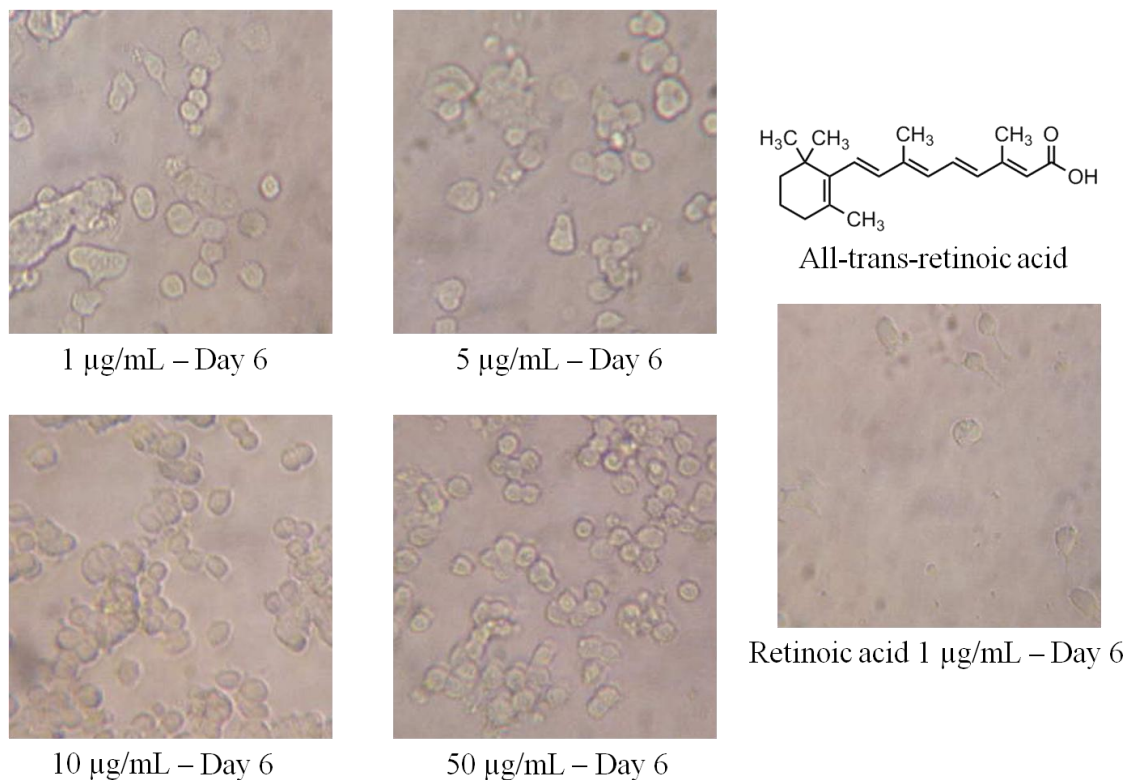


Figure 33. Neurite outgrowth assay

PC-12 cells were incubated with 1, 5, 10, or 50 µg/mL of dimethyl furan-2,4-dicarboxylate for 6 days. All-trans-retinoic acid (1 µg/mL) was used as the control of neuronal differentiation. Retinoic acid made PC-12 cells stop dividing and start differentiating.

SIGNIFICANCE

It has been shown that dimethyl furan-2,4-dicarboxylate, which is overproduced by the *aziA2* disruption mutant of *S. sahachiroi*, does not share antitumor or antibacterial activity with the azinomycins. The molecule neither displays antifungal activity nor enhances neurite outgrowth of PC-12 cells. The compound may be generated as a

replacement for azinomycins, but it is not biologically active or has a narrow spectrum of activity. This may be the beginning of evolution process, in which the bacterium starts synthesizing a new secondary metabolite which could or could not be bioactive. It is also possible that dimethyl furan-2,4-dicarboxylate was not produced as a replacement for azinomycins, but was produced for other purposes. This may be caused by lack of azinomycin production or *aziA2* dysfunction, which could cause an internal environmental change of *S. sahachiroi* comparing to the wild type. Production of antibiotics is not essential for the organism in a research lab because there are no competitors in the sterilized culture medium. The compound was possibly produced for other biosynthetic pathways which might be limited by lack of energy consumed by azinomycin production in the wild type *S. sahachiroi*. Therefore, it is possible that Δ *aziA2* *S. sahachiroi* activates a gene cluster to synthesize a novel natural product if the disruptant is exposed to the external stimulus including the existence of competitors or other stress factors.

The other interesting topic of AziA2 is the mystery of its unusual architecture, which will be evaluated in the future. AziA2 has sequential domains of C-PCP-C domains whose first C domain is thought to catalyze a transfer of 3-methoxy-5-methyl-1-naphthoic acid to the PCP domain from another PCP domain of AziA1 (A-PCP module), and the second C domain is thought to catalyze a condensation between the naphthoic acid and a substrate of AziA3 (A-KR-PCP module), putatively 3-methyl-2-oxo-but-3-enoic acid. Why does this unique protein contain extra C and PCP domains for the condensation between the substrates? The direct analysis of the protein is difficult because it is a module which does not perform a catalytic reaction alone and is a part of the NRPS/PKS hybrid containing four other modules. It is essential to examine the overall function of AziA2 in the presence of substrate bound AziA1 and AziA3. The necessity and function of the extra C-PCP domains could be assessed by various experiments including mutation and disruption studies on these domains to evaluate if a mutant lacking these domains is still able to catalyze the condensation reaction. Overexpression of only these domains could be useful in examining the transfer of the

naphthoic acid. Understanding of the function of AziA2 would shed new light on the activity and function of this NRPS/PKS hybrid.

MATERIALS AND METHODS

Chemicals and General Procedures

Jurkat clone E6-1, PC-12, culture medium RPMI 1640, fetal bovine serum (FBS), and antibiotic penicillin-streptomycin solution (x100) were purchased from American Type Culture Collection (ATCC, Manassas, VA, USA). Heat-inactivated horse serum (HHS) was purchased from Life Technologies (Termo Fisher Scientific, Waltham, MA, USA). Frozen stock of Jurkat cells was cultivated in a sterilized Petri dish with 15 mL RPMI with 10 % FBS and 150 μ L antibiotic solution at 37 °C in 5 % CO₂ for 3-4 days. Before the culture medium turned yellow, 5 mL of the medium was transferred into 75 cm² culture flasks where 25 mL of fresh RPMI medium with FBS and 250 μ L of antibiotic solution were added. This step was repeated every 3-4 days to keep the cells from being overgrown and unhealthy. PC-12 cells were cultivated in the same manner except for the following. Collagen coated dishes (Collagen Type IV, BioCoat, Becton Dickinson, Franklin Lakes, NJ, USA) were used culturing. The medium contained 5 % FBS and 10 % HHS but did not contain antibiotic.

Cytotoxicity Assay against Jurkat Cells, Human Cell Line of T Lymphocyte

Jurkat cells were cultivated in the cell culture medium (RPMI 1640 with 10% fetal bovine serum) and maintained in 75 cm² culture flasks at 37 °C in 5% CO₂. Cells were harvested by centrifugation (10 min at 1000 rpm), washed twice with the fresh culture medium without serum, and resuspended in the fresh culture medium. The number of cells was counted by hemocytometer, and the medium volume was adjusted to give 2,000,000 cells/mL. 100 μ L of cells (200,000 cells) was added to 600 μ L of cell culture medium in 24-well plates which contained either dimethyl furan-2,4-dicarboxylate or aziA2 disruption mutant and wild type extracts at a final concentration

of 1, 10, or 25 $\mu\text{g}/\text{mL}$. Cells were incubated for 24 hours and transferred to 1.5 mL eppendorf tubes to centrifuge for 15 min at 14,000 rpm. The medium was removed, and cells were washed with phosphate buffered saline (PBS) without manganese and calcium ions. Cells were lysed and stained by CyQUANT® Cell Proliferation Assay Kit (Invitrogen), and subsequently placed in a black 96-well plate and analyzed using a Bio-Tek fluorometer to measure relative fluorescence.

Chemotaxis Assay against Jurkat Cells, Human Cell Line of T Lymphocyte

Cells were harvested and counted as detailed above. Transwell®, 24 well plates with permeable supports (5.0 μm polycarbonate membrane, Boyden chamber, Costar) were used. The bottom well contained 600 μL of cell culture medium with 1 $\mu\text{g}/\text{mL}$, 10 $\mu\text{g}/\text{mL}$, or 25 $\mu\text{g}/\text{mL}$ of either dimethyl furan-2,4-dicarboxylate or 25 $\mu\text{g}/\text{mL}$ of *aziA2* disruption mutant and wild type extracts. 100 μL of cells (200,000 cells) was added to the top well. After incubation for 24 hours, cells were collected from the bottom well to assess how many cells migrated. Cells were collected and analyzed by the same method as detailed for the cytotoxicity assay.

Anti-Bacterial and Anti-Fungal Assays

Escherichia coli (DH10b) was cultivated in 5 mL of LB medium at 37 °C overnight. Cells were diluted with the fresh medium to give $\text{OD}_{600} = 0.1$. 100 μL of diluted cells was added to 96-well plates containing the final concentrations of 0, 1, 5, 25, 50 $\mu\text{g}/\text{mL}$ of dimethyl furan-2,4-dicarboxylate. Following incubation at 37 °C for 24 hours, the cell density was measured with a Bio-Tek microplate reader. For *Bacillus subtilis*, nutrient broth (Difco, Becton Dickinson) was used as the culture medium, and for *Saccharomyces cerevisiae*, cells were cultured in YPG medium (yeast extract, 10 g; peptone, 20 g; galactose, 20 g for 1 L) at 30 °C. The final concentrations of the compound for these two were 0, 1, 10, 50, 100 $\mu\text{g}/\text{mL}$.

Neurite Outgrowth Assay

PC-12 neuronal cells were cultivated in 100 mm Collagen Type IV dishes at 37 °C in 5% CO₂ with RPMI 1640, supplemented with 10% HHS and 5% FBS. The cells were collected from the culture dish by flushing with the serum free medium and transferred to a 15 mL falcon tube. The cells were centrifuged for 15 min at 1000 rpm, washed twice with the serum free medium, and resuspended in RPMI 1640 with a trace amount of serum (0.5 % heat-inactivated horse serum and 0.25 % fetal bovine serum) to give 50,000 cells/mL. The cells (200 µL) were transferred to a 96-well Collage Type IV plate (10,000 cells/well). Following 24 h incubation for to allow the cells to adhere to the plate, dimethyl furan-2,4-dicarboxylate was added to give final concentrations of 1, 5, 10, and 50 µg/mL. Each well was visually monitored over 1 week for neurite outgrowth and intercellular connections.

CHAPTER IV

DISCOVERY AND EVALUATION OF MACRO-LACTONE ANTI-METASTATIC MARINE NATURAL PRODUCT, NUIAPOLIDE*

INTRODUCTION

Natural product extracts have been used as crude drugs for thousands of years in locations all over the world, such as Mesopotamia, Egypt, India, and China.¹⁷⁻²⁰ They have been used in combinations of diverse natural products produced by one or more organisms for treating various diseases and symptoms including pain, inflammation, and infection. The history of herbal drug use clearly shows the significance of natural products as medicines. The techniques utilized to prepare and develop these therapies have occasionally misled physicians, sometimes leading to treatment of patients with unbeneficial or even toxic substances. This was especially common before robust statistical analysis methods had been developed. The natural product industry entered into a new era after the discovery of penicillin in 1928, which was the first pure antibiotic isolated from the fungus *Penicillium rubens*.^{12, 29} Although it took more than ten years for penicillin to be clinically applied, the remarkable success led researchers to the large-scale exploration of other microorganisms in all kind of environments on earth. This has provided a great diversity of compounds with high selectivity and specificity of action. This is difficult to reproduce when studying synthetic compounds. In the period of 01/1981-12/2010, natural product relating compounds occupy 50.3 % of all the new approved drugs.¹ The search for bioactive natural products has been hastened by the development of high throughput screening (HTS) methods in early 1990s, which

*Majority of the data reported in this chapter is reprinted from “Macrolactone Nuiapolide, Isolated from a Hawaiian Marine Cyanobacterium, Exhibits Anti-Chemotactic Activity” by Mori, S.; Williams, H.; Cagle, D.; Karanovich, K.; Horgen, F. D.; Smith, R., III; Watanabe, C. M. H., 2015. *Mar. Drugs*, 13, 6274-6290, Copyright [2015] by the authors, Licensed by MDPI, Basel, Switzerland.

currently can assess more than 250,000 samples per day.¹⁴²

The most important source of natural products is *Streptomyces* consisting of more than 500 species and thousands of strains, which makes it the largest genus of Actinobacteria.¹⁴³ *Streptomyces* species have large genomes for bacteria, containing substantial numbers of genes involved in the production of secondary metabolites. This allows the species to produce more than two-thirds of all known antibiotics of natural origin, including streptomycin, chloramphenicol, tetracycline, etc.¹⁴⁴ Another aspect making the bacteria popular is their relative ease to collection and cultivation. The species is predominantly found in soil which is easy to access and study in a regular biological laboratory. It has been hypothesized that environments that people cannot easily investigate possess a much greater source of natural products.¹⁴⁵ The ocean covers more than 70% of the earth's surface. The microbial population in seawater samples was examined based on the data collected by Sorcerer II Global Ocean Sampling (GOS), and it was estimated that there were more than 6,000,000 proteins available. This is nearly twice the number of proteins existing in the previous database, and some of them had no similarities to known proteins.¹⁴⁶ The data supports the idea that there is a high diversity of natural products in ocean microbial communities.

Halichondrin B is a recent example of a successful marine natural product. It was isolated from a marine sponge *Halichondria okadai* and found to have anticancer activity in 1986.¹⁴⁷ Through the synthetic study of the compound, it was revealed that the simplified analog of the natural product, named eribulin, possessed the same level of activity as the parent compound.^{148, 149} Eribulin was eventually approved by the Food and Drug Administration (FDA) in 2010, by the European Medicines Agency (EMA) in 2011, and subsequently by other countries.^{150, 151} Other marine natural products and/or their derivatives have also been marketed such as ziconotide (Prialt®, Elan Pharmaceuticals) from a tropical cone snail for the treatment of pain, cytarabine (Cytosar-U, Teva Pharmaceuticals) and ecteinascidin 743 (Yondelis®, Pharma Mar S.A.) for the treatment of cancer, and omega-2-acid ethyl esters (Lovza®, GlaxoSmithKline) for the treatment of hypertriglyceridemia.¹⁵²⁻¹⁵⁴

Natural products are investigated as therapies for various types of disease, including cancer which is the greatest cause of human death in many developed countries.⁴⁰⁻⁴³ Cancers appear when living cells fail to destroy themselves by apoptosis after mutations in certain directions caused by genetics, life styles, exposure to carcinogens, or their combination.¹⁵⁵ Because all adult cells have the potential to become cancer cells, there are countless types of cancer. This creates a substantial hurdle for cancer treatment. There are two additional barriers which make treatment complicated. One is the fact that human immunity, which people naturally possess, rarely destroys cancer cells once they start growing because they arose from normal cells which are not attacked by immune cells.¹⁵⁶ Therefore, cancer cells do not stop growing until they finally kill the patient. The other major problem of cancer is metastasis, a phenomenon of the cancer spread from one location to another through the circulatory system of the body, such as cardiovascular and lymphatic systems.¹⁵⁷ Because many cancers are not visible and do not cause symptoms until they grow sufficiently large, they may hide in other parts of the body for months or years even though cancer at the original site is well treated. This ultimately tends to be the source of death for the patients. Therefore, preventing metastasis is equally important to annihilating cancer cells.

Cancer metastasis is enhanced by chemotaxis, the migration of a cell by response to a chemical stimulus.¹⁵⁸ Chemotaxis is seen in almost all organisms, including single-cell and multicellular organisms. Single-cell organisms, such as bacteria, approach nutritional chemicals but flee from toxic chemicals.¹⁵⁹ Multicellular organisms utilize the phenomenon for single cell functions, such as the movement of sperm toward an egg or of immune cells toward their targets.^{160, 161} The process, however, also inevitably enables some cancer cells to migrate from one location to another, triggering the development of cancers at the new site. Because many cancers are not visible and do not present symptoms until they grow sufficiently large, they may hide in other parts of the body for months or years even though the original cancer has been eliminated. Therefore, finding a chemical which blocks the chemotactic activity of cancer cells adds a new strategy toward cancer treatment as an anti-metastatic agent.¹⁶² The chemical is also desired to

have no cytotoxicity because cytotoxic chemicals to cancer cells tend to be cytotoxic to the normal cells leading to adverse reactions.

RESULTS AND DISCUSSION

Evaluation of Hawaiian Marine Natural Product Extracts for Anti-Chemotactic Behavior

To identify putative immunosuppressive or anti-metastatic agents from natural products, microorganisms in Hawaiian ocean were assessed in several steps. A total of 560 crude extract samples, which include various organisms and various extraction methods, were evaluated for their ability to inhibit the chemotactic activity of Jurkat cells.¹³⁶ Jurkat is an immortalized line of human T lymphocyte cells that are capable of exhibiting migration toward a nutrient source, fetal bovine serum (FBS).¹⁶³ Boyden chambers were used to assess the activity of the extracts because Jurkat cells are suspension cells.¹³⁶ FTY720, a derivative of the natural product myriocin and an approved drug for the treatment of multiple sclerosis (MS), was utilized as a control substance.¹³⁷

The crude extract samples were assayed at 25.0 µg/mL which is considered as micro-molar concentration scale for a majority of natural products. The result was visually observed with an inverted microscope (Figure 34). It was clearly shown that there was cell migration when the chemotactic agent fetal bovine serum (FBS) was present (Figure 34-b comparing to Figure 34-a), but the cells did not approach the high concentrated nutrient location when an active compound was present (Figure 34-c and Figure 34-d). However, the dead cells were observed in the presence of FTY720 which is known as a cytotoxic agent, but the cells were alive with the CL13-F10 sample. 50 samples including CL13-F10 were found to inhibit the chemotactic activity of Jurkat cells, which were subjects to assess for cytotoxicity.

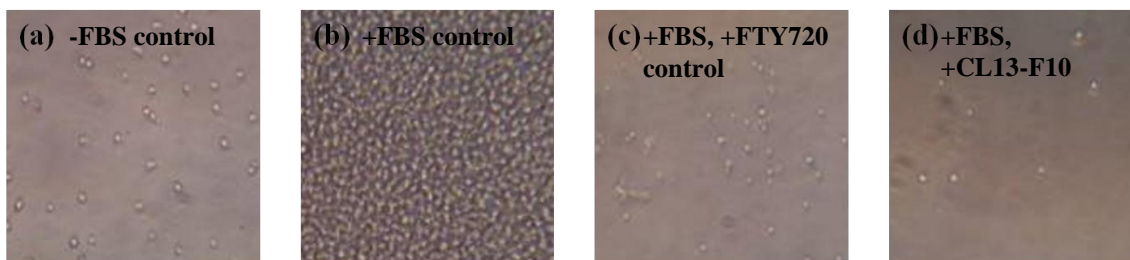


Figure 34. Evaluation of Jurkat cultures in the Boyden chamber assay

Microscopic images of the bottom well of Boyden chambers after 24 h incubation; **(a)**: – FBS and – chemotactic agent, **(b)**: + FBS and – chemotactic agent, **(c)**: + FBS and + FTY720, **(d)**: + FBS and + CL13-F10. Shrinkage of cells in (c) is indicative of cell death.

Cytotoxicity Assay for Active Crude Extracts

An ideal natural product with anti-metastatic potential would be one which inhibits the chemotactic activity but does not have cytotoxicity because most chemicals which are cytotoxic to cancer cells are also cytotoxic to healthy cells. 50 samples capable of inhibiting Jurkat cell chemotaxis were assessed for their cytotoxicity. The relative number of live cells was counted by fluorescent emission followed by green fluorescent (GR) dye staining, and it was compared to the relative number of live cells in the control sample which did not contain the test substances. It was shown that 7 out of 50 samples did not demonstrate cytotoxicity against Jurkat cells at the concentration of 25.0 $\mu\text{g/mL}$ (Figure 35).

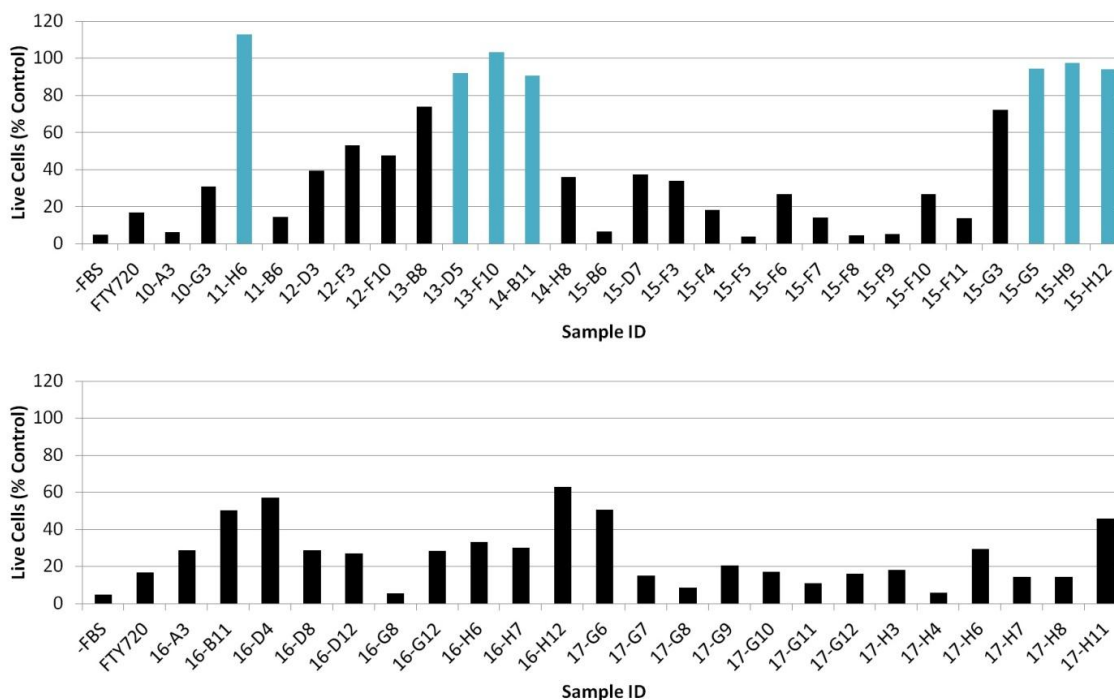


Figure 35. Cytotoxicity profile analysis of extracts

The turquoise bar represents samples where the percentage of live cells is > 90 % of the control. The black bar represents samples where the percentage of live cells is < 90 %. Controls included wells grown without FBS (-FBS) and with FTY720 (5 $\mu\text{g/mL}$). Sample codes are library plate number and coordinate on the plate.

Evaluation of Fractionated Extracts for Anti-Chemotactic Behavior

The sample CL013-F10 (SM 1-12-16), which was the water and solid phase extract of the Cyanobacterium 071905-NII-01, was chosen for further evaluation because it had better chemotaxis inhibition activity at lower dosage, and it did not kill cells at these concentrations (10 $\mu\text{g/mL}$) (Appendix Figure 81). The active samples, which were extracted with dichloromethane (FR022) or methanol (FR023), were fractionated (1 min/fraction) into 24 wells in a 96-well plate for further chemotaxis assays. Each fraction from both extracts was examined for anti-chemotactic activity of Jurkat cells. Each extract provided three active fractions. The retention times of the active fractions for each extract were different from one another. The active fractions from FR022 were A3 (4-5 min), A11 (12-13 min), and A12 (13-14 min) (Figure 36-a),

and the active fractions from FR023 were A8 (9-10 min), B2 (15-16 min), and B3 (16-17 min) (Figure 36-b).

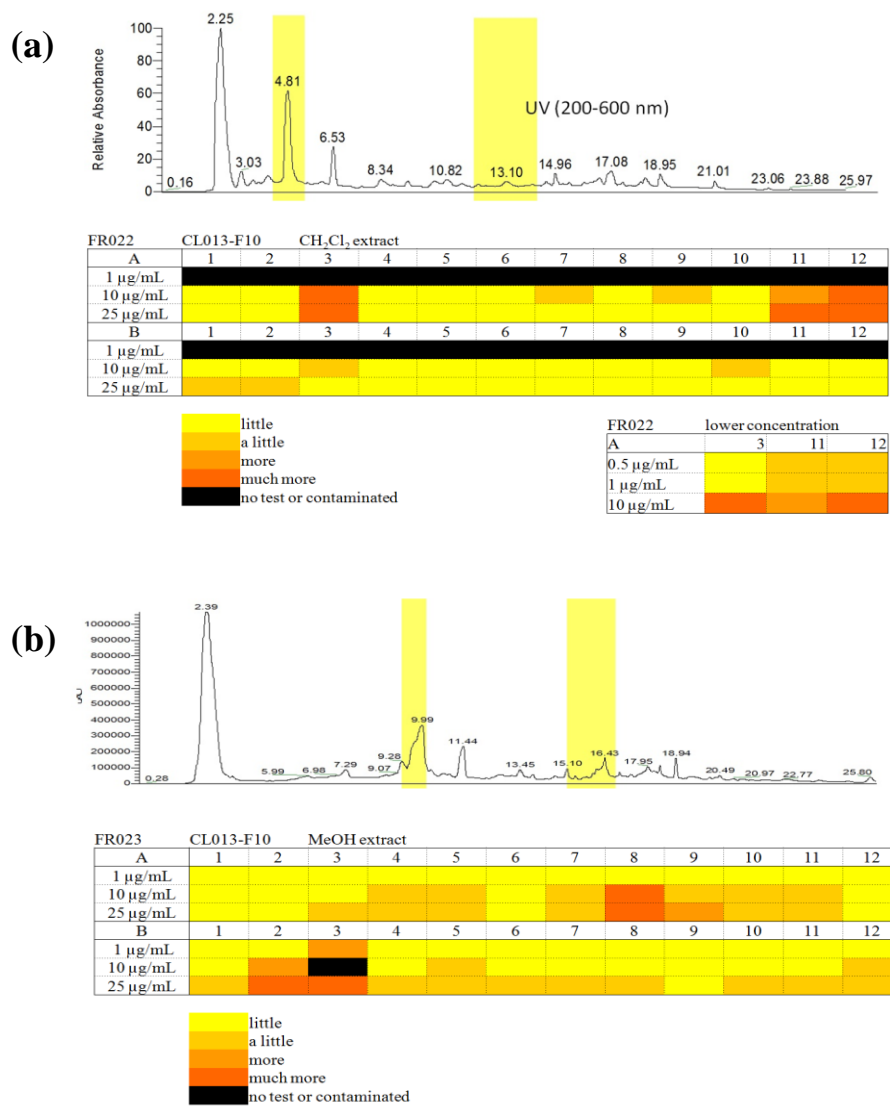


Figure 36. Fragmentation of CL013-F10 (Dr. David Horgen) and chemotaxis assays
 The samples were extracted with (a) dichloromethane (FR022) and (b) methanol (FR023), and each fraction was assessed for inhibition Jurkat chemotactic activity. The yellow bars in the LC profile are the active fractions. Yellow to orange colors in the table represents the level of activity.

The LC profiles and activity patterns of FR022 and FR023 showed similar patterns except the retention times of the active components were shifted reflecting the different gradients of the separation. This suggested the same active components were present in both samples with FR022 fractions A3 and A11/A12 corresponding to FR023 fractions A8 and B2/B3, respectively and likewise, activity at A11 and A12 from FR022 (corresponding to B2 and B3 from FR023). This was confirmed by photodiode array (PDA) map and LC-MS (Appendix Figure 82-Appendix Figure 86). Fractions FR022-A3/FR023-A8 showed a major component with a mass of 788.6 ± 0.2 Da (m/z 789.6, compound **56**). These two natural products, which had molecular masses of 788.6 ± 0.2 Da (compound **56**) and 982.7 ± 0.2 Da (NP982), respectively, were subjected to purification by LC-MS. Compound **56** was isolated to purity, its anti-chemotactic activity confirmed and was obtained in sufficient quantities for further analysis (Appendix Figure 87). Nuiapolide (**56**) showed chemotactic activity at concentrations as low as $1 \mu\text{g/mL}$ ($1.3 \mu\text{M}$) (Figure 37 and Appendix Figure 87). Isomeric components of NP982 and low isolated yields precluded further analysis.

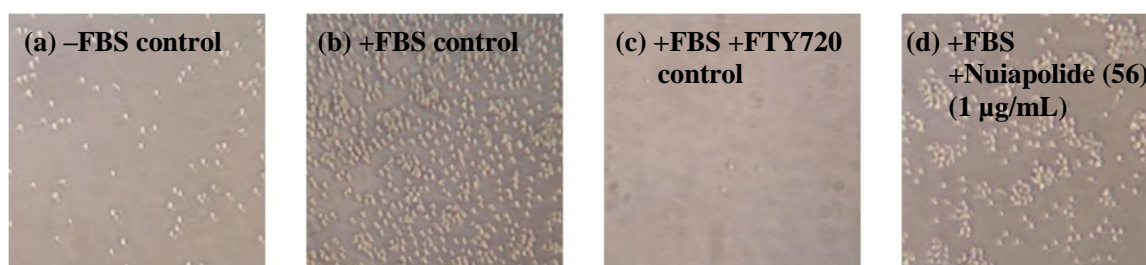


Figure 37. Evaluation of nuiapolide (56**) activity at $1 \mu\text{g/mL}$**

Images of microscope fields of the bottom well after 24 h of incubation; (a): bottom well received no FBS and no test substance, (b): bottom well received 10 % FBS and no test substance, (c): bottom well received 10 % FBS and FTY720 ($5 \mu\text{g/mL}$), (d): bottom well received 10 % FBS and Nuiapolide (**56**) ($1 \mu\text{g/mL}$).

Cell Cycle Analysis of Nuiapolide (56)

The effect of Nuiapolide (56) to Jurkat cell cycle was analyzed by flow cytometry. The population ratio in the cell cycle phases of the living cells was calculated from the histogram of flow cytometry, which distinguishes the state of cells into three distinct phases; Gap 0 (G0) or Gap 1 (G1), Synthesis (S), and Gap 2 (G2) or Mitosis (M) phases.^{164, 165} The cell cycle is divided into four phases and one resting phase, G0 in which cells leave the cycle and stop dividing. In the interphase state where cells continue growing the size and synthesizing a new copy of DNA, there are three phases, G1, S, and G2. G1 phase is the growth or Gap 1 phase and represents the first of the four phases of the cell cycle. The G1/S phase transition is a major checkpoint in the cell cycle, with S-phase representing the point in the cell cycle when DNA replication occurs. G2 phase is a period of rapid cell growth and protein synthesis as the cell prepares itself for cell division. The G2/M phase transition is another major checkpoint in the cell cycle, with M phase representing the final phase of the cell cycle; the cell's nucleus is separated into two identical sets of chromosomes and cytokinesis occurs, *i.e.* the cell divides into two daughter cells.

The Jurkat cells were incubated with nuiapolide (56) for up to 6 h. The flow cytometry analysis showed the significant decrease of ratio of G0/G1 phase in all the incubation times in comparison to the control (0 h). S phase decreased but G2/M phase increased over time, which displayed that the cells could progress into S and following G2/M phase but arrested at the last stage. It suggested that nuiapolide (56) allows cells to synthesize new DNAs, but it inhibits the efficient cell division (Figure 38 and Appendix Figure 88). We did not observe any 8N cells; the cell cycle is perturbed where there is a slowing or block in G2/M.

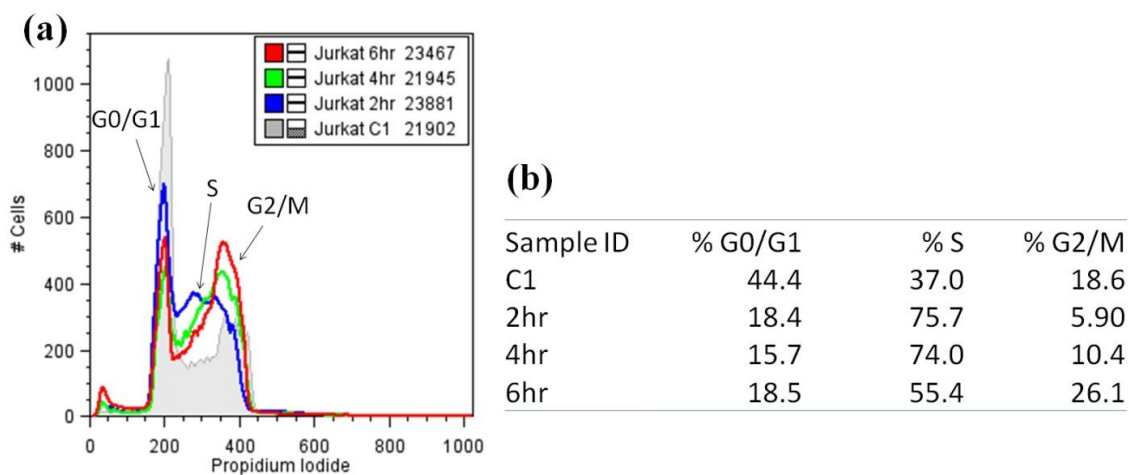


Figure 38. Cell cycle analysis of nuiapolide (56) treated Jurkat cells

The Jurkat cells were analyzed by flow cytometry after 2, 4, and 6 h incubation with nuiapolide (56). It was shown that change of the ratio of G0/G1, S, and G2/M phases over the time course including the control which was prior to nuiapolide (56) treatment was shown in a histogram (a) and on a table (b). In the histogram, the peak around at 200 nm absorption, a gap between two peaks, and the peak around at 400 nm absorption represent G0/G1, S, and G2/M phases respectively.

Structural Analysis of Nuiapolide (56)

The molecular formula of nuiapolide (56) was established as $C_{44}H_{84}O_{11}$ based on HRMS (m/z $[M+H]^+$ 789.6076, calcd for $C_{44}H_{85}O_{11}$, 789.6092; $[M+Na]^+$ 811.5895, calcd for $C_{44}H_{84}O_{11}Na$, 811.5911) and requires three degrees of unsaturation. The structure was elucidated by 1H NMR, ^{13}C NMR, ^{13}C NMR DEPT, COSY, TOCSY, HSQC, HSQC-TOCSY, in methanol- d_4 and DMSO- d_6 (Figure 40-Figure 55 and Table 3). ^{13}C NMR showed 15 distinct signals, some of which (δ_C 20.8-21.5, 36.2-37.4, and 69.8-70.8) were overlapped with multiple peaks. HSQC correlation paired the 1H and ^{13}C NMR signals. C-40 at δ_C 33.91, C-1 at δ_C 166.90, and C-3 at δ_C 161.20, which were absent in the HSQC correlation and DEPT, were predicted as R_4C for C-40 and a substituted alkene or carbonyl carbon for C-1 and C-3. In HMBC, C-40 correlated with H-41-43 (δ_H 0.93) and H-39 (δ_H 5.02). As nine protons were predicted to be at H-41-43, C-40 and C-41-43 are due to a tert-butyl group attached to C-39. Based on the chemical

shift and HMBC correlation between H-39 and C-1, C-39 and C-1 were assigned as an α -carbon on an oxygen linkage and carbonyl carbon respectively, indicating that the molecule is an ester. C-1 had an HMBC correlation with alkene proton H-2. H-2 correlated with C-3, which also exhibited correlations with H-4 and H-44. Since H-44 consisted of 3 protons, this gives methyl substitution on the alkene C-3 on which C-4 extends the carbon chain further. No additional unsaturated carbons or substitutions were found except for hydroxyl groups present in the molecule, thus confirming that nuiapolide (**56**) is a macrolactone with an alkene and two side chains locating near the ester functional group (Figure 39) and nine hydroxyl groups distributed throughout the saturated hydrocarbon ring structure.

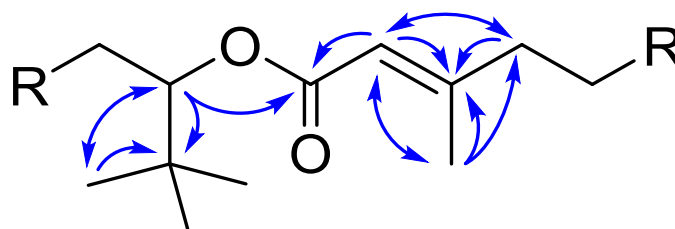


Figure 39. Partial structure of nuiapolide (56**) with key HMBC correlations**

Since three distinct signals of protons on hydroxyl carbons were found in the ^1H NMR, this signified three different environments for these hydroxyl groups. These protons (locations) were indicated as H-a, H-b, and H-c at δ_{H} 3.78, 3.57, and 3.42, respectively. H-a contains two protons which had TOCSY correlations with H-4 and H-b, but they neither had nor shared COSY correlation. This suggested that there were at least two carbons between H-a and others. In HSQC-TOCSY, in addition to correlations with carbons at δ_{C} 36.2-37.4, there was a correlation with C-8 (δ_{C} 43.51), which was proposed as the carbon between each H-a. H-c consists of one proton correlated with H-39 and H-b in TOCSY but not in COSY. H-c and H-39, however, shared a correlation in COSY. These indicated that there is one carbon between H-c and H-39 and at least two

carbons between H-c and H-b. Six protons in H-b were almost identical, thus their positions were likely equally distributed and spread enough not to affect each other. Two distinct HSQC-TOCSY correlations with δ_C 36.2-37.4 and 20.8-21.5 indicated there were two isolated environments between each H-b. This confirmed that the hydroxyl groups at H-b appear at every four carbons. Because of the ring size, there cannot be more than four carbons between H-b and H-a or H-c, indicating there are three carbons between these.

The proposed location of hydroxyl groups was confirmed by the number of carbons in environments through the ring structure (Appendix Figure 89). Nine hydroxyl carbons were found at δ_C 67.58 (C-37) and δ_C 69.8-70.8 (C-7, C-9, C-13, C-17, C-21, C-25, C-29, and C-33). There were 16 α -carbons of hydroxyl groups (except for C-8) at δ_C 37.55 (C-38) and 36.2-37.4 (C-6, C-10, C-12, C-14, C-16, C-18, C-20, C-22, C-24, C-26, C-28, C-30, C-32, C-34, and C-36). Seven β -carbons (except for C-5) were located at δ_C 20.8-21.5 (C-11, C-15, C-19, C-23, C-27, C-31, and C-35). The location of hydroxyl groups was further confirmed by ^1H NMR, ^{13}C NMR, COSY, TOCSY, and HMBC in DMSO- d_6 which showed signals of hydroxyl protons (Table 3 and Figure 50-Figure 55). The new peaks appeared at δ_H 4.14, 4.15, 4.44, and 4.47. COSY correlations showed that the peaks at δ_H 4.44 and 4.47 were from hydroxyl groups at position H-a, the peak at δ_H 4.14 was from H-b hydroxyl groups, and the peak at δ_H 4.15 was from position H-c, which was confirmed by a TOCSY correlation with H-39. HMBC showed correlations between δ_H 4.44/4.47 and C-8, between δ_H 4.14 and δ_C 36.2-37.4/69.8-70.8, and between δ_H 4.15 and C-38. Based on the above analyses, the structure of nuiapolide (**56**) was determined, as shown in Figure 40.

The structure suggested that the compound belongs to the polyketide class of natural products and displays structural similarity to the caylobolides, which were shown to be cytotoxic against some cancer cell lines.^{166, 167} Nuiapolide (**56**) and caylobolides A (**57**) and B (**58**) share the core structure of a macro-lactone. They contain a large saturated carbohydrate ring with several hydroxyl groups and similar side chains around the ester functional group. The number of carbons in the ring structure, however, was

slightly greater in compound **56** (39 carbons) than in caylobolides (35 carbons). Given the structure of **56** and its Hawaiian origins, we named it nuiapolide (**56**). Nuiapo means big circle in Hawaiian and “ide” indicates the macrolide.

Table 3. NMR spectral data for nuiapolide (56)

Position ^a	δ_{H} (<i>J</i> in Hz) in MeOH- <i>d</i> ₄	δ_{H} (<i>J</i> in Hz) in DMSO- <i>d</i> ₆	δ_{C} in MeOH- <i>d</i> ₄ , type	δ_{C} in DMSO- <i>d</i> ₆ , type	TOCSY	HSQC-TOCSY ^b	HMBC ^c
1	-	-	166.90, C	166.04, C	-	-	-
2	5.74, s	5.67, s	115.73, CH	116.69, CH	4, 44, 41-43	44	1, 3, 4, 44
3	-	-	161.20, C	160.04, C	-	-	-
4	2.58, m and 2.83, m	2.59, m	32.69, CH ₂	33.11, CH ₂	2, Ha, 5, 6, HC ^f	5	2, 3, 5
5	1.60, m	1.49, m	23.86, CH ₂	24.08, CH ₂	4, H-a, a-OH, HC ^f	-	4, C-i, C-iii
6 (C-i) ^d	1.49, m	1.31, m	36.2-37.4, CH ₂	37.2-38.1, CH ₂	4, H-a, a-OH, HC ^f	-	C-i, C-iii
7 (H-a) ^e (C-iii) ^d	3.78, s	3.58, s	69.8-70.8, CH	69.2-70.2, CH	4, a-OH, H-b, HC ^f	C-i, 8	-
(7)-OH	-	4.44, d (4.4) or 4.47, d (4.2)	-	-	H-a, HC ^f	-	8, C-i, C-iii
8	1.56, m	1.37	43.51, CH ₂	44.67, CH ₂	H-a, a-OH, HC ^f	C-i, C-ii, C-iii	C-iii
9 (H-a) ^e (C-iii) ^d	3.78, s	3.58	69.8-70.8, CH	69.2-70.2, CH	4, a-OH, H-b, HC ^f	C-i, 8	-
(9)-OH	-	4.44, d (4.4) or 4.47, d (4.2)	-	-	H-a, HC ^f	-	8, C-i, C-iii
10 (C-i) ^d	1.48-1.59, m	1.24-1.41, m	36.2-37.4, CH ₂	37.2-38.1, CH ₂	H-a, HC ^f	C-i, C-ii, C-iii	C-i, C-ii, C-iii
11 (C-ii) ^d	1.31-1.55, m	1.19-1.37, m	20.8-21.5, CH ₂	21.4-22.0, CH ₂	H-b, HC ^f	C-i, C-ii, C-iii	C-i, C-iii
12 (C-i) ^d	1.48-1.59, m	1.24-1.41, m	36.2-37.4, CH ₂	37.2-38.1, CH ₂	H-b, HC ^f	C-i, C-ii, C-iii	C-i, C-ii, C-iii
13 (H-b) ^e (C-iii) ^d	3.57, s	3.37, s	69.8-70.8, CH	69.2-70.2, CH	H-a, H-c, HC ^f	C-i, C-ii	-
(13)-OH	-	4.14, d (4.1)	-	-	H-b, HC ^f	-	C-i, C-iii
14 (C-i) ^c	1.48-1.59, m	1.24-1.41, m	36.2-37.4, CH ₂	37.2-38.1, CH ₂	H-b, HC ^f	C-i, C-ii, C-iii	C-i, C-ii, C-iii

Table 3 Continued

Position ^a	δ_{H} (<i>J</i> in Hz) in MeOH- <i>d</i> ₄	δ_{H} (<i>J</i> in Hz) in DMSO- <i>d</i> ₆	δ_{C} in MeOH- <i>d</i> ₄ , type	δ_{C} in DMSO- <i>d</i> ₆ , type	TOCSY	HSQC- TOCSY ^b	HMBC ^c
15 (C-ii) ^d	1.31-1.55, m	1.19-1.37, m	20.8-21.5, CH ₂	21.4-22.0, CH ₂	H-b, HC ^f	C-i, C-ii, C- iii	C-i, C-iii
16 (C-i) ^d	1.48-1.59, m	1.24-1.41, m	36.2-37.4, CH ₂	37.2-38.1, CH ₂	H-b, HC ^f	C-i, C-ii, C- iii	C-i, C-ii, C- iii
17 (H-b) ^e (C- iii) ^d	3.57, s	3.37, s	69.8-70.8, CH	69.2-70.2	H-a, H-c, HC ^f	C-i, C-ii	-
(17)-OH	-	4.14, d (4.1)	-	-	H-b, HC ^f	-	C-i, C-iii
18 (C-i) ^d	1.48-1.59, m	1.24-1.41, m	36.2-37.4, CH ₂	37.2-38.1, CH ₂	H-b, HC ^f	C-i, C-ii, C- iii	C-i, C-ii, C- iii
19 (C-ii) ^d	1.31-1.55, m	1.19-1.37, m	20.8-21.5, CH ₂	21.4-22.0, CH ₂	H-b, HC ^f	C-i, C-ii, C- iii	C-i, C-iii
20 (C-i) ^c	1.48-1.59, m	1.24-1.41, m	36.2-37.4, CH ₂	37.2-38.1, CH ₂	H-b, HC ^f	C-i, C-ii, C- iii	C-i, C-ii, C- iii
21 (H-b) ^e (C- iii) ^d	3.57, s	3.37, s	69.8-70.8, CH	69.2-70.2, CH	H-a, H-c, HC ^f	C-i, C-ii	-
(21)-OH	-	4.14, d (4.1)	-	-	H-b, HC ^f	-	C-i, C-ii
22 (C-i) ^d	1.48-1.59, m	1.24-1.41, m	36.2-37.4, CH ₂	37.2-38.1, CH ₂	H-b, HC ^f	C-i, C-ii, C- iii	C-i, C-ii, C- iii
23 (C-ii) ^d	1.31-1.55, m	1.19-1.37, m	20.8-21.5, CH ₂	21.4-22.0, CH ₂	H-b, HC ^f	C-i, C-ii, C- iii	C-i, C-iii
24 (C-i) ^d	1.48-1.59, m	1.24-1.41, m	36.2-37.4, CH ₂	37.2-38.1, CH ₂	H-b, HC ^f	C-i, C-ii, C- iii	C-i, C-ii, C- iii
25 (H-b) ^e (C- iii) ^d	3.57, s	3.37, s	69.8-70.8, CH	69.2-70.2, CH	H-a, H-c, HC ^f	C-i, C-ii	-
(25)-OH	-	4.14, d (4.1)	-	-	H-b, HC ^f	-	C-i, C-iii
26 (C-i) ^d	1.48-1.59, m	1.24-1.41, m	36.2-37.4, CH ₂	37.2-38.1, CH ₂	H-b, HC ^f	C-i, C-ii, C- iii	C-i, C-ii, C- iii
27 (C-ii) ^d	1.31-1.55, m	1.19-1.37, m	20.8-21.5, CH ₂	21.4-22.0, CH ₂	H-b, HC ^f	C-i, C-ii, C- iii	C-i, C-iii
28 (C-i) ^d	1.48-1.59, m	1.24-1.41, m	36.2-37.4, CH ₂	37.2-38.1, CH ₂	H-b, HC ^f	C-i, C-ii, C- iii	C-i, C-ii, C- iii
29 (H-b) ^e (C- iii) ^d	3.57, s	3.37, s	69.8-70.8, CH	69.2-70.2, CH	H-a, H-c, HC ^f	C-i, C-ii	-
(29)-OH	-	4.14, d (4.1)	-	-	H-b, HC ^f	-	C-i, C-iii
30 (C-i) ^d	1.48-1.59, m	1.24-1.41, m	36.2-37.4, CH ₂	37.2-38.1, CH ₂	H-b, HC ^f	C-i, C-ii, C- iii	C-i, C-ii, C- iii
31 (C-ii) ^d	1.31-1.55, m	1.19-1.37, m	20.8-21.5, CH ₂	21.4-22.0, CH ₂	H-b, HC ^f	C-i, C-ii, C- iii	C-i, C-iii

Table 3 Continued

Position ^a	δ_{H} (<i>J</i> in Hz) in MeOH- <i>d</i> ₄	δ_{H} (<i>J</i> in Hz) in DMSO- <i>d</i> ₆	δ_{C} in MeOH- <i>d</i> ₄ , type	δ_{C} in DMSO- <i>d</i> ₆ , type	TOCSY	HSQC-TOCSY ^b	HMBC ^c
32 (C-i) ^d	1.48-1.59, m	1.24-1.41, m	36.2-37.4, CH ₂	37.2-38.1, CH ₂	H-b, HC ^f	C-i, C-ii, C-iii	C-i, C-ii, C-iii
33 (H-b) ^e (C-iii) ^d	3.57, s	3.37, s	69.8-70.8, CH	69.2-70.2, CH	H-a, H-c, HC ^f	C-i, C-ii	-
(33)-OH	-	4.14, d (4.1)	-	-	H-b, HC ^f	-	C-i, C-iii
34 (C-i) ^d	1.48-1.59, m	1.24-1.41, m	36.2-37.4, CH ₂	37.2-38.1, CH ₂	H-b, HC ^f	C-i, C-ii, C-iii	C-i, C-ii, C-iii
35 (C-ii) ^d	1.31-1.55, m	1.19-1.37, m	20.8-21.5, CH ₂	21.4-22.0, CH ₂	H-b, HC ^f	C-i, C-ii, C-iii	C-i, C-iii
36 (C-i) ^d	1.42, m	1.28, m	36.2-37.4, CH ₂	37.2-38.1, CH ₂	H-b, HC ^f	37, C-i, C-ii, C-iii	C-i, C-ii, C-iii
37 (H-c) ^e	3.42, m	3.25, m	67.58, CH	67.25, CH	H-b, c-OH, 39	C-i	-
(37)-OH	-	4.15, d (5.58)	-	-	39, H-b, HC ^f	-	38, C-i, C-iii
38	1.58, m	1.44, m	37.55, CH ₂	38.56, CH ₂	H-c, c-OH, HC ^f	37, 39	C-i, C-iii
39	5.02, dd (9.7, 2.5)	4.94, dd (9.7, 2.5)	76.82, CH	76.91, CH	H-c, c-OH, 41-43, 44, HC ^f	38	1, 37, 38, 40, 41-43
40	-	-	33.91, C	34.60, C	-	-	-
41-43	0.93, s	0.85, s	25.00, CH ₃	26.27, CH ₃	2, 39	-	39, 40
44	1.96, s	1.87, s	23.89, CH ₃	24.91, CH ₃	39	2, 5	2, 3, 4

^a ¹H NMR and ¹³C NMR in methanol-*d*₄ and DMSO-*d*₆ in the left four columns and 2D NMR correlations in the right four columns for each position were shown on the table.

^b HSQC-TOCSY correlations are ¹H → ¹³C, and correlations at the same position are excluded.

^c HMBC correlations are ¹H → ¹³C.

^d Three grouped ¹³C NMR peaks are marked as C-i, C-ii, and C-iii.

^e Three ¹H NMR peaks of protons on hydroxyl carbons are marked as H-a, H-b, and H-c.

^f HC is overlapped hydrocarbon peaks at 1.31-1.59 (methanol-*d*₄) and 1.19-1.41 (DMSO-*d*₆) in ¹H NMR.

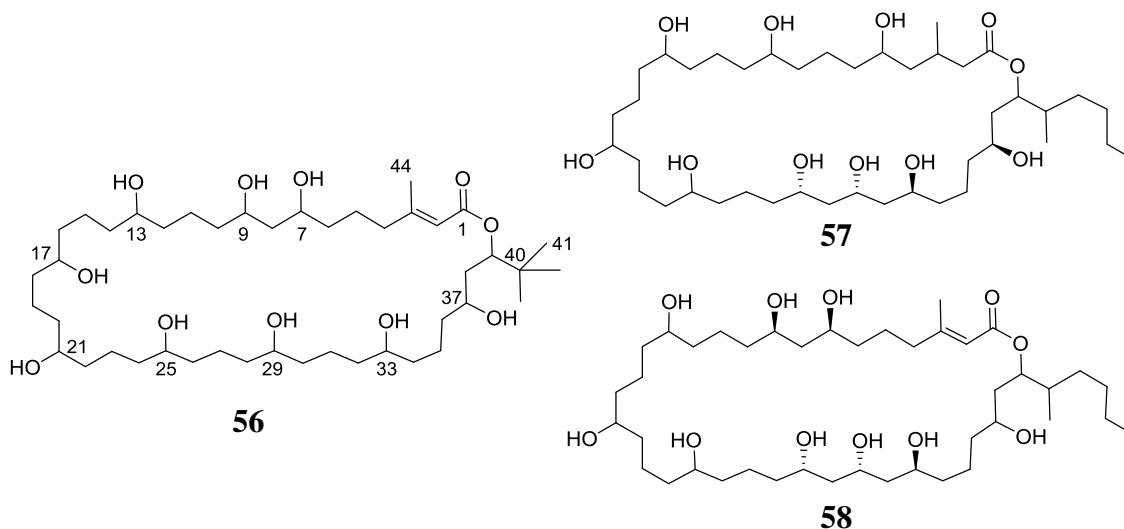


Figure 40. Structure of nuiapolide (56) and caylobolides A (57) and B (58)

SIGNIFICANCE

A novel bioactive natural product, nuiapolide (**56**) isolated from the marine Cyanobacterium has been shown anti-chemotactic activity against Jurkat cells at concentrations as low as 1.3 μM . The compound has been identified as a macrolactone containing 40 membered ring structure with 9 almost equally distributed hydroxyl groups. The compound also contains isobutyl at the α position of oxygen linkage of the ester functional group, and an alkene and methyl substitution at the α and β positions of carbon linkage respectively. This structure is closely related to the previously described class of antitumor natural products, caylobolides, which were also isolated from Cyanobacteria *Lyngbya majuscula* for caylobolide A and *Phormidium spp.* for caylobolide B.^{166, 167}

Cyanobacteria is a phylum of bacteria which produce energy through photosynthesis. Because of gaseous oxygen produced as a byproduct of photosynthesis, it is believed that the bacterial metabolism was the primary cause of oxidation of the ancient earth. This allowed the planet to be habitable for most current organisms which

rely on cellular respiration. Cyanobacteria are found almost everywhere in the terrestrial and aquatic habitats, and aquatic Cyanobacteria are known as producers of toxic secondary metabolites, cyanotoxins. When they bloom on the surface of lake or ocean, the concentrated bacteria produce a variety of toxic natural products, including the groups of cyclic peptides, alkaloids, and polyketides.^{168, 169} These and other bioactive secondary metabolites are recently recognized as research targets through the development of harvesting, cultivation, and isolation techniques of single bacterium.¹⁷⁰⁻¹⁷² The novel product evaluated in this project provides an example in the database of Cyanobacterial bioactive natural products.

The structure of nuiapolide (**56**) suggests that the backbone of the compound is produced by PKSs, and the sequential substitutions of hydroxyl groups in every four carbons suggests that the majority of the carbon chain is extended in an iterative PKS containing at least KR, DH, and ER domains in addition to fundamental AT, KS, and ACP domains. Evaluation of the biosynthesis of the molecule would be one future project. It is essential to identify the species of the Cyanobacterium and to obtain the biosynthetic gene cluster of nuiapolide (**56**). Understanding of the biosynthetic pathway would lead to the bio-engineered production of its bioactive analogs. The other interest of the natural product is to identify the mechanism of action. It shares several features with caylobolides, such as simple substitutions around the ester functional group, a long cyclic carbon chain, and several hydroxyl substitutions on the chain. Through the synthetic and analogous bioactive studies, the pharmacophore of the compounds could be determined, and synthetic small molecules which share the pharmacophore may be useful for cancer or other disease therapies.

METHODS AND MATERIALS

General Experimental Procedures

High resolution ESI-MS spectra were measured on an Agilent 6530 QTOF mass spectrometer with an Agilent 1200 HPLC system. Unit-resolution ESI-MS spectra were

performed on a Thermo Finnigan LCQ Deca XP Max ion trap mass spectrometer using ESI ionization interfaced with an Agilent 1100 HPLC, Thermo Finnigan Surveyor photodiode array (PDA) detector, and a SEDEX 75 Evaporative light scattering detector (ELSD). Preparative HPLC was performed using an Agilent 1100 binary preparative system with an Agilent multi-wavelength UV detector. An inverted microscope (VWR, Radnor, Pennsylvania, USA) was used for evaluation of Jurkat cells. Photographs of the cells were taken with X100 magnification (X10 ocular and X10 objective lens) and a camera (Olympus, Shinjuku, Tokyo, Japan) equipped with a modified lens piece, which fits over the microscope eyepiece. Cell cycle analysis of Jurkat cells was performed with a flow cytometer (FACSCalibur, Becton Dickinson, Franklin Lakes, New Jersey, USA). NMR spectra were acquired on a Bruker Avance III 500 MHz spectrometer equipped with a 5 mm H-C-N cryoprobe (Bruker Corporation, Billerica, Massachusetts, USA) at 500 MHz for ^1H NMR and 125 MHz for ^{13}C NMR in methanol- d_4 or DMSO- d_6 .

Reagents and Chemicals

Jurkat clone E6-1, its culture medium RPMI 1640, and fetal bovine serum (FBS) were purchased from American Type Culture Collection (ATCC, Manassas, VA, USA). Triton X-100, DNase-free RNase, propidium iodide, and ampules of NMR solvents (methanol- d_4 and DMSO- d_6) were purchased from Sigma-Aldrich (St. Louis, MO, USA).

Sample Preparation for Assay Analysis (Hawaii Pacific University)

The 560 crude extracts were prepared from freeze dried samples of microorganisms collected from near-shore environments in the main Hawaiian islands. Active sample 13-F10, was prepared from a colonial cyanobacterium (071905-NII-01). Specifically, the freeze-dried cyanobacterium sample (105 mg) was extracted in H_2O (10 mL) with sonication. The water extracted was filtered and loaded on a C-4 solid phase extraction (SPE) cartridge (500 mg, 300 Å). The cartridge was washed with H_2O (10 mL) and the H_2O wash was discarded. The column was then eluted with methanol/water

mixtures (33:67, 67:33, and 100:0; 6 mL each). The combined fractions were dried under vacuum (3.9 mg) and added to our extract libraries as 13-F10. Prior to assay, a small portion of the extract was dissolved in methanol/ethyl acetate/*t*-butyl methyl ether (60:30:10) (MET) and transferred to a 96-well plate. The plates were stored desiccated and vacuum packed at -20 °C. Each 96-well plate of extracts was solubilized in MET and evaluated in our chemotaxis transwell assay.

Details on Cyanobacteria Biomass (Hawaii Pacific University)

Colonies of the red filamentous cyanobacterium were collected by hand on July 19, 2005 at a depth of 12-20 m in waters adjacent to Lehua Rock, an islet off the east shore of Niihau, Hawaii. Samples were kept on ice in the field before freezing at -15 °C. The frozen samples were then freeze-dried. A dried voucher specimen (071905-NII-01) is deposited in the Department of Natural Sciences, Hawaii Pacific University and a partial 16S rRNA gene sequence was deposited in the NCBI GenBank under the accession number KT852581.

DNA Extraction and Sequencing (Hawaii Pacific University)

DNA was extracted using a Qiagen DNeasy kit. A small portion of frozen biomass was thawed and warmed to 55 °C. Lysis buffer (“ATL” buffer, 180 µL) and proteinase K solution (600 mAU/mL; 20 µL) were added, and the mixture was vortexed, then incubated overnight at 55 °C. After warming the mixture to 70 °C, the sample was again vortexed, and chaotropic “AL” buffer (200 µL) was added, followed by a 10 min incubation. The sample was then mixed thoroughly with ethanol (200 µL) and pipetted into the DNeasy mini-spin column, which was placed in a collection tube and centrifuged at 6,000 g for 1 min. The column was washed by centrifuging again at 6,000 g for 1 min after adding the chaotropic elution buffer “AW1” (500 µL) and again with wash buffer “AW2” (500 µL) and centrifuging again at 20,000 g for 3 min. Elution buffer “AE” (100 µL) was added and incubated at room temperature for 1 min, before centrifuging at 6,000 g for 1 min. The DNA eluate was collected and stored at -20 °C.

Primers were developed by Nubel and coworkers (1997) to amplify an approximate 700 bp region of 16S that allows the specific amplification of cyanobacterial 16S genes sequences.¹⁷³ The partial sequencing of 16S was accomplished by adding 1 μ L of thawed isolated DNA to a mixture of H₂O (26 μ L), dNTP (1.0 μ L, Eppendorf), forward primer (1.0 μ L, 20 pmol/ μ L, CYA106F: CGGACGGGTGAGTAACGCGTGA), and reverse primers (1.0 μ L, 20 pmol/ μ L, a 1:1 ratio of CYA781Ra: GACTACTGGGGTATCTAATCCCATT and CYA781Rb: GACTACAGGGGTATCTAATCCCTTT) in a PCR tube. The mixture was heated to 95 °C for 2 min and the following mixture was added: 14.75 μ L H₂O, 5 μ L 10X reaction buffer, and 0.25 μ L Taq polymerase (Eppendorf). The following cycles were applied: 10 cycles, 95 °C for 30 sec, 65 °C for 30 sec, the cool -1 °C; 30 cycles, 95 °C for 30 sec, 55 °C for 30 sec, 68 °C for 1 min. Finally, the PCR product was held at 68 °C for 7 min and then stored at 4 °C. The PCR product was checked for a single correctly sized product by agarose gel electrophoresis, and the band was prepared for sequencing using a Qiagen QIAquick spin kit per instructions. Sequencing was conducted by the by the Greenwood Molecular Biology Facility (University of Hawaii) employing the ABI Prism BigDye Terminator and Primer Cycle Sequencing Chemistries and an ABI 377XL capillary sequencer.

A tblastx search against the NCBI database with E-value cutoff of $\leq 1.0E-3$ revealed a highly significant hit to *Okeania plumata* (KC986934.1).¹⁷⁴

Scaled-Up Extraction of the Active Cyanobacterial Species (Hawaii Pacific University)

For process and storage efficiency, the bulk of our library samples are routinely extracted in organic solvents. Sample 071905-NII-01 (5.6 g dry wt) was extracted repeatedly with methanol (65 mL and 2 x 50 mL) followed by dichloromethane (2 x 50 mL). The methanol extracts were combined and solvent was removed under vacuum to yield 1.8 g of extract residue. The dichloromethane extracts were also combined and solvent removed under vacuum to yield 34 mg. Analytical amounts of both extracts were

subject to bioassay-linked fractionation in order to identify the active component(s) of the organism.

Bioassay-Linked Fractionation of Methanol and Dichloromethane Extracts of the Cyanobacterium 071905-NII-01 (Hawaii Pacific University)

Both extracts (dichloromethane, 1.7 mg, FP1; methanol, 2.0 mg, FP2) were fractionated in two runs each by reversed-phase HPLC (Phenomenex Luna C18-2 column, 5 μm , 4.6 \times 250 mm) using a linear gradient of acetonitrile/water (FP1: 50:50 to 100:0 over 0-15 min, then 100% acetonitrile from 15-26 min; FP2: 20:80 to 100:0 over 0-15 min, then 100% acetonitrile from 15-26 min; flow rate: 1.0 mL/min; UV detection: 200-600 nm). Extract components eluting between 2.0-26.0 min were collected as 60-sec fractions into a deep 96-well plate. For each extract, both HPLC runs were collected into the same deep-well plate and solvent was removed from the plates under vacuum in a centrifugal concentrator at room temperature. Fractions were reconstituted with MET and apportioned into low profile 96-well plates for bioassay, averaging 45 and 60 μg /well for FP1 and FP2, respectively. Prior to assay, the fractions were reconstituted and diluted in MET and tested as average concentrations of 1, 10, and 25 μg /mL. For FP1, the activity concentrated in fractions eluting at 4.0-5.0 and 12.0-14.0 min. And for FP2, activity concentrated in fractions eluting at 9.0-10.0 and 16.0-17.0 min. Taken together, LCMS of both active regions in both fraction plates indicated the presence of the same components in each of the two active regions. FP1 fractions had only very minor impurities. The major component in the earliest active region for each fraction was absent from adjacent inactive fractions and showed a molecular weight of 788.6 (ESI-positive mode m/z 789.6, MH^+ ; ESI-negative mode m/z 787.6 [$\text{M-H}]^-$). The second active region in FP1 showed of a single low-yielding compound that was absent from adjacent inactive fractions. The major component had a molecular weight of 982.7 (ESI-positive mode m/z 983.5, MH^+ , m/z 1005.5, MNa^+ ; ESI-negative mode m/z 981.9 [$\text{M-H}]^-$).

Isolation of Nuiapolide (56) (Hawaii Pacific University)

The major component from the first active fraction in FP1 and FP2 was isolated from the methanol extract, guided by LCMS (ESI-positive mode m/z 789.6, MH⁺; ion trap analyzer). The methanol extract (1,020 mg) was dissolved in methanol and cleaned up for HPLC by eluting in 7 batches from an SPE column (C18 silica, 1 g, EM 110167-4) with methanol (17 mL each). The eluate was concentrated under vacuum to dryness (996 mg), reconstituted in methanol/water 90:10 (14 mL) and chromatographed in 7 portions by preparative reversed phase HPLC (Phenomenex Luna C18-2 column, 5 μ m, 22 \times 250 mm; flow rate: 18 mL/min; methanol/water linear gradient 70:30 to 100:0 from 0-15 min, then 100% methanol from 15-30 min). Peaks were collected based on absorbance at 210 nm and analyzed by LCMS. Compound **1**, nuiapolide, eluted at 8.6 min (50.7 mg, 0.89% yield, dry wt). The purity of nuiapolide (**1**) (>95%) was determined by LCMS-ELSD analysis (Phenomenex Luna C18-2 column, 5 μ m, 2 \times 250 mm; flow rate: 0.20 mL/min; acetonitrile/water gradient 50:50 to 100:0 over 0-10 min, then 100% acetonitrile 10-20 min; ELSD 50 $^{\circ}$ C; PDA 200-600 nm).

Structural Analysis of Nuiapolide (56)

Nuiapolide (56): chartreuse amorphous solid; $[\alpha]_D^{25}$ -12 (CH₃OH, c 0.341); ¹H and ¹³C NMR data (methanol-*d*₄ and DMSO-*d*₆), see Table 3 and Figure 41-Figure 55; HR-TOF-ESIMS, m/z [M+H]⁺ 789.6076 (calcd for C₄₄H₈₅O₁₁, 789.6092, Δ -2.2 ppm), [M+Na]⁺ 811.5895 (calcd for C₄₄H₈₄O₁₁Na, 811.5911, Δ -2.0 ppm). NMR spectra were recorded on a Bruker Avance III. The purified sample (500 μ g) was dissolved in 500 μ L of methanol-*d*₄ or DMSO-*d*₆, which was transferred into a 3 mm NMR sample tube (Wilmad LabGlass, Vinelandk, NJ, USA). ¹H NMR, ¹³C NMR, ¹³C NMR DEPT, COSY, TOCSY, HSQC, HSQC-TOCSY, and DMSO-*d*₆ were acquired in methanol-*d*₄ at 298 K (Figure 41-Figure 49 for spectra; Table 3 for assignments), and ¹H NMR, ¹³C NMR, COSY, TOCSY, and HMBC were recorded in DMSO-*d*₆ at 315 K (Figure 50-Figure 55).

Chemotaxis and Cytotoxicity Assay against Jurkat Cells, Human Cell Line of T Lymphocyte

Chemotaxis and cytotoxicity assays of crude or purified extracts against Jurkat cells were performed as described in Chapter III assessing the activities of *aziA2* disruption mutant and dimethyl furan-2,4-dicarboxylate (**55**) except for the solvent, which was MET solution.

Cell Cycle Analysis by Flow Cytometry

The effect of nuiapolide (**56**) on the cell cycle was assessed by flow cytometry. Jurkat cells were harvested by centrifugation and counted following the same procedures as detailed in previous sections. Cells were added to RPMI cell culture medium in 24-well plates to give a final concentration of 400,000 cells/mL, 500 μ L total volume. Nuiapolide (**56**) was added (5.0 μ g/mL) and the cells were incubated at 37 °C in 5% CO₂ for 2, 4, or 6 h. The resulting cells were prepared for flow cytometry analysis based on published procedures.¹⁷⁵ Cells were transferred into a 15-mL falcon tube and harvested by centrifugation at 1,000 rpm for 10 min. Cells were subsequently washed with 5 mL of PBS and pelleted at 1,000 rpm for 6 min. The supernatant was removed and the cells were resuspended in 0.5 mL of PBS. The cell suspension was transferred into 4.5 mL of ice cold ethanol and stored on ice (or -20 °C) for more than 2 h. The ethanol fixed cells were collected by centrifugation at 1,000 rpm for 5 min. The cell pellet was resuspended in 5 mL of PBS, incubated for 1 min and centrifuged again at 1,000 rpm for 5 min. The cell pellet was finally resuspended in 1 mL of freshly prepared staining solution (PBS, 0.1% of Triton X-100, and 0.2 mg/mL of DNase-free RNase, and 0.02 mg/mL of propidium iodide), and incubated at room temperature for 30 min before analyzing the samples by flow cytometry using a 488 nm argon laser.

Spectral Data of Nuiapolide (56)

Nuaipolide (**56**): ¹H NMR (methanol-d₄, 500 MHz): δ_{H} 0.93 (9H, s, CH₃41, CH₃42, and CH₃43), 1.31-1.55 (14H, overlapped m, CH₂11, CH₂15, CH₂19, CH₂23, CH₂27, CH₂31,

and CH₂35), 1.48-1.59 (26H, overlapped m, CH₂10, CH₂12, CH₂14, CH₂16, CH₂18, CH₂20, CH₂22, CH₂24, CH₂26, CH₂28, CH₂30, CH₂32, and CH₂34), 1.42 (2H, m, CH₂36), 1.49 (2H, m, CH₂6), 1.56 (2H, m, CH₂8), 1.58 (2H, m, CH₂38), 1.60 (2H, m, CH₂5), 1.96 (3H, s, CH₃44), 2.58 (1H, m, H4'), 2.83 (1H, m, H4''), 3.42 (1H, m, H37), 3.57 (6H, s, H13, H17, H21, H25, H29, and H33), 3.78 (2H, s, H7 and H9), 5.02 (1H, dd, $J = 9.7, J = 2.5$ Hz, H39) 5.74 (1H, s, H2). ¹H NMR (dimethyl sulfoxide-d₆, 500 MHz): δ_{H} 0.85 (9H, s, CH₃41, CH₃42, and CH₃43), 1.19-1.37 (14H, overlapped m, CH₂11, CH₂15, CH₂19, CH₂23, CH₂27, CH₂31, and CH₂35), 1.24-1.41 (26H, overlapped m, CH₂10, CH₂12, CH₂14, CH₂16, CH₂18, CH₂20, CH₂22, CH₂24, CH₂26, CH₂28, CH₂30, CH₂32, and CH₂34), 1.28 (2H, m, CH₂36), 1.31 (2H, m, CH₂6), 1.37 (2H, m, CH₂8), 1.44 (2H, m, CH₂38), 1.49 (2H, m, CH₂5), 1.87 (3H, s, CH₃44), 2.59 (2H, m, CH₂4), 3.25 (1H, m, H37), 3.37 (6H, s, H13, H17, H21, H25, H29, and H33), 3.58 (2H, s, H7 and H9), 4.14 (6H, d, $J = 4.1$ Hz, OH13, OH17, OH21, OH25, OH29, and OH33), 4.15 (1H, d, $J = 5.6$ Hz, OH37), 4.44 (1H, d, $J = 4.4$ Hz, OH7 or OH9), 4.47 (1H, d, $J = 4.2$ Hz, OH7 or OH9), 4.94 (1H, dd, $J = 9.7, J = 2.5$ Hz, H39), 5.67 (1H, s, H2). ¹³C NMR (methanol-d₄, 500 MHz): δ_{C} 20.8-21.5 (C11, C15, C19, C23, C27, C31, and C35), 23.86 (C5), 23.89 (C44), 25.00 (C41, C42, and C43), 32.69 (C4), 33.91 (C40), 36.2-37.4 (C6, C10, C12, C14, C16, C18, C20, C22, C24, C26, C28, C30, C32, C34, and C36), 37.55 (C38), 43.51 (C8), 67.58 (C37), 69.8-70.8 (C7, C9, C13, C17, C21, C25, C29, and C33), 76.82 (C39), 115.73 (C2), 161.20 (C3), 166.90 (C1). ¹³C NMR (dimethyl sulfoxide-d₆, 500 MHz): δ_{C} 21.4-22.0 (C11, C15, C19, C23, C27, C31, and C35), 24.08 (C5), 24.91 (C44), 26.27 (C41, C42, and C43), 33.11 (C4), 34.60 (C40), 37.2-38.1 (C6,

C10, C12, C14, C16, C18, C20, C22, C24, C26, C28, C30, C32, C34, and C36), 38.56 (C38), 44.67 (C8), 67.25 (C37), 69.2-70.2 (C7, C9, C13, C17, C21, C25, C29, and C33), 76.91 (C39), 116.69 (C2), 160.04 (C3), 166.04 (C1). HR-TOF-ESIMS, m/z [M+H]⁺ 789.6076 (calcd for C₄₄H₈₅O₁₁, 789.6092, Δ -2.2 ppm), [M+Na]⁺ 811.5895 (calcd for C₄₄H₈₄O₁₁Na, 811.5911, Δ -2.0 ppm).

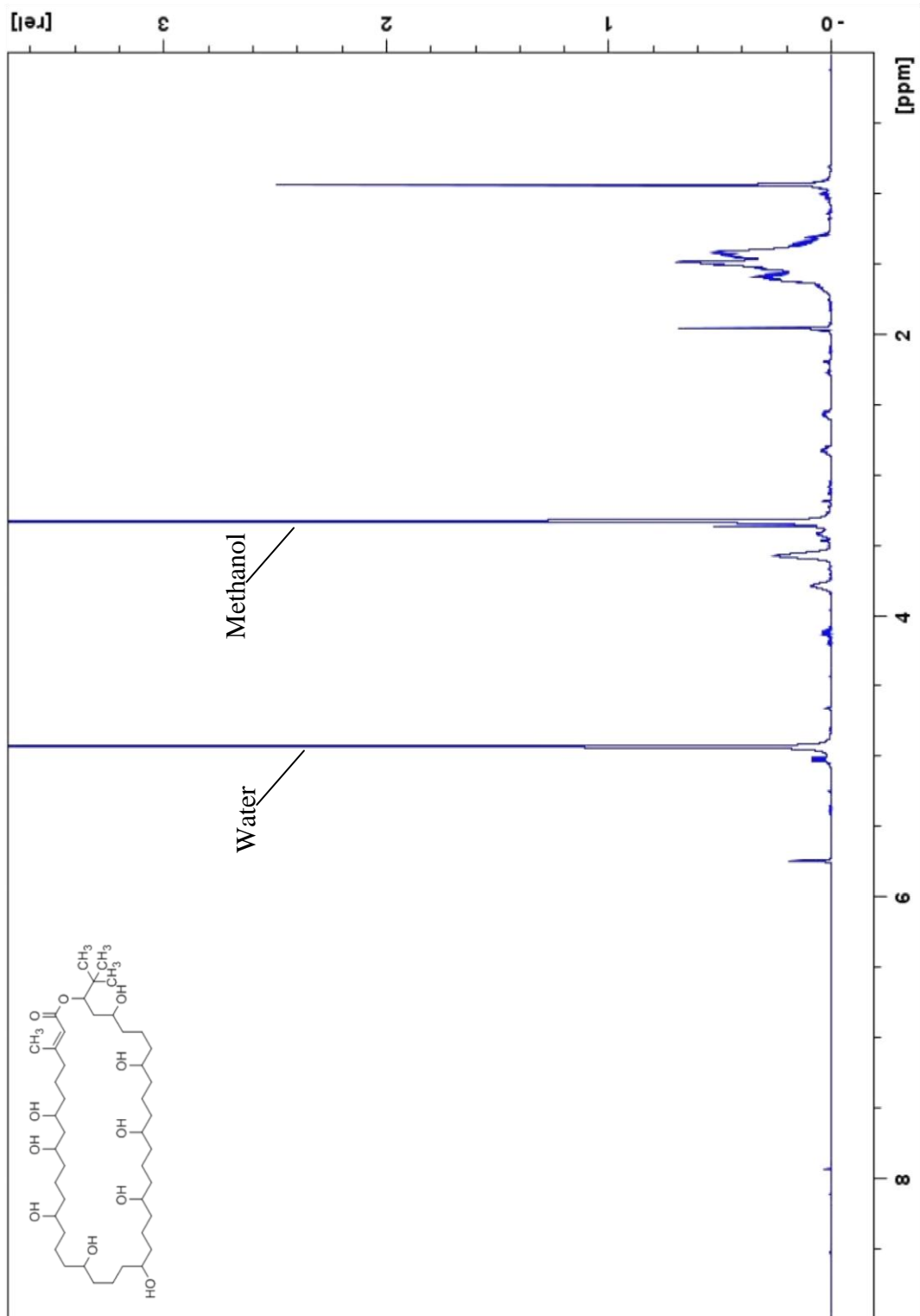


Figure 41. ^1H NMR of nuiapolide (56) in methanol- d_4

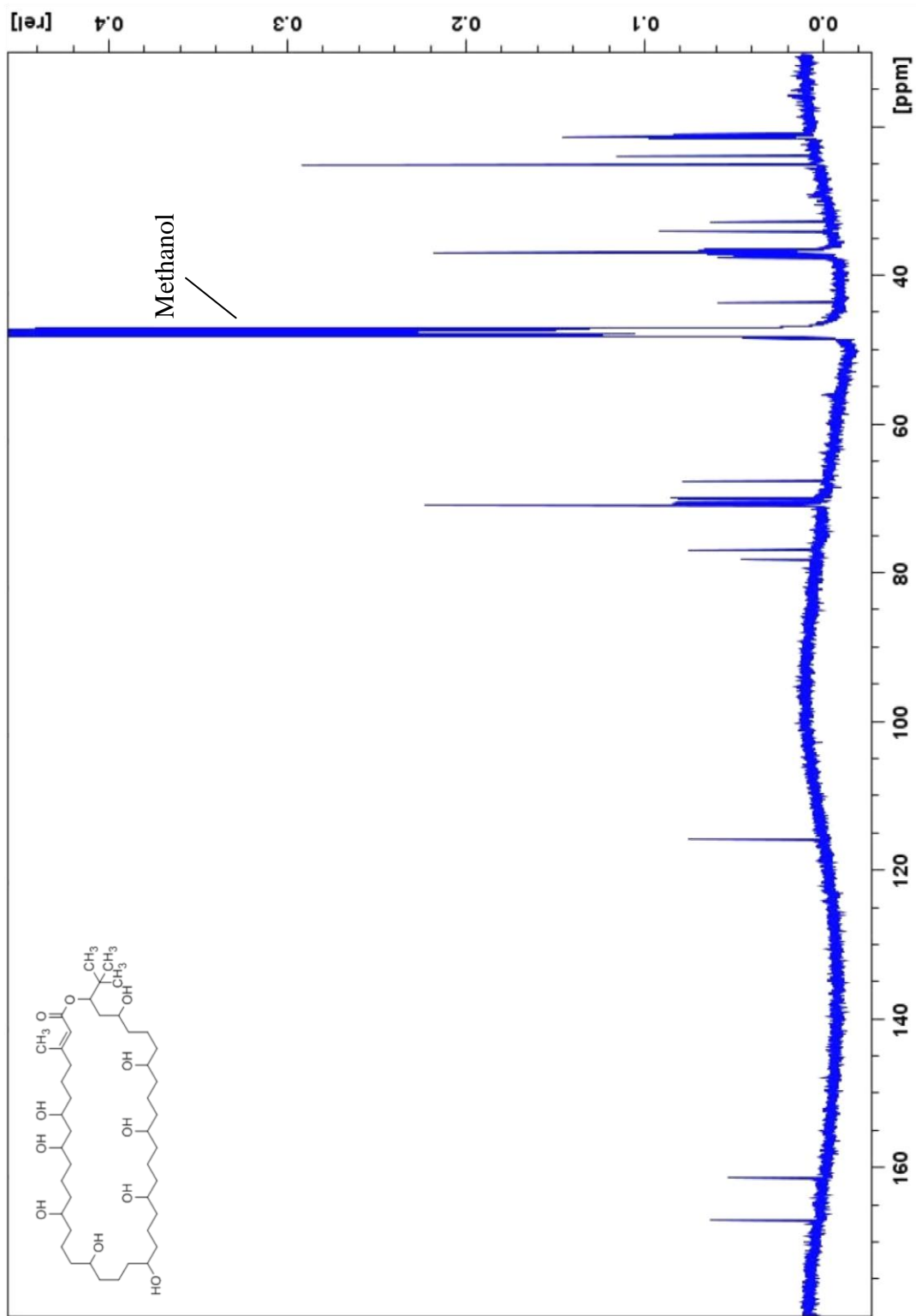


Figure 42. ^{13}C NMR of nuiapolide (56) in methanol- d_4

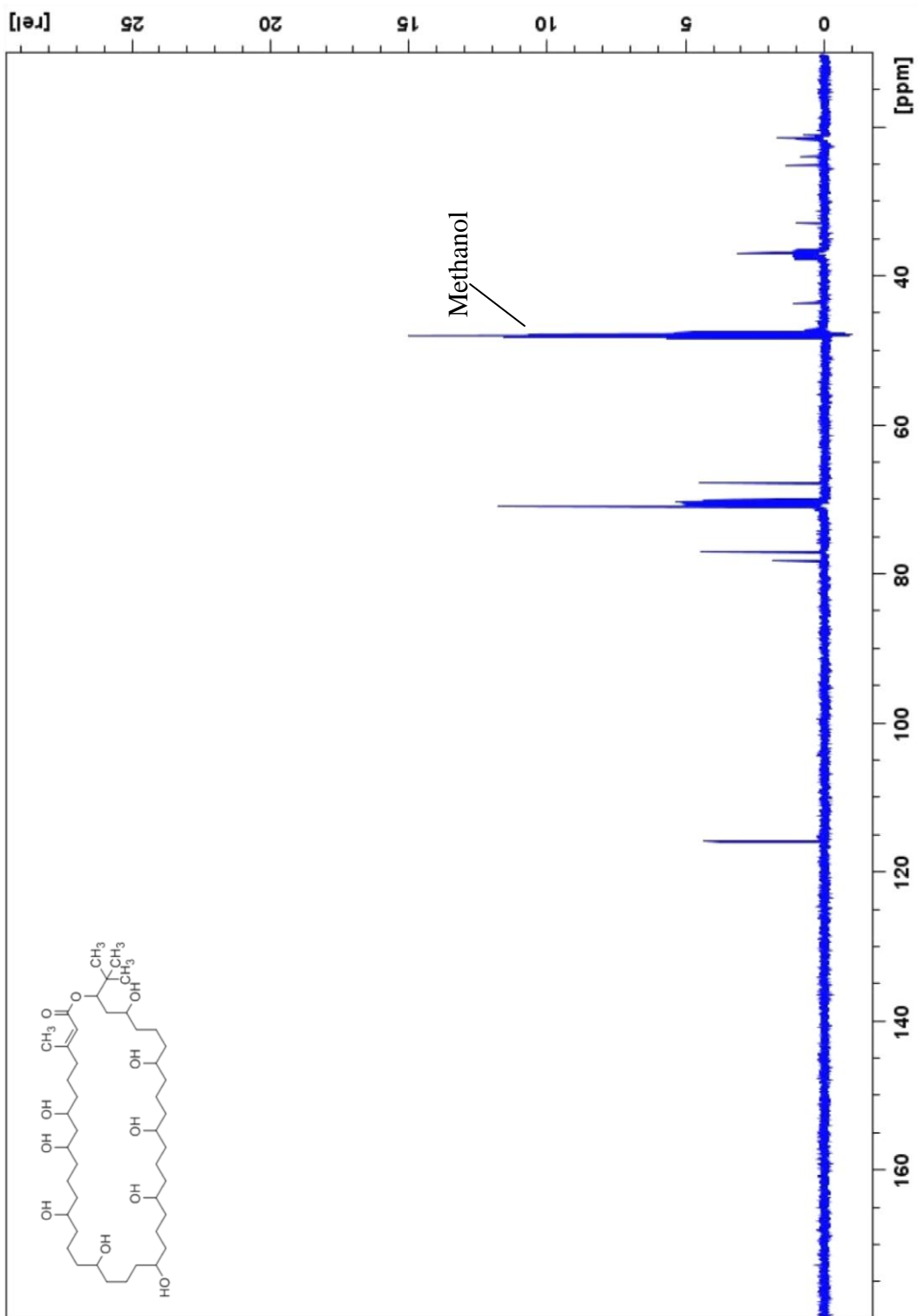


Figure 43. DEPT-90 of nuiapolide (56) in methanol-*d*₄

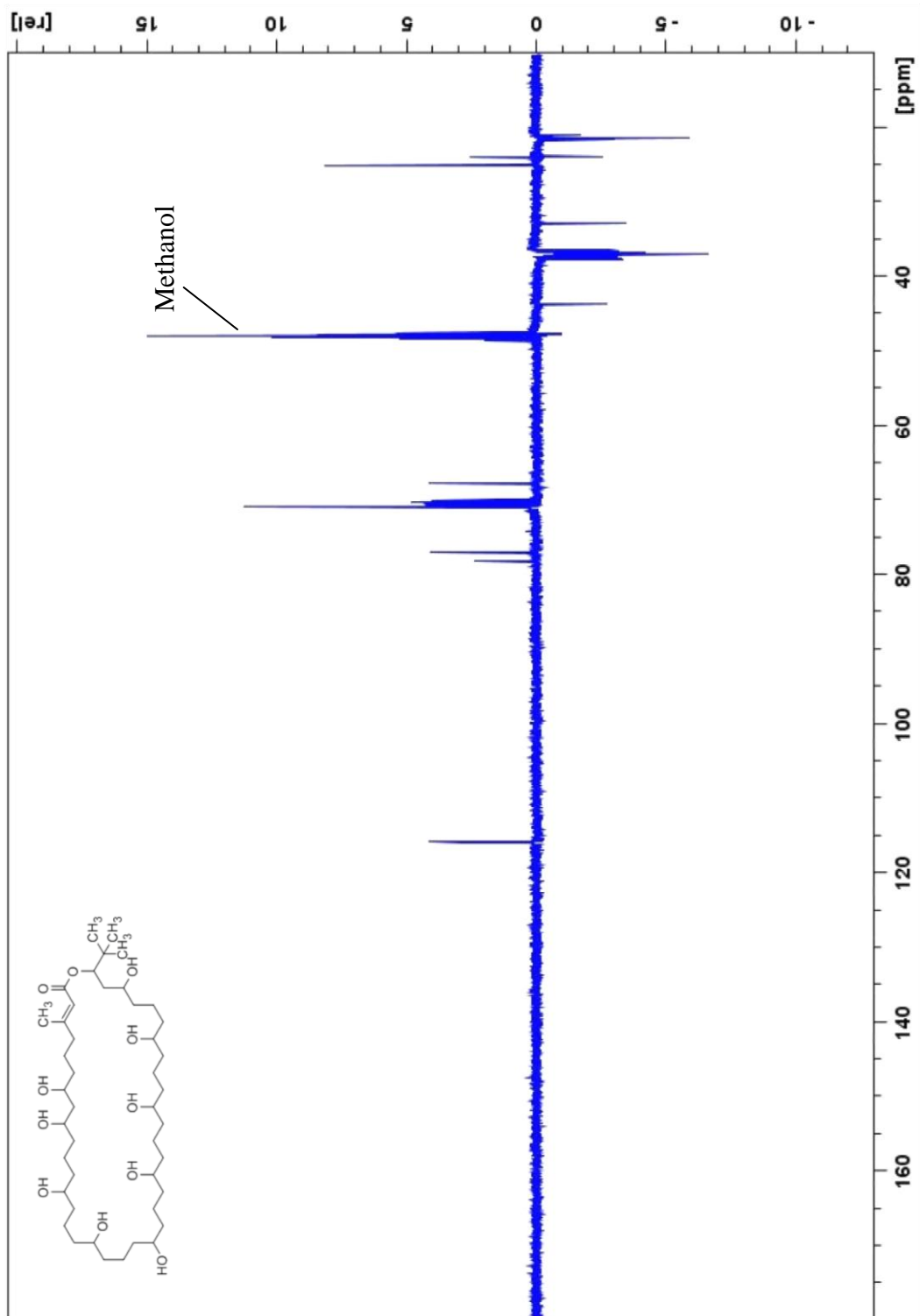


Figure 44. DEPT-135 of nuiapolide (56) in methanol- d_4

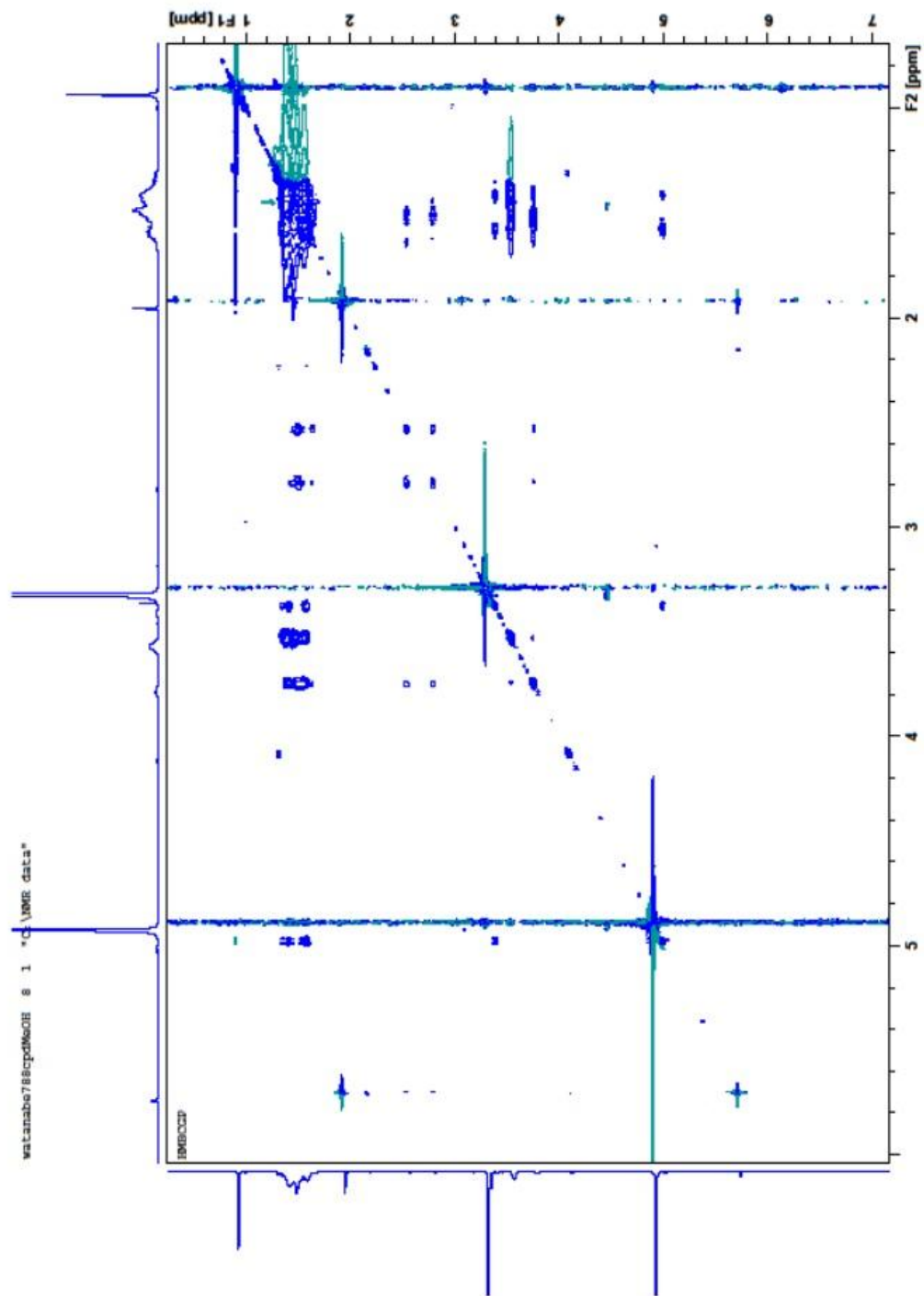


Figure 45. COSY of nuiapolide (56) in methanol- d_4

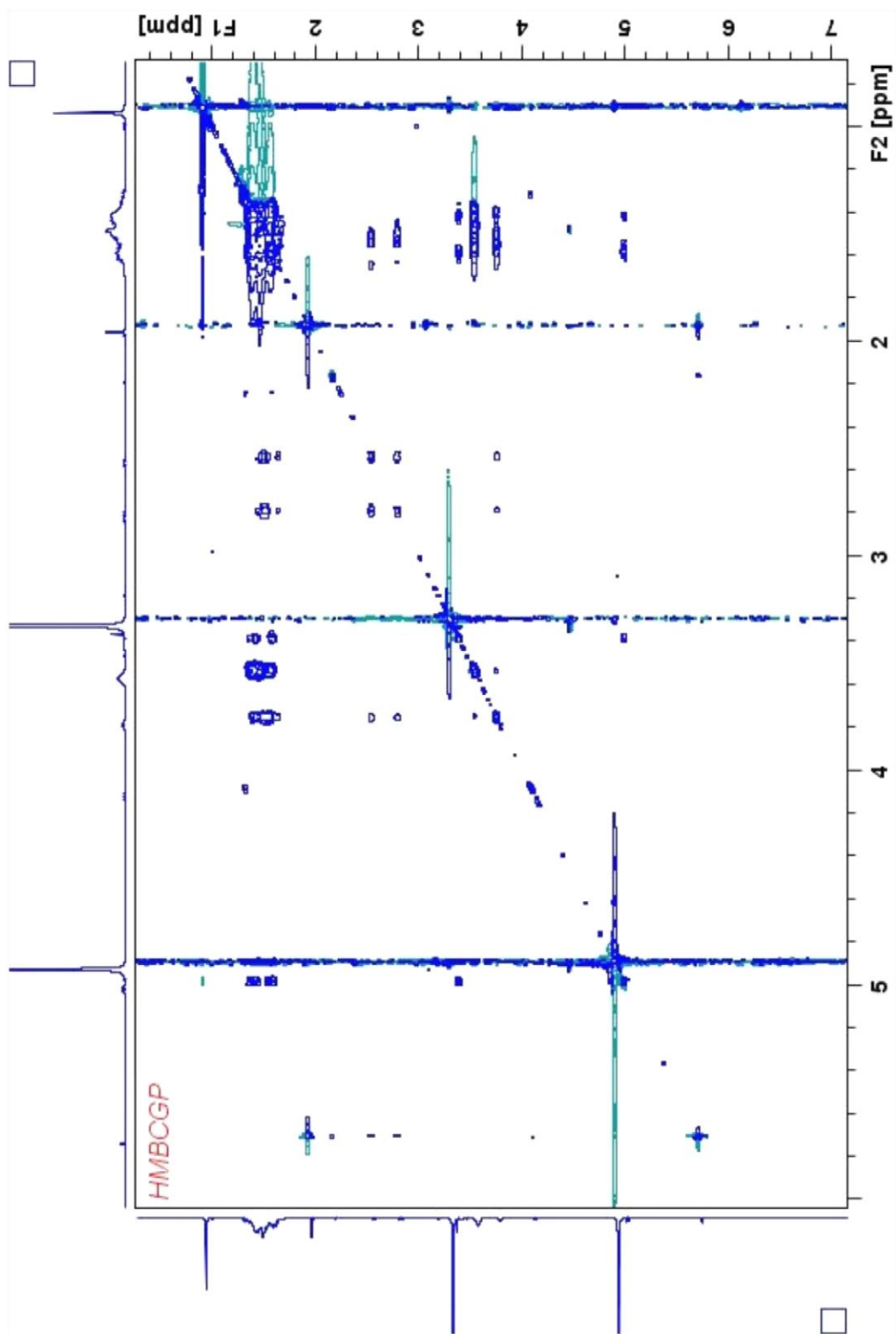


Figure 46. TCOSY of nuiapolide (56) in methanol-*d*₄

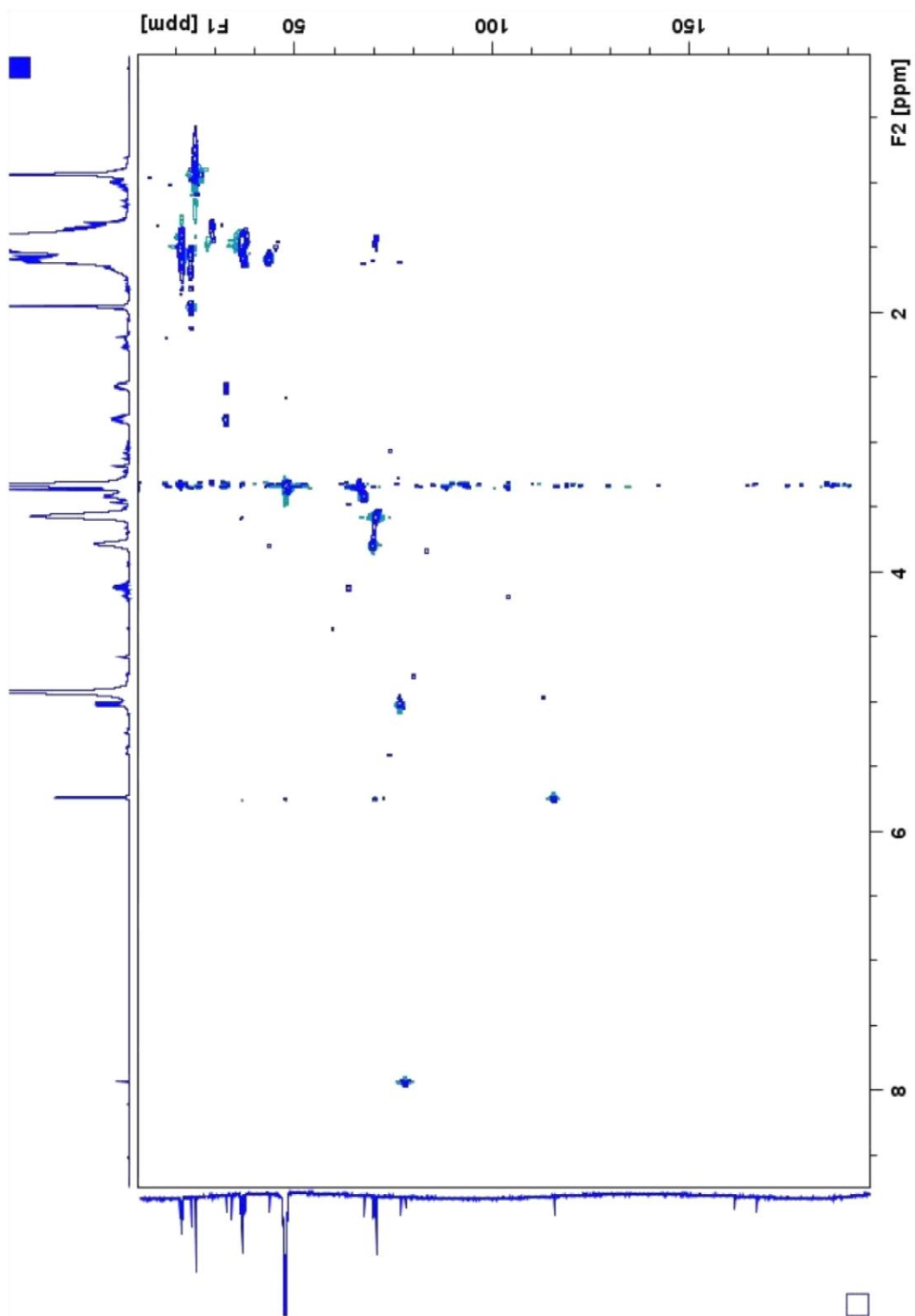


Figure 47. HSQC of nuiapolide (56) in methanol-*d*₄

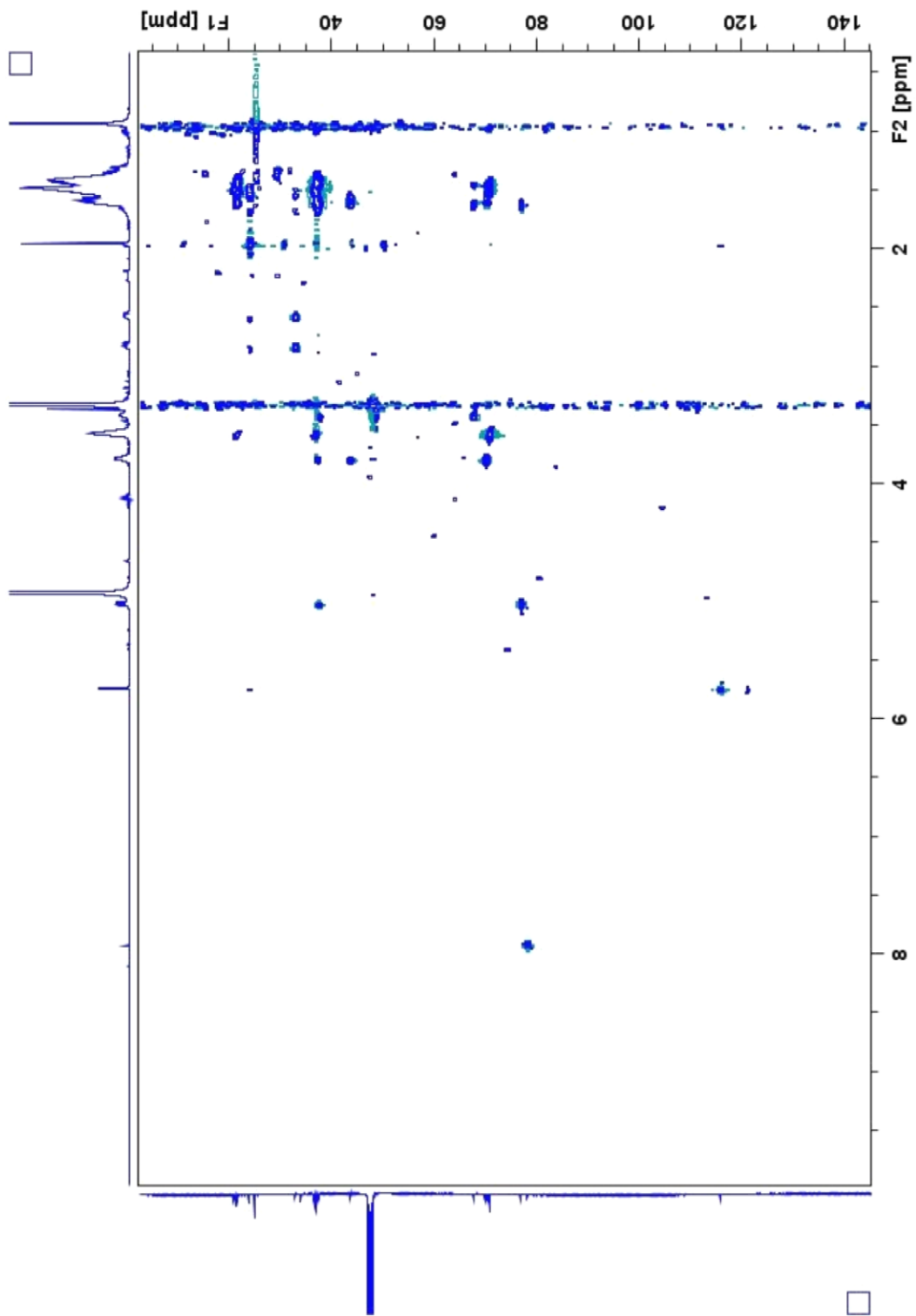


Figure 48. HSQC-TOCSY of nuiapolide (56) in methanol- d_4

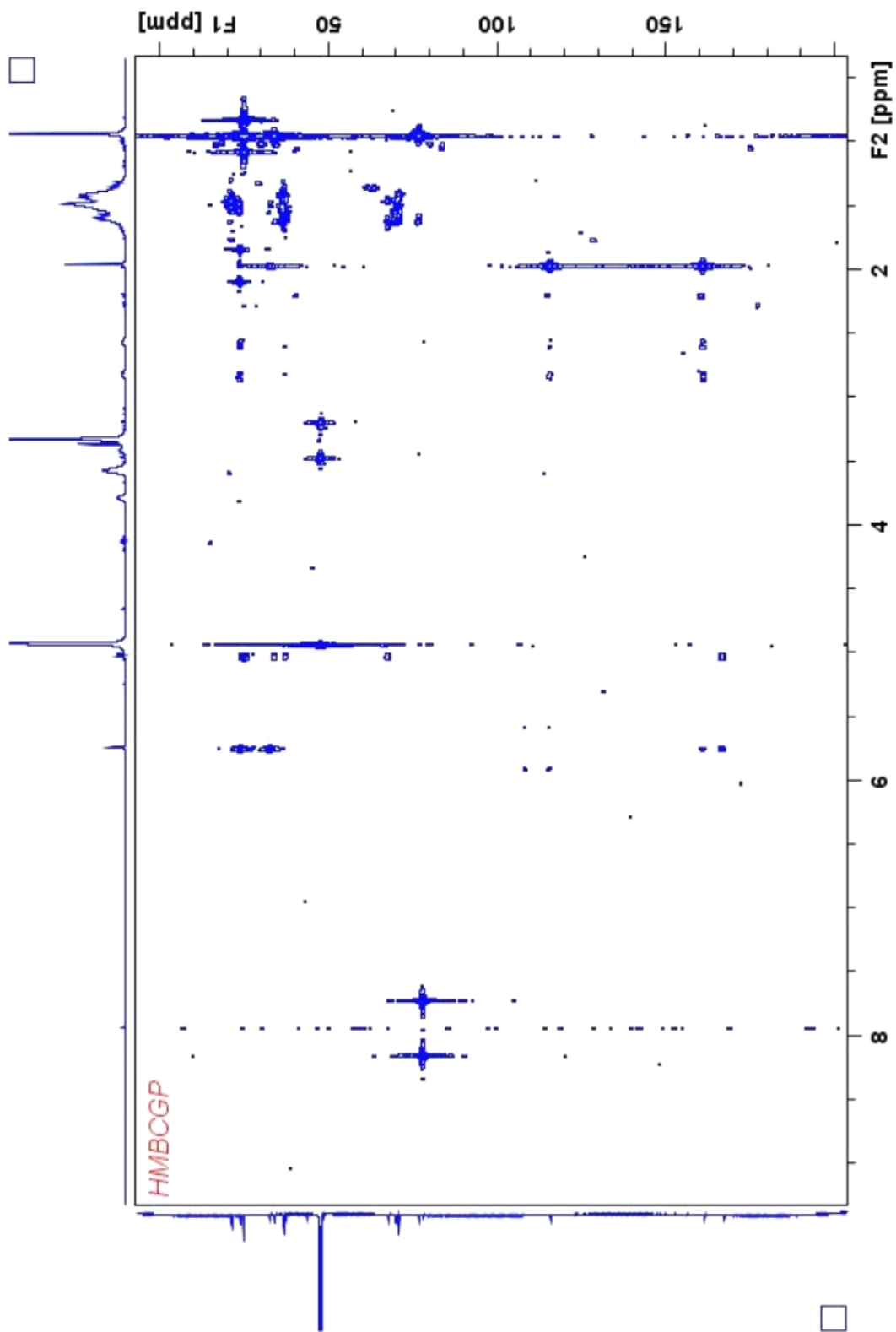


Figure 49. HMBC of nuiapolide (56) in methanol-*d*₄

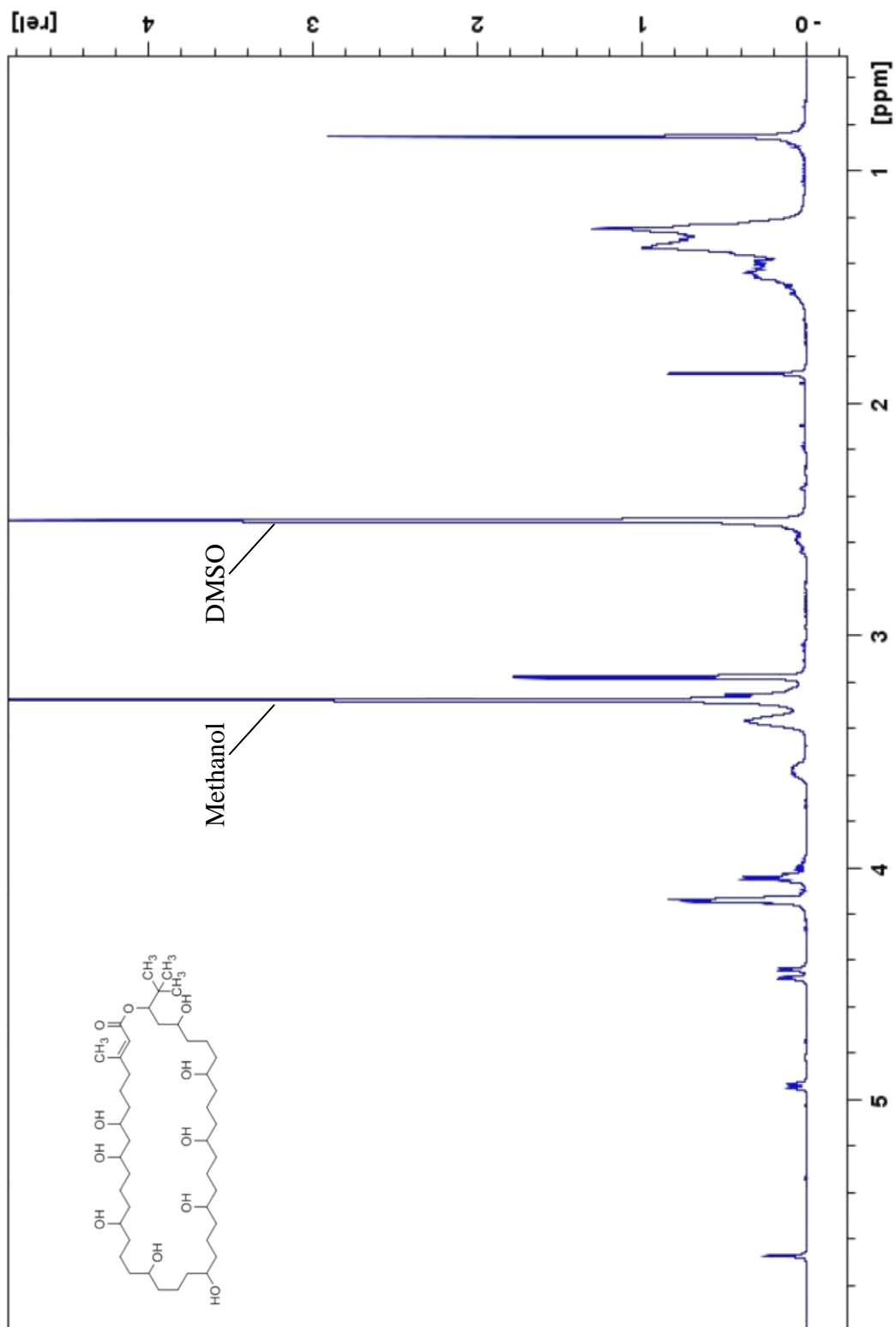


Figure 50. ^1H NMR of nuiapolid (56) in $\text{DMSO}-d_6$

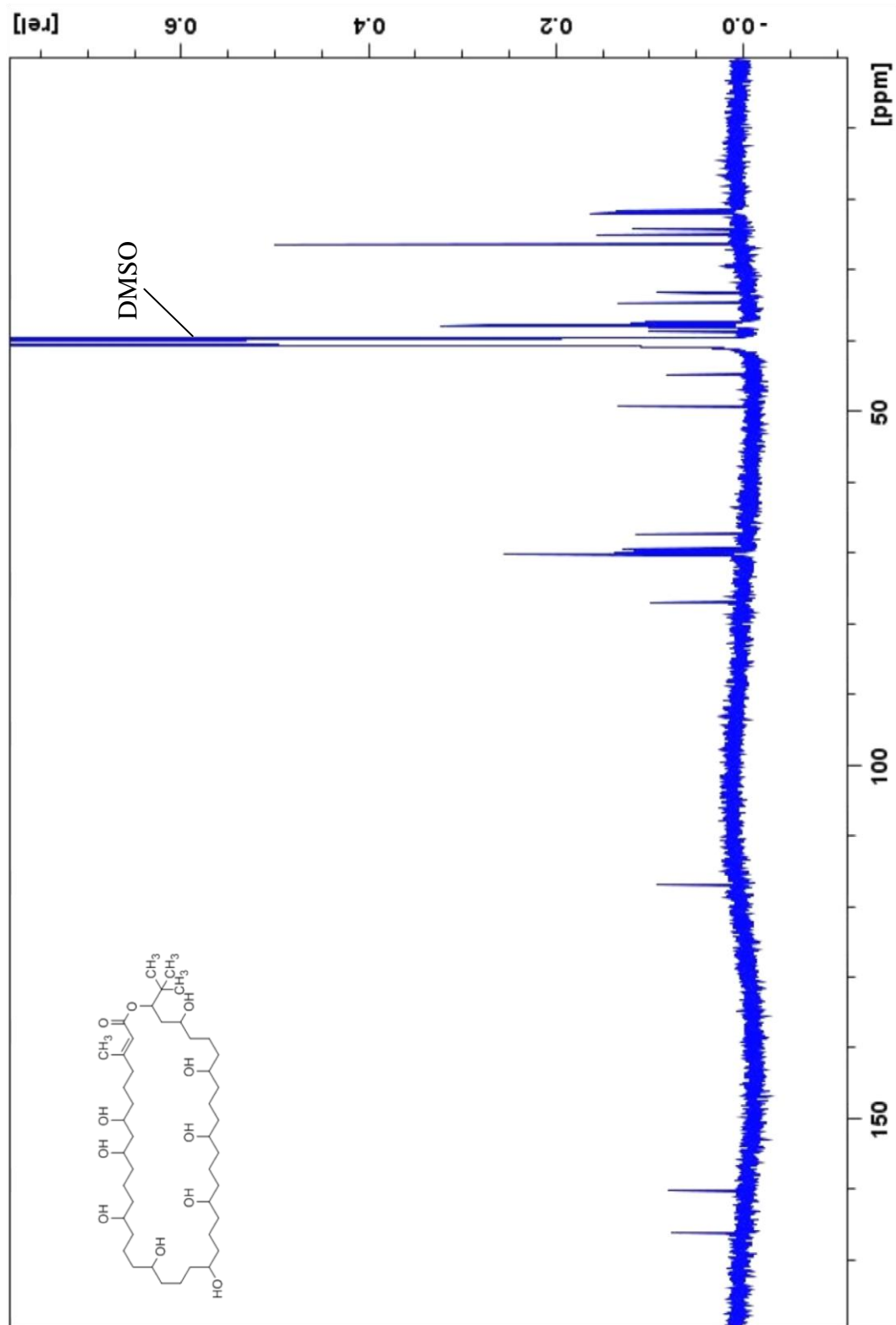


Figure 51. ^{13}C NMR of nuiapoxide (56) in DMSO-d_6

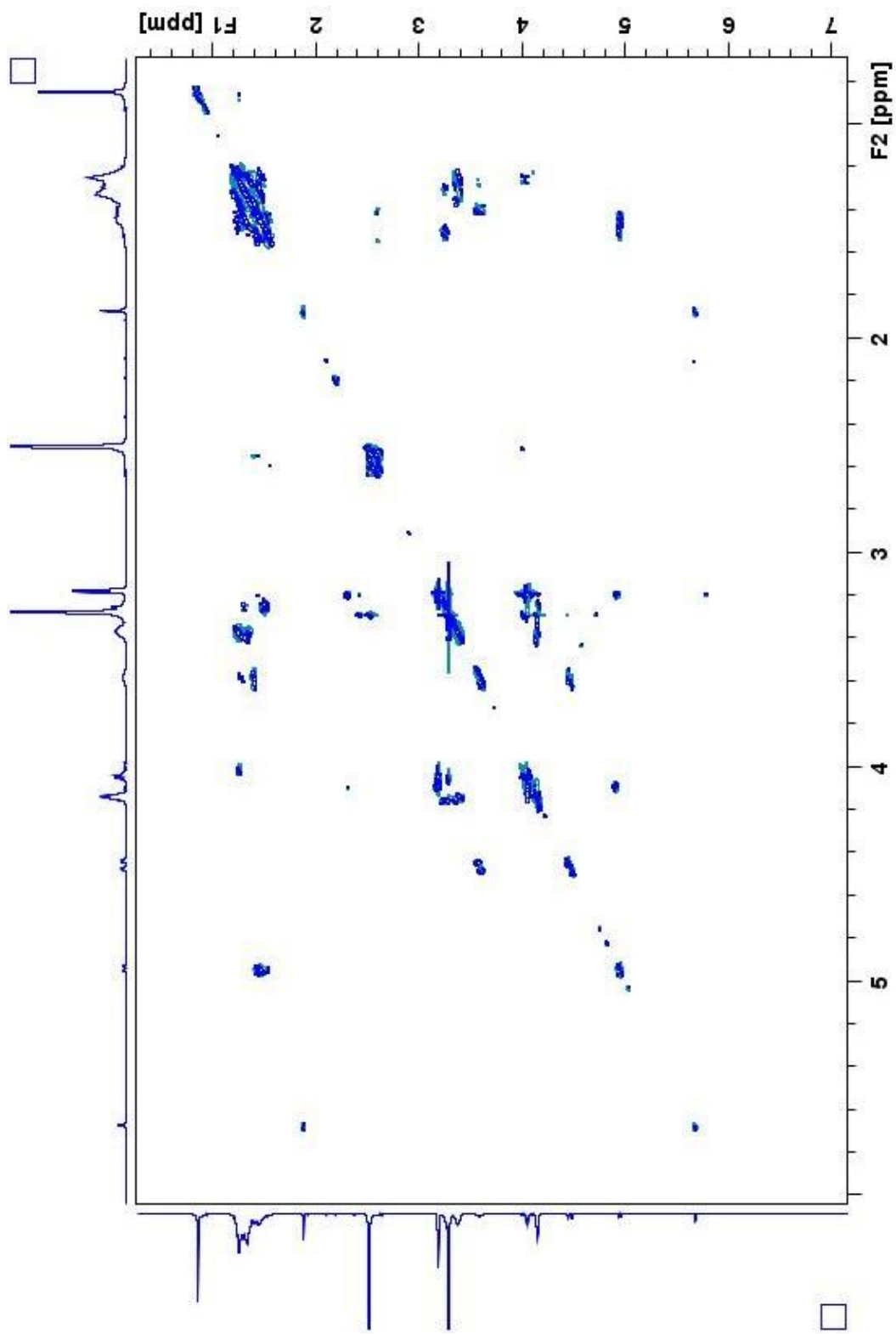


Figure 52. COSY of nuiapolide (56) in DMSO- d_6

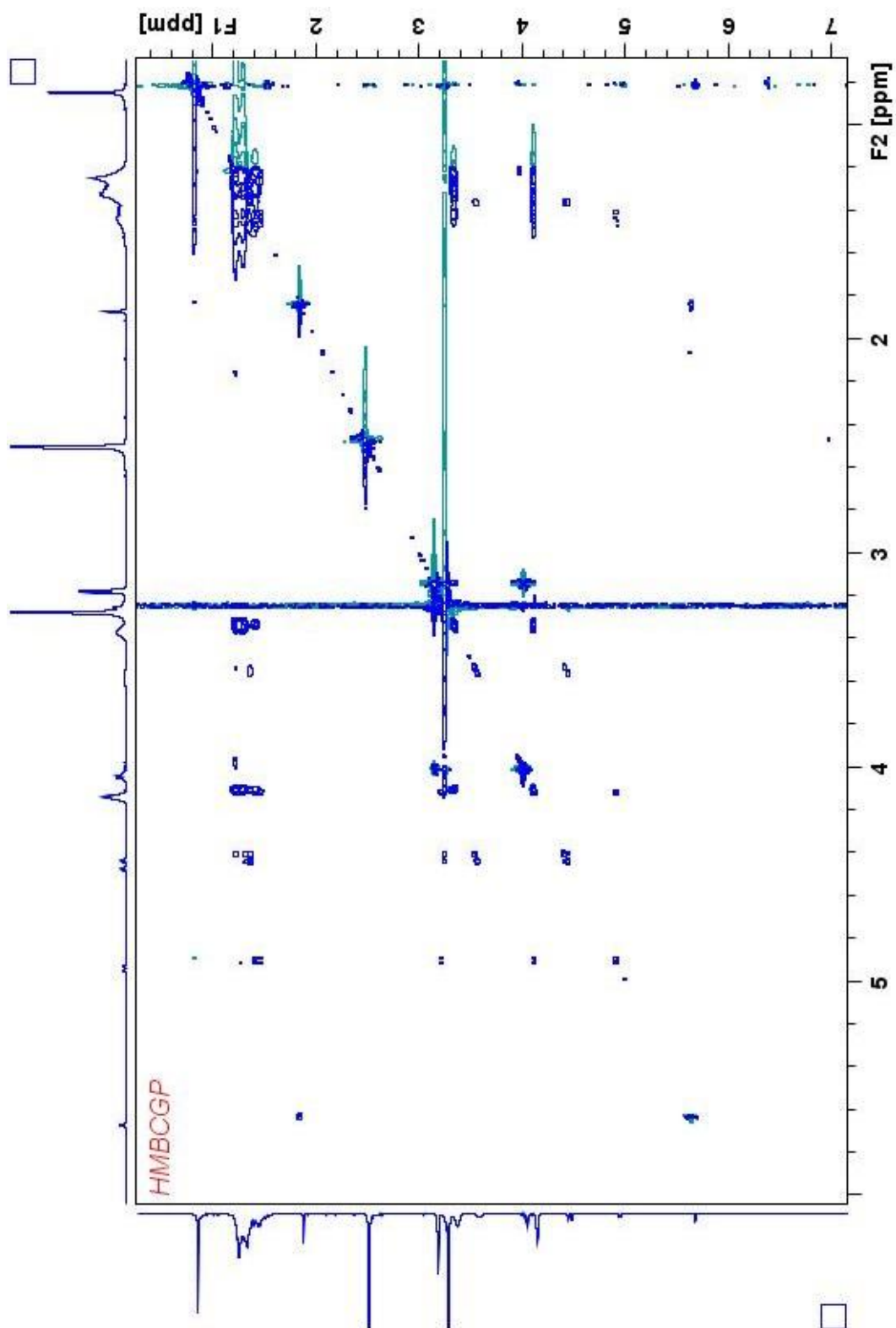


Figure 53. TOCSY of nuiapolidine (56) in DMSO-*d*₆

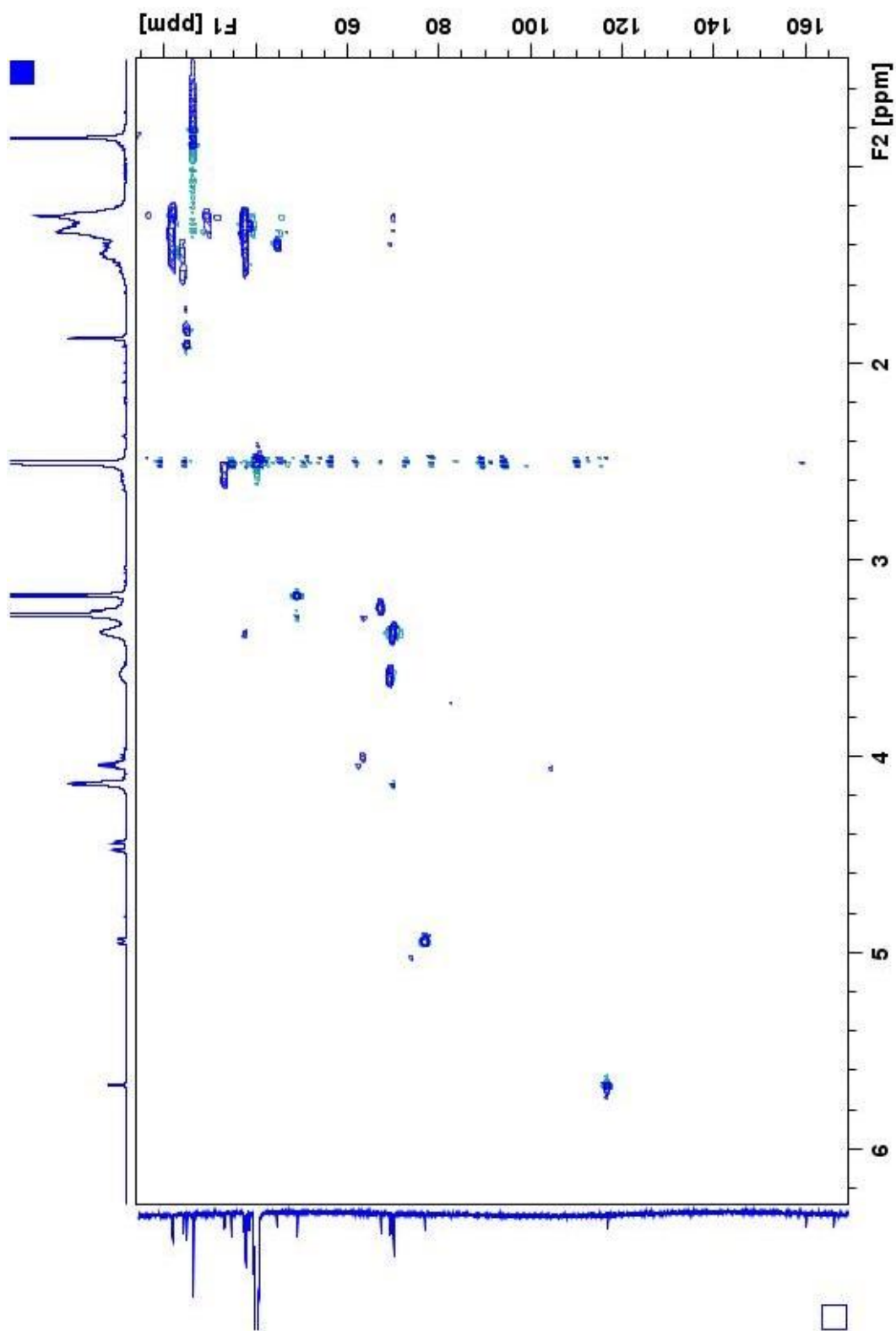


Figure 54. HSQC of nuiapolide (56) in DMSO-*d*₆

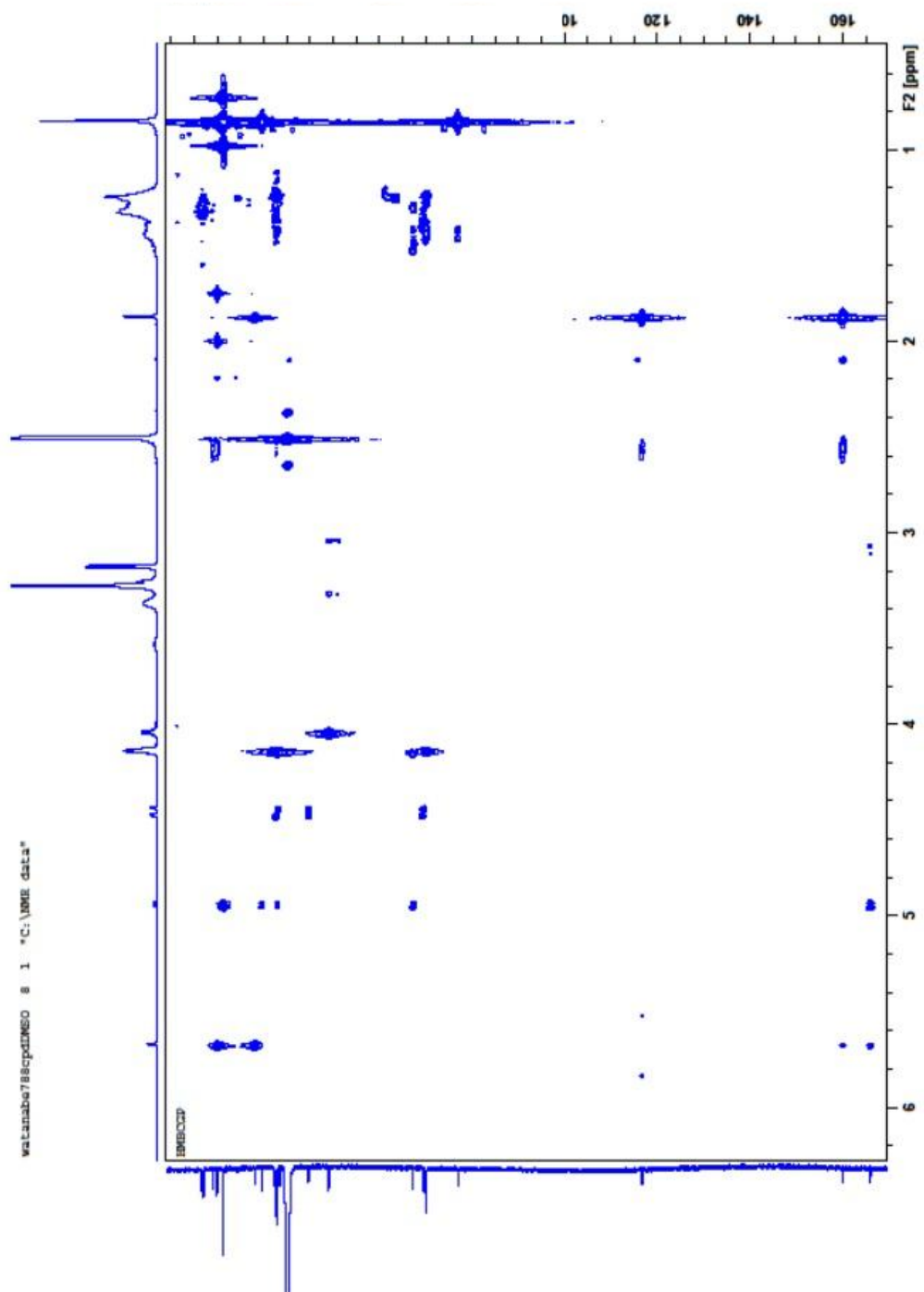


Figure 55. HMBN of nuiapolide (56) in DMSO- d_6

CHAPTER V

CONCLUSION

Natural products have been used as therapeutic agents since the beginning of human history and still play an important role in drug discovery. Use of natural products for therapeutic purposes is thought to be one of the most primitive behaviors of human beings because it is seen even in animals such as mammals and birds. Humans could investigate how natural products affected their health and inherited the knowledge over generations. Natural product drugs have become purer and purer through the technological and scientific advancement. From crude drugs found within an organisms' extract, single natural product drugs were established by the discovery of penicillin in 1928. Since then, scientists started exploring novel natural products from plants or microorganisms, which led to a great expansion of the bioactive compound database. The database keeps enlarging not only with new natural products but also with chemically or biologically modified non-natural natural products. These modification techniques are very important in current drug discovery, however both techniques have limitations. The chemical modification tends to yield reasonable amount of analogous products, but it often cannot replicate the complexities of natural products. The biological modification can replicate these complexities, but it does not produce a high amount of engineered products. Understanding of biosynthetic pathway and enzyme functions is essential for the efficient utilization of combinatorial biosynthesis.

Azinomycins, antitumor agents produced by the soil bacterium *Streptomyces sahachiroi*, are suitable targets to further our enzymatic understanding because they are biosynthesized by a combination of large enzyme families: NRPSs, PKSs, and alkaloid producing enzymes. Evaluation of their functions and interactions would greatly benefit bioengineering utilizing these common enzymatic families together. Even the seemingly simplest part of their biosynthesis, production of the naphthoate moiety by the PKS (AziB), was shown to be more complex than the well studied biosynthesis of aromatic

polyketides; AziB required interaction with a TE domain (AziG) to yield the fully elongated product. This implies the database which is used for bioinformatic studies would not be large enough to accurately predict enzymatic functions and would lack the crucial information for protein-protein or domain-domain interactions. Our enzymatic knowledge, in other words, needs to be improved more for effective engineered biosynthesis of non-natural natural products.

Assembling the naphthoic acid into the azinomycin structure by NRPSs is another mystery whose mechanism could not be drawn only by bioinformatic studies due to an extra domain, AziA2. Transferring the naphthoic acid from AziA1 to AziA2 without any structural modifications seems to be energetically inefficient. However, disruption of *aziA2* in the genomic DNA of *S. sahachiroi* revealed that this domain was essential for the azinomycin production. The same phenomenon can be observed in other PKS or NRPS biosynthetic pathways containing apparently unnecessary domains. This indicates again that our enzymatic knowledge has a lot room to improve. The *aziA2* disruption mutant also displayed an example of bacterial adaptation. Overproduction of dimethyl furan-2,4-dicarboxylate in the disruption mutant suggested that a gene cluster which is silenced in the wild type *S. sahachiroi* was activated by a change of the internal environment, in this case the absence of azinomycin production. This suggests that yield of a natural product could be increased by disruption of other natural products' biosynthesis in an organism.

Most natural products isolated to date are found in terrestrial organisms because of their ease to harvest and culture. Oceans cover 70 % of earth's surface and have been thought to be a large source of novel natural products. Recent technological and scientific advancement has allowed researchers to explore marine natural products, which have successfully provided potent therapeutic agents. The novel macrolactone bioactive natural product nuiapolide was discovered and isolated from a marine cyanobacterium. The proposed anti-metastatic activity could provide a solution or hint for therapies targeting cancer metastasis which is one of the critical barriers in cancer treatment. The molecular structure of nuiapolide resembles a previously described class

of anti-tumor natural products, the caylobolides, which were also isolated from cyanobacteria. Further evaluation of these compounds for their biosynthetic pathway would be beneficial for bio-engineering purposes, and the large but relatively simple structure would ease the synthetic study to identify the pharmacophore and to produce bioactive analogs.

The following topics were discussed in this dissertation: the novel PKS-TE domain interaction involved in polyketide biosynthesis, bioactivity assays of dimethyl furan-2,4-dicarboxylate which was overproduced in *S. sahachiroi aziA2* disruption mutant, and discovery of the novel bioactive marine natural product nuiapolide. Each project provided different outcomes; the first one provided enzymatic perspective in the polyketide production, the second displayed bacterial adaptation, and the last added a compound into the marine natural product database. These achievements would present novel scientific insights into natural product chemistry.

REFERENCES

1. Newman, D.J. and Cragg, G.M., Natural products as sources of new drugs over the 30 Years from 1981 to 2010. *Journal of Natural Products*, **2012**, *75* 311-335.
2. Newman, D.J. and Giddings, L.A., Natural products as leads to antitumor drugs. *Phytochemistry Reviews*, **2014**, *13* 123–137.
3. Sun, H.; Liu, Z.; Zhao, H.; and Ang, E.L., Recent advances in combinatorial biosynthesis for drug discovery. *Drug Design, Development and Therapy*, **2015**, *9* 823–833.
4. Armstrong, R.W.; Salvati, M.E.; and Nguyen, M., Novel interstrand cross-links induced by the antitumor antibiotic carzinophilin/azinomycin B. *Journal of the American Chemical Society*, **1992**, *114* 3144-3145.
5. Coleman, R.S.; Perez, R.J.; Burk, C.H.; and Navarro, A., Studies on the mechanism of action of azinomycin B: definition of regioselectivity and sequence selectivity of DNA cross-link formation and clarification of the role of the naphthoate. *Journal of the American Chemical Society*, **2002**, *124* (44), 13008-13017.
6. Fujiwara, T.; Saito, I.; and Sugiyama, H., Highly efficient DNA interstrand crosslinking induced by an antitumor antibiotic, carzinophilin. *Tetrahedron Letters*, **1999**, *40* (2), 315-318.
7. Foulke-Abel, J.; Agbo, H.; Zhang, H.; Mori, S.; and Watanabe, C.M.H., Mode of action and biosynthesis of the azabicyclic-containing natural products azinomycin and ficellomycin. *natural Product Reports*, **2011**, *28* 693–704.
8. Kelly, G.T.; Liu, C.; Smith, R., 3rd; Coleman, R.S.; and Watanabe, C.M.H., Cellular effects induced by the antitumor agent azinomycin B. *Chemistry & Biology*, **2006**, *13* (5), 485-92.
9. Williams, D.H.; Stone, M.J.; Hauck, P.R.; and Rahman, S.K., Why are secondary metabolites (natural products) biosynthesized? *Journal of Natural Products*, **1989**, *52* (6), 1189-1208.

10. Croteau, R.; Kutchan, T.M.; and Lewis, N.G., *Natural products (secondary metabolites), in Biochemistry & Molecular Biology of Plants*, Buchanan, B.B.; Gruissem, W.; and Jones, R.L., Editors. 2000, John Wiley & Sons: Hoboken. p. 1250-1318.
11. Butler, M.S., The role of natural product chemistry in drug discovery. *Journal of Natural Products*, **2004**, 67 (12), 2141–2153.
12. Fleming, A., On the antibacterial action of cultures of a penicillium, with a special reference to their use in the isolation of *B. influenza*. *the British Journal of Experimental Pathology*, **1929**, 10 226-236.
13. Miller, E.L., The penicillins: a review and update. *Journal of Midwifery & Women's Health*, **2002**, 47 (6), 426-434.
14. Solecki, R.S., Shanidar IV, a neanderthal flower burial in northern Iraq. *Science*, **1975**, 190 (4217), 880-881.
15. Hardy, K.; Buckley, S.; Collins, M.J.; Estalrich, A.; Brothwell, D.; Copeland, L.; García-Taberner, A.; García-Vargas, S.; de la Rasilla, M.; Lalueza-Fox, C.; Huguet, R.; Bastir, M.; Santamaría, D.; Madella, M.; Wilson, J.; Cortés, Á.F.; and Rosas, A., Neanderthal medics? Evidence for food, cooking, and medicinal plants entrapped in dental calculus. *Naturwissenschaften*, **2012**, 99 (8), 617-626.
16. Lalueza-Fox, C.; Gigli, E.; de la Rasilla, M.; Fortea, J.; and Rosas, A., Bitter taste perception in Neanderthals through the analysis of the TAS2R38 gene. *Biology Letters*, **2009**, 5 (6), 809-811.
17. Attinger, P., La médecine mésopotamienne. *Journal des Médecines Cunéiformes*, **2008**, 11-12 1-96.
18. Nunn, J., Ancient Egyptian medicine, in University of Oklahoma Press. **2002**.
19. Aggarwal, B.B.; Sundaram, C.; Malani, N.; and Ichikawa, H., Curcumin: the Indian solid gold. *Advances in Experimental Medicine and Biology*, **2007**, 595 1–75.
20. Hong, F., History of medicine in China. *McGill Journal of Medicine*, **2004**, 8 (1), 7984.

21. Rodriguez, E. and Wrangham, R., Zoopharmacognosy: the use of medicinal plants by animals. *Phytochemical Potential of Tropical Plants*, **1993**, 27 89–105.
22. Wrangham, R.W. and Nishida, T., *Aspilia* spp. Leaves: a puzzle in the feeding behavior of wild chimpanzees. *Primates* **1983**, 24 (2), 276-282.
23. Wrangham, R.W. and Goodall, J., Understanding chimpanzees in Harvard University Press. **1989**: Cambridge, MA.
24. Rodriguez, E.; Aregullin, M.; Nishida, T.; Uehara, S.; Wrangham, R.W.; Abramowski, Z.; Finlayson, A.; and Towers, G.H.N., Thiarubrine-A, a bioactive constituent of *Aspilia* (Asteraceae) consumed by wild chimpanzees. *Experientia*, **1985**, 41 419-420.
25. Ali, S., Do birds employ ants to rid themselves of ectoparasites? *Journal of the Bombay Natural History Society*, **1936**, 38 (3), 628–631.
26. Revis, H.C. and Waller, D.A., Bactericidal and fungicidal activity of ant chemicals on feather parasites: an evaluation of anting behavior as a method of self-medication in songbirds. *The Auk* **2004**, 121 (4), 1262–1268.
27. Beutler, J.A., *Natural products as a foundation for drug discovery*, in *Current Protocols in Pharmacology*, Enna, S.J., et al., Editors. 2009. p. 11.1–9.11.21.
28. Mishra, B.B. and Tiwari, V.K., Natural products: an evolving role in future drug discovery. *European Journal of Medical Chemistry*, **2011**, 46 4769-4807.
29. Houbraken, J.; Frisvad, J.C.; and Samson, R.A., Fleming's penicillin producing strain is not *Penicillium chrysogenum* but *P. rubens*. *IMA Fungus*, **2011**, 2 (1), 87-95.
30. Chain, E.; Florey, H.W.; Gardner, A.D.; Heatley, N.G.; Jennings, M.A.; Orr-Ewing, J.; and Sanders, A.G., Penicillin as a chemotherapeutic agent. *Lancet*, **1940**, 239 226-228.
31. Abraham, E.P.; Chain, E.; Fletcher, C.M.; Gardner, A.D.; Heatley, N.G.; Jennings, M.A.; and Florey, H.W., Further observations on penicillin. *Lancet*, **1941**, 241 177-189.

32. Myers, W.G., Review papers: penicillin: a potent new chemotherapeutic agent. *The Ohio Journal of Science*, **1944**, 44 (6), 278-286.
33. David, D.; Wolfender, J.L.; and Dias, D.A., The pharmaceutical industry and natural products: historical status and new trends. *Phytochemistry Reviews*, **2014**, 1–17.
34. Agrestia, J.J.; Antipovc, E.; Abatea, A.R.; Ahna, K.; Rowata, A.C.; Barete, J.C.; Marquezf, M.; Klibanovc, A.M.; Griffiths, A.D.; and Weitz, D.A., Ultrahigh-throughput screening in drop-based microfluidics for directed evolution. *Proceedings of the National Academy of Sciences*, **2010**, 107 (9), 4004–4009.
35. Patwardhan, B. and Mashelkar, R.A., Traditional medicine-inspired approaches to drug discovery: can Ayurveda show the way forward? *Drug Discovery Today*, **2009**, 14 (15-16), 804–811.
36. Ji, H.F.; Li, X.J.; and Zhang, H.Y., Natural products and drug discovery. Can thousands of years of ancient medical knowledge lead us to new and powerful drug combinations in the fight against cancer and dementia? *EMBO Reports*, **2009**, 10 (3), 194-200.
37. Mayer, A.M.; Glaser, K.B.; Cuevas, C.; Jacobs, R.S.; Kem, W.; Little, R.D.; McIntosh, J.M.; Newman, D.J.; Potts, B.C.; and Shuster, D.E., The odyssey of marine pharmaceuticals: a current pipeline perspective. *Trends in Pharmacological Sciences*, **2010**, 31 (6), 255-265.
38. Harvey, A.L., Toxins and drug discovery. *Toxicon*, **2014**, 92 193-200.
39. Murphy, S.L.; Xu, J.; and Kochanek, K.D., Deaths: final data for 2010. *National Vital Statistics Reports* **2013**, 61 (4),
40. Eurostat. *Causes of death statistics*. Statistics Explained 2015 2 March 2015 [cited 2015 15 March]; Available from: http://ec.europa.eu/eurostat/statistics-explained/index.php/Causes_of_death_statistics.
41. Haikerwal, M.C., Australian burden of disease study fatal burden of disease 2010, in Australian Burden of Disease Study Series, Haikerwal, M.C., Editor. **2015**, Australian Institute of Health and Welfare: Canberra.
42. CCS, Canadian cancer statistics 2014, Statistics, C.C.S.s.A.C.o.C., Editor. **2014**, Canadian Cancer Society: Toronto, ON.

43. Takayama, S., Cancer statistics in Japan - 2013, in Cancer Statistics in Japan, Takayama, S., Editor. **2013**, *Foundation of Promotion of Cancer Research*.
44. Mann, J., Natural products in cancer chemotherapy: past, present and future. *Nature Reviews Cancer*, **2002**, 2 143-148.
45. Blunt, J.W.; Copp, B.R.; Keyzers, R.A.; Munroa, M.H.G.; and Prinsep, M.R., Marine natural products. *Natural Product Reports*, **2014**, 31 160–258.
46. Newman, D.J. and Cragg, G.M., Marine-sourced anti-cancer and cancer pain control agents in clinical and late preclinical development. *Marine Drugs*, **2014**, 12 255-278.
47. Suffness, M. and Douros, J., Current status of the NCI plant and animal product program. *Journal of Natural Products*, **1982**, 45 1-14.
48. Stierle, A.; Strobel, G.; and Stierle, D., Taxol and taxane production by *Taxomyces andreanae*, an endophytic fungus of Pacific yew. *Science*, **1993**, 260 (5105), 214-216.
49. Walsh, V. and Roux, M.L., Contingency in innovation and the role of national systems: taxol and taxotere in the USA and France. *Research Policy*, **2004**, 33 1307–1327.
50. Holton, R., Method for preparation of taxol using an oxazinone, in European Patent. **1991**: US.
51. Holton, R., Method for preparation of taxol using alpha-lactam, in European Patent. **1992**: US.
52. Cavalletti, E.; Crippa, L.; Mainardi, P.; Oggioni, N.; Cavagnoli, R.; Bellini, O.; and Sala, F., Pixantrone (BBR 2778) has reduced cardiotoxic potential in mice pretreated with doxorubicin: comparative studies against doxorubicin and mitoxantrone. *Investigational New Drugs*, **2007**, 25 (3), 187-195.
53. Gordon, E.M.; Barrett, R.W.; Dower, W.J.; Fodor, S.P.A.; and Gallop, M.A., Applications of combinatorial technologies to drug discovery. 2. Combinatorial organic synthesis, library screening strategies, and future directions. *Journal of Medicinal Chemistry*, **1994**, 37 (10), 1385–1401.

54. Armstrong, R.W.; Combs, A.P.; Tempest, P.A.; Brown, S.D.; and Keating, T.A., Multiple-component condensation strategies for combinatorial library synthesis. *Accounts of Chemical Research*, **1996**, *29* 123-131.
55. Paul, S.M.; Mytelka, D.S.; Dunwiddie, C.T.; Persinger, C.C.; Munos, B.H.; Lindborg, S.R.; and Schacht, A.L., How to improve R&D productivity: the pharmaceutical industry's grand challenge. *Nature Reviews Drug Discovery*, **2010**, *9* 203-214.
56. Cane, D.E.; Walsh, C.T.; and Khosla, C., Harnessing the biosynthetic code: combinations, permutations, and mutations. *Science*, **1998**, *282* (5386), 63-68.
57. Hunter, I.S. and Hill, R.A., *Tetracyclines, in Biotechnology of Antibiotics*, Strohl, W.R., Editor. 1997, Marcel Decker: New York. p. 659-682.
58. Kima, E.-S.; Bibbb, M.J.; Butlerc, M.J.; Hopwoodb, D.A.; and Sherman, D.H., Sequences of the oxytetracycline polyketide synthase-encoding *otc* genes from *Streptomyces rimosus*. *Gene*, **1994**, *141* (1), 141-142.
59. Cortes, J.; Haydock, S.F.; Roberts, G.A.; Bevitt, D.J.; and Leadlay, P.F., An unusually large multifunctional polypeptide in the erythromycin-producing polyketide synthase of *Saccharopolyspora erythraea*. *Nature*, **1990**, *348* 176-178.
60. Donadio, S. and Katz, L., Organization of the enzymatic domains in the multifunctional polyketide synthase involved in erythromycin formation in *Saccharopolyspora erythraea*. *Gene*, **1992**, *111* 551-560.
61. Donadio, S.; Staver, M.J.; McAlpine, J.B.; Swanson, S.J.; and Katz, L., Modular organization of genes required for complex polyketide biosynthesis. *Science*, **1991**, *252* 675-679.
62. Kevany, B.M.; Rasko, D.A.; and Thomas, M.G., Characterization of the complete zwittermicin A biosynthesis gene cluster from *Bacillus cereus*. *Applied and Environment Microbiology*, **2009**, *75* (4), 1144-1155.
63. Du, L.; Sánchez, C.; Chen, M.; Edwards, D.J.; and Shen, B., The biosynthetic gene cluster for the antitumor drug bleomycin from *Streptomyces verticillus* ATCC15003 supporting functional interactions between nonribosomal peptide synthetases and a polyketide synthase. *Chemistry & Biology*, **2000**, *7* (8), 623-642.

64. Fischbach, M.A. and Walsh, C.T., Assembly-line enzymology for polyketide and nonribosomal peptide antibiotics: logic, machinery, and mechanisms. *Chemical Reviews*, **2006**, *106* 3468-3496.
65. Lambalot, R.H.; Gehring, A.M.; Flugel, R.S.; Zuber, P.; LaCelle, M.; Marahiel, M.A.; Reid, R.; Khosla, C.; and Walsh, C.T., A new enzyme superfamily — the phosphopantetheinyl transferases. *Chemistry & Biology*, **1996**, *3* (11), 923-936.
66. Hertweck, C.; Luzhetskyy, A.; Rebets, Y.; and Bechthold, A., Type II polyketide synthases: gaining a deeper insight into enzymatic teamwork. *Natural Product Reports*, **2007**, *24* 162-190.
67. Hertweck, C.; Luzhetskyy, A.; Rebets, Y.; and Bechthold, A., Type II polyketide synthases: gaining a deeper insight into enzymatic teamwork. *Natural Product Reports*, **2007**, *24* 162–190.
68. Tseng, C.C.; McLoughlin, S.M.; Kelleher, N.L.; and Walsh, C.T., Role of the active site cysteine of DpgA, a bacterial type III polyketide synthase. *Biochemistry*, **2004**, *43* (4), 970-980.
69. Wageningen, A.A.v.; Kirkpatrick, P.N.; Williams, D.H.; Harris, B.R.; Kershaw, J.K.; Lennard, N.J.; Jones, M.; Jones, S.J.M.; and Solenberg, P.J., Sequencing and analysis of genes involved in the biosynthesis of a vancomycin group antibiotic. *Chemistry & Biology*, **1998**, *5* (3), 155–162.
70. Bushley, K.E.; Raja, R.; Jaiswal, P.; Cumbie, J.S.; Nonogaki, M.; Boyd, A.E.; Owensby, C.A.; Knaus, B.J.; Elser, J.; Miller, D.; Di, Y.; McPhail, K.L.; and Spatafora, J.W., The genome of *Tolypocladium inflatum*: evolution, organization, and expression of the cyclosporin biosynthetic gene cluster. *PLoS Genetics*, **2013**, *9* (6).
71. Gokhale, R.S.; Hunziker, D.; Cane, D.E.; and Khosla, C., Mechanism and specificity of the terminal thioesterase domain from the erythromycin polyketide synthase. *Chemistry & Biology*, **1999**, *6* (2), 117–125.
72. Shaw-Reid, C.A.; Kelleher, N.L.; Losey, H.C.; Gehring, A.M.; Berg, C.; and Walsh, C.T., Assembly line enzymology by multimodular nonribosomal peptide synthetases: the thioesterase domain of *E. coli* EntF catalyzes both elongation and cyclolactonization. *Chemistry & Biology*, **1999**, *6* 385-400.

73. Gaudelli, N.M. and A., T.C., Epimerization and substrate gating by a TE domain in β -lactam antibiotic biosynthesis. *Nature Chemical Biology*, **2014**, *10* 251-258.
74. Gaudelli, N.M.; Long, D.H.; and A., T.C., beta-Lactam formation by a non-ribosomal peptide synthetase during antibiotic biosynthesis. *Nature*, **2015**, *520* 383-387.
75. Fujii, I.; Watanabe, Y.; Sankawa, U.; and Ebizuka, Y., Identification of Claisen cyclase domain in fungal polyketide synthase WA, a naphthopyrone synthase of *Aspergillus nidulans*. *Chemistry & Biology*, **2001**, *8* 189-197.
76. Crawford, J.M. and Townsend, C.A., New insights into the formation of fungal aromatic polyketides. *Nature Reviews Microbiology*, **2010**, *8* 879-889.
77. Fujii, I.; Watanabe, Y.; Kubo, Y.; Tsuji, G.; and Ebizuka, Y., Enzymatic synthesis of 1,3,6,8-tetrahydroxynaphthalene solely from malonyl coenzyme A by a fungal iterative type I polyketide synthase PKS1. *Biochemistry*, **2000**, *39* 8853-8858.
78. Crawford, J.M.; Vagstad, A.L.; Whitworth, K.P.; Ehrlich, K.C.; and Townsend, C.A., Synthetic strategy of nonreducing iterative polyketide synthases and the origin of the classical "starter unit effect". *ChemBioChem*, **2008**, *9* 1019-1023.
79. Vagstad, A.L.; Hill, E.A.; Labonte, J.W.; and Townsend, C.A., Characterization of a fungal thioesterase having Claisen cyclase and deacetylase activities in melanin biosynthesis. *Chemistry & Biology*, **2012**, *19* 1525-1534.
80. Bravo-Rodriguez, K.; Ismail-Ali, A.F.; Klopries, S.; Kushnir, S.; Ismail, S.; Fansa, E.K.; Wittinghofer, A.; Schulz, F.; and Sanchez-Garcia, E., Predicted incorporation of non-native substrates by a polyketide synthase yields bioactive natural product derivatives. *ChemBioChem*, **2014**, *15* (13), 1991-1997.
81. Hata, T.; Koga, F.; Sano, Y.; Kanamori, K.; Matsumae, A.; Sugawara, R.; Hoshi, T.; and Shima, T., Carzinophilin, a new tumor inhibitory substance produced by *Streptomyces*. *The Journal of Antibiotics. Series A.*, **1954**, *7* (4), 107-112.
82. Nagaoka, K.; Matsumoto, M.; Oono, J.; Yokoi, K.; Ishizeki, S.; and Nakashima, T., Azinomycins A and B, new antitumor antibiotics. I. Producing organism, fermentation, isolation, and characterization. *Journal of Antibiotics (Tokyo)*, **1986**, *39* (11), 1527-32.

83. Ishizeki, S.; Ohtsuka, M.; Irinoda, K.; Kukita, K.; Nagaoka, K.; and Nakashima, T., Azinomycins A and B, new antitumor antibiotics. III. Antitumor activity. *Journal of Antibiotics (Tokyo)*, **1987**, *40* (1), 60-65.
84. Yokoi, K.; Nagaoka, K.; and Nakashima, T., Azinomycins A and B, new antitumor antibiotics. II. Chemical structures. *Chemical & Pharmaceutical Bulletin (Tokyo)*, **1986**, *34* (11), 4554-4561.
85. Terawaki, A. and Greenberg, J., Effect of carzinophillin on bacterial deoxyribonucleic acid: formation of inter-strand cross-links in deoxyribonucleic acid and their disappearance during post-treatment incubation. *Nature*, **1966**, *209* 481-484.
86. Terawaki, A. and Greenberg, J., Inactivation of transforming deoxyribonucleic acid by carzinophillin and mitomycin C. *Biochimica et Biophysica Acta*, **1966**, *119* (1), 59-64.
87. Lown, J.W. and Majumdar, K.C., Studies related to antitumor antibiotics. Part IX. Reactions of carzinophillin with DNA assayed by ethidium fluorescence. *Canadian Journal of Biochemistry*, **1977**, *55* (6), 630-635.
88. LePla, R.C.; Landreau, C.A.; Shipman, M.; and Jones, G.D., On the origin of the DNA sequence selectivity of the azinomycins. *Organic & Biomolecular Chemistry* **2005**, *3* (7), 1174-1175.
89. Hodgkinson, T.J.; Kelland, L.R.; Shipman, M.; and Suzenet, F., Chemical synthesis and cytotoxicity of some azinomycin analogues devoid of the 1-azabicyclo[3.1.0]hexane subunit. *Bioorganic & Medicinal Chemistry Letters*, **2000**, *10* (3), 239-41.
90. David-Cordonnier, M.H.; Casely-Hayford, M.; Kouach, M.; Briand, G.; Patterson, L.H.; Bailly, C.; and Searcey, M., Stereoselectivity, sequence specificity and mechanism of action of the azinomycin epoxide. *Chembiochem*, **2006**, *7* (11), 1658-61.
91. Coleman, R.S.; Woodward, R.L.; Hayes, A.M.; Crane, E.A.; Artese, A.; Ortuso, F.; and Alcaro, S., Dependence of DNA sequence selectivity and cell cytotoxicity on azinomycin A and B epoxyamide stereochemistry. *Organic Letters*, **2007**, *9* (10), 1891-1894.

92. Coleman, R.S.; Burk, C.H.; Navarro, A.; Brueggemeier, R.W.; and Diaz-Cruz, E.S., Role of the azinomycin naphthoate and central amide in sequence-dependent DNA alkylation and cytotoxicity of epoxide-bearing substructures. *Organic Letters*, **2002**, *4* (20), 3545-3548.
93. Zang, H. and Gates, K.S., DNA binding and alkylation by the "left half" of azinomycin B. *Biochemistry*, **2000**, *39* (48), 14968-14975.
94. Landreau, C.A.; LePla, R.C.; Shipman, M.; Slawin, A.M.; and Hartley, J.A., Delineating noncovalent interactions between the azinomycins and double-stranded DNA: importance of the naphthalene substitution pattern on interstrand cross-linking efficiency. *Organic Letters*, **2004**, *6* (20), 3505-3507.
95. Hashimoto, M.; Matsumoto, M.; Yamada, K.; and Terashima, S., Synthesis, chemical property, and cytotoxicity of the carzinophilin congeners carrying a 2-(1-acylamino-1-alkoxycarbonyl)methylidene-1-azabicyclo[3.1.0]hexane system. *Tetrahedron Letters*, **1994**, *35* (14), 2207-2210.
96. Hashimoto, M.; Yamada, K.; and Terashima, S., Synthesis, chemical reactivity, and cytotoxicity of 2-bis(alkoxycarbonyl)methyliden-1-azabicyclo[3.1.0]hexane systems related to antitumor antibiotic carzinophilin A. *Chemistry Letters*, **1992**, *21* (6), 975-978.
97. Hodgkinson, T.J.; Kelland, L.R.; Shipman, M.; and Vile, J., Synthesis and reactivity of some chiral, nonracemic 1-azabicyclo[4.1.0]heptanes related to the azinomycins. *Tetrahedron*, **1998**, *54* 6029-6034.
98. Hashimoto, M. and Terashima, S., A stereoselective synthesis of a novel model compound of carzinophilin carrying the C6-C13 unit with correct stereochemistry. *Chemistry Letters*, **1994**, *23* (6), 1001-1002
99. Hashimoto, M.; Matsumoto, M.; Yamada, K.; and Terashima, S., Synthetic studies of carzinophilin. Part 4: Chemical and biological properties of carzinophilin analogues. *Tetrahedron*, **2003**, *59* 3089-3097.
100. Hartley, J.A.; Hazrati, A.; Kelland, L.R.; Khanim, R.; Shipman, M.; Suzenet, F.; and Walker, L.F., A synthetic azinomycin analogue with demonstrated DNA cross-linking activity: insights into the mechanism of action of this class of antitumor agent *Angewandte Chemie International Edition*, **2000**, *39* 3467-3470.

101. LePla, R.C.; Landreau, C.A.; Shipman, M.; Hartley, J.A.; and Jones, G.D., Azinomycin inspired bisepoxides: influence of linker structure on in vitro cytotoxicity and DNA interstrand cross-linking. *Bioorganic & Medicinal Chemistry Letters*, **2005b**, *15* (11), 2861-2864.
102. Finerty, M.J.; Bingham, J.P.; Hartley, J.A.; and Shipman, M., Azinomycin bisepoxides containing rigid aromatic linkers: synthesis, cytotoxicity and DNA interstrand cross-linking activity. *Tetrahedron Letters*, **2009**, *50* (26), 3648–3650.
103. Corre, C. and Lowden, P.A., The first biosynthetic studies of the azinomycins: acetate incorporation into azinomycin B. *Chemical Communications (Cambridge)*, **2004**, (8), 990-991.
104. Corre, C.; Landreau, C.A.; Shipman, M.; and Lowden, P.A., Biosynthetic studies on the azinomycins: the pathway to the naphthoate fragment. *Chemical Communications (Cambridge)*, **2004**, (22), 2600-2601.
105. Kelly, G.T.; Sharma, V.; and Watanabe, C.M.H., An improved method for culturing *Streptomyces sahachiroi*: biosynthetic origin of the enol fragment of azinomycin B. *Bioorganic Chemistry*, **2008**, *36* (1), 4-15.
106. Sharma, V.; Kelly, G.T.; Foulke-Abel, J.; and Watanabe, C.M.H., Aminoacetone as the penultimate precursor to the antitumor agent azinomycin A. *Organic Letters*, **2009**, *11* (17), 4006-4009.
107. Sharma, V.; Kelly, G.T.; and Watanabe, C.M.H., Exploration of the molecular origin of the azinomycin epoxide: timing of the biosynthesis revealed. *Organic Letters*, **2008**, *10* (21), 4815-8.
108. Zhao, Q.; He, Q.; Ding, W.; Tang, M.; Kang, Q.; Yu, Y.; Deng, W.; Zhang, Q.; Fang, J.; Tang, G.; and Liu, W., Characterization of the azinomycin B biosynthetic gene cluster revealing a different iterative type I polyketide synthase for naphthoate biosynthesis. *Chemistry & Biology*, **2008**, *15* (7), 693-705.
109. Simkhada, D.; Zhang, H.; Mori, S.; Williams, H.; and Watanabe, C.M.H., Activation of cryptic metabolite production through gene disruption: dimethyl furan-2,4-dicarboxylate produced by *Streptomyces sahachiroi*. *Beilstein Journal of Organic Chemistry*, **2013**, *9* 1768–1773.

110. Wang, S.; Zhao, R.; Liu, K.; Zhu, M.; Li, A.; and He, J., Essential role of an unknown gene aziU3 in the production of antitumor antibiotic azinomycin B verified by utilizing optimized genetic manipulation systems for *Streptomyces sahachiroi*. *FEMS Microbiology Letters*, **2012**, *337* 147–154.
111. Foulke-Abel, J.; Kelly, G.T.; Zhang, H.; and Watanabe, C.M.H., Characterization of AziR, a resistance protein of the DNA cross-linking agent azinomycin B. *Molecular bioSystems*, **2011**, *7* 2563–2570.
112. Song, F.; Thoden, J.B.; Zhuang, Z.; Latham, J.; Trujillo, M.; Holden, H.M.; and Dunaway-Mariano, D., The catalytic mechanism of the hotdog-fold enzyme superfamily 4-hydroxybenzoyl-CoA thioesterase from *Arthrobacter* sp. strain SU. *Biochemistry*, **2012**, *51* 7000-7016.
113. Jia, X.-Y.; Tian, Z.-H.; Shao, L.; Qu, X.-D.; Zhao, Q.-F.; Tang, J.; Tang, G.-L.; and Liu, W., Genetic characterization of the chlorothricin gene cluster as a model for spirotetronate antibiotic biosynthesis. *Chemistry & Biology*, **2006**, *13* 575-585.
114. Liu, W.; Nonaka, K.; Nie, L.; Zhang, J.; Christenson, S.D.; Bae, J.; Lanen, S.G.V.; Zazopoulos, E.; Farnet, C.M.; Yang, C.F.; and Shen, B., The neocarzinostatin biosynthetic gene cluster from *Streptomyces carzinostaticus* ATCC 15944 involving two iterative type I polyketide synthases. *Chemistry & Biology*, **2005**, *12* 293-302.
115. Daum, M.; Peintner, I.; Linnenbrink, A.; Frerich, A.; Weber, M.; Paululat, T.; and Bechthold, A., Organisation of the biosynthetic gene cluster and tailoring enzymes in the biosynthesis of the tetracyclic quinone glycoside antibiotic polyketomycin. *ChemBioChem*, **2009**, *10* 1073-1083.
116. Sánchez, C.; Du, L.; Edwards, D.J.; Toney, M.D.; and Shen, B., Cloning and characterization of a phosphopantetheinyl transferase from *Streptomyces verticillus* ATCC15003, the producer of the hybrid peptide[^]polyketide antitumor drug bleomycin. *Chemistry & Biology*, **2001**, *8* (7), 725-738.
117. Dillon, S.C. and Bateman, A., The hotdog fold: wrapping up a superfamily of thioesterases and dehydratases. *BMC Bioinformatics*, **2004**, *5* (109).

118. Song, F.; Zhuang, Z.; Finci, L.; Dunaway-Mariano, D.; Kniewel, R.; Buglino, J.A.; Solorzano, V.; Wu, J.; and Lima, C.D., Structure, function, and mechanism of the phenylacetate pathway hot dog-fold thioesterase PaaI. *Journal of Biological Chemistry*, **2006**, 281 (16), 11028-11038.
119. Teufela, R.; Mascaraqueb, V.; Ismaila, W.; Vossa, M.; Pererab, J.; Eisenreichc, W.; Haehnel, W.; and Fuchs, G., Bacterial phenylalanine and phenylacetate catabolic pathway revealed. *Proceedings of the National Academy of Sciences*, **2010**, 107 (32), 14390-14395.
120. Thoden, J.B.; Zhuang, Z.; Dunaway-Mariano, D.; and Holden, H.M., The structure of 4-hydroxybenzoyl-CoA thioesterase from *Arthrobacter* sp. strain SU. *Journal of Biological Chemistry*, **2002**, 278 (44), 43709-43716.
121. Wu, R.; Latham, J.A.; Chen, D.; Farelli, J.; Zhao, H.; Matthews, K.; Allen, K.N.; and Dunaway-Mariano, D., Structure and catalysis in the Escherichia coli hotdog-fold thioesterase paralogs YdiI and YbdB. *Biochemistry*, **2014**, 53 (29), 4788-4805.
122. Kunishima, N.; Asada, Y.; Sugahara, M.; Ishijima, J.; Nodake, Y.; Sugahara, M.; Miyano, M.; Kuramitsu, S.; Yokoyama, S.; and Sugahara, M., A novel induced-fit reaction mechanism of asymmetric hot dog thioesterase PaaI. *Journal of Molecular Biology*, **2005**, 352 (1), 212-228.
123. Tsai, S.C.; Miercke, L.J.; Krucinski, J.; Gokhale, R.; Chen, J.C.; Foster, P.G.; Cane, D.E.; Khosla, C.; and Stroud, R.M., Crystal structure of the macrocycle-forming thioesterase domain of the erythromycin polyketide synthase: versatility from a unique substrate channel. *Proceedings of the National Academy of Sciences*, **2001**, 98 (26), 14808-14813.
124. Bruner, S.D.; Weber, T.; Kohli, R.M.; Schwarzer, D.; Marahiel, M.A.; Walsh, C.T.; and Stubbs, M.T., Structural basis for the cyclization of the lipopeptide antibiotic surfactin by the thioesterase domain SrfTE. *Structure*, **2002**, 10 (3), 301-310.
125. Pemble, C.W.t.; Johnson, L.C.; Kridel, S.J.; and Lowther, W.T., Crystal structure of the thioesterase domain of human fatty acid synthase inhibited by orlistat. *Nature Structural & Molecular Biology*, **2007**, 14 (8), 704-709.

126. Korman, T.P.; Crawford, J.M.; Labonte, J.W.; Newman, A.G.; Wong, J.; Townsend, C.A.; and Tsai, S.C., Structure and function of an iterative polyketide synthase thioesterase domain catalyzing Claisen cyclization in aflatoxin biosynthesis. *Proceedings of the National Academy of Sciences*, **2010**, *107* (14), 6246-6251.
127. Cantu, D.C.; Ardèvol, A.; Rovira, C.; and Reilly, P.J., Molecular mechanism of a hotdog-fold acyl-CoA thioesterase. *Chemistry - A European Journal*, **2014**, *20* (29), 9045–9051.
128. Brobst, S.W. and Townsend, C.A., The potential role of fatty acid initiation in the biosynthesis of the fungal aromatic polyketide aflatoxin B₁. *Canadian Journal of Chemistry*, **1993**, *72* 200-207.
129. Watanabe, C.M.H.; Wilson, D.; Linz, J.E.; and Townsend, C.A., Demonstration of the catalytic roles and evidence for the physical association of type I fatty acid synthases and a polyketide synthase in the biosynthesis of aflatoxin B₁. *Chemistry & Biology*, **1996**, *3* 463-469.
130. Ellman, G.L., Tissue sulfhydryl groups. *Archives of Biochemistry and Biophysics*, **1959**, *82* (1), 70-77.
131. Cassayre, J.Y.; Renold, P.; Pitterna, T.; Bobosik, V.; El, Q.M.; Dalencon, A.J.; Zambach, W.; Godfrey, C.R.; Jung, P.J.; and Pabba, J., Insecticidal compounds. **2010**, *Google Patents*.
132. Barba, O.; Dawson, G.J.; Krulle, T.M.; Rowley, R.J.; Smyth, D.; and Thomas, G.H., Dihydroimidazothiazole derivatives. **2006**, *Google Patents*.
133. Otwinowski, Z. and Minor, W., *Processing of X-ray Diffraction Data Collected in Oscillation Mode*, in *Methods Enzymol.*, Carter, C.W.J. and Sweet, R.M., Editors. 1997, Academic Press: New York. p. 307-326.
134. Ding, W.; Deng, W.; Tang, M.; Zhang, Q.; Tang, G.; Bi, Y.; and Liu, W., Biosynthesis of 3-methoxy-5-methyl naphthoic acid and its incorporation into the antitumor antibiotic azinomycin B. *Molecular BioSystems* **2010**, *6* (6), 1071-81.

135. Bentley, S.D.; Chater, K.F.; Cerdeño-Tárraga, A.-M.; Challis, G.L.; Thomson, N.R.; James, K.D.; Harris, D.E.; Quail, M.A.; Kieser, H.; Harper, D.; Bateman, A.; Brown, S.; Chandra, G.; Chen, C.W.; Collins, M.; Cronin, A.; Fraser, A.; Goble, A.; Hidalgo, J.; Hornsby, T.; Howarth, S.; Huang, C.-H.; Kieser, T.; Larke, L.; Murphy, L.; Oliver, K.; O'Neil, S.; Rabinowitsch, E.; Rajandream, M.-A.; Rutherford, K.; Rutter, S.; Seeger, K.; Saunders, D.; Sharp, S.; Squares, R.; Squares, S.; Taylor, K.; Warren, T.; Wietzorrek, A.; Woodward, J.; Barrell, B.G.; Parkhill, J.; and Hopwood, D.A., Complete genome sequence of the model actinomycete *Streptomyces coelicolor* A3(2). *Nature*, **2002**, *417* 141-147.
136. Boyden, S.V., The chemotactic effect of mixtures of antibody and antigen on polymorphonuclear leucocytes. *Journal of Experimental Medicine*, **1962**, *115* (3), 453-466.
137. Adachi, K. and Chiba, K., FTY720 story. Its discovery and the following accelerated development of sphingosine 1-phosphate receptor agonists as immunomodulators based on reverse pharmacology. *Perspectives in Medicinal Chemistry*, **2007**, *1* 11-23.
138. Greene, L.A. and Tischler, A.S., Establishment of a noradrenergic clonal line of rat adrenal pheochromocytoma cells which respond to nerve growth factor. *Proceedings of the National Academy of Sciences*, **1976**, *73* (7), 2424-2428.
139. Rydel, R.E. and Greene, L.A., Acidic and basic fibroblast growth factors promote stable neurite outgrowth and neuronal differentiation in cultures of PC12 cells. *Journal of Neuroscience*, **1987**, *7* (11), 3639-3653.
140. Jones-Villeneuve, E.M.; McBurney, M.W.; Rogers, K.A.; and Kalnins, V.I., Retinoic acid induces embryonal carcinoma cells to differentiate into neurons and glial cells. *Journal of Cell Biology*, **1982**, *94* (2), 253-262.
141. Scheibe, R.J.; Ginty, D.D.; and Wagner, J.A., Retinoic acid stimulates the differentiation of PC12 cells that are deficient in cAMP-dependent protein kinase. *Journal of Cell Biology*, **1991**, *113* (5), 1173-1182.
142. Cragg, G.M. and Newman, D.J., Natural products: a continuing source of novel drug leads. *Biochimica et Biophysica Acta*, **2013**, *1830* 3670-3695.
143. Mitchell, W., Natural products from synthetic biology. *Current Opinion in Chemical Biology*, **2011**, *15* (4), 505-515.

144. Procópioa, R.E.d.L.; Silvaa, I.R.d.; Martinsa, M.K.; Azevedoa, J.L.d.; and Araújo, J.M.d., Antibiotics produced by *Streptomyces*. *The Brazilian Journal of Infectious Diseases*, **2012**, *16* (5), 466–471.
145. Stewart, E.J., Growing unculturable bacteria. *Journal of Bacteriology*, **2012**, *194* (16), 4151-4160.
146. Rusch, D.B.; Halpern, A.L.; Sutton, G.; Heidelberg, K.B.; Williamson, S.; Yooseph, S.; Wu, D.; Eisen, J.A.; Hoffman, J.M.; Remington, K.; Beeson, K.; Tran, B.; Smith, H.; Baden-Tillson, H.; Stewart, C.; Thorpe, J.; Freeman, J.; Andrews-Pfannkoch, C.; Venter, J.E.; Li, K.; Kravitz, S.; Heidelberg, J.F.; Utterback, T.; Rogers, Y.H.; Falcón, L.I.; Souza, V.; Bonilla-Rosso, G.; Eguiarte, L., E.; Karl, D.M.; Sathyendranath, S.; Platt, T.; Bermingham, E.; Gallardo, V.; Tamayo-Castillo, G.; Ferrari, M.R.; Strausberg, R.L.; Neelson, K.; Friedman, R.; Frazier, M.; and Venter, J.C., The Sorcerer II global ocean sampling expedition: northwest Atlantic through eastern tropical Pacific. *PLoS Biology*, **2007**, *5* (3).
147. Hirata, Y. and Uemura, D., Halichondrins - antitumor polyether macrolides from a marine sponge. *Pure and Applied Chemistry*, **1986**, *58* (5), 701-710.
148. Yu, M.J.; Kishi, Y.; and Littlefield, B.A., *Discovery of E7389, a fully synthetic macrocyclic ketone analogue of halichondrin B, in Anticancer agents from natural products*, Newman, D.J.; Kingston, D.G.I.; and Cragg, G.M., Editors. 2005.
149. Towle, M.J.; Salvato, K.A.; Budrow, J.; Wels, B.F.; Kuznetsov, G.; Aalfs, K.K.; Welsh, S.; Zheng, W.; Seletsk, B.M.; Palme, M.H.; Habgood, G.J.; Singer, L.A.; Dipietro, L.V.; Wang, Y.; Chen, J.J.; Quincy, D.A.; Davis, A.; Yoshimatsu, K.; Kishi, Y.; Yu, M.J.; and Littlefield, B.A., *In vitro* and *in vivo* anticancer activities of synthetic macrocyclic ketone analogues of halichondrin B. *Cancer Research*, **2001**, *61* (3), 1013-1021.
150. USFDA, FDA approves new treatment option for late-stage breast cancer, in FDA NEWS RELEASE. **2010**.
151. Eisai, Halaven™ (eribulin) Receives European Commission Approval For Advanced Breast Cancer. **2011**.
152. Martins, A.; Vieira, H.; Gaspar, H.; and Santos, S., Marketed marine natural products in the pharmaceutical and cosmeceutical industries: tips for success. *Marine Drugs*, **2014**, *12* (2), 1066-1101.

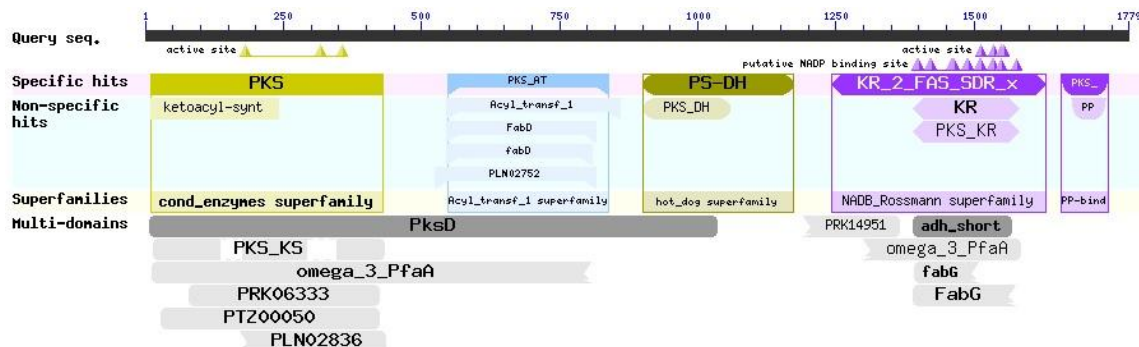
153. Molinski, T.F.; Dalisay, D.S.; Lievens, S.L.; and Saludes, J.P., Drug development from marine natural products. *Nature Reviews Drug Discovery*, **2009**, 8 (1), 69-85.
154. Carter, N.J. and Keam, S.J., Trabectedin : a review of its use in the management of soft tissue sarcoma and ovarian cancer. *Drugs*, **2007**, 67 (15), 2257-2276.
155. Stewart, B. and Wild, C.P., eds. *World cancer report 2014*. 2014, World Health Organization.
156. Dzivenu, O.K. and O'Donnell-Tormey, J., Cancer and the immune system: the vital connection. *Cancer Research Institute*, **2003**.
157. Chaffer, C.L. and Weinberg, R.A., A perspective on cancer cell metastasis. *Science*, **2011**, 331 (6024), 1559-1564.
158. Roussos, E.T.; Condeelis, J.S.; and Patsialou, A., Chemotaxis in cancer. *Nature Reviews Cancer*, **2011**, 11 (8), 573-587.
159. Wadhams, G.H. and Armitage, J.P., Making sense of it all: bacterial chemotaxis. *Nature Reviews Molecular Cell Biology*, **2004**, 5 1024-1037.
160. Kaupp, U.B.; Keshikar, N.D.; and Weyand, I., Mechanisms of sperm chemotaxis. *Annual Review of Physiology*, **2008**, 70 93-117.
161. Oppenheim, J.J. and Yang, D., Alarmins: chemotactic activators of immune responses. *Current Opinion in Immunology*, **2005**, 17 (4), 359-365.
162. Wong, M.S.; Sidik, S.M.; Mahmud, R.; and Stanslas, J., Molecular targets in the discovery and development of novel antimetastatic agents: current progress and future prospects. *Clinical and Experimental Pharmacology and Physiology*, **2013**, 40 (5), 307-319.
163. Schneider, U.; Schwenk, H.; and Bornkamm, G., Characterization of EBV-genome negative "null" and "T" cell lines derived from children with acute lymphoblastic leukemia and leukemic transformed non-Hodgkin lymphoma. *International Journal of Cancer*, **1977**, 19 (5), 621-626.
164. Schafer, K.A., The cell cycle: a review. *Veterinary Pathology*, **1998**, 35 461-478.

165. Vermeulen, K.; Bockstaele, D.R.V.; and Berneman, Z.N., The cell cycle: a review of regulation, deregulation and therapeutic targets in cancer. *Cell Proliferation*, **2003**, *36* 131-149.
166. MacMillan, J.B. and Molinski, T.F., Caylobolide A, a unique 36-membered macrolactone from a Bahamian *Lyngbya majuscula*. *Organic Letters*, **2002**, *4* (9), 1535-1538.
167. Salvador, L.A.; Paul, V.J.; and Luesch, H., Caylobolide B, a macrolactone from symplostatin 1-producing marine cyanobacteria *Phormidium* spp. from Florida. *Journal of Natural Products*, **2010**, *73* 1606-1609.
168. Carmichael, W.W., Cyanobacteria secondary metabolites - the cyanotoxins. *Journal of Applied Microbiology*, **1992**, *72* (6), 445-459.
169. Zanchett, G. and Oliveira-Filho, E.C., Cyanobacteria and cyanotoxins: from impacts on aquatic ecosystems and human health to anticarcinogenic effects. *Toxins (Basel)*, **2013**, *5* (10), 1896-1917.
170. Burja, A.M.; Banaigs, B.; Abou-Mansour, E.; Burgess, J.G.; and Wright, P.C., Marine cyanobacteria - a prolific source of natural products. *Tetrahedron*, **2001**, *57* 9347-9377.
171. Tan, L.T., Bioactive natural products from marine cyanobacteria for drug discovery. *Phytochemistry*, **2007**, *68* 954-979.
172. Welker, M.; Dittmann, E.; and Döhren, H.v., *Cyanobacteria as a source of natural products*, in *Methods in Enzymology*, Hopwood, D.A., Editor. 2012, Elsevier: Amsterdam. p. 23-46.
173. Nübel, U.; Garcia-Pichel, F.; and Muyzer, G., PCR primers to amplify 16S rRNA genes from cyanobacteria. *Applied and Environment Microbiology*, **1997**, *63* (8), 3327-3332.
174. Engene, N.; Paul, V.J.; Byrum, T.; Gerwick, W.H.; Thor, A.; and Ellisman, M.H., Five chemically rich species of tropical marine cyanobacteria of the genus *Okeania* gen. nov. (Oscillatoriales, Cyanoprokaryota). *Journal of Phycology*, **2013**, *49* (6), 1095-1106.

175. Darzynkiewicz, Z. and Juan, G., *Unit 7.5 DNA content measurement for DNA ploidy and cell cycle analysis*, in *Current Protocols in Cytometry*, Chambers, K., Editor. 1997, International Society for Advancement of Cytometry.
176. Olsen, J.G.; Kadziola, A.; Wettstein-Knowles, P.v.; Siggaard-Andersen, M.; Lindquist, Y.; and Larsen, S., The X-ray crystal structure of beta-ketoacyl (acyl carrier protein) synthase I. *FEBS Letters*, **1999**, *460* 46-52.
177. Tang, Y.; Kim, C.-Y.; Mathews, I.I.; Cane, D.E.; and Khosla, C., The 2.7-Å crystal structure of a 194-kDa homodimeric fragment of the 6-deoxyerythronolide B synthase. *Proceedings of the National Academy of Sciences*, **2006**, *103* (30), 11124-11129.
178. Keatinge-Clay, A., Crystal structure of the erythromycin polyketide synthase dehydratase. *Journal of Molecular Biology*, **2008**, *384* 941-953.
179. Akey, D.L.; Razelun, J.R.; Tehranisa, J.; Sherman, D.H.; Gerwick, W.H.; and Smith, J.L., Crystal structures of dehydratase domains from the curacin polyketide biosynthetic pathway. *Structure*, **2010**, *18* 94-105.
180. Keatinge-Clay, A.T. and Stroud, R.M., The structure of a ketoreductase determines the organization of the beta-carbon processing enzymes of modular polyketide synthases. *Structure*, **2006**, *14* 737-748.
181. Alekseyev, V.V.; Liu, C.W.; Cane, D.E.; Puglisi, J.D.; and Khosla, C., Solution structure and proposed domain-domain recognition interface of an acyl carrier protein domain from a modular polyketide synthase. *Protein Science*, **2007**, *16* 2093-2107.

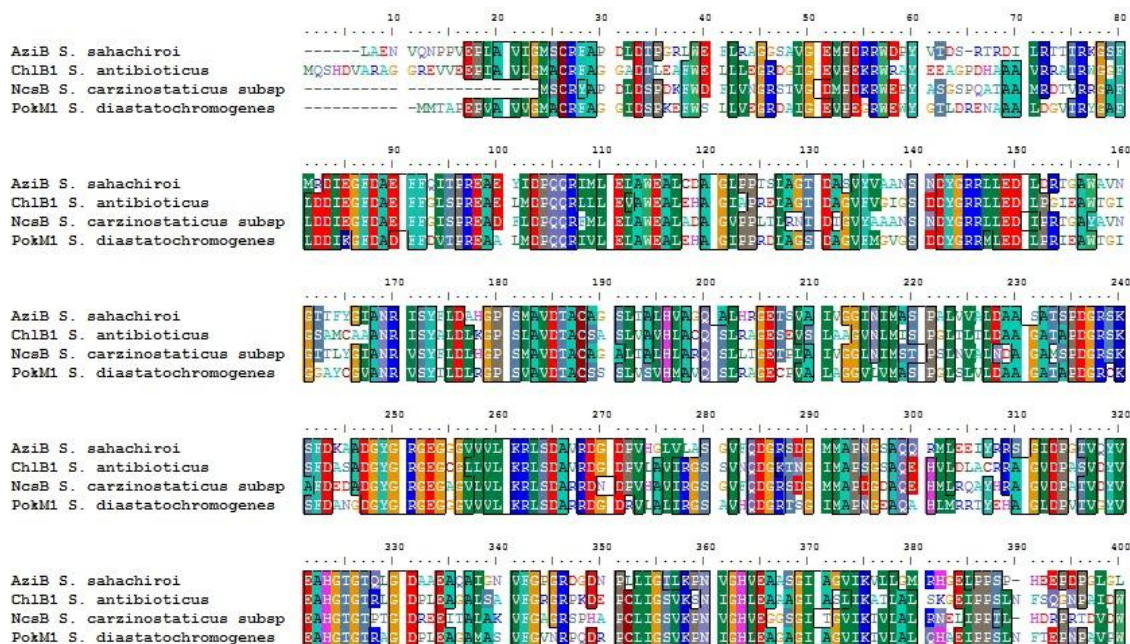
APPENDIX

FIGURES AND TABLES



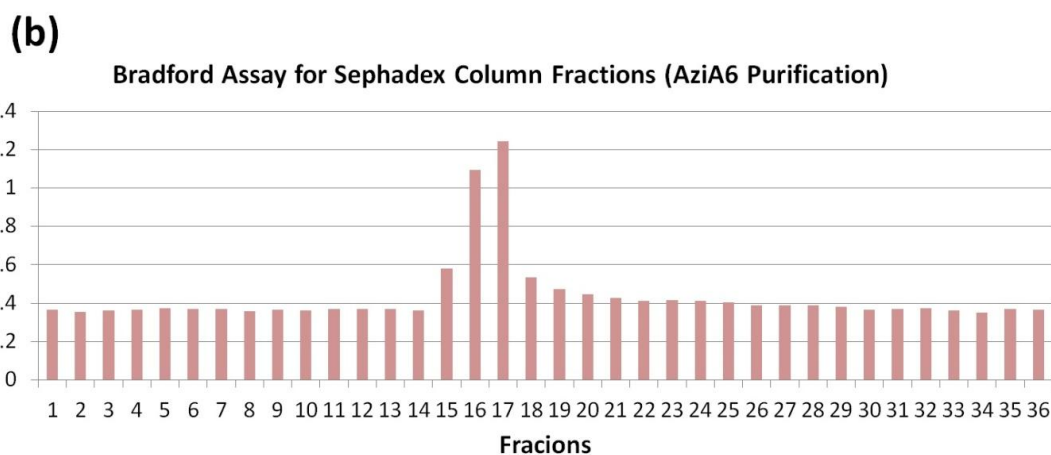
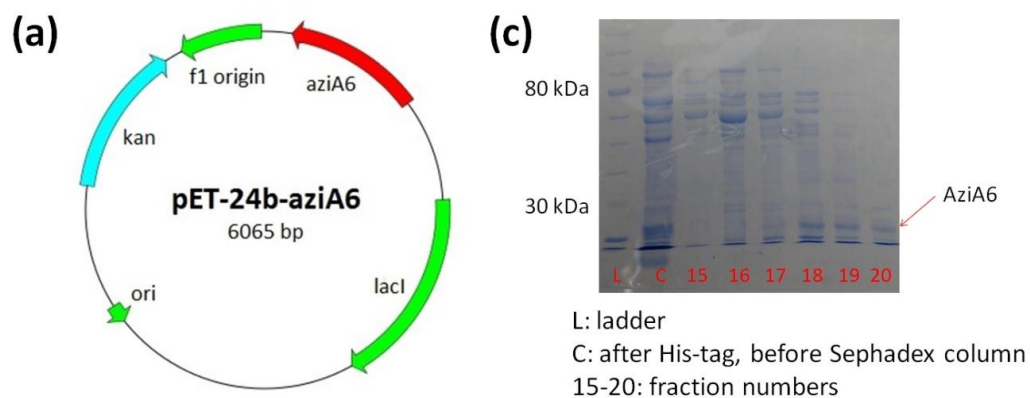
Appendix Figure 56. BLAST search of AziB

AziB peptide sequence was searched for homology by BLAST. It shows the distinct five domains including KS,¹⁷⁶ AT,¹⁷⁷ DH,^{112, 178, 179} KR,¹⁸⁰ and ACP¹⁸¹ domains.



Appendix Figure 57. Multiple alignment of AziB and its homologous enzymes (0-400 aa)

ChlB1 (Identity: 45%, NCBI accession number: AAZ77673.1),¹¹³ NcsB (52%, AAM77986.1),¹¹⁴ and PokM1 (46%, ACN64831.1).¹¹⁵



Appendix Figure 58. Preparation of pure AziA6

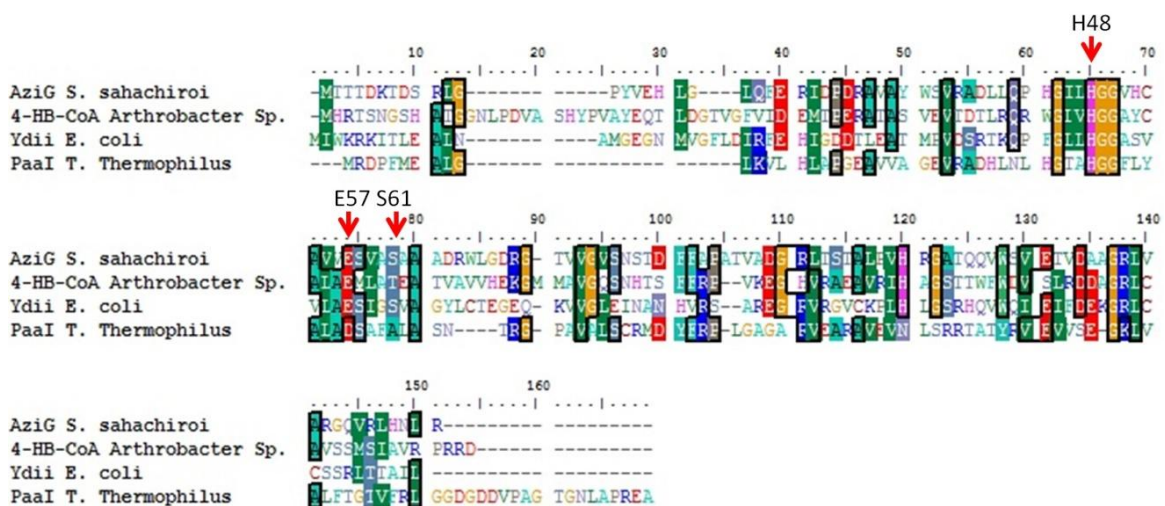
(a): Cloned expression vector of AziA6. (b): Bradford assay for each fraction in Sephadex column filtration. (c): SDS-PAGE analysis of Sephadex column fractions.



Appendix Figure 59. BLAST search of AziG

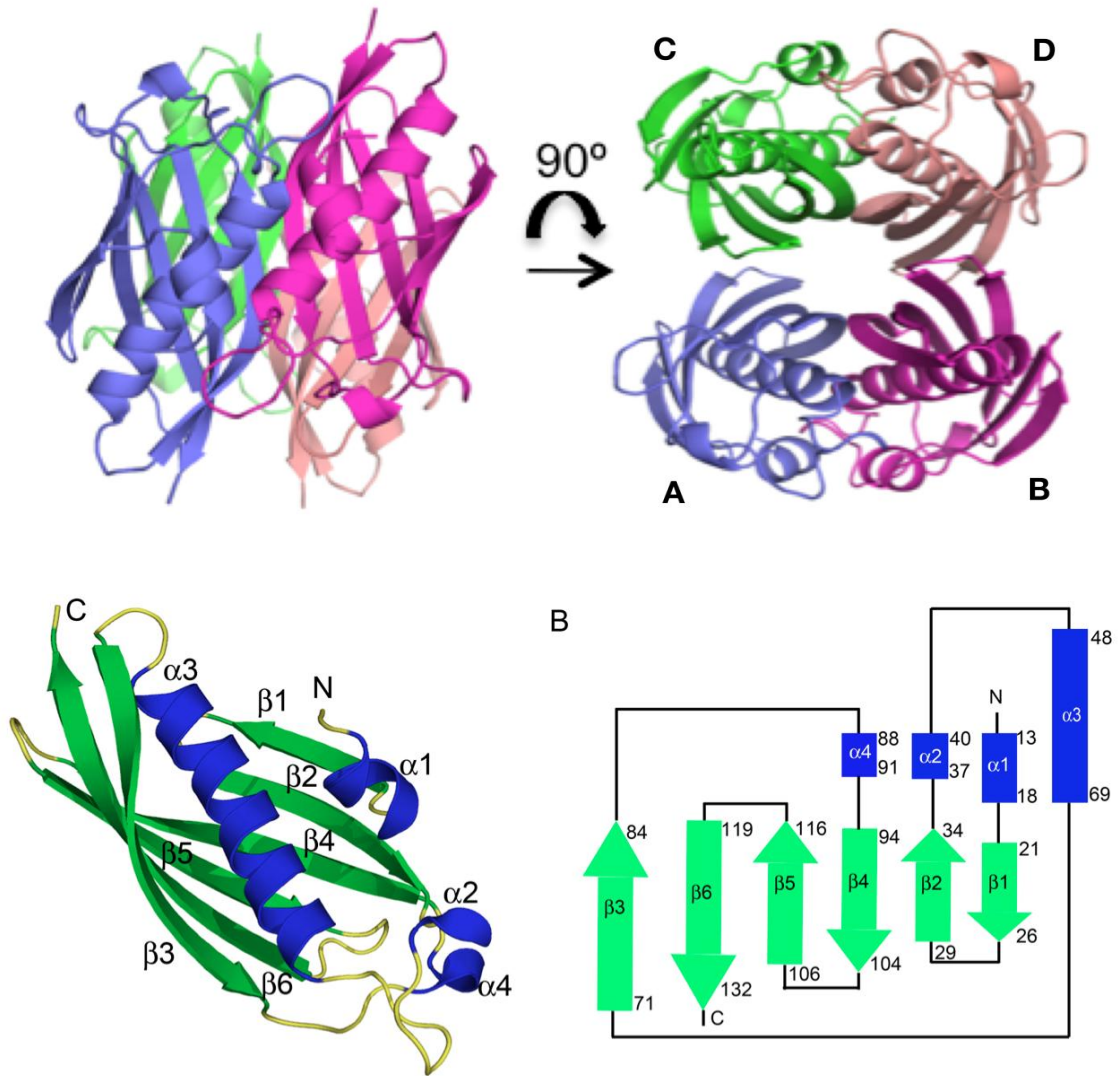
Appendix Table 4. Characterized homologous enzymes of AziG

Accession no.	Organism	Protein	E-value	Identity/similarity (%)
AziG (comparison with TEs characterized by crystallography and kinetics)				
1Q4S_A	<i>Arthrobacter</i> sp. SU	PaaI TE (hotdog)	4e-14	37/56
4K49_C	<i>E. coli</i> K-12	PaaI TE (hotdog)	4e-12	33/45
1J1Y_A	<i>Thermus Thermophilus</i> Hb8	PaaI TE (hotdog)	1e-09	35/51



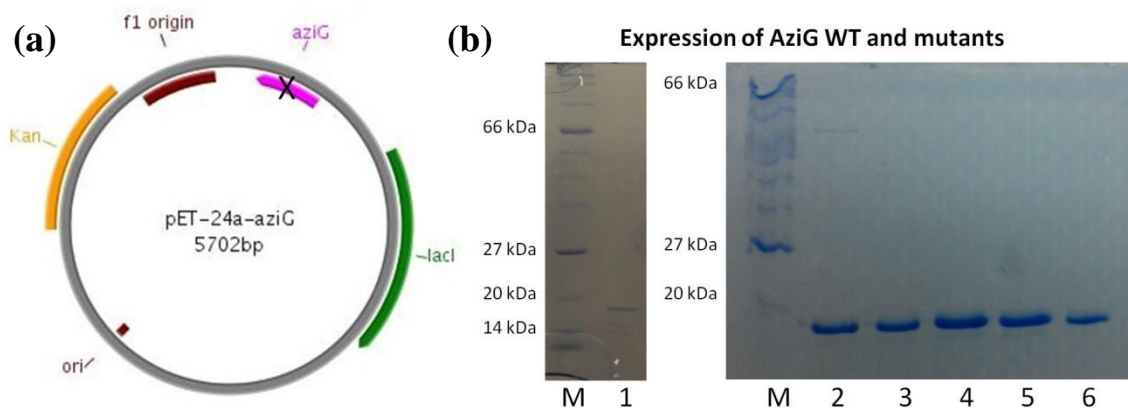
Appendix Figure 60. Multiple alignment of AziG and its characterized homologous enzymes which share the conserved active site

4-HB-CoA TE (Identity: 37%, Similarity: 56%, PDB accession number: 1Q4S_A).¹²⁰
 Ydii (33%, 45%, 4K49_C),¹²¹ PaaI (35%, 51%, 1J1Y_A),¹²²



Appendix Figure 61. AziG tetramer and monomer

The monomer adopts the characteristic hotdog fold with the β -sheet of each monomer facing the core and the main α -helices facing outward.



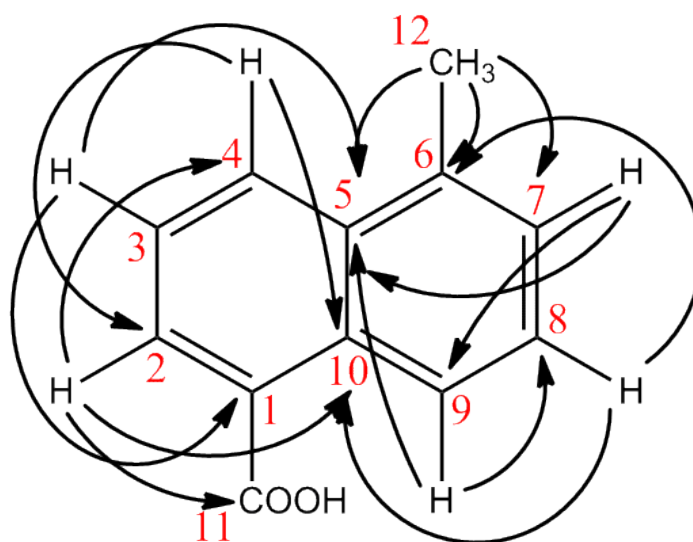
Appendix Figure 62. Expression plasmid of AziG (and its mutants) and SDS-PAGE analysis of overexpression and purification

(a): *aziG* was cloned into pET-24a and was mutated by site-directed mutagenesis. (b): SDS-PAGE analysis after overexpression and purification of AziG WT and mutants (M: protein marker, 1: WT, 2: H44A, 3: H48A, 4: E57A, 5: S58A, 6: S61A).

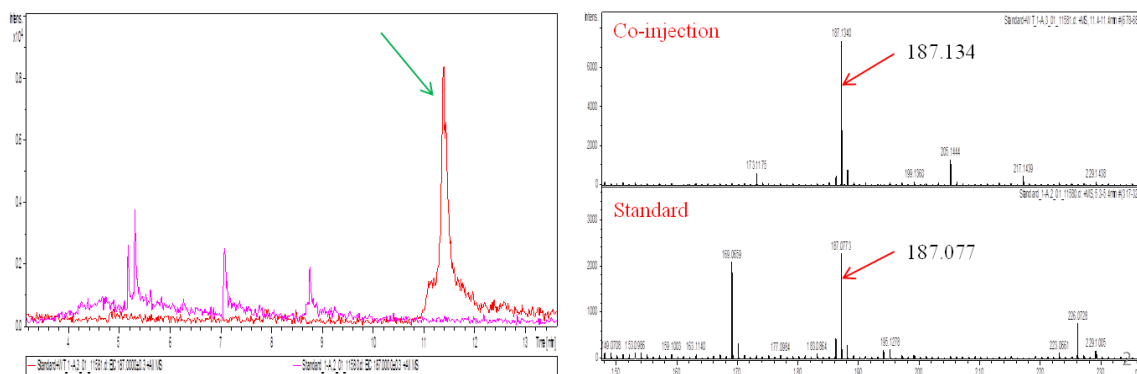
Appendix Table 5. NMR spectral data for 5-methyl-1-naphthoic acid (49**) (500 MHz, CD₃OD).**

5-methyl-1-naphthoic acid (49)			
Position	δ_C , type	δ_H (J in Hz)	HMBC ^a
1	125.8, C		
2	130.4, CH	8.120, d (7.8)	4, 10, 11
3	125.5, CH	7.574, t (7.8)	1, 5
4	130.0, CH	8.268, d (8.4)	2, 10
5	134.3, C		
6	135.9, C		
7	128.0, CH	7.388, d (7.1)	5, 9
8	128.1, CH	7.450, t (9.1)	6, 10
9	125.0, CH	8.649, d (9.1)	5, 8
10	132.6, C		
11	171.5, C		
12	20.0, CH ₃	2.704	5, 6, 7

^a HMBC correlations are ¹H→¹³C

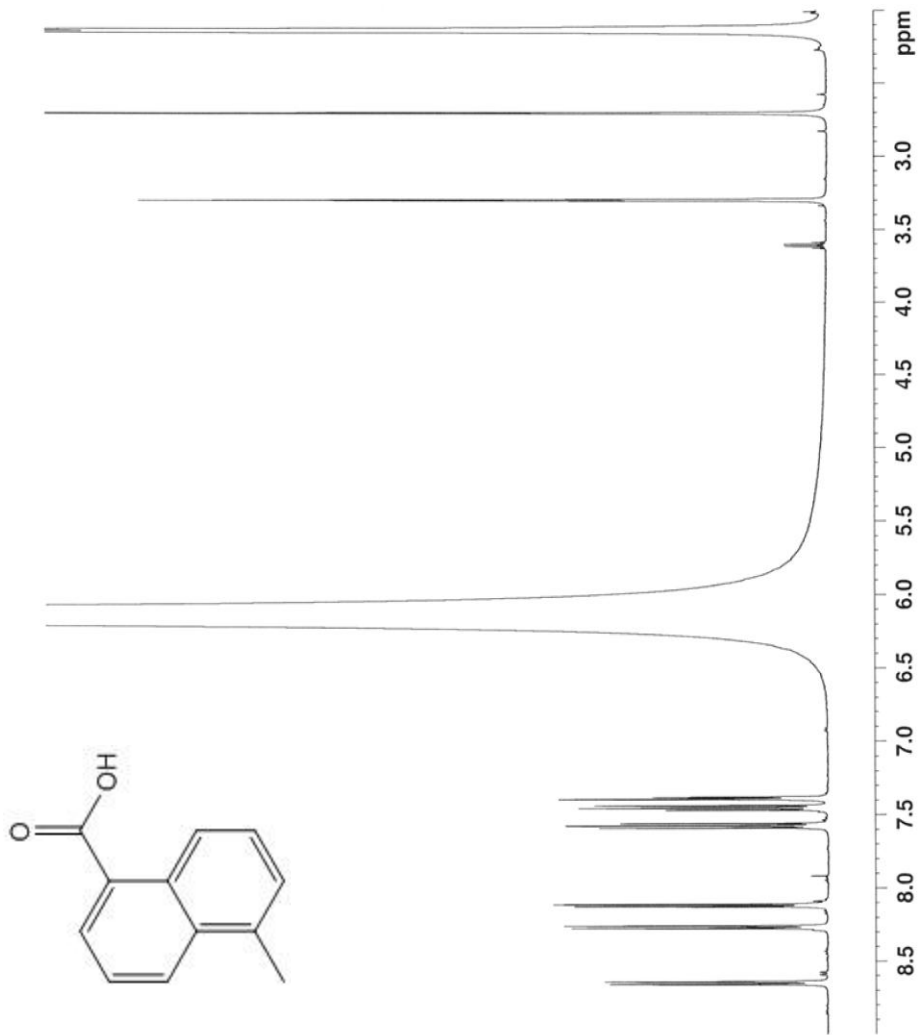


Appendix Figure 63. Numbering of 5-methyl-1-naphthoic acid (49) and HMBC correlations

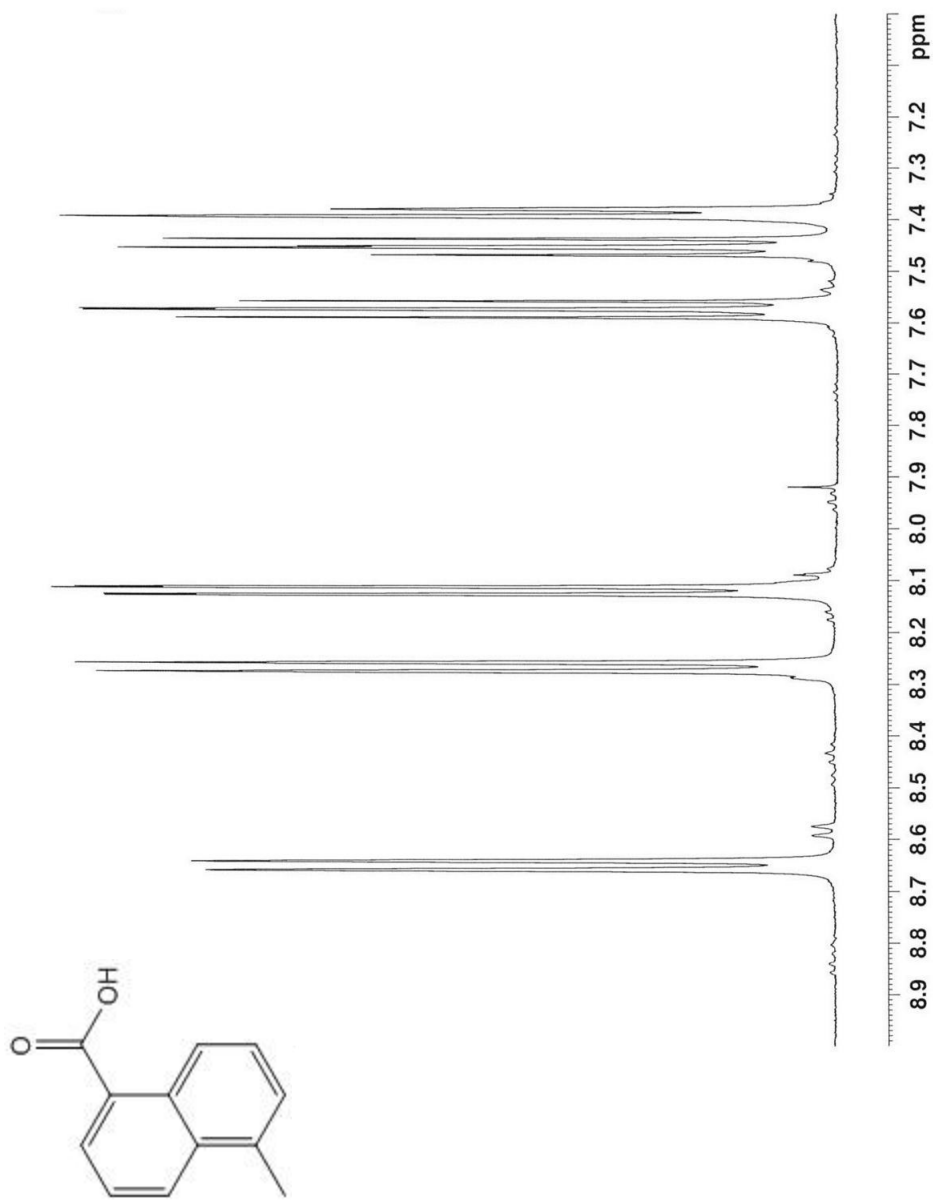


Appendix Figure 64. LC-MS analysis with the standard

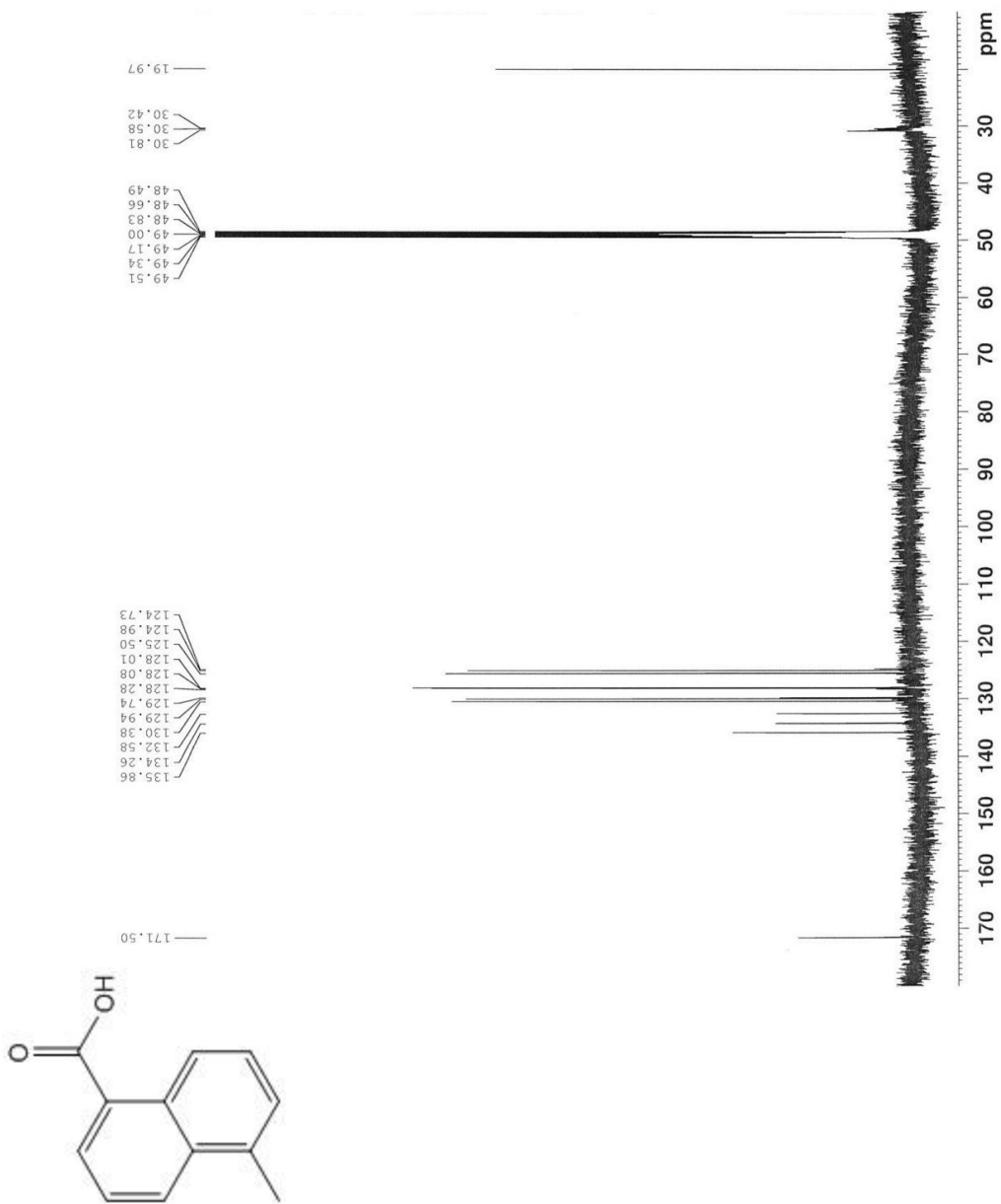
The crude standard gave multiple peaks in the LC profile (pink line), but when it was co-injected with the AziB-AziG product (red line), only one peak appeared (green arrow) which matches the mass of the AziB-AziG product.



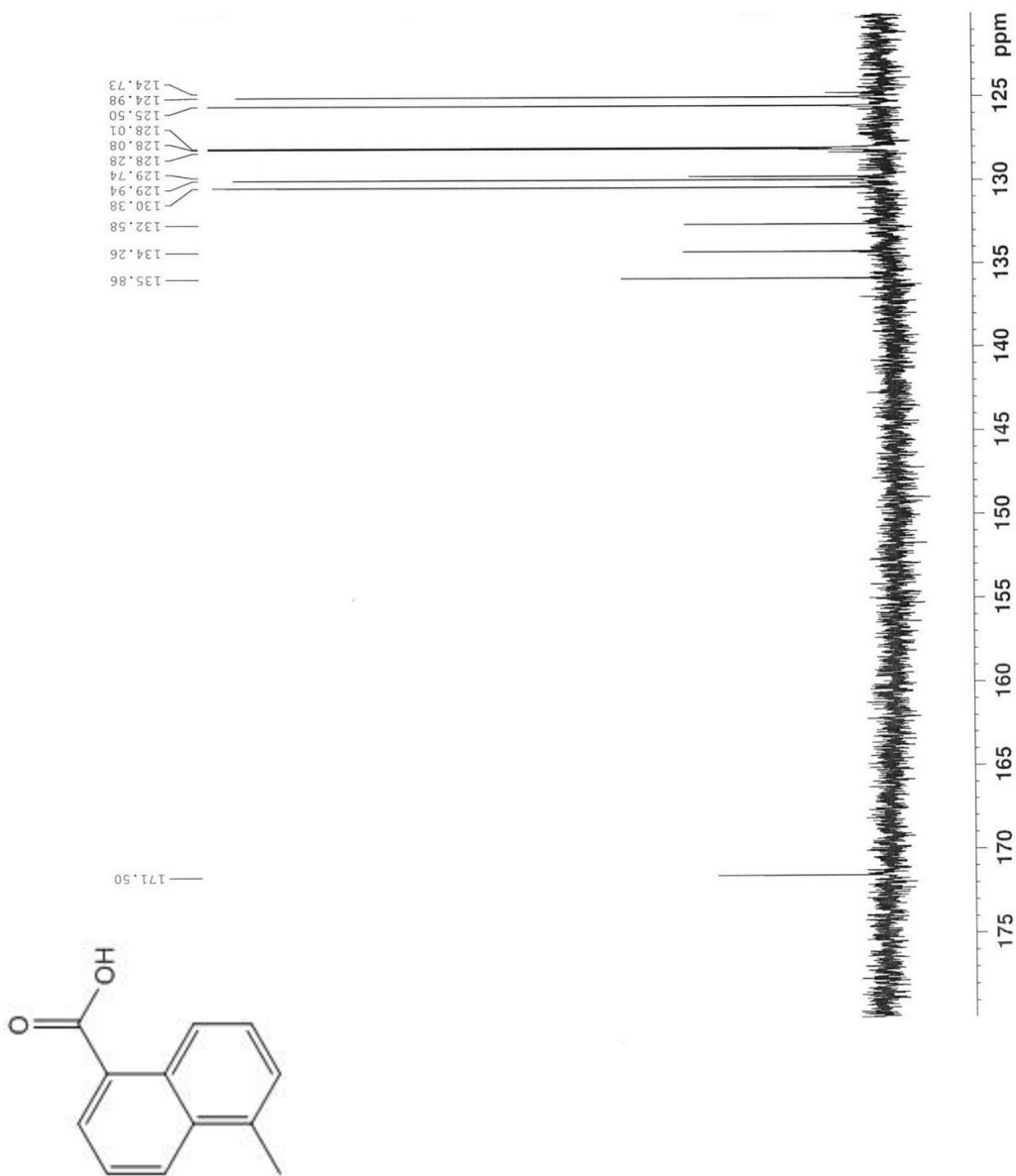
Appendix Figure 65. ^1H NMR (500 MHz, CD_3OD) for 5-methyl-1-naphthoic acid (49)



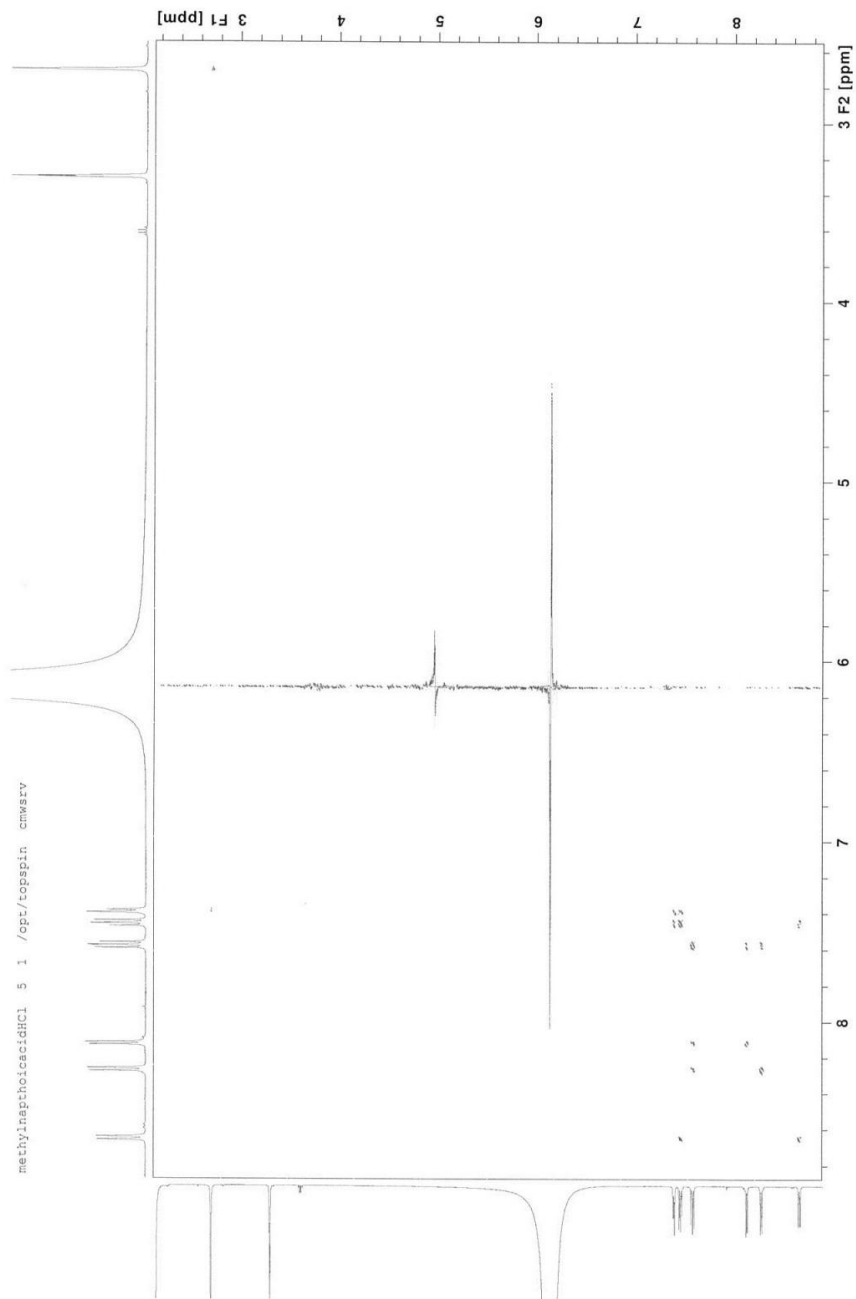
Appendix Figure 66. ¹H NMR (500 MHz, CD₃OD) for 5-methyl-1-naphthoic acid (49), 7.0-9.0 ppm



Appendix Figure 67. ^{13}C NMR (500 MHz, CD_3OD) for 5-methyl-1-naphthoic acid (49)

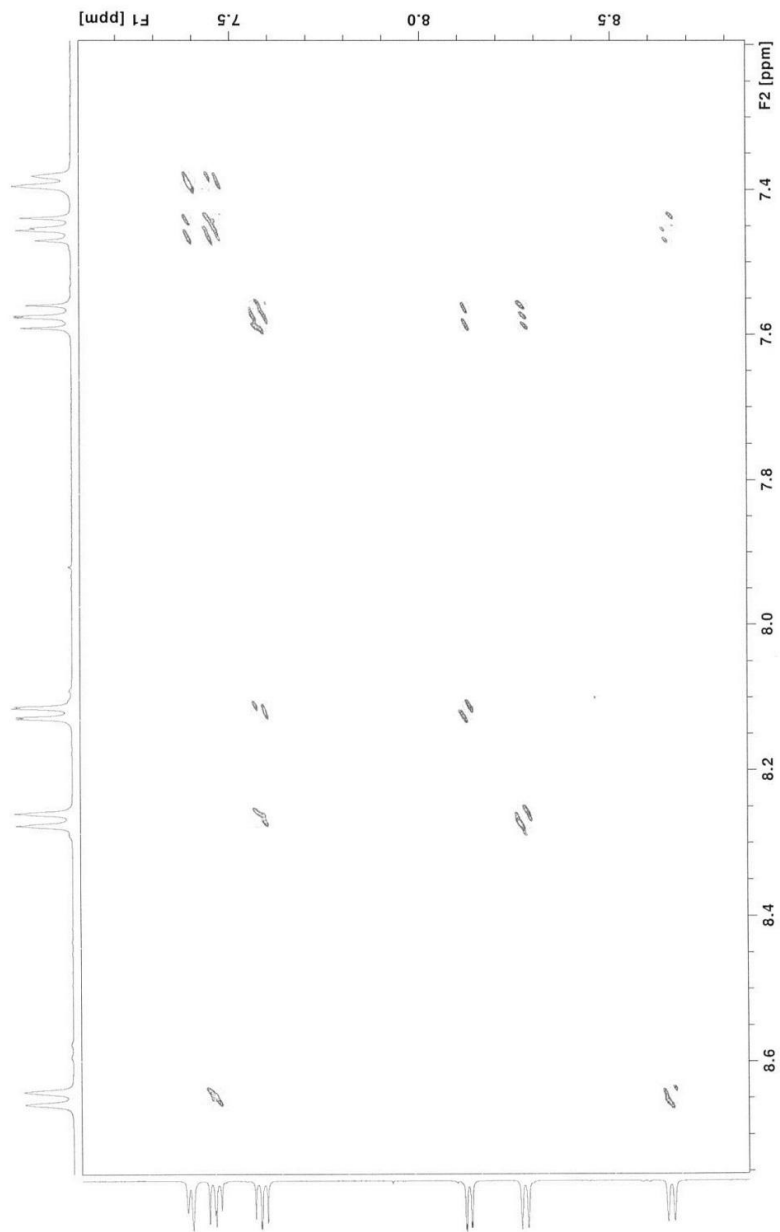


Appendix Figure 68. ¹³C NMR (500 MHz, CD₃OD) for 5-methyl-1-naphthoic acid (49), >120 ppm

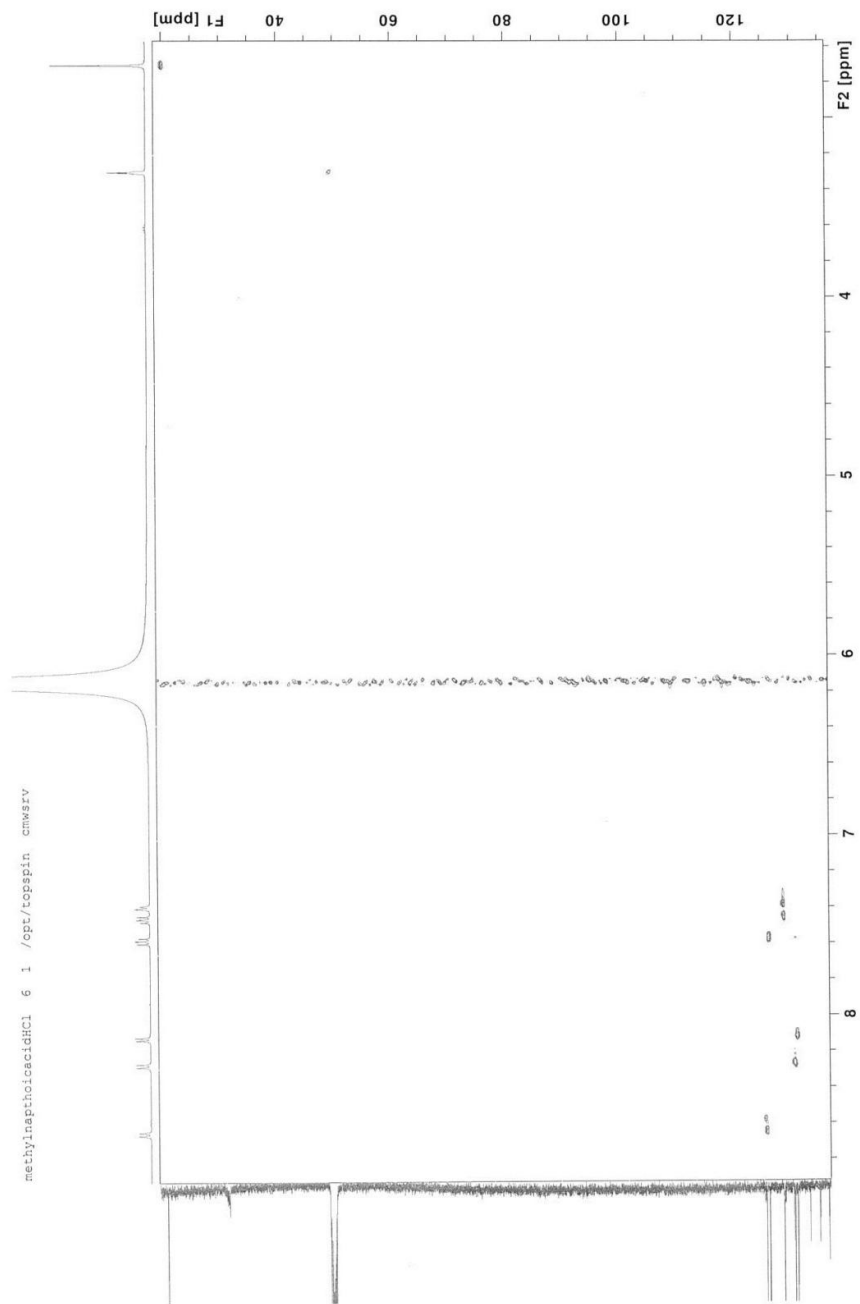


Appendix Figure 69. COSY (500 MHz, CD₃OD) for 5-methyl-1-naphthoic acid (49)

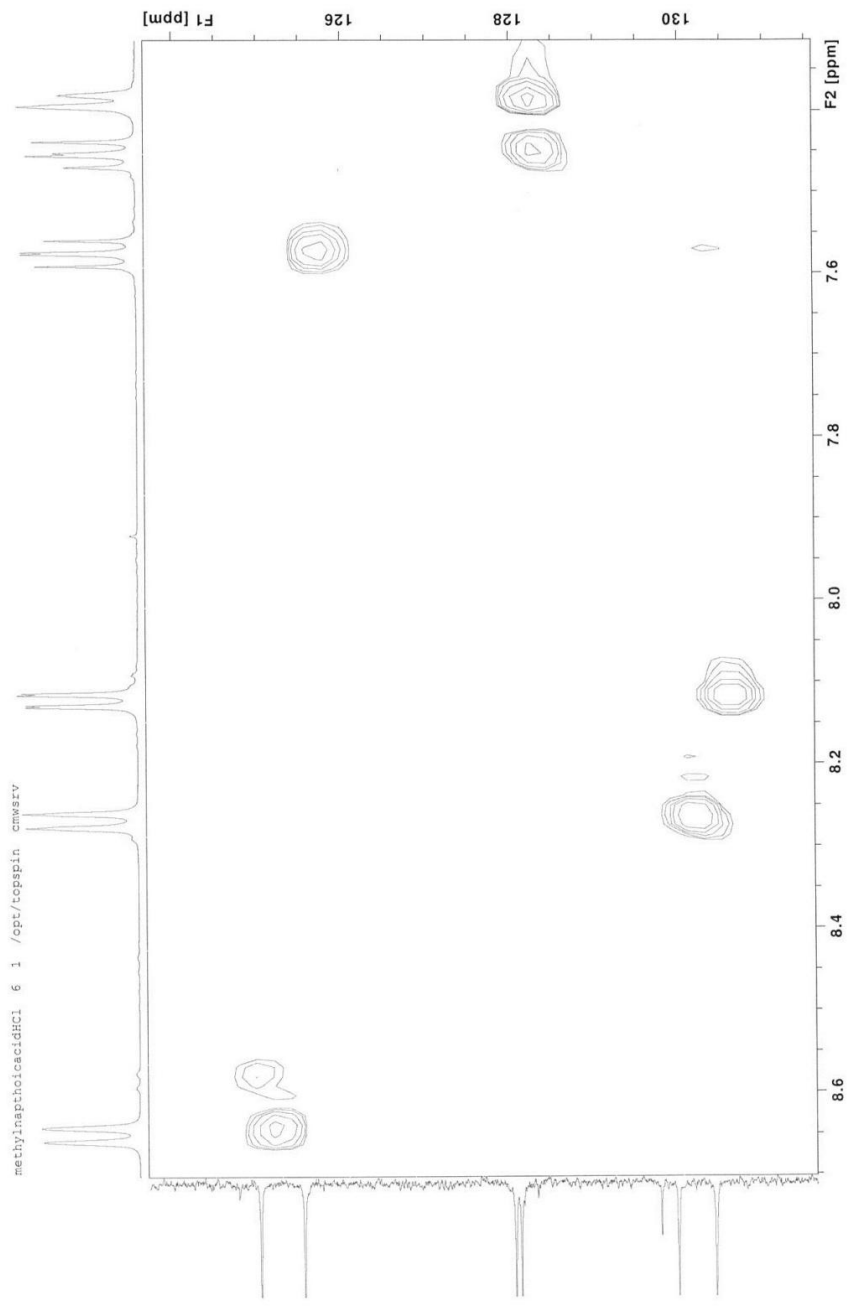
methylnapthoicacidHCl 5 1 /opt/cosyprn cmwsvr



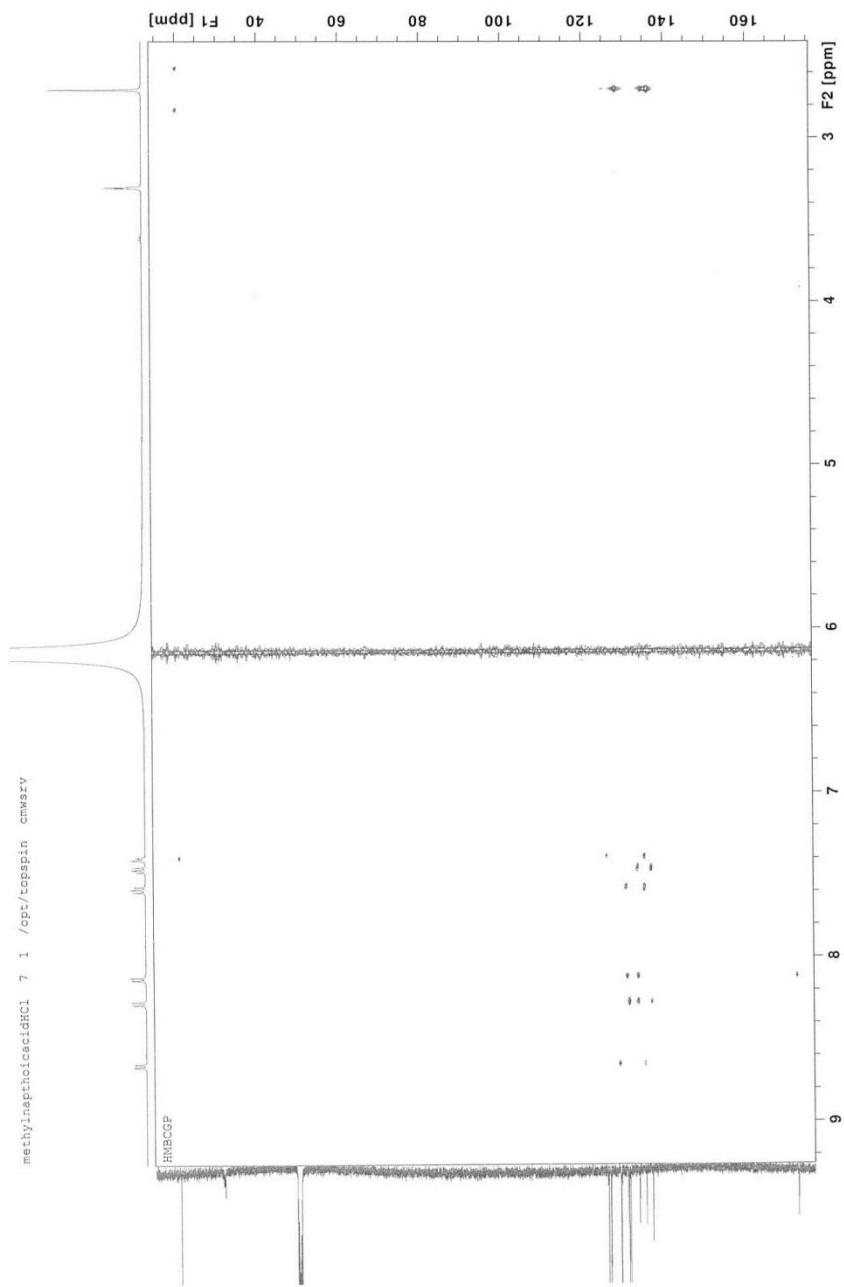
Appendix Figure 70. COSY (500 MHz, CD₃OD) for 5-methyl-1-naphthoic acid (49), 7.0-9.0 ppm



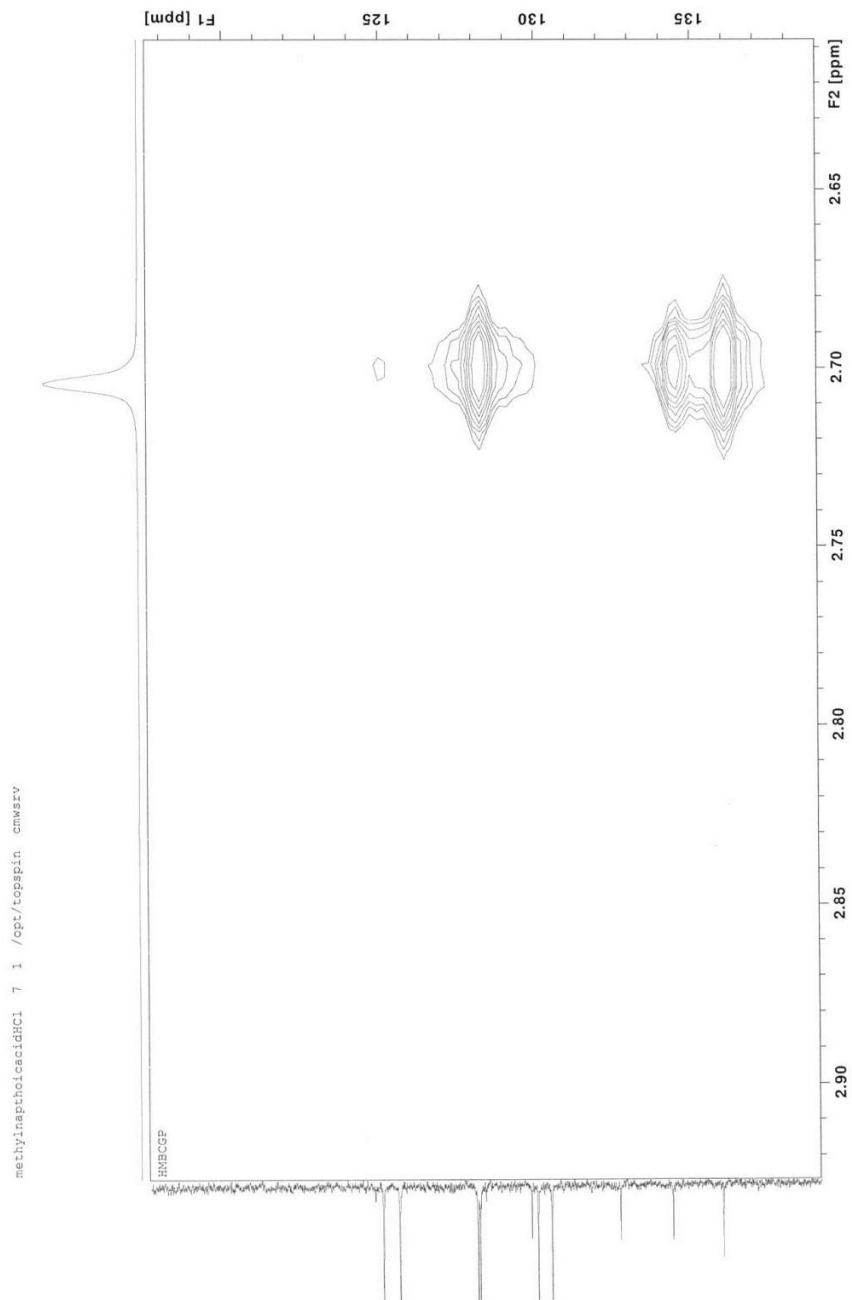
Appendix Figure 71. HSQC (500 MHz, CD₃OD) for 5-methyl-1-naphthoic acid (49)



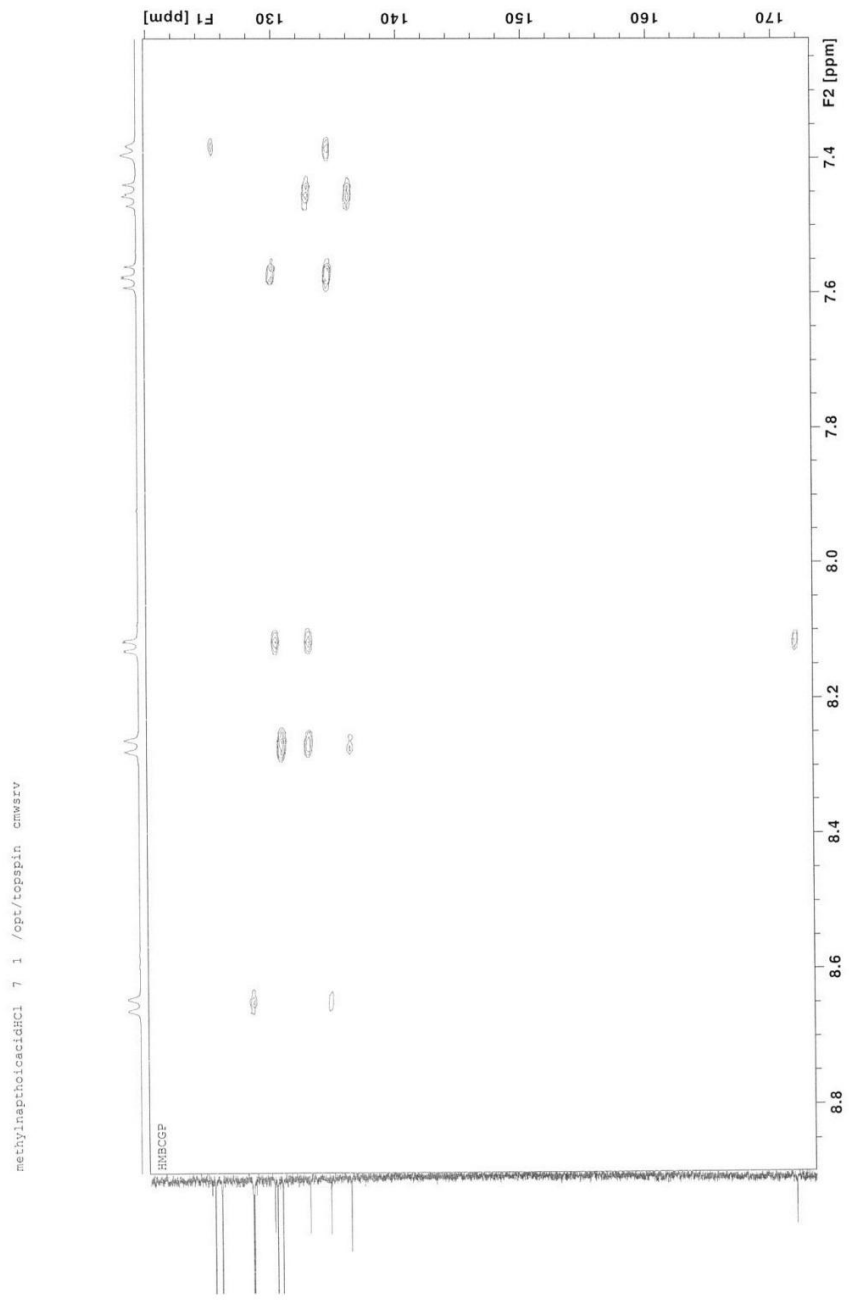
Appendix Figure 72. HSQC (500 MHz, CD₃OD) for 5-methyl-1-naphthoic acid (49), aromatic region



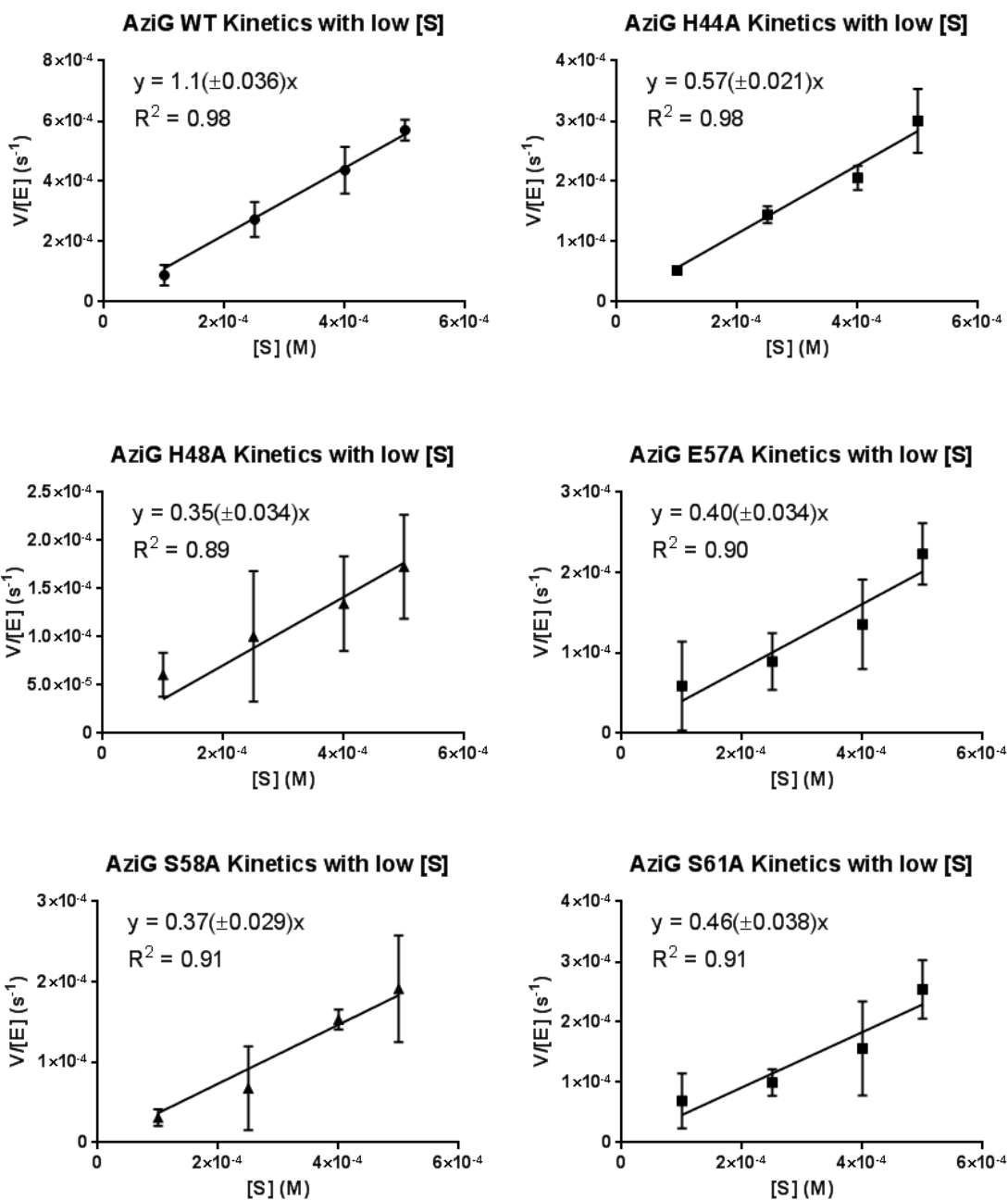
Appendix Figure 73. HMBC (500 MHz, CD₃OD) for 5-methyl-1-naphthoic acid (49)



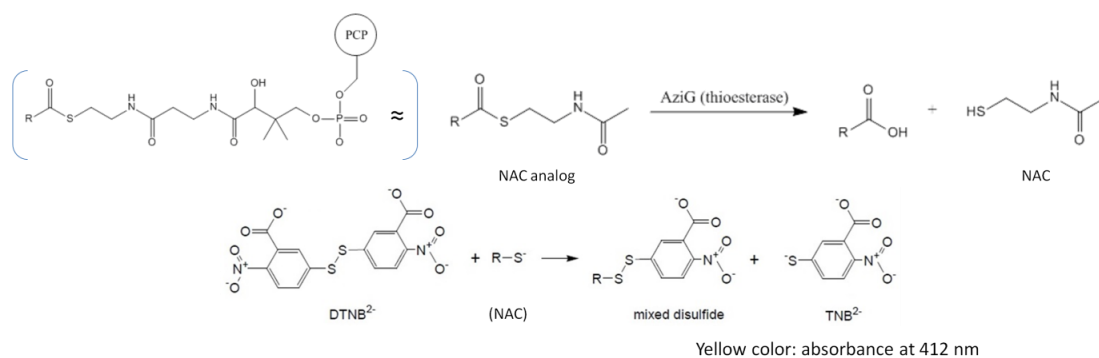
Appendix Figure 74. HMBBC (500 MHz, CD_3OD) for 5-methyl-1-naphthoic acid (49), methyl group region



Appendix Figure 75. HMBBC (500 MHz, CD₃OD) for 5-methyl-1-naphthoic acid (49), aromatic region

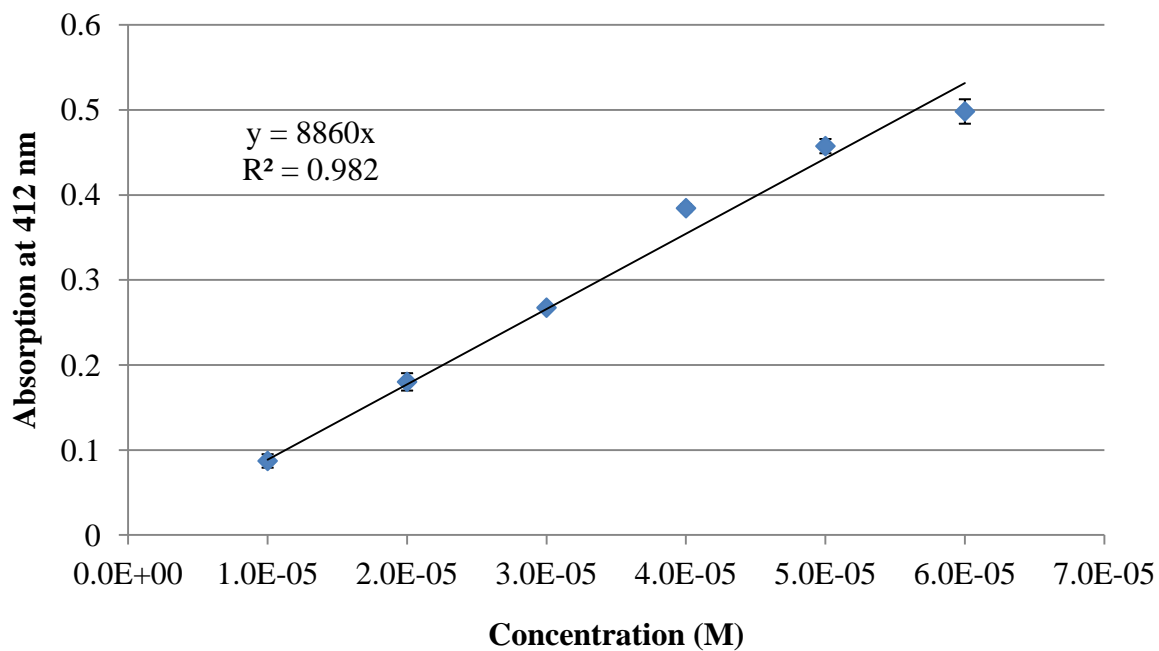


Appendix Figure 76. Individual kinetic parameters including R^2 values and error bars of standard deviations

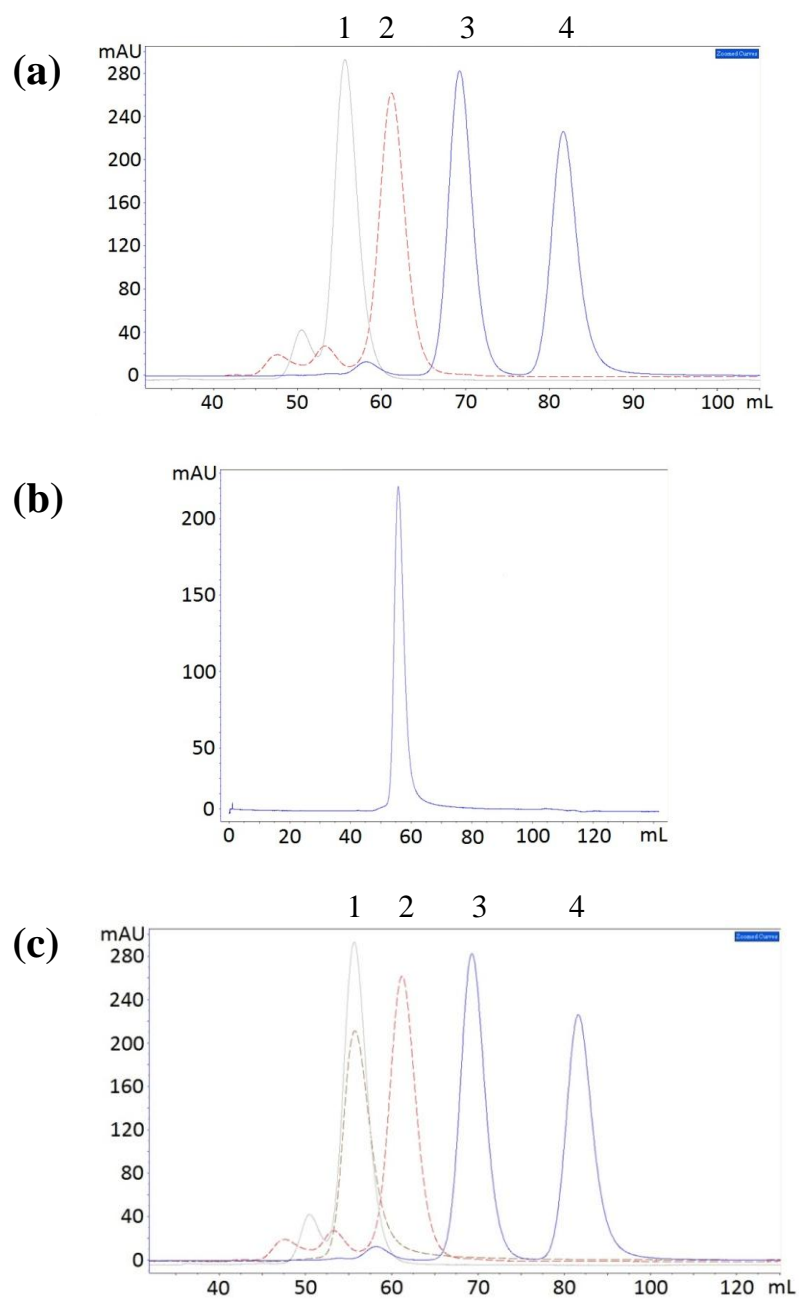


Appendix Scheme 5. AziG kinetic experiment utilizing Ellman's reagent

Molar absorptivity of Ellman's reagent

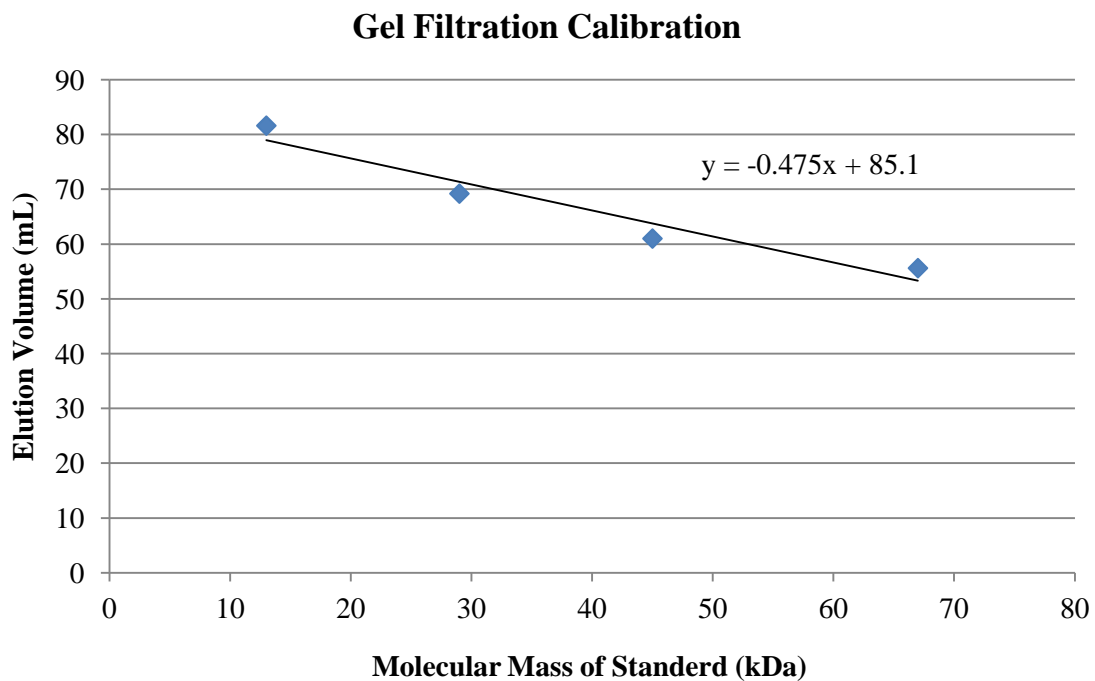


Appendix Figure 77. Determination of molar absorptivity of Ellman's reagent in the reaction buffer



Appendix Figure 78. Gel filtration of native AziG

(a): Elution profile of 1 bovine serum albumin, 2 ovalbumin, 3 carbonic anhydrase, and 4 cytochrome C, (b): native AziG, (c): overlay of AziG with standards.



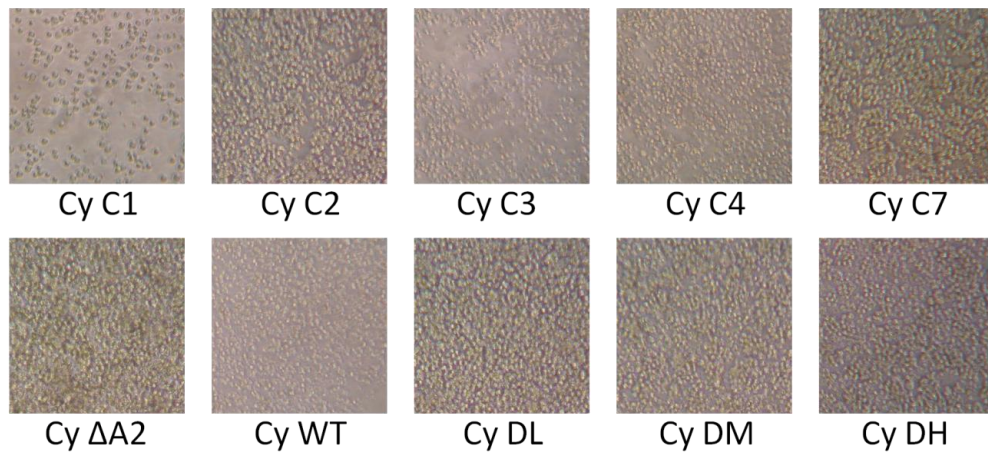
Proteins	Molecular Mass (kDa)	Elution Volume (mL)
BSA	67	55.6
ovalbumin	45	61.0
Carbonic anhydrase	29	69.2
Cytochrome C	13	81.6
AziG	62	55.6

Appendix Figure 79. Gel filtration analysis of AziG: calibration curves and tabulated data

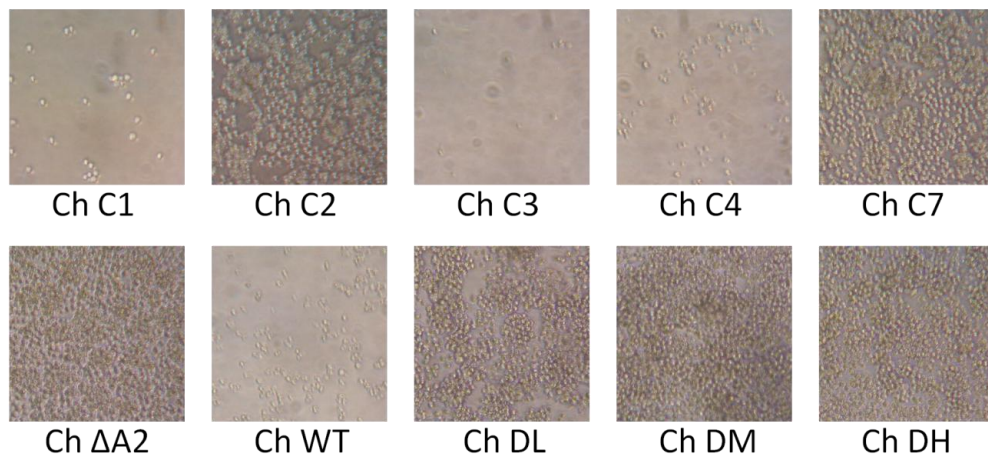
Appendix Table 6. AziG data collection and refinement statistics

	AziG	AziG/3-hydroxy-2-
beamline	CHESS F1	NE-CAT ID-E
resolution (Å)	2.15	2.4
wavelength (Å)	0.9183	0.97919
space group	<i>I</i> 4 ₁ 22	<i>I</i> 4 ₁ 22
a (Å)	68.5	68.2
c (Å)	139.6	139.7
Matthews coefficient	2.73	2.71
% solvent	54.9	54.6
mol/asu	1	1
Measured reflections	62888	36636
Unique reflections	9373	6783
Average I/σ	37.3(5.8)	22.2(3.6)
Redundancy	6.7(5.7)	5.4(5.5)
Completeness (%)	99.5(100)	99.6(100)
R _{merge} (%) ^b	9.1(38.6)	9.4(35.6)
No. of protein atoms	920	927
No. of ligand atoms	0	14
No. of water atoms	34	28
Reflections in working	8883	6448
Reflections in test set	446	323
R-factor (%)	22.2	20.2
R _{free} (%)	26.6	25.0
rms deviation from		
bonds (Å)	0.007	0.008
angles (deg)	1.17	1.101
average B factor for	45.2	26.4
Ramachandram plot		
most favored (%)	95.1	96.7
allowed (%)	4.9	3.3
disallowed (%)	0	0

Cytotoxicity assay

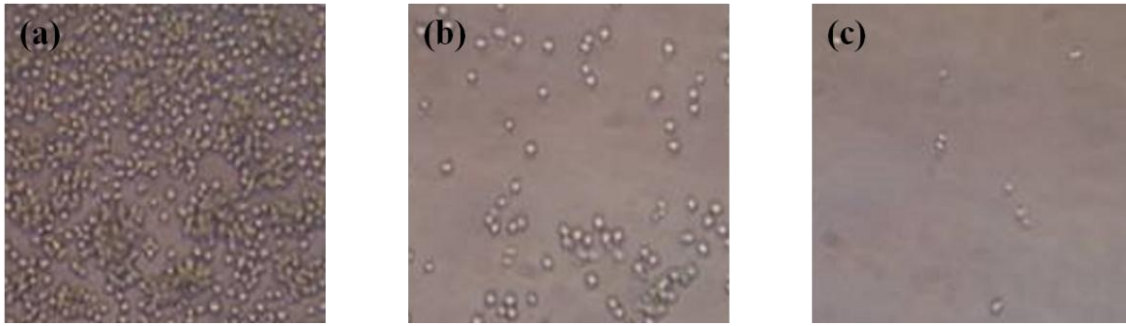


Chemotaxis assay



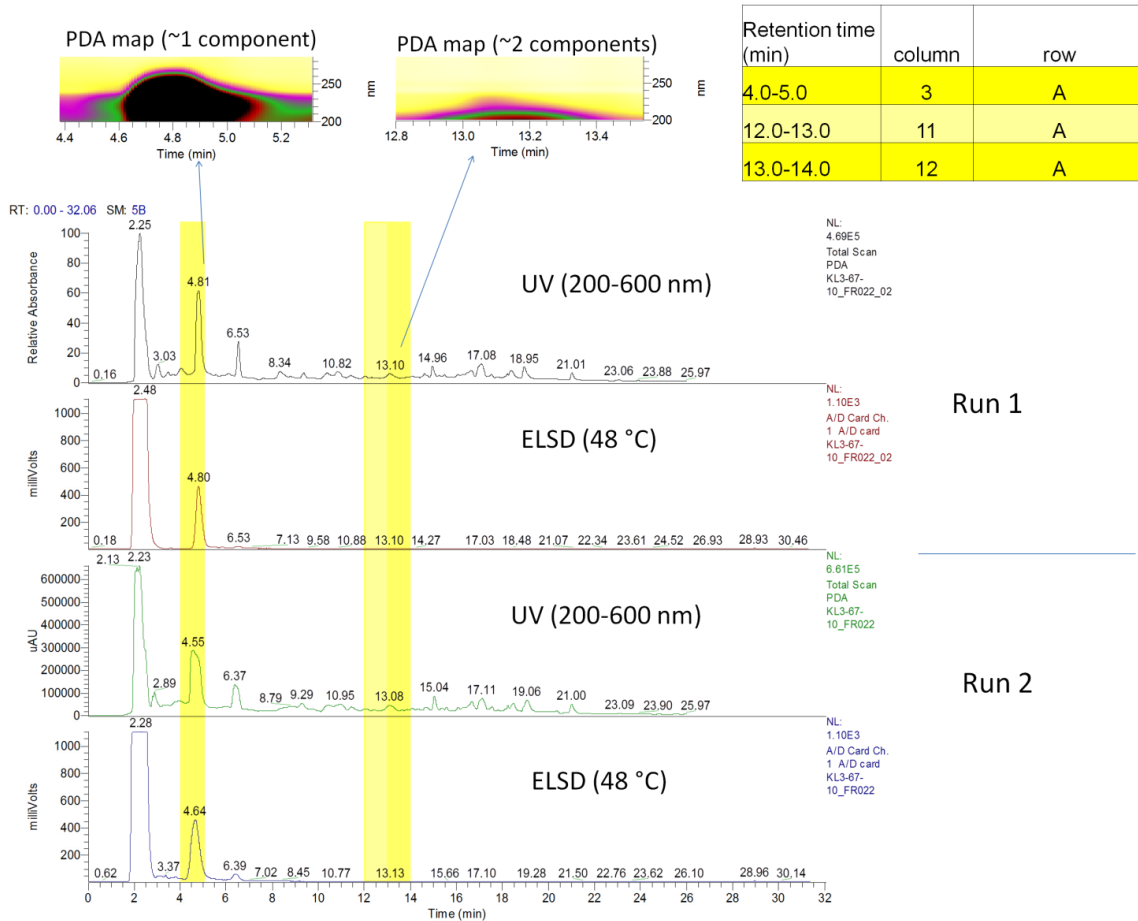
Appendix Figure 80. Cytotoxicity and chemotaxis assay against Jurkat cells

Microscopic images of the assays. **Cytotoxicity assay:** Cy C1: control without FBS in the culture medium, Cy C2: control without any samples, Cy C3: control with FTY720 (1.0 $\mu\text{g/mL}$), Cy C4: control with FTY720 (0.75 $\mu\text{g/mL}$), Cy C7: control with 1 μL of stock solution (methanol/ethyl acetate/t-butyl methyl ether = 60/30/10), Cy Δ A2: *aziA2* disruption mutant extract, Cy WT: wild type extract, Cy DL: 1 $\mu\text{g/mL}$ of dimethyl furan-2,4-dicarboxylate, Cy DM: 10 $\mu\text{g/mL}$, Cy DH: 25 $\mu\text{g/mL}$. **Chemotaxis assay:** Ch C1: control without FBS in the bottom well, Ch C2: control without any samples, Ch C3: control with FTY720 (1.0 $\mu\text{g/mL}$), Ch C4: control with FTY720 (0.75 $\mu\text{g/mL}$), Ch C7: control with 1 μL of stock solution, Ch Δ A2: *aziA2* disruption mutant extract, Ch WT: wild type extract, Ch DL: 1 $\mu\text{g/mL}$ of dimethyl furan-2,4-dicarboxylate, Ch DM: 10 $\mu\text{g/mL}$, Ch DH: 25 $\mu\text{g/mL}$.

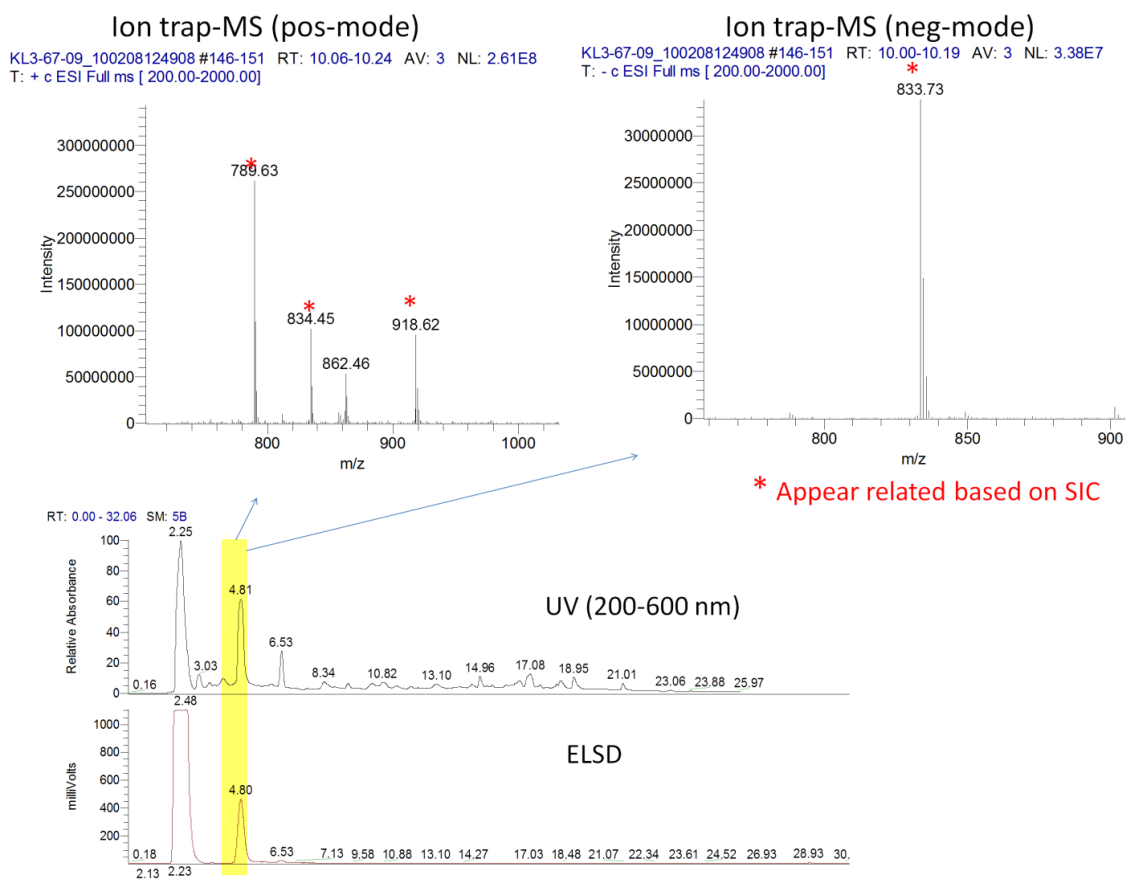


Appendix Figure 81. Chemotaxis assay of CL013-F10 at lower doses

Microscopic images of the bottom well of Boyden chambers after 24 h incubation; (a): 1 µg/mL, (b): 10 µg/mL, and (c): 25 µg/mL of CL013-F10.

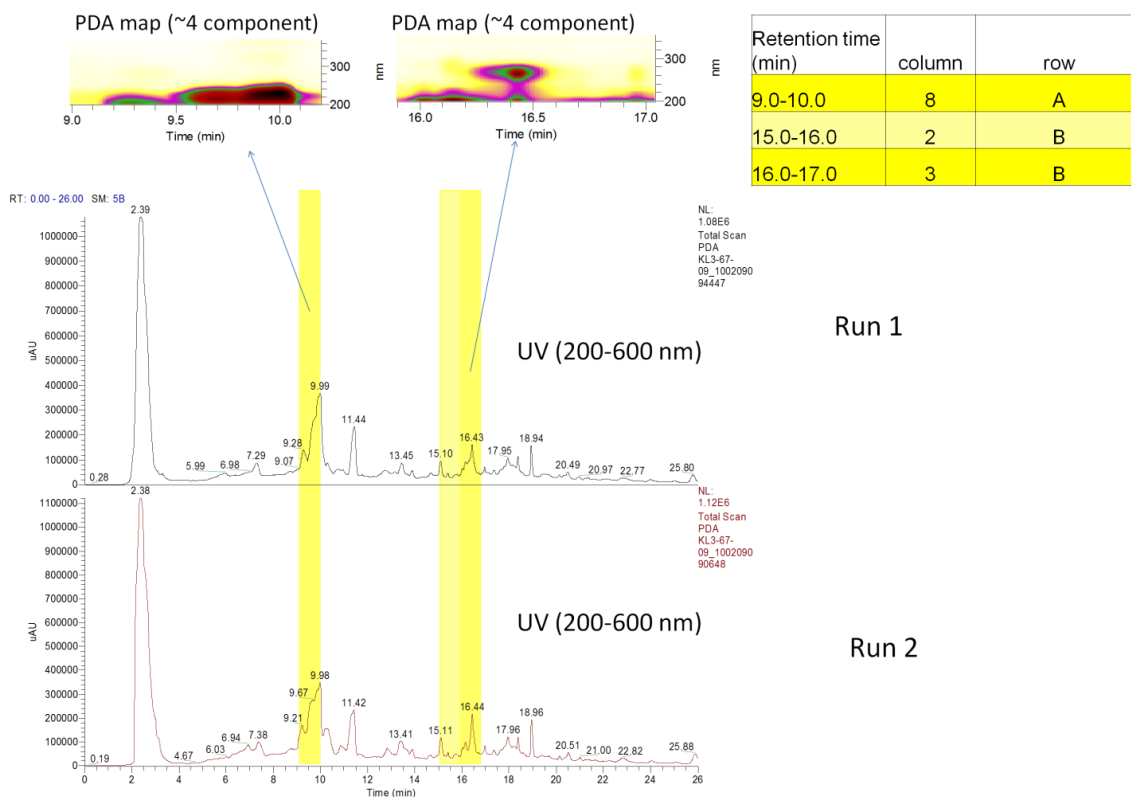


Appendix Figure 82. PDA map of active fractions in FR022

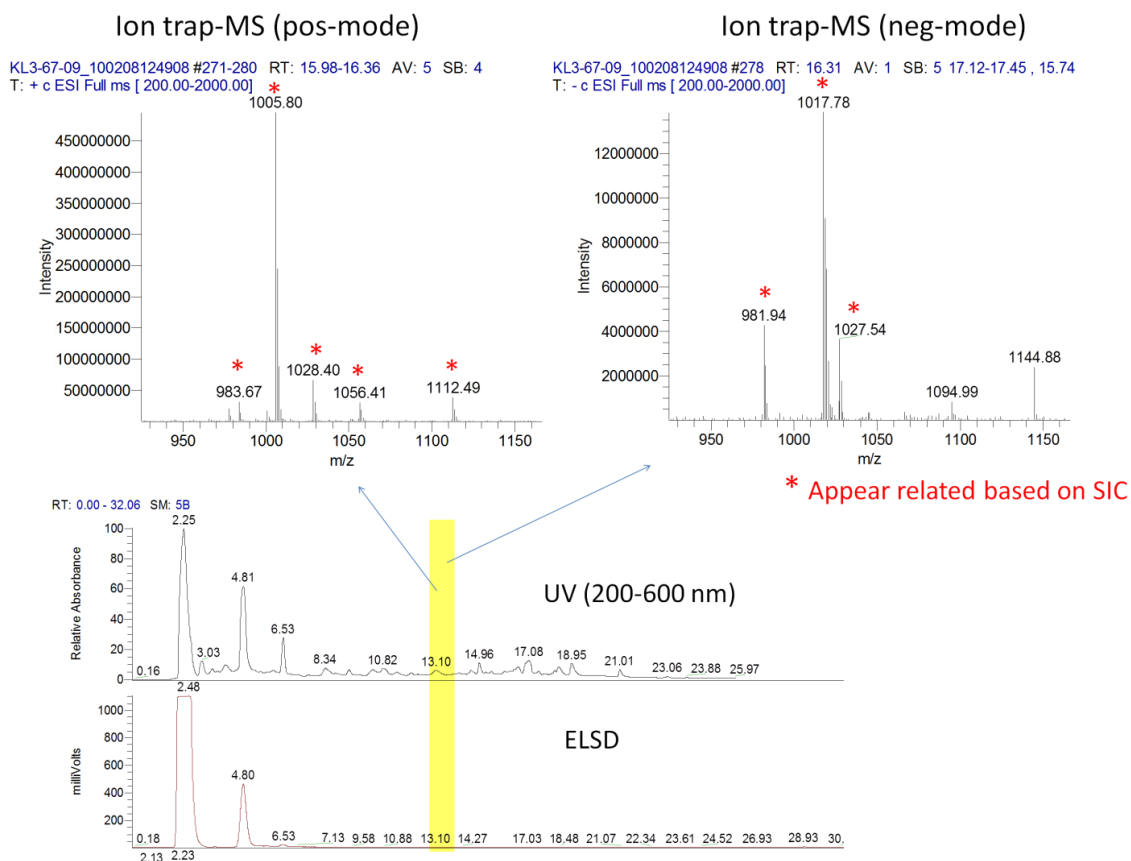


Appendix Figure 83. LCMS analysis of FR022

The molecular weight was determined as 788.6 ± 0.2 Da based on monomer and dimer adducts.



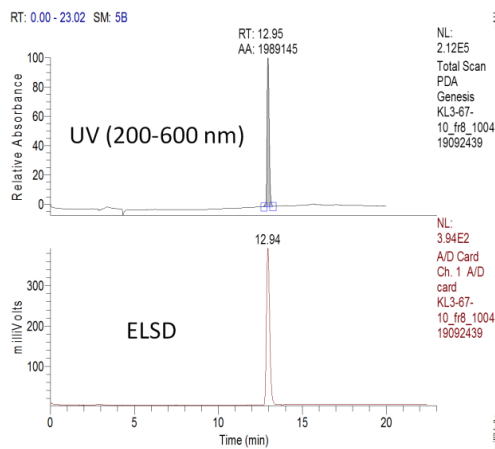
Appendix Figure 84. PDA map of active fractions in FR023



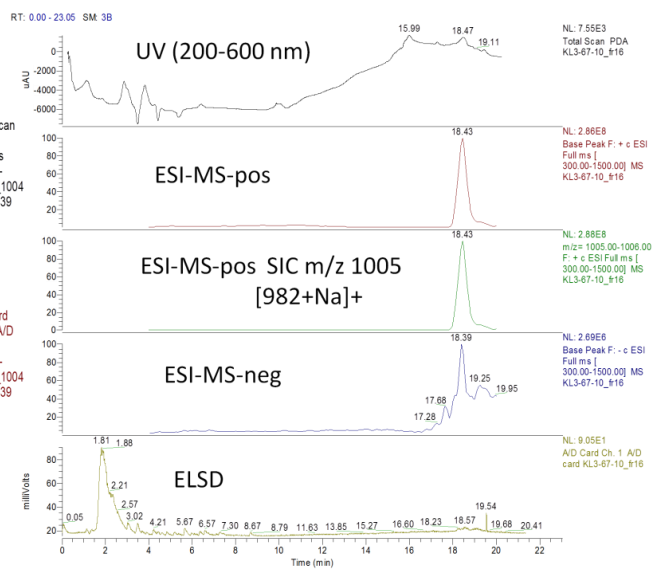
Appendix Figure 85. LCMS analysis of NP988

The molecular weight was determined as 982.7 ± 0.2 Da based on monomer adducts.

(a) NP788 (KK1-62-08)

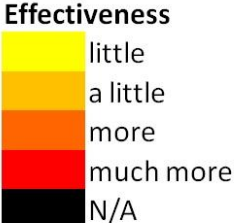


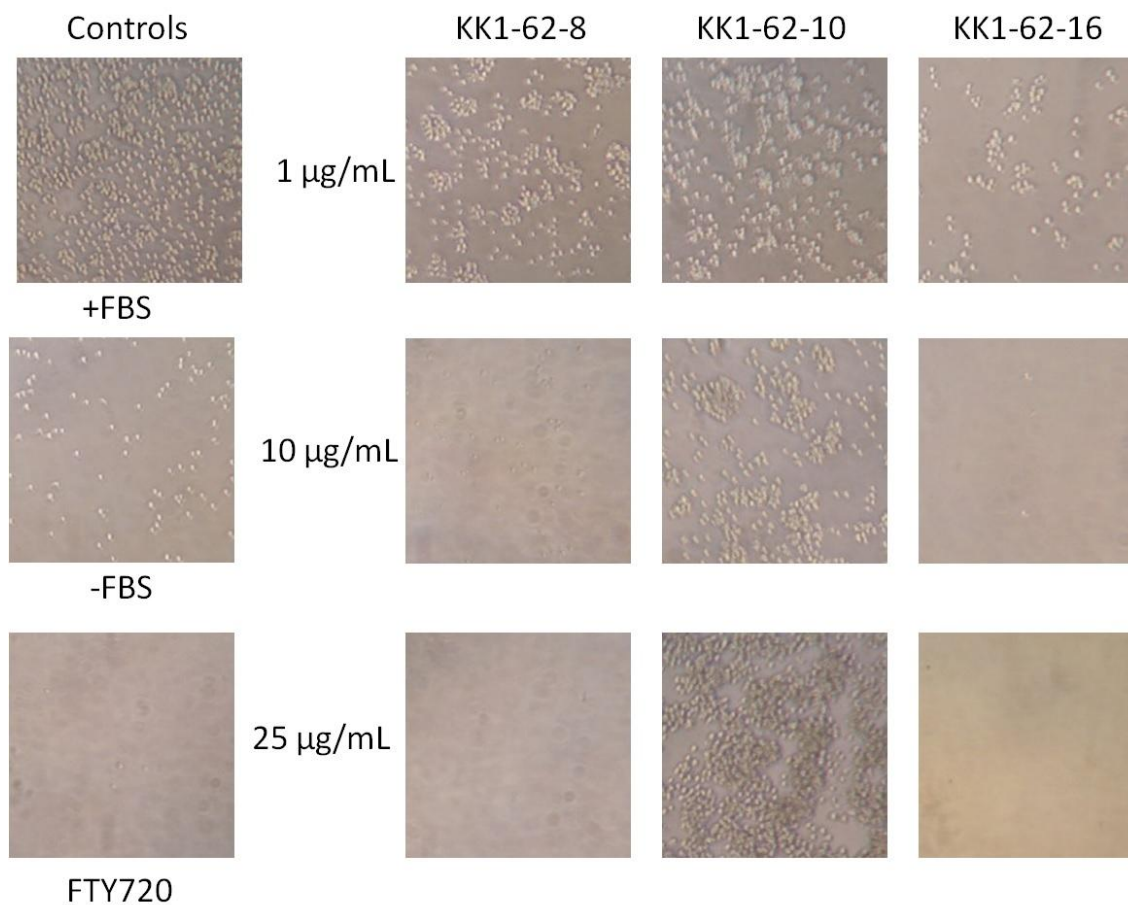
(b) NP982 (KK1-62-16)



Appendix Figure 86. Purified nuiapolide (56) and NP982

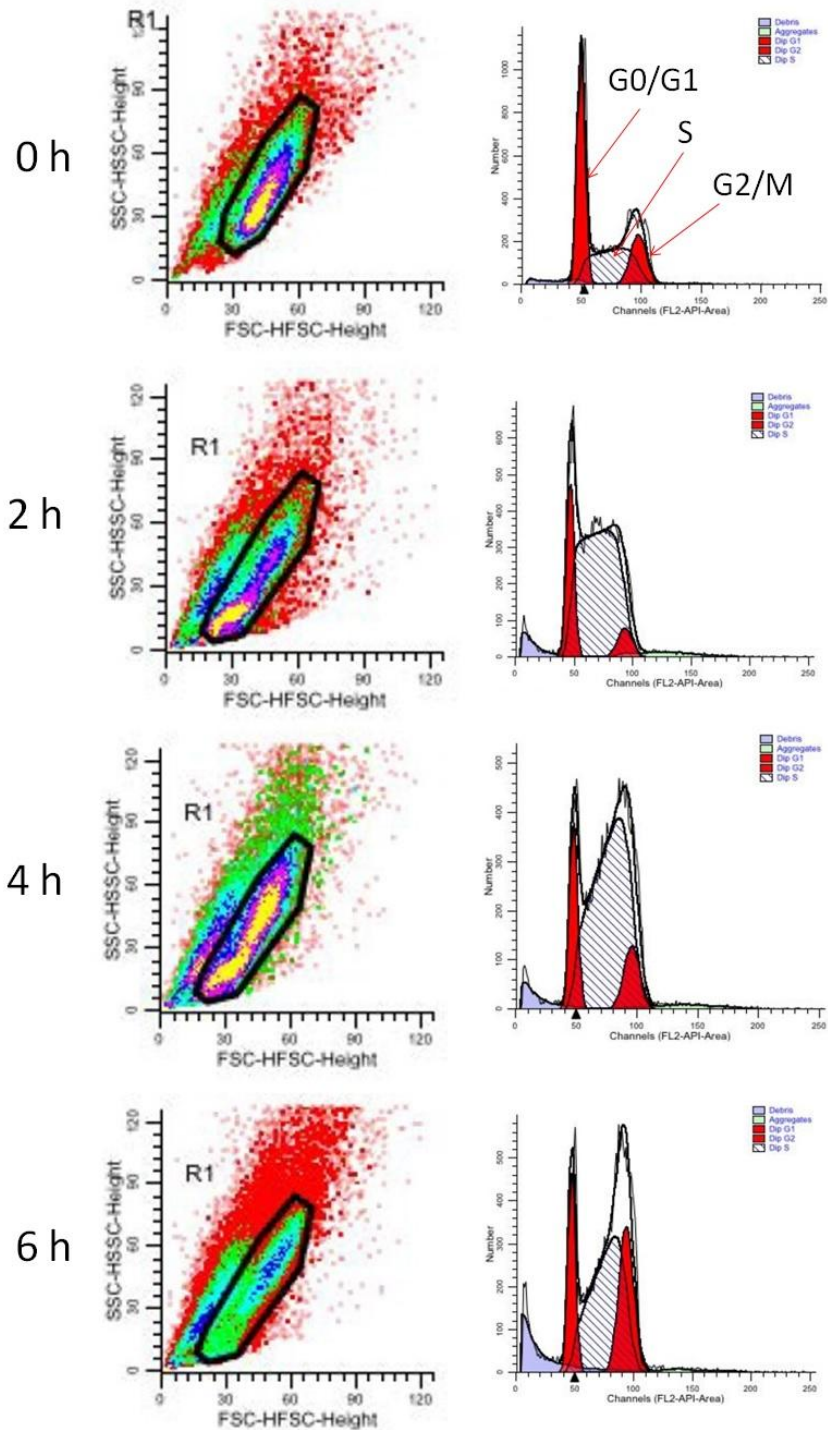
(a): Nuiapolide (56, NP788) was purified sufficient amount. **(b):** NP982 was purified insufficient amount.

KK1-62-8 (Nuiapolide)	1 $\mu\text{g}/\text{mL}$	10 $\mu\text{g}/\text{mL}$	25 $\mu\text{g}/\text{mL}$	Effectiveness 
KK1-62-10	1 $\mu\text{g}/\text{mL}$	10 $\mu\text{g}/\text{mL}$	25 $\mu\text{g}/\text{mL}$	
KK1-62-16 (NP982)	1 $\mu\text{g}/\text{mL}$	10 $\mu\text{g}/\text{mL}$	25 $\mu\text{g}/\text{mL}$	



Appendix Figure 87. Chemotaxis assay for purified active fractions

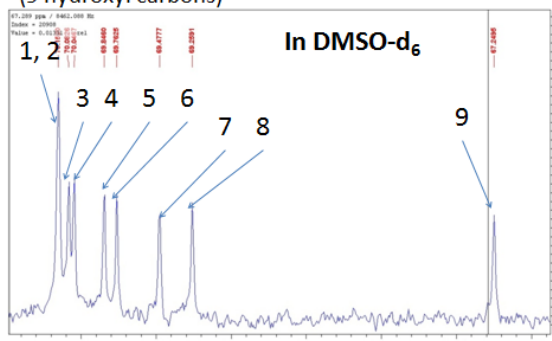
The fractions were assessed for ability of inhibiting chemotaxis of Jurkat cells at the concentrations of 1, 10, and 25 $\mu\text{g}/\text{mL}$. The other sample KK1-62-10 was the fraction between active fractions, indicating no activity of the fraction.



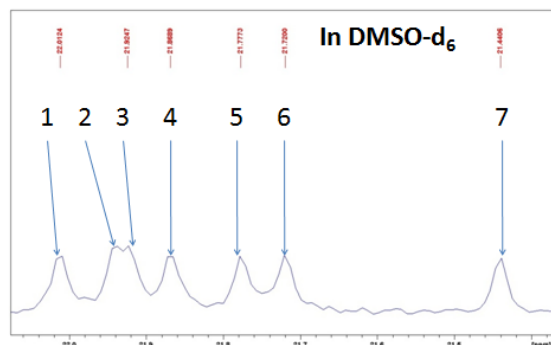
Appendix Figure 88. Cell cycle analysis of nuiapolide (56) treated Jurkat cells
 Left: light-scattering properties of cells/nuclei, Middle: Histogram with modeled cell cycle components, and Right: appearance of cells

Number of carbons in ^{13}C NMR grouped regions

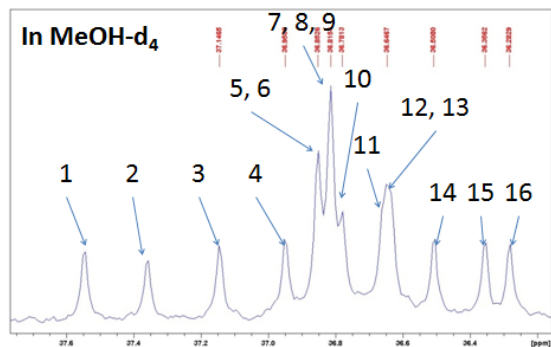
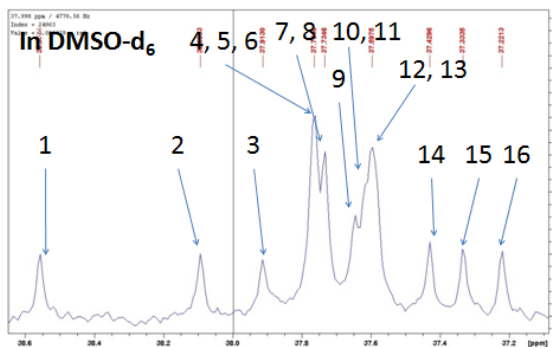
C7, C9, C13, C17, C21, C25, C29, C33, C37
(9 hydroxyl carbons)



C11, C15, C19, C23, C27, C31, C35 (7 β -carbons)



C6, C10, C12, C14, C16, C18, C20, C22, C24, C26, C28, C30, C32, C34, C36, C38 (16 α -carbons)



Appendix Figure 89. Number of carbons in ^{13}C NMR grouped regions

Top right: 21.4-22.0 ppm in DMSO- d_6 . Top left: 69.2-70.2 ppm in DMSO- d_6 . Bottom right: 36.2-37.4 ppm in methanol- d_4 . Bottom left: 37.2-38.1 ppm in DMSO- d_6 .